UNIVERSIDADE FEDERAL DE VIÇOSA

Understanding the environmental dynamics of the Pantanal: Pedological, phytosociological, and machine learning applications for landscape evolution and inundation monitoring studies

Iórrana Figueiredo Sacramento
Doctor Scientiae

VIÇOSA - MINAS GERAIS
2025

IÓRRANA FIGUEIREDO SACRAMENTO

Understanding the environmental dynamics of the Pantanal: Pedological, phytosociological, and machine learning applications for landscape evolution and inundation monitoring studies

Thesis submitted to the Soil Science and Plant Nutrition Graduate Program of the Universidade Federal de Viçosa in partial fulfillment of the requirements for the degree of *Doctor Scientiae*.

Adviser: Carlos E. G. R. Schaefer

Co-advisers: Elpidio I. F. Filho
Guilherme R. Corrêa

VIÇOSA - MINAS GERAIS
2025

Ficha catalográfica elaborada pela Biblioteca Central da Universidade Federal de Viçosa - Campus Viçosa

T
S123u
2025

Sacramento, Iórrana Figueiredo, 1995-
Understanding the environmental dynamics of the Pantanal: pedological, phytosociological, and machine learning applications for landscape evolution and inundation monitoring studies / Iórrana Figueiredo Sacramento. – Viçosa, MG, 2025.
1 tese eletrônica (259 f.): il. (algumas color.).

Texto em inglês.
Inclui apêndices.
Orientador: Carlos Ernesto Gonçalves Reynaud Schaefer.
Tese (doutorado) - Universidade Federal de Viçosa, Departamento de Solos, 2025.
Inclui bibliografia.
DOI: https://doi.org/10.47328/ufvbbt.2025.234
Modo de acesso: World Wide Web.

1. Ciência do solo. 2. Paisagens - Pantanal Mato-grossense (MT e MS). 3. Pedologia. 4. Solos - Inundação. 5. Aprendizado do computador. I. Schaefer, Carlos Ernesto Gonçalves Reynaud, 1965-. II. Universidade Federal de Viçosa. Departamento de Solos. Programa de Pós-Graduação em Solos e Nutrição de Plantas. III. Título.

CDD 22. ed. 631.4

Bibliotecário(a) responsável: Bruna Silva CRB-6/2552

IÓRRANA FIGUEIREDO SACRAMENTO

Understanding the environmental dynamics of the Pantanal: Pedological, phytosociological, and machine learning applications for landscape evolution and inundation monitoring studies

Thesis submitted to the Soil Science and Plant Nutrition Graduate Program of the Universidade Federal de Viçosa in partial fulfillment of the requirements for the degree of *Doctor Scientiae*.

APPROVED: January 30, 2025.

Assent:

_____

Iórrana Figueiredo Sacramento
Author

_____

Carlos Ernesto Goncalves Reynaud Schaefer
Adviser

To my parents: Edna and Cleiton.

ACKNOWLEDGMENTS

To the Federal University of Viçosa, for providing the opportunity to complete this postgraduate course.
To my adviser, Carlos Ernesto, for his valuable guidance, support, and trust.
To my co-advisers, Guilherme and Elpídio, for their incentive and mentorship during field and laboratory work.
To the professors Francis, Danilo, Frederico, Márcio, Edgar, Marcelo, José João, Maurício, João Ker, Liovando, Isabela, for their assistance and valuable teachings.
To the administrative and laboratory staff, Claudinha, Carol, Nayan, Adriana, Josemar, Maurício, Carlinhos, Paloma, and João José, for their support and collaboration.
To my trainees and graduate students, Carol, Raíssa, Júlia, Riquelme, Vitor, Felipe, and Antônio, for their fundamental contributions to the laboratory work.
To my friends and colleagues, Prímula, Palucci, Cássio, Clara, Fabrício, Ramon, Diego, Alex, and Diogo, whose assistance significantly contributed to the development of this work.
To God for the blessings and strength.
To my parents, Cleiton and Edna, my sister Beatriz, and all my family for their unconditional love and essential support.
To all of my friends, for their affection, encouragement, and patience during the most challenging and joyful moments of my path.
This work has been sponsored by the following Brazilian research agencies: Coordination for the Improvement of Higher Education Personnel (CAPES; Financing code 001), Minas Gerais State Foundation for Research Aid (FAPEMIG) and National Council of Scientific and Technological Development (CNPq).

“Eu sei de muito pouco. Mas tenho a meu favor tudo o que não sei. Tudo o que não sei é a minha parte maior e melhor: é a minha largueza. É com ela que eu compreenderia tudo. Tudo o que não sei é que constitui a minha verdade”.
(Clarice Lispector)

ABSTRACT

SACRAMENTO, Iórrana Figueiredo, D.Sc., Universidade Federal de Viçosa, January, 2025. **Understanding the environmental dynamics of the Pantanal: Pedological, phytosociological, and machine learning applications for landscape evolution and inundation monitoring studies**. Adviser: Carlos Ernesto Goncalves Reynaud Schaefer. Co-advisers: Elpidio Inacio Fernandes Filho and Guilherme Resende Corrêa.

The Pantanal, one of the world's largest continental wetlands, hosts immense biodiversity and is shaped by a unique flooding regime. Nhecolândia, the second biggest Pantanal sub-region, is distinguished by its abundance of lakes and geoenvironmental diversity. Studying the Pantanal's landscape is crucial for understanding its dynamics and supporting sustainable management. Seasonal climatic variability significantly impacts vegetation composition, structure, and soil moisture, influencing plant community distribution. Soils exhibit distinct morphological and physico-chemical characteristics, shaped by past and present processes. In the last few decades, inappropriate land use and climate change have disrupted the Pantanal's flood regime. This study investigated soil genesis, soil-vegetation-landscape relationships, lansdcape evolution, in the Pantanal Nhecolândia, and inundation frequency along the Upper Paraguay River Basin (UPRB), where the Pantanal is inserted. For the pedogenesis study, thirty soil profiles from the main Nhecolândia landscape units, were collected, and analyzed by their morphological, physical, chemical, mineralogical, and geochemical characteristics. For the soil-vegetation relationship study, vegetation was described, phytosociological parameters were obtained, and composite soil samples were collected and analyzed by their physical and chemical characteristics. For the landscape evolution study, carbon stable isotopes analysis, and chronological analyzes, such as radiocarbon and optically stimulated luminesce datings, were applied. For the water frequency monitoring, water was mapped using radar images, associated with multi-source data and the Random Forest, a machine learning classification algorithm. The pedological differentiation in the Nhecolândia Pantanal is mainly caused by topographical variations, climate, and biological activity. Despite the sandy texture, each environment differed in some aspect: the Salinas stand out with greater clay and base cation contents, due to predominance of salinization, gleization, and bissialitization processes. The Baías and Murundus, affected by paludization and termite activity, respectively, showed higher organic carbon content. Acidic soils dominated in the Vazantes due to podzolization and ferrolisis. The Campos soils are dystrophic due to intense leaching. Non-floodable areas

(Cordilheiras and Murundus) presented higher species richness and composition, due to nutrient availability. Floodable areas, particularly the Salinas, presented the lowest species richness and composition due to high Na+ levels. During the Late Holocene, Salinas transitioned from a cerrado (savanna) to a grassy environment, while the higher Vazantes, with mixed C3-C4 grass cover, evolved to a C4-dominated grassland. In contrast, lower areas, such as the Baías and lower Vazantes, remained dominated by hydrophilic and aquatic macrophytes due to a more persistent flooding regime. Between 2018 to 2021, areas with higher inundation frequency occurred in the western portion of the UPRB, near to the Paraguay River, and in the southern portion, where the Nhecolândia's lakes occur, and a decreasing trend in water extent was observed during the wet season. Understanding soil-vegetation-landscape interactions and monitoring flood dynamics are fundamental for mitigating climate change impacts and conserving this complex ecosystem.

Keywords: soil-landscape; edaphology; pedology; flooding; machine learning

RESUMO

SACRAMENTO, Iórrana Figueiredo, D.Sc., Universidade Federal de Viçosa, janeiro de 2025. **Compreendendo as dinâmicas ambientais do Pantanal: Aplicações pedológicas, fitossociológicas e de aprendizado de máquinas para estudos de evolução da paisagem e monitoramento de inundações.**. Orientador: Carlos Ernesto Goncalves Reynaud Schaefer. Coorientadores: Elpidio Inacio Fernandes Filho e Guilherme Resende Corrêa.

O Pantanal, uma das maiores áreas úmidas continentais do mundo, abriga uma imensa biodiversidade e é moldado por um regime de inundações singular. A Nhecolândia, segunda maior sub-região do Pantanal, destaca-se pela abundância de lagoas e diversidade geoambiental. Estudar a paisagem do Pantanal é crucial para entender sua dinâmica e apoiar sua sustentabilidade. A variabilidade climática sazonal impacta significativamente a composição e estrutura da vegetação, e a umidade do solo, influenciando a distribuição das comunidades vegetais. Os solos apresentam características distintas, moldadas por processos passados e presentes. Nas últimas décadas, o uso inadequado da terra e as mudanças climáticas têm afetado o regime de inundações do Pantanal. Este estudo investigou a gênese do solo, as relações solo-vegetação, a evolução da paisagem do Pantanal da Nhecolândia e a frequência de inundação ao longo da Bacia do Alto Rio Paraguai (BARP), onde o Pantanal está inserido. Para o estudo da pedogênese, trinta perfis de solo distribuídos em seis unidades de paisagem da Nhecolândia foram coletados e analisados quanto às suas características morfológicas, físicas, químicas, mineralógicas e geoquímicas. Para o estudo das relações solo-vegetação, foram obtidos parâmetros fitossociológicos e amostras compostas de solo, que passaram por análises de suas características físicas e químicas. Para o estudo da evolução da paisagem, análises de isótopos estáveis de carbono e análises cronológicas, como datação por radiocarbono e por luminescência opticamente estimulada, foram aplicadas. Para o monitoramento da frequência de inundações, a água foi mapeada usando imagens de radar, associadas a dados de múltiplas fontes e o algoritmo de classificação por aprendizado de máquina Random Forest. A diferenciação pedológica no Pantanal da Nhecolândia é causada principalmente por variações topográficas, clima e atividade biológica. As Salinas se destacaram por maior teor de argila e cátions básicos, predominando processos de salinização, gleização e bissialitização. As Baías e os Murundus, influenciados pela paludização e pela atividade de cupins, respectivamente, apresentaram maior teor de carbono orgânico. Solos ácidos dominaram nas Vazantes devido à podzolização e à ferrólise. Os

solos dos Campos são distróficos devido à intensa lixiviação. Áreas não inundáveis (Cordilheiras e Murundus) apresentaram maior riqueza e composição de espécies devido à disponibilidade de nutrientes. Áreas inundáveis, particularmente as Salinas, apresentaram menor riqueza e composição de espécies devido ao alto teor de Na+. Durante o Holoceno tardio, as Salinas passaram de cerrado para um ambiente gramíneo, enquanto as Vazantes mais altas, com cobertura mista de gramíneas C3-C4, evoluíram para gramíneas dominadas por plantas C4. Em contraste, as áreas mais baixas, como as Baías e Vazantes baixas, permaneceram dominadas por vegetação hidrófila e macrófitas aquáticas devido a um regime de inundações mais persistente. Entre 2018 e 2021, áreas com maior frequência de inundações ocorreram na porção oeste da BARP, próximo ao Rio Paraguai, e na porção sul, onde estão as lagoas da Nhecolândia, com uma tendência de redução da extensão de água durante a estação chuvosa. Compreender as interações solo-vegetação-paisagem e monitorar a dinâmica das inundações são fundamentais para mitigar os impactos das mudanças climáticas e conservar este ecossistema complexo.

Palavras-chave: solo-paisagem; edafologia; pedologia; inundação; aprendizado de máquinas

SUMMARY

1 GENERAL INTRODUCTION

The Pantanal is a unique wetland landscape in the Brazilian territory. According to Ab'Sáber (2011), the Pantanal is considered a contact zone and a major extension of terrestrial and aquatic ecosystems. It is one of the world's largest continental flooded areas and the second most preserved Brazilian biome (Keddy *et al*., 2009; MapBiomas, 2024). It was designated as a National Heritage site by the Brazilian Constitution in 1988 and a Biosphere Reserve by UNESCO in 2000 (Boin *et al*., 2019). The Pantanal presents a mosaic landscape, incorporating ecosystems from surrounding biomes, such as the Cerrado (uppercase C for the biogeographic province), Amazonia, Chaco (Bolivia, Paraguay and Argentina), Atlantic Forest, and fragments of Caatinga (Ab'Sáber, 2011; Boin *et al*., 2019). This heterogeneity results in a landscape with distinctive hydrological, pedological, and floristic characteristics, one of the reasons for the use of the plural term "Pantanals" (Pott *et al*., 2011).

The Nhecolândia, one of the eleven subregions of the Pantanal, is distinguished by its abundance of alkaline-saline and freshwater lakes, an intriguing characteristic of the landscape (Assine, 2015; Furian *et al*., 2013). The diversity of soil and vegetation types, together with a complex hydrography, generates a diversity of landscape units, locally referred to as *Salinas* (saline or alkaline lakes), *Baías* (freshwater lakes), *Cordilheiras* (sand levees), *Vazantes* (seasonal floodwater courses), *Murundus* (termite mounds), and *Campos* (grasslands fields) (Boin *et al*., 2009; de Oliveira; Pla-Pueyo; Hackney, 2019; Furquim; Vidoca, 2021). The Nhecolândia forms part of the Taquari megafan, a depositional system shaped by alternating humid and dry periods since the Late Pleistocene (McGlue *et al*., 2017). The climatic evolution is imprinted on the region's landforms, through the presence of abandoned lobes, degradational channels, and ponds (Assine, Mario Luis *et al*., 2015; Gradella *et al*., 2011).

The environmental dynamic of the Pantanal landscape is deeply related to changes in climatic conditions. The flooding regime in the Pantanal is primarily driven by the increased volume of the Paraguay river and its tributaries, which is influenced by the low slope and seasonal rainfall, occurring mainly in the surrounding uplands (Adámoli, 1984a). In the northern Pantanal, inundation begins during the rainy season in January/February and reaches the southern portion about three months later, around April/May (Carvalho, 1984). In the Nhecolândia, composed by an unconsolidated sandy substrate, water flows along *Vazantes* and permanent channels (*Corixos*) during the inundation season (Assine *et al*., 2015; McGlue *et al*., 2017). During floods, the *Baías* integrate with the *Vazantes*, while the *Salinas* remain isolated due to surface and subsurface barriers created by the surrounding *Cordilheiras* and a low

permeable soil horizon, respectively, which contribute to the soil alkalinization process (Barbiero *et al*., 2008; Costa-Silva *et al*., 2024; McGlue *et al*., 2017).

The seasonal hydrological changes that occur annually in the Pantanal are responsible for expanding and retracting habitats, which create different conditions for plant development and are the main factors influencing the richness and diversity of plant species and phytophysiognomies in the Pantanal's ecosystems (Alho, 2008; Ravaglia *et al*., 2011). Another factor is the habitats insularization, particularly observed in the *Murundus* fields. According to the theory of island biogeography, species richness is a function of habitat size and decreases as the area becomes smaller (Bordignon *et al*., 2007), among other factors such as migration. In general, plant communities in the Pantanal differentiate and occur across three basic landforms in relation to flooding: flood-free ridges (*Cordilheiras*) with trees, seasonally flooded plains with grasslands, and water bodies with aquatic macrophytes (Pott; Pott, 2004). The influence of flooding on plant distribution in the Pantanal is so significant that amazonian species located in its southern portion can survive even during dry season, due to inundation caused by the delayed water flow mentioned earlier (Pott *et al*., 2011). The woody savanna of the Cerrado biogeographic province, called cerrado (with a lowercase "c" to refer to the vegetation form), predominates in the sandy areas influenced by Taquari River deposition and is the only extensive area where cerrado occurs over Quaternary sediments (Adámoli, 1984b).

The soils are also influenced by seasonal flooding and exhibit distinct morphological and physico-chemical characteristics across the different landscape units of the Pantanal (Amaral Filho, 1984; Couto *et al*., 2023; Cunha, 1980). Pedological studies in the Nhecolândia have focused on the salt-affected soils and their relationships with the *Salinas*, aiming to understand the origins of these intriguing landscape features (Andrade *et al*., 2020; Bacani *et al*., 2010; Barbiero *et al*., 2008; Costa-Silva *et al*., 2024; Furquim *et al*., 2010; Merdy *et al*., 2022; Schiavo *et al*., 2012). Formed from a uniform sandy substrate, soil differentiation in the Nhecolândia subregion depends on climatic, topographic and hydrological variations, which influence many pedological processes, such as the translocation of metal-organic complexes, salinization, oxidation-reduction, and mineral neoformation (Bacani *et al*., 2010; Barbiero *et al*., 2016; Furquim *et al*., 2008; Oliveira *et al*., 2022). Paleoenvironmental studies, using an integrated approach that includes pedological analyses, radiocarbon and optically stimulated luminescence dating, microfossils, and stable carbon isotope ratios, have been important for understanding the evolution of the Nhecolândia landscape (Becker *et al*., 2018; McGlue *et al*., 2017; Rasbold *et al*., 2024).

In recent decades in the Pantanal, inappropriate land use for agriculture and cattle husbandry, as well as the construction of small hydroelectric plants, have led to an increase in erosive and aggradation processes, which directly affects biodiversity and the flooding regime (Alho *et al*., 2019; Junk *et al*., 2006; Junk; Cunha, 2005). Fires, which are considered natural in the Pantanal, have increased due to agriculture and pasture, with 2020 setting records for the number of fire foci and burned areas (Marques *et al*., 2021). In Nhecolândia, the main threat is the deforestation of the *Cordilheiras* for cultivated pasture, a process that has been intensified due to the increasing competition with the cattle ranches on the surrounding upland (Junk *et al*., 2006). The loss of *Cordilheiras* vegetation has caused the erosion of sand ridges, which has affected *Salinas* dynamics. During the inundation season, freshwater reaches the *Salinas*, contributing to the acidification of waters, diluting soil solutions, and promoting overall leaching, which cause the degradation of Saline-Sodic soils into Sodic soils (Andrade *et al*., 2020; Furquim *et al*., 2017).

As demonstrated so far, the inundation regime is the main characteristic of the Pantanal and the principal factor driving the ecological dynamic. Any change in water supply in the Pantanal may directly impact on the sustainability of its ecosystems. In addition to the local impacts of land-use change, future global climate change projections indicate that temperatures could rise, and rainfall could decrease, causing longer dry periods and, consequently, affecting the regional water balance (Marengo; Oliveira; Alves, 2015). Inundation monitoring studies have been conducted in the Pantanal to evaluate and predict the impacts of human actions and future climate changes (Antunes; Esquerdo, 2015; Evans *et al*., 2010; Moraes; Pereira; Cardozo, 2013; Paz *et al*., 2011). Different techniques and approaches have been applied for flood monitoring at various scales, with the synthetic aperture radar remote sensing being a promising tool, once it can measure through clouds and vegetation cover with high spatial and temporal resolutions (Hess; Melack; Simonett, 1990; Shen *et al*., 2019).

Thus, this study aims to address the following key questions: What are the soil-landscape relationships of the Nhecolândia Pantanal? How do soil characteristics influence the assembly of different vegetational communities? What are the main soil-forming processes in each landscape unit? How has the Nhecolândia landscape evolved? What is the spatiotemporal dynamic of inundations in the Upper Paraguay River Basin?

1.1 REFERENCES

AB'SÁBER, A. N. **Brasil, paisagens de exceção: o litoral e o Pantanal mato-grossense, patrimônios básicos**. 4. ed. Cotia: Ateliê Editorial, 2011.

ADÁMOLI, J. A dinâmica das inundações no Pantanal. In: Simpósio sobre Recursos Naturais e Sócio-econômicos do Pantanal, 1, 1984a, Corumbá. **Anais...** Corumbá: EMBRAPA-DDT, 1984a. p. 51.

ADÁMOLI, J. Fitogeografia do Pantanal. In: Simpósio sobre Recursos Naturais e Sócio-econômicos do Pantanal, 1, 1984b, Corumbá. **Anais...** EMBRAPA-DDT, 1984b. p. 105–6.

ALHO, C. J. R. *et al*. Ameaças à biodiversidade do Pantanal brasileiro pelo uso e ocupação da terra. **Ambiente & Sociedade**, [s. l.], v. 22, 2019. Disponível em: http://lattes.cnpq.

ALHO, C. J. R. Biodiversity of the Pantanal: response to seasonal flooding regime and to environmental degradation. **Brazilian Journal of Biology**, [s. l.], v. 68, n. 4, p. 957–966, 2008.

AMARAL FILHO, Z. P. do. Solos do Pantanal Mato-grossense. Simpósio sobre Recursos Naturais e Sócio-econômicos do Pantanal, 1, 1984, **Anais...** Corumbá. EMBRAPA-DDT, 1984. p. 91–104.

ANDRADE, G. R. P. *et al*. Transformation of clay minerals in salt-affected soils, Pantanal wetland, Brazil. **Geoderma**, [s. l.], v. 371, p. 114-380, 2020.

ANTUNES, J. F. G.; ESQUERDO, J. C. D. M. Quantification of flooded areas of Pantanal by sub-pixel classification of MODIS time-series data. **Geografia**, [s. l.], v. 40, p. 1–16, 2015.

ASSINE, M. L. Brazilian Pantanal: A Large Pristine Tropical Wetland. In: VIEIRA, B. C.; S., RODRIGUES, A. A.; SANTOS, L. J. C. (org.). **Landscapes and Landforms of Brazil**. [S. l.]: Springer Dordrecht, 2015. p. 135–146.

ASSINE, M. L. *et al*. **Geology and Geomorphology of the Pantanal Basin**. In: [S. l.: s. n.], 2015. p. 23–50.

ASSINE, M. L. *et al*. The Quaternary alluvial systems tract of the Pantanal Basin, Brazil. **Brazilian Journal of Geology**, [s. l.], v. 45, n. 3, p. 475–489, 2015.

BACANI, V. M. *et al*. Caracterização das diferenças microclimáticas e pedomorfológicas do entorno de uma lagoa salina no pantanal da Nhecolândia, MS. **Geografia**, [s. l.], v. 35, n. 1, p. 149–163, 2010.

BARBIERO, L. *et al*. Organic control of dioctahedral and trioctahedral clay formation in an alkaline soil system in the Pantanal Wetland of Nhecolândia, Brazil. **PLOS ONE**, [s. l.], v. 11, n. 7, p. 1-23, 2016.

BARBIERO, L. *et al*. Soil morphological control on saline and freshwater lake hydrogeochemistry in the Pantanal of Nhecolândia, Brazil. **Geoderma**, [s. l.], v. 148, n. 1, p. 91–106, 2008.

BECKER, B.F. *et al*. Late Holocene palynology of a saline lake in the Pantanal of Nhecolândia, Brazil. **Palynology**, [s. l.], v. 42, n. 4, p. 457–465, 2018.

BOIN, M. N. *et al*. Pantanal: The Brazilian Wetlands. In: SALGADO, RODRIGUES, A. A.; SANTOS, L. J. C.; PAISANI, J. C. (org.). **The Physical Geography of Brazil**. [S. l.]: Springer Cham, 2019. p. 75–91.

BORDIGNON, L. *et al*. Ilhas Vegetacionais no Pantanal Matogrossense: um teste da Teoria de Biogeografia de Ilhas. **Revista Brasileira de Biociências**, [s. l.], v. 5, p. 387–389, 2007.

CARVALHO, N. de O. Hidrologia da Bacia do Alto Paraguai. In: Simpósio sobre Recursos Naturais e Sócio-econômicos do Pantanal, 1, Corumbá. **Anais...** Corumbá: EMBRAPA-DDT, 1984. p. 43–50.

COSTA-SILVA, A. R. *et al*. Soils surrounding saline-alkaline lakes of Nhecolândia, Pantanal, Brazil: Toposequences, mineralogy and chemistry. **Geoderma Regional**, [s. l.], v. 36, p. e00746, 2024.

COUTO, E. G. *et al*. Soils of Pantanal: The Largest Continental Wetland. In: Schaefer, C.E.G.R. (eds). **The Soils of Brazil**. Switzerland: Springer, Cham, 2023, p. 239-267.

CUNHA, N. G. da. **Considerações sobre os solos da sub-região da Nhecolândia, Pantanal Mato-grossense**. Corumbá: EMBRAPA, 1980.

DE OLIVEIRA, E. C.; PLA-PUEYO, S.; HACKNEY, C. R. Natural and anthropogenic influences on the Nhecolândia wetlands, SE Pantanal, Brazil. **Geological Society**, [s. l.], v. 488, n. 1, p. 167–180, 2019.

EVANS, T. L. *et al*. Using ALOS/PALSAR and RADARSAT-2 to Map Land Cover and Seasonal Inundation in the Brazilian Pantanal. **IEEE Journal of Selected Topics in Applied Earth Observations and Remote Sensing**, [s. l.], v. 3, n. 4, p. 560–575, 2010.

FURIAN, S. *et al*. Chemical diversity and spatial variability in myriad lakes in Nhecolândia in the Pantanal wetlands of Brazil. **Limnology and Oceanography**, [s. l.], v. 58, n. 6, p. 2249–2261, 2013.

FURQUIM, S. A. C. *et al*. Mineralogy and Genesis of Smectites in an Alkaline-Saline Environment of Pantanal Wetland, Brazil. **Clays and Clay Minerals**, [s. l.], v. 56, n. 5, p. 579–595, 2008.

FURQUIM, S. A. C. *et al*. Neoformation of micas in soils surrounding an alkaline-saline lake of Pantanal wetland, Brazil. **Geoderma**, [s. l.], v. 158, n. 3–4, p. 331–342, 2010.

FURQUIM, S. A. C. *et al*. Salt-affected soils evolution and fluvial dynamics in the Pantanal wetland, Brazil. **Geoderma**, [s. l.], v. 286, p. 139–152, 2017.

FURQUIM, S. A. C.; VIDOCA, T. T. Salt-Affected Soils of Pantanal Wetland. In: TALEISNIK, E.; LAVADO, R. S. (org.). **Saline and Alkaline Soils in Latin America**. Cham: Springer International Publishing, 2021. p. 229–254.

GRADELLA, F. dos S. *et al*. Geomorphology and deposition events in Nhecolandia Pantanal Wetland. **Geografia**, [s. l.], v. 36, p. 107–117, 2011.

HESS, L. L.; MELACK, J. M.; SIMONETT, D. S. Radar detection of flooding beneath the forest canopy: a review. **International Journal of Remote Sensing**, [s. l.], v. 11, n. 7, p. 1313–1325, 1990.

JUNK, W. J. *et al*. Biodiversity and its conservation in the Pantanal of Mato Grosso, Brazil. **Aquatic Sciences**, [s. l.], v. 68, n. 3, p. 278–309, 2006.

JUNK, W. J.; CUNHA, C. N. de. Pantanal: a large South American wetland at a crossroads. **Ecological Engineering**, [s. l.], v. 24, n. 4, p. 391–401, 2005.

KEDDY, P. A. *et al*. Wet and Wonderful: The World's Largest Wetlands Are Conservation Priorities. **BioScience**, [s. l.], v. 59, n. 1, p. 39–51, 2009.

MAPBIOMAS. **Projeto MapBiomas - Mapeamento Anual de Cobertura e Uso da Terra no Brasil - Coleção 9**. [S. l.], 2024.

MARENGO, J. A.; OLIVEIRA, G. S.; ALVES, L. M. Climate Change Scenarios in the Pantanal. In: BERGIER, I; ASSINE, M. L. **Dynamics of the Pantanal Wetland in South America**. Switzerland: Springer, Cham, 2015. p. 227–238.

MARQUES, J. F. *et al*. Fires dynamics in the Pantanal: Impacts of anthropogenic activities and climate change. **Journal of Environmental Management**, [s. l.], v. 299, p. 113586, 2021.

MCGLUE, M. M. *et al*. Holocene stratigraphic evolution of saline lakes in Nhecolândia, southern Pantanal wetlands (Brazil). **Quaternary Research**, [s. l.], v. 88, n. 3, p. 472–490, 2017.

MERDY, P. *et al*. Processes and rates of formation defined by modelling in alkaline to acidic soil systems in Brazilian Pantanal wetland. **Catena**, [s. l.], v. 210, p. 105876, 2022.

MORAES, E. C.; PEREIRA, G.; CARDOZO, F. da S. Evaluation of reduction of Pantanal wetlands in 2012. **Geografia**, [s. l.], v. 38, p. 1–14, 2013.

OLIVEIRA, N. de S. *et al*. Pedogenesis of soils with accumulation of organic carbon in the subsurface horizons in a saline lake in the Pantanal wetland of Nhecolândia, Brazil. **Journal of South American Earth Sciences**, [s. l.], v. 117, p. 1-15, 2022.

PAZ, A. R. da *et al*. Large-scale modelling of channel flow and floodplain inundation dynamics and its application to the Pantanal (Brazil). **Hydrological Processes**, [s. l.], v. 25, n. 9, p. 1498–1516, 2011.

POTT, A. *et al*. Plant diversity of the Pantanal wetland. **Brazilian Journal of Biology**, [s. l.], v. 71, n. 1, p. 265–273, 2011.

POTT, A.; POTT, V. J. Features and conservation of the Brazilian Pantanal wetland. **Wetlands Ecology and Management**, [s. l.], v. 12, p. 547–552, 2004.

RASBOLD, G. G. *et al*. Holocene limnological changes in saline and freshwater lakes, Lower Nhecolândia, Pantanal, Brazil. **Hydrobiologia**, [s. l.], v. 851, n. 7, p. 1723–1739, 2024.

RAVAGLIA, A. G. *et al*. **Mapeamento das unidades de paisagem das sub-regiões da Nhecolândia e Poconé, Pantanal Mato-Grossense**. 1. ed. Corumbá: Embrapa Pantanal, 2011.

SCHIAVO, J. A. *et al*. Characterization and classification of soils in the Taquari river basin - Pantanal region, state of Mato Grosso do Sul, Brazil. **Revista Brasileira de Ciência do Solo**, [s. l.], v. 36, n. 3, p. 697–708, 2012.

SHEN, Xinyi *et al*. Inundation Extent Mapping by Synthetic Aperture Radar: A Review. **Remote Sensing**, [s. l.], v. 11, n. 7, p. 879, 2019.

2 CHAPTER 1: Soil-landscape interplays in the sandy domain of the Nhecolândia Pantanal, western Brazil

2.1 ABSTRACT

The Pantanal is one of the largest wetlands, hosting immense biodiversity. The landscape of the Nhecolândia subregion is considered a mosaic of plants and environments. Understanding the soil-landscape interactions are fundamental for better planning and management of Pantanal natural resources. In this study, we aimed to characterize soil-landscape relationships across the landscape units of Nhecolândia. These units include *Baía* and *Salina* (freshwater and alkaline lakes, respectively), *Vazante* (flooding lowlands), *Cordilheira* (sand ridges), *Campo* (flooding fields), and *Murundus* (termite mounds, described here for the first time). Vegetation and soil were described, collected, and classified using the Brazilian Soil Classification System and the World Reference Base for Soil Resources. Granulometry and chemical routine fertility analyses were performed, alongside statistical analyses (descriptive, multivariate and non-parametric variance analyses). Cerrado vegetation predominates, with trees and shrubs species mainly in non-flooded areas (*Cordilheiras* and *Murundus*), and herbaceous fields in seasonally waterlogged areas (*Salina*, *Baía*, *Vazante*, and *Campo*). Arenosols dominated due to sandy fluvial sediments, but *Salinas* showed high pedodiversity, with clay-rich, alkaline, and fertile soils, displaying redoximorphic features and salt accumulation. *Baías* soils had high surface total organic carbon (TOC) due to prolonged water saturation, while *Vazantes* soils are base-poor and rich in Al^{3+}, reflecting leaching and ferrolysis. *Cordilheiras* soils are sandy, with higher fertility and TOC due to fauna influence and litter accumulation. *Murundus* and *Campos* soils were similar, but *Murundus* had high TOC, due to termite activity, favoring pedoturbation. This study highlighted the hydrological regime's influence on soil, vegetation, and biological activity, shaped by topographical and substrate interactions, which drive the unique diversity of the Nhecolândia landscape.

Keywords: Wetland. Pedoenvironment. Saline soils. Pedoturbation.

2.2 INTRODUCTION

The Pantanal is one of the largest continental wetlands of the world and home to an immense diversity of plant and fauna species. It is considered a National Heritage site by the Constitution of Brazil, a World Heritage Area, a Reserve of Biosphere by UNESCO, and an area with international importance by the Ramsar Convention of Wetlands (Furquim; Vidoca, 2021). A wetland can be defined as an ecosystem at the interface between aquatic and terrestrial environments, permanently or periodically inundated by shallow water or consist of waterlogged soils (Junk *et al*., 2014). The Pantanal is in western Brazil, in the Upper Paraguay River Basin (UPRB), and it is formed by a mosaic of environments, with distinctive pedological, vegetational, and hydrological characteristics (Pott *et al*., 2011; Silva; Abdon, 1998). The Nhecolândia, one of the eleven Pantanal's subregions, is known by its hundreds of alkaline-saline and freshwater lakes, salt-affected soils on a sandy plain, and its environmental heterogeneity, comprising a complex regional landform and hydrography (Ab'Sáber, 2011; de Oliveira; Pla-Pueyo; Hackney, 2019).

During the Quaternary, climatic and geomorphological changes have been responsible for altering the river dynamic and creating relict depositional landforms in Pantanal (Assine, 2015; Latrubesse *et al.*, 2005). One of these relict landforms are the alkaline-saline lakes of the lower Nhecolândia, which preserves their alkaline geochemical pattern since ~2,500 cal yrs BP (Rasbold *et al*., 2024). Recent studies have evidenced that the varying salinity of these lakes is the result of the effects of the Late Holocene complex hydroclimate variability and local geomorphological characteristics of the floodplains (Freitas et al., 2019, McGlue *et al*., 2017; Merdy *et al*., 2022, Rasbold *et al*., 2024).

The flooding regime in Pantanal is mainly caused by the increasing volume of the main regional rivers and tributaries, flat relief, and seasonal rainfall in the surrounding uplands (Boin *et al*., 2019). Terrestrial habitats expand during the dry season, and retract with flooding, which affect the relationships of aquatic and terrestrial communities, and, consequently, the richness of vegetation and productivity of the system (Alho, 2008; Ivory *et al*., 2019). Little variations in the soil moisture cause significant differences in the composition and distribution of the plant communities (Pott, 1981), making pedological studies very relevant for understanding the ecosystem dynamic of Pantanal.

The Pantanal soils exhibit distinct morphological and physical-chemical characteristics across various landscape units (Cardoso *et al*., 2016, 2011; Cunha, 1980; Ferreira-Júnior *et al*., 2016). These characteristics results from different pedogenetic processes,

such as gleization, salinization, solonization, plinthization, paludization, argilluviation, and podzolization, associated with the seasonal variations of the groundwater (Couto *et al*., 2023; Furquim; Vidoca, 2021). Soils are the result of complex interactions among various landscape components (geology, relief, climate, and organisms) over time (Jenny, 1941). Therefore, integrated soil-landscape studies are essential for understanding environmental dynamics. Furthermore, considering that the Nhecolândia wetland is a heterogeneous environment conditioned by water dynamics, a soil-landscape approach helps to provide a deeper understanding of the impacts of climatic and land use changes on ecosystems. It also serves as a valuable tool for effective terrestrial planning and management.

Nhecolândia is the second-largest subregion of the Pantanal, and its significant size contributes to the diversity of environments and soil characteristics found within it. However, most pedological studies in this subregion have been concentrated to the low Nhecolândia sector (Mato Grosso do Sul state), specifically at the Nhumirim Farm, property of the Brazilian Agricultural Research Corporation (EMBRAPA), and have focused on understanding the formation of the saline lakes. In this study, we aimed to characterize the soil-landscape relationships among all different landscape units of Nhecolândia, covering a broader sampling area and integrating vegetation and landforms relationships.

2.3 MATERIAL AND METHODS

2.3.1 Study area

The Brazillian Pantanal is located in the Upper Paraguai River Basin (UPRB), in the states of Mato Grosso and Mato Grosso do Sul. The Pantanal covers an area of 138.183 km² and was sub-divided into 11 sub-regions according to differences related to flood regime, relief, soil and vegetation (Silva; Abdon, 1998). The Nhecolândia covers an area of 26.921 km², and is in the southern portion of the Taquari megafan (Silva; Abdon, 1998). It is placed in the municipalities of Corumbá, Aquidauana and Rio Verde de Mato Grosso, in Mato Grosso do Sul state, ranging from the latitudes 18°12'52.76"S and 19°40'12.46"S, and the longitudes 54°52'39.21"W and 57°13'24.67"W (Figure 1).

The climate of the Pantanal is classified as Aw, according to the Köppen system, indicating a tropical continental climate with dry winter. In the Nhecolândia, the approximate annual average air temperature is 26 ºC and the average annual rainfall is 1206 mm (Garcia, 1984). The rainy season occurs between November and March, while the period of strong

pluvial deficit ranges from August to October (Garcia, 1984). The flooding season occurs from March to May (Garcia, 1984), and is mainly caused by local precipitation or groundwater elevation (Gradella; Quénol; Sakamoto, 2009; Padovani, 2010).

Figure 1 – Location map of the study area and the Nhecolândia landscape units: a) Freshwater lake – *Baías*; b) Saline-alkaline lakes – *Salinas*; c) Sandy ridges – *Cordilheira*; d) Seasonal floodable lowlands – *Vazantes*; e) Termite mounds – *Murundus*; f) Occasionally flooded grasslands – *Campo*.

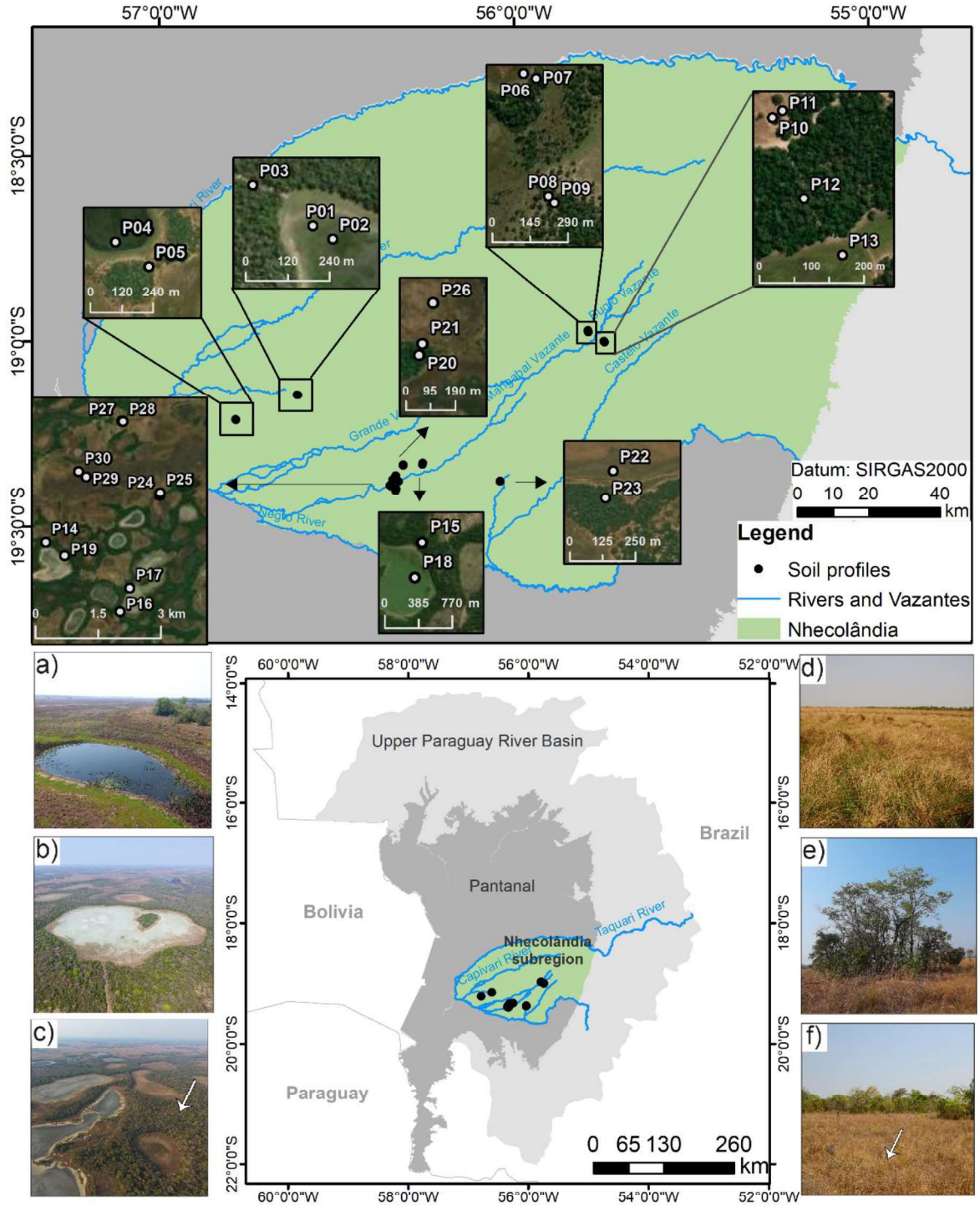

Source: The author.

The sedimentary lithology of the Pantanal consists of poorly consolidated fine- to coarse-grained sandstones, which form the Pantanal Formation (Godoi; Martins; Mello, 2001). The Pantanal depression is seismically active and was formed as a result of the uplift of the Central Andes (Ussami; Shiraiwa; Dominguez, 1999). The depression of the UPRB evolved into the Pantanal basin due to fluvial dissection, subsidence, and sedimentation processes during the Quaternary (Ab'Sáber, 2011; Assine, 2015). The upper areas of the UPRB, ranging from 200 to 1200 m above sea level, are remnants of the uplift of the Sul-Americana surface during the early Cenozoic, before the formation of the Pantanal basin, which ranges from 80 to 150 m above sea level (Alho, 2005a; Assine, 2015). The Nhecolândia is part of the abandoned fan lobe of the Taquari megafan, characterized by flat relief and low slope gradients, with more than 10,000 shallow lakes and extensive sandy dunes (Assine *et al*., 2015; Zani; Assine; Mcglue, 2012).

The Pantanal has a heterogenous landscape, shaped by the flooding regime. The landscape units of Nhecolândia, with typical regional designations, were based on the works of Ab'Sáber (2011), Brasil (1982), Calheiros and Fonseca Júnior (1996), and Valverde (1972).

The lakes can be differentiated into *Baías* and *Salinas*. The *Baías* (Figure 1a) are freshwater lakes, with varied size and depth, which can be temporary or permanent, and are influenced by the seasonal flooding, presenting a surface-groundwater connection (Furian *et al*., 2013). The *Salinas* (Figure 1b) are shallow saline or oligosaline lakes permanently isolated from the surface and subsurface drainage network. This is explained due to the presence of sandy ridges that surround the *Salinas* and the occurrence of a low permeable soil horizon that acts as a barrier for infiltration (Barbiero 2008; Furian *et al*., 2013; Furquim 2010a, 2010b).

The sandy levees surrounding the *Salinas* are called *Cordilheiras* (Figure 1c) and they are characterized by sandy and narrow elevations covered by cerrado vegetation (a vegetation type of the Cerrado biome). The formation of the *Cordilheiras* is associated with deflation and remobilization of fluvial sands from the Nhecolândia fan lobe in the arid early Holocene, which allowed the formation of depressions (the lakes) and complex marginal sand ridges (*Cordilheiras*) (McGlue *et al*., 2017).

The *Vazantes* (Figure 1d), also called floodable lowlands, are natural channels of intermitent rivers that connect the *Baías* during the high floods. They are wide and low areas, considered to be an aquatic-terrestrial transition zone (Calheiros; Fonseca Júnior, 1996). The *Murundus* (termite mounds; Figure 1e) are recognized as biogenic landforms created by the long-term pedoturbation by termites (Couto; Oliveira, 2010). They are widely distributed round

elevations (0.5-20 m in diameter, and 0.2 – 2.0 m high) covered by woody cerrado trees and shrubs (Eiten, 1972a; Ribeiro, Jose Felipe; Walter, 1998). The *Campos* (Figure 1f), grassy areas surrounding the *Murundus*, are covered by herbaceous vegetation and occasionally flooded during inundation season.

The Pantanal is a unique combination of the Brazilian biomes Cerrado (Savanna), Atlantic Forest, Amazon, and some fragments of Caatinga (Brazilian steppe vegetation). According to Pott *et al*. (2011), the Pantanal is considered a mosaic of formations, with gallery forests, palmlands, grasslands, savannas, grasslands and well-drained ridges. In the Pantanal depression there are 1863 phanerogam plant species listed and 250 species of aquatic plants (Alho, 2008). The fauna is biodiverse and composed by many species of birds, mammals, reptiles, amphibious, and fishes, which reflect the heterogeneity of the Pantanal environment (Guimarães *et al*., 2014).

The economic activities in Pantanal are associated with traditional cattle ranching, based on the native pasture, and tourism, and the main threat to the Pantanal conservation is associated with the erosion caused by the land use of the surrounding highlands (Pott; Pott, 2004).

2.3.2 Soil survey and vegetation description

The fieldwork occurred during the dry periods of 2016, 2019 and 2021. A total of 30 soil profiles were collected from the different landscape units of the Pantanal of Nhecolândia: five in the *Salinas*, six in the *Baías*, three in the *Vazantes*, ten in the *Cordilheiras*, three in the *Murundus*, and three in the *Campos*. Soil description followed Lemos and Santos (1996), and the classification was based on the Brazilian Soil Classification System (Santos *et al*., 2018) and the World Reference Base for Soil Resources (IUSS Working Group WRB, 2022). The vegetation covering each soil profile was described according to Pott and Pott (1994, 2000).

2.3.3 Physical and chemical analyses

Soil samples were air dried, crushed and passed through a 2 mm sieve, and submitted to physical and chemical analyses in the Routine Soil Fertility Laboratory of the Soil Department of the Federal University of Viçosa, Brazil, which follows standard methods described below (Silva *et al*., 2017). The standard pipette method was used for granulometric

analysis, obtaining coarse sand (2 - 0.2 mm), fine sand (0.2 - 0.05 mm), silt (0.05 - 0.002 mm) and clay (<0.002 mm) fractions.

The pH was measured in water and in 1 mol L^{-1} KCl 1:2.5 soil:solution. The available cations K and Na and P contents, and the micronutrients Cu, Mn, Fe and Zn were extracted by the Mehlich-1 method (HCl 0.05 mol L^{-1} and H_2SO_4 0.0125 mol L^{-1}). The determinations were done by photocolorimetry (P), flame photometry (Na and K) and atomic absorption spectroscopy (micronutrients). The exchangeable Ca^{2+}, Mg^{2+} and Al^{3+} (exchangeable acidity) were extracted by KCl 1 mol L^{-1} and determined by atomic absorption spectroscopy (Ca^{2+} and Mg^{2+}) and titration with 0.025 mol L^{-1} NaOH solution (Al^{3+}). The potencial acidity (H+Al) was obtained by a 0.5 mol L^{-1} calcium acetate solution buffered at 7 pH and determined by titration with 0.025 mol L^{-1} NaOH solution. The available S was extracted with a monocalcium phosphate in a 2 mol L^{-1} acetic acid solution and determined by photocolorimetry. The remaining phosphorous (P-Rem) was determined with a 0.01 mol L^{-1} $CaCl_2$ solution and by photocolorimetry. Total organic carbon (TOC) was obtained by the wet-combustion method (Yeomans; Bremner, 1988), using a 0.0667 mol L^{-1} potassium dichromate extraction reagent and titration with 0.102 mol L^{-1} ammonium iron (II) sulfate. From these analyzes, the bases sum (BS), effective cation exchange capacity (eCEC), potencial cation exchange capacity (pCEC), bases saturation (PBS), aluminum saturation index (Al_{sat}) sodium saturation index (Na-SI) were calculated.

The electrical conductivity (EC), soluble salts, and $CaCO_3$ equivalent analyzes were conducted following Teixeira *et al*. (2017). We extracted the soil solution of selected soil samples applying the saturated paste method. For some samples, we used the 1:1 soil-water extractions. Soil EC was measured using a benchtop conductivity measurement equipment. Soluble Ca^{2+} and Mg^{2+} were determined by atomic absorption spectroscopy and soluble Na^{+} and K^{+} were determined by flame photometry. Chlorates were determined by titration using a 0.05 mol L^{-1} $AgNO_3$ solution and 5% K_2CrO_4 as indicator. $CaCO_3$ equivalent (CCE) was determined by attacking the soil with excess of 0.5 mol L^{-1} HCl with a 0.25 mol L^{-1} NaOH solution. This procedure is not adjusted for Mg, K, or Na carbonates or organic matter which may be present.

Fe and Al content of amorphous oxides from selected samples of Podzols and Arenosols were extracted with ammonium oxalate (McKeague; Day, 1966) and determined by atomic absorption spectroscopy.

2.3.4 Statistical analyses

Physical and chemical attributes of the soil samples were used to perform the Principal Component Analysis (PCA), in order to identify the importance of the soil variables for each landscape unit and the correlation between them. The first two dimensions were selected for the analysis, once they explain the highest percentage of the variance of the dataset. The most important soil attributes were used in the non-parametric Kruskall-Wallis analysis and the post-hoc Dunn' test, considering a 5% probability value or less ($p \leq 0.05$). All of these statistical analyses were performed using the software R (R Core Team, 2024) and the following packages: stats for the PCA and Kruskal-Wallis analyses, and rstatix for the Dunn's test.

2.4 RESULTS

2.4.1 Vegetation description of the landscape units

The landscape units of the Pantanal of Nhecolândia presented two phytophysiognomies: i) forest, which comprises the *Cordilheira* and *murundu* units; and ii) the herbaceous field, which include the *Salinas*, *Baías*, *Vazantes*, and *Campos* units. Some *Salinas* (profiles 17 and 18) had bare soils.

On the well-drained *Cordilheiras*, where both semi-deciduous forest and savannah forest vegetation types occur, such as *Protium heptaphyllum* (Aubl.) Marchand (popular name: *Almacega*), *Attalea phalerata* (Mart.) ex Spreng (popular name: *Acuri* or *Bacuri*), *Emmotum nitens* (Benth.) Miers, *Casearia silvestris* Sw. (popular name: *chá-de-frade*), and *Qualea parviflora* Mart. (popular name: *pau-terra*). All these species are used as forage for cattle, except the *Emmotum nitens* (Benth.) Miers which have an ornamental use (Pott; Pott, 1994). The *Mouriri elliptica* Mart. (*coroa-de-frade*) predominate in the *Murundus* and *Elyonurus cf. muticus (*Spreng.) Kuntze (popularly known as *capim-carona*) was more frequent in the *Campos* environment, which occasionally experiences short flooding.

In the inundated environments, the herbaceous phytophysiognomy is composed by aquatic and terrestrial species. In the *Vazantes* environment, *Paspalum acuminatum* Raddi (popular name: *pastinho d'água*), *Bulbostylis* sp., and *Schizachyrium tenerum* Nees species occur, which are species tolerant to prolonged inundation periods. Surrounding the *Salinas*, *Paspalum vaginatum* Sw. (popular name: *grama-de-salina*), an amphibious grass, was dominant. In the *baía*, *Typha domingensis* Pers. (popular name: *taboa*) and

Eichhornia azurea (Sw.) Kunth (popular name: *camalote*), both aquatics, were the dominant species.

2.4.2 Soil morphological characterization

The *Salinas* environment is located at an average of 104.6 m of altitude, in average, having soils classified as Gleysols, Podzol, and Solonetz (Table 1). The soil colors varied from olive to olive gray, indicating reducing conditions and green micas, such as ferric illite (Table 2), as also observed by Furquim *et al.* (2010b). Soil texture varied between sandy to clay, associated with the semiconsolidated sandy-clay sedimentary substrate. These soils were the most structured of all soils with weak to moderate angular or subangular blocks. The dry and moist consistency were, respectively, very hard and very friable. The Gleysols presented few, fine, and distinct mottles. The Podzol presented abundant mottles and nodules in the B horizons (30% in the Bsc3, 40% in the Bsc2, and 50% in the Bsc1 horizons), and the Solonetz (soil profile 18) presented fine and irregular nodules between the A and E horizons. The Solonetz (soil profile 17) presented cementation, due to Na dispersion.

Soils of the *Baías* are located at 109 m of altitude, in average, and corresponded to Arenosols, Podzol, and Planosols (Table 1). They showed a very dark gray predominant color, which is related both to reduction conditions and organic matter accumulation (Table 2). Most soils are sandy and structureless, with single grain structure. The dry and moist consistencies were soft and very friable, respectively. The Planosol presented few mottles, and some Arenosols (soil profiles 6 and 26) presented common, medium and distinct-diffuse mottles. None of the profiles presented cementation.

Arenosols and the Podzol were the soils of the *Vazantes* landscape unit, located at an average altitude of 116 m (Table 1). Brown colors are predominant, due to organic matter influence (Table 2). Most soils are sandy and structureless, with loose and friable consistencies in dry and moist states, respectively. The Podzol (soil profile 29) presented Fe oxides cementation in the B horizon.

The soils of the *Cordilheiras* are Arenosols (Table 1), at a higher mean altitude (128 m). Main soil color was dark yellowish brown and structureless (Table 2). The dry and moist consistency were, respectively, loose and very friable. One Arenosol (P20) showed great clay content and subsurface cementation.

Further up, the *Murundus* soils are located at a mean altitude of 121.66 m, all Arenosols (Table 1), with a dark grayish brown color, loamy sandy texture, structureless, loose

and very friable, and without subsurface cementation (Table 2). The soils of the *Campos* were also classified as Arenosols, at slightly higher altitude 127 m) (Table 1). They are brown, sandy, and similar to the *Murundus* already described (Table 2).

Table 1 – Soil classes of the soil profiles collected in the Pantanal of Nhecolândia, according to the Brazillian Soil Classification System (SiBCS) and the International Soil Classification System (WRB/FAO).

Landscape unit	Soil Profile	Altitude (m)	SiBCS	WRB/FAO
Salinas	1	110	GLEISSOLO HÁPLICO Sódico típico hipocarbonático êutrico	Reductigleyic Eutric Gleysol (Clayic, Alcalic, Sideralic, Humic, Protospodic, Uterquic)
	2	106	GLEISSOLO HÁPLICO Sódico típico hipocarbonático	Reductigleyic Eutric Gleysol (Arenic, Alcalic, Ochric, Sodic, Uterquic)
	17	110	PLANOSSOLO NÁTRICO Órtico arênico	Albic Solonetz (Arenic, Differentic, Endic, Hypernatric)
	18	108	PLANOSSOLO NÁTRICO Sálico mésico hipocarbonático	Albic Nudinatric Protosalic Stagnic Gleyic Solonetz (Arenic, Differentic, Endic. Ochric, Hypernatric)
	19	89	ESPODOSSOLO FERRILÚVICO Hidromórfico arênico	Stagnic Gleyic Entic Podzol (Arenic, Epic, Eutric, Sideralic)
	Mean	104.6		
	SD*	8.88		
Baías	4	91	PLANOSSOLO HÁPLICO Eutrófico gleissólico solódico	Eutric Albic Gleyic Histic Planosol (Arenic, Alcalic, Sideralic, Humic, Sodic)
	6	129	NEOSSOLO QUARTZARÊNICO Hidromórfico típico	Dystric Brunic Arenosol (Ochric, Protoargic)
	21	106	ESPODOSSOLO HUMILÚVICO Hidromórfico arênico	Albic Podzol (Arenic, Epic, Eutric, Oxyaquic, Sideralic)
	22	113	NEOSSOLO QUARTZARÊNICO Hidromórfico típico	Eutric Sideralic Arenosol (Ochric, Claric)
	24	110	NEOSSOLO QUARTZARÊNICO Hidromórfico espodossólico	Eutric Sideralic Gleyic Brunic Arenosol (Humic, Claric, Protospodic)
	26	105	NEOSSOLO QUARTZARÊNICO Hidromórfico organossólico	Eutric Sideralic Brunic Gleyic Arenosol (Humic)
	Mean	109		
	SD*	12.38		
Vazantes	13	138	NEOSSOLO QUARTZARÊNICO Hidromórfico plintossólico	Dystric Sideralic Gleyic Arenosol (Ochric)

	29	103	ESPODOSSOLO FERRILÚVICO Hidromórfico arênico dúrico	Gleyic Histic Albic Ortsteinic Podzol (Arenic, Abruptic, Epic, Sideralic)
	30	107	NEOSSOLO QUARTZARÊNICO Órtico típico	Dystric Sideralic Arenosol (Ochric)
	Mean	116		
	SD*	19.15		
Cordilheiras	3	119	NEOSSOLO QUARTZARÊNICO Órtico típico	Dystric Sideralic Brunic Arenosol (Ochric, Claric)
	5	104	NEOSSOLO QUARTZARÊNICO Órtico gleissólico	Eutric Sideralic Brunic Arenosol (Ochric, Claric)
	7	137	NEOSSOLO QUARTZARÊNICO Órtico típico	Eutric Sideralic Brunic Arenosol (Ochric, Rubic)
	12	146	NEOSSOLO QUARTZARÊNICO Órtico típico	Dystric Sideralic Brunic Arenosol (Ochric)
	14	175	NEOSSOLO QUARTZARÊNICO Órtico típico	Eutric Sideralic Brunic Arenosol (Ochric)
	15	117	NEOSSOLO QUARTZARÊNICO Órtico típico	Dystric Sideralic Brunic Arenosol (Ochric)
	16	139	NEOSSOLO QUARTZARÊNICO Órtico típico	Dystric Sideralic Brunic Arenosol (Ochric)
	20	114	PLANOSSOLO HÁPLICO Eutrófico solódico espessarênico	Eutric Sideralic Brunic Arenosol (Ochric, Protoargic, Claric, Protospodic)
	23	120	NEOSSOLO QUARTZARÊNICO Órtico típico	Dystric Sideralic Brunic Arenosol (Ochric)
	25	112	NEOSSOLO QUARTZARÊNICO Órtico gleissólico	Eutric Sideralic Gleyic Brunic Arenosol (Ochric)
	Mean	128		
	SD*	21.15		
Murundus	8	134	NEOSSOLO QUARTZARÊNICO Órtico típico	Dystric Sideralic Brunic Arenosol (Ochric, Isopteric Claric)
	10	123	NEOSSOLO QUARTZARÊNICO Órtico típico	Dystric Brunic Arenosol (Humic, Isopteric, Claric)
	28	108	NEOSSOLO QUARTZARÊNICO Órtico típico	Dystric Brunic Arenosol (Ochric, Isopteric)
	Mean	121.66		
	SD*	13.05		

Campos	9	139	NEOSSOLO QUARTZARÊNICO Órtico típico	Eutric Sideralic Brunic Arenosol (Ochric)
	11	136	NEOSSOLO QUARTZARÊNICO Órtico típico	Dystric Sideralic Brunic Arenosol (Ochric, Claric)
	27	106	NEOSSOLO QUARTZARÊNICO Órtico gleissólico	Dystric Sideralic Brunic Arenosol (Ochric)
	Mean	127		
	SD*	18.25		

Source: The author.
Note: *SD – standard deviation.

Table 2 – Predominant soil morphological attributes in each soil profile of the landscape units.

Landscape unit	Soil Profile	Altitude (m)	Color (moist)		Texture	Structure(1) (grade/size/type)	Consistency(2) (dry/moist)	Cementation(3)
Salinas	1	110	5Y 4/2	Olive gray	Clay	st/f-m/pr	vh/fi	nc
	2	106	2,5Y 5/2	Olive gray	Sandy	sg	vh/vfr-fr	nc
	17	110	5Y 5/3	Olive	Loamy sandy	w/f-m/abk	vh/fi	wc
	18	108	5Y 5/2	Olive gray	Loamy sandy	w/m-co/sbk	so/vfr	nc
	19	89	5Y 5/2	Olive gray	Sandy	sg	l/vfr	nc
Baías	4	91	5Y 3/1	Very dark gray	Sandy	sg	so/vfr	nc
	6	129	10YR 5/3	Brown	Sandy	sg	l/fr	nc
	21	106	2,5YR 2,5/1	Reddish black	Sandy	sg	so/vfr	nc
	22	113	2,5YR 5/2	Weak red	Sandy	sg	so/vfr	nc
	24	110	2,5Y 3/1	Very dark gray	Loamy sandy	sg	so/vfr	nc
	26	105	10YR 4/3	Brown	Sandy	sg	l/vfr	nc
Vazantes	13	138	10YR 6/4	Light yellowish brown	Sandy	sg	so/fr	nc
	29	103	7,5YR 4/6	Brown	Loamy sandy	sg	l/vfr	mc
	30	107	7,5YR 3/2	Dark brown	Sandy	sg	l/fr	nc
Cordilheiras	3	119	10YR 5/3	Brown	Sandy	sg	l/fr-vfr	nc
	5	104	10YR 5/3	Brown	Sandy	sg	l/vfr	nc
	7	137	10YR 4/4	Dark yellowish brown	Sandy	sg	l/vfr	nc
	12	146	10YR 5/3	Brown	Sandy	sg	l/vfr	nc
	14	175	10YR 3/3	Dark Brown	Sandy	sg	l/vfr	nc
	15	117	10YR 4/4	Dark yellowish brown	Sandy	sg	so/vfr	nc

	16	139	10YR 4/4	Dark yellowish brown	Sandy	sg	l/vfr	nc
	20	114	2,5Y 4/2	Dark grayish brown	Sandy	sg	l/vfr	wc
	23	120	10YR 6/6	Brownish yellow	Sandy	sg	l/vfr	nc
	25	112	2,5Y 5/3	Light olive brown	Sandy	sg	l/vfr	nc
Murundus	8	134	10YR 4/2	Dark grayish brown	Loamy sandy	sg	l/vfr	nc
	10	123	10YR 3/2	Dark grayish brown	Loamy sandy	sg	l/vfr	nc
	28	108	7,5YR 4/2	Brown	Sandy	sg	l/vfr	nc
Campos	9	139	10YR 4/2	Dark grayish brown	Sandy	sg	l/vfr	nc
	11	136	10YR 5/3	Brown	Sandy	sg	l/vfr	nc
	27	106	7,5YR 4/3	Brown	Sandy	sg	l/vfr	nc

Source: The author.
Note: (1) w – weak; st: strong; f – fine; m – medium; co – coarse; abk – angular blocky; sbk – subangular blocky; sg – single grain; pr – prismatic.
(2) l – loose; so – soft; vfr – very friable; fr – friable; vh – very hard; fi – firm;
(3) nc – non-cemented; wc – weakly cemented; mc – moderately cemented.

2.4.3 Soil physico-chemical and mineralogical characterization

The first two dimensions (Dim 1 and Dim2) explained 53.74% of the total data variance (Figure 2). The Dim1 explained 37% and the variables that most contributed to explain the data variance were $_{e}$CEC, clay, K, Ca^{2+}, Na, P-Rem, water pH, silt, PBS, NaSI and Mg^{2+}. The Dim2 explained 16.8%, and was influenced mainly by H+Al, TOC, Zn, Fe, water pH, PBS, Cu, and silt. The variables that better explained the soils of the *Salinas* was related with salt accumulation, such as, PBS, $_{e}$CEC, water pH, and clay contents. The TOC, H+Al, Zn, and Fe were the most important variables to explain the variance of the *Baías* soils and H+Al, and Zn were most important for the *Vazantes*. Both pedoenvironments are influenced by flooding, which favors organic matter accumulation. The *Cordilheiras* soils were influenced by P-Rem, and coarse and fine sand, indicating a very low P retention due to a sandy texture. The soils of the *murundu* and *campo* are better explained by Al^{3+}, Al_{sat} and coarse and fine sand contents.

Figure 2 – Principal component analysis of the physical and chemical attributes of the soil samples of the landscape units of the Nhecolândia subregion.

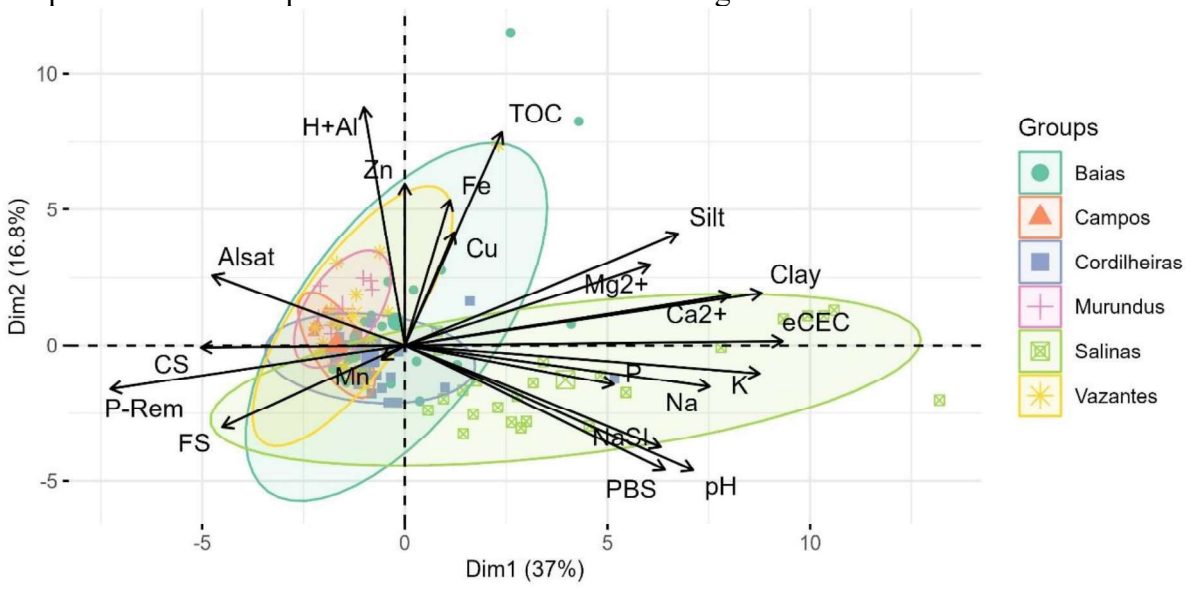

Source: The author.
Note: Al_{sat} – Al saturation; CS – coarse sand; Cu, Zn, Fe, and Mn – microelements; FS – fine sand; eCEC – exchangeable cation exchange capacity; H+Al – potential acidity; Mg^{2+}, Ca^{2+}, Na^{+}, and K^{+} – exchangeable cations; NaSI – Na saturation index; $_{p}CEC$ – potential cation exchange capacity; P – available P; P-Rem - remaining phosphorous; TOC – total organic carbon.

In relation to soil granulometry, the *Murundus* and *Campos* soil were similar with reference to the coarse sand fraction (Table 3), presenting the highest mean values (416.1 and 478.7 g kg^{-1}, respectively) (Figure 4). Regarding the fine sand fraction, the *Vazantes*, *Cordilheiras* and *Baías* presented the higher contents (642.2, 650.9, and 616.6 g kg^{-1}, respectively). The *Salinas* soils presented the highest clay content (mean of 212.7 g kg^{-1}), contrasting with all other environments. The *Baías* and *Vazantes* have varying clay contents.

The *Salinas* have the most alkaline and eutric soils, with significant differences in water pH, P, Na, Ca^{2+}, BS, PBS, and NaSI in relation to the other soil groups (Table 3), presenting the highest values (Figure 4). On the other hand, the *Murundus*, *Campos*, and *Vazantes* presented the most acidic (mean pH of 4.43, 5.1, and 5.07, respectively) and dystric soils (mean PBS of 10, 35.5 and 15%, respectively), associated with high Al^{3+} (mean of 0.76, 0.35, and 0.47 $cmol_c\ kg^{-1}$, respectively), and Al_{sat} (mean of 74.1, 70.4, and 58.4%, respectively). The statistical differences according to the TOC, Zn, and Cu values were non-significant among the landscape units. In the case of the TOC, the *Baías*, *Murundus* and *Vazantes* soils presented the highest mean values (1.05, 1.03, and 0.6% respectively), with a *Baías* surface horizon reaching 11.3%, representing a Histic epipedon. The H+Al contents were also higher for the *Baías, Murundus and Vazantes* soils (1.9, 2.6, and 1.8 $cmol_c\ kg^{-1}$, respectively). The Fe content

was higher in the *Baías*, *Salinas*, and *Vazantes* soils (mean of 241.9, 132.7, and 95.2 mg kg^{-1}, respectively) mainly due to reducing conditions.

Table 3 – Kruskal-Wallis (KW) and Dunn test results for comparing the physical and chemical soil attributes of the Pantanal of Nhecolândia landscape units. Significance level of 5% ($p \leq 0.05$). $^{*}P < 0.05$, $^{**}P < 0.01$ and $^{***}P < 0.001$.

Soil attribute	KW	*Salinas*	*Baías*	*Cordilheiras*	*Campos*	*Vazantes*	*Murundus*
TOC	ns	a	a	a	a	a	a
Zn	ns	a	a	a	a	a	a
Cu	ns	a	a	a	a	a	a
Mg^{2+}	**	ab	a	a	ab	b	ab
CS	***	c	c	bc	a	c	ab
FS	***	ab	a	a	b	a	b
Silt	***	ab	a	b	b	a	ab
Clay	***	a	b	b	b	b	ab
Water pH	***	a	bd	b	cd	bcd	c
P	***	a	c	ab	bc	c	bc
K^{+}	***	a	b	b	b	b	ab
Na^{+}	***	a	c	bc	b	bc	bc
Ca^{2+}	***	a	ab	b	c	c	c
Al^{3+}	***	c	bc	cd	ab	ab	a
H+Al	***	c	ab	b	bc	ab	a
BS	***	a	b	b	bc	c	bc
pCEC	***	a	b	b	b	b	ab
eCEC	***	a	b	b	b	b	ab
PBS	***	a	b	b	bc	c	c
Alsat	***	c	bc	b	a	a	a
NaSI	***	a	c	bc	b	bc	bc
P-Rem	***	b	a	a	a	a	ab
Mn	***	a	ab	ab	c	bc	abc
Fe	***	ac	b	ac	c	ab	abc

Note: Al^{3+} – exchangeable acidity; Al_{sat} – Al saturation; BS – base sum; CS – coarse sand; Zn, Cu, Fe, and Mn – microelements; FS – fine sand; eCEC – exchangeable cation exchange capacity; H+Al – potential acidity; Mg^{2+}, Ca^{2+}, Na^{+}, and K^{+} – exchangeable cations; NaSI – Na saturation index; $_{p}$CEC – potential cation exchange capacity; P – available P; PBS – percentage of base saturation P-Rem - remaining phosphorous; TOC – total organic carbon.

Figure 4 – Box plots of selected physical and chemical attributes of the soil landscape units of the Nhecolândia subregion.

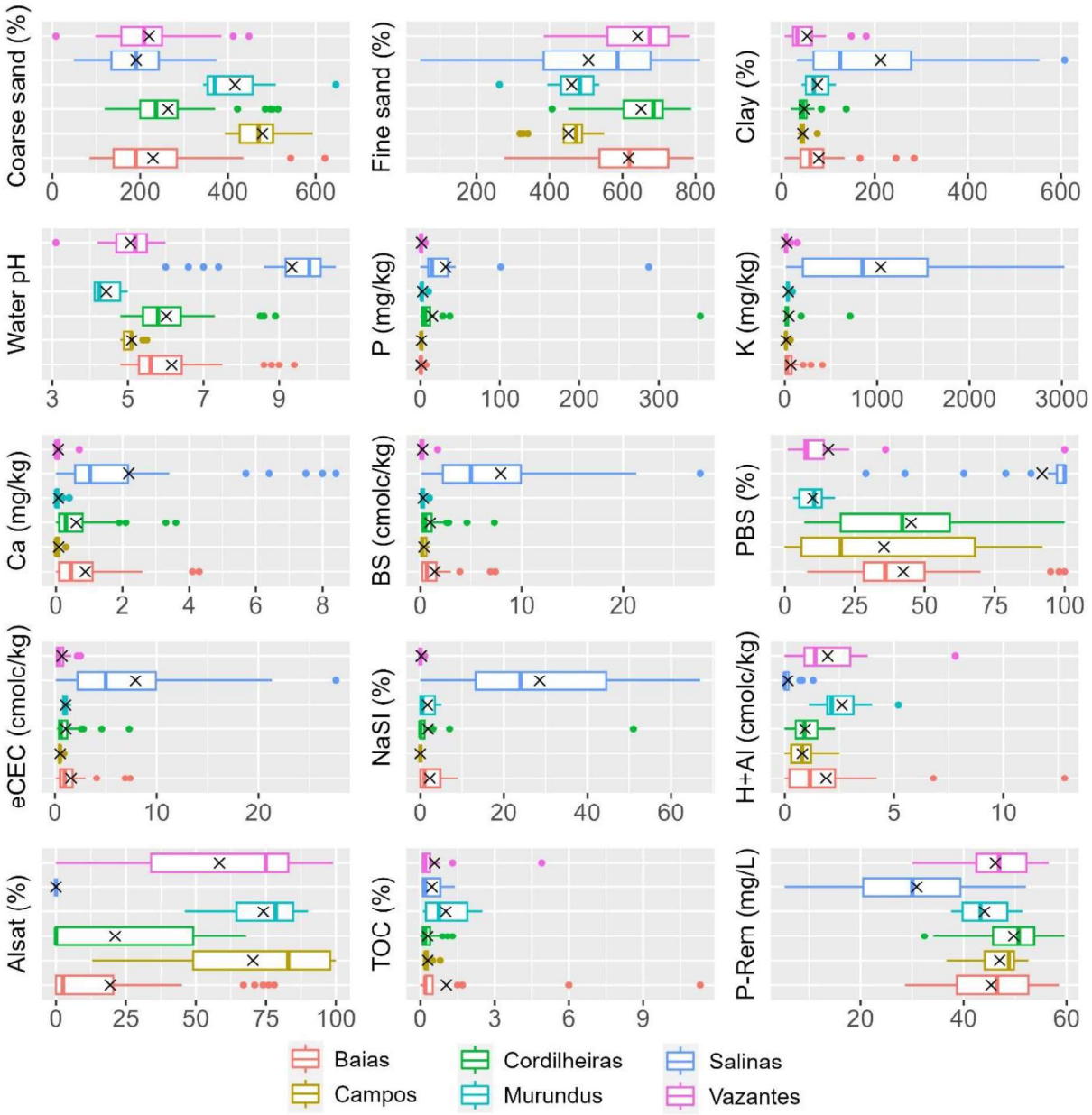

Source: The author.
Note: Al_{sat} – Al saturation; BS – base sum; eCEC – exchangeable cation exchange capacity; H+Al – potential acidity; Ca^{2+}, and K^{+} – exchangeable cations; NaSI – Na saturation index; P – available P; PBS – percentage of base saturation P-Rem - remaining phosphorous; TOC – total organic carbon.

In relation to the soluble salts of the soils of the *Salinas*, the Solonetz (soil profile 18) exhibits an EC greater than 7 dS m^{-1}, indicating a salic character (as defined by the SiBCS) and the highest water pH values, driven by higher concentrations of all soluble salt ions except Cl^{-} (Table 4). Another Solonetz (soil profile 17) also presented a high water pH, mainly due to elevated Na^{+} and HCO_3^{-} concentrations. The Podzol (soil profile 19) displays an EC greater than 4 dS m^{-1} at the surface, attributed to high levels of Ca^{2+}, Mg^{2+}, Cl^{-}, CO_3^{2-}, HCO_3^{-}, and

$CaCO_3$, giving it a saline character. The water pH values of the Gleysols showed little variation throughout the profiles and were mainly influenced by Ca^{2+}, Mg^{2+}, HCO_3^-, and $CaCO_3$.

Table 4 – Soluble salts and $CaCO_3$ equivalent contents of the soils of the *Salinas* and one soil of *Cordilheira* (P20).

Horizon/ Depth	Water pH	CE	Ca^{2+}	Mg^{2+}	K^+	Na^+	Cl^-	$CO3^{2-}$	HCO_3^-	CCE
cm		dS m^{-1}	---------- $cmol_c$ kg^{-1} ----------				--------- $cmol_c$ L^{-1} --------			g kg^{-1}
P1 - Reductigleyic Eutric Gleysol (Clayic, Alcalic, Sideralic, Humic, Protosodic, Uterquic)										
An (0-11)	9.09	0.89	461.1	594.91	0.40	0.95	0.20	0.20	10.75	77.82
ABgn (11-23)	9.12	1.19	252.7	145.12	0.38	1.30	0.19	0	12.90	49.04
Bgn1 (23-57)	9.35	0.70	267.8	285.43	0.22	0.73	1.95	0.38	8.45	96.51
Bgn2 (57-88)	9.43	0.80	351.7	522.71	0.27	0.86	0.95	0	10.70	94.96
Cn (88-110+)	9.09	0.95	54.9	127.68	0.07	0.17	-	0	10.80	18.85
Mean	9.35	0.89	267.84	285.43	0.27	0.86	0.57	0.00	10.75	77.82
SD	0.35	0.18	149.54	214.64	0.13	0.41	0.83	0.17	1.57	33.20
P2 - Reductigleyic Eutric Gleysol (Arenic, Alcalic, Ochric, Sodic, Uterquic)										
An1 (0-9)	9.35	1.21	272.9	110.19	0.40	1.20	0.20	0.50	12.40	60.68
An2 (9-16)	9.46	0.71	223.3	200.21	0.24	0.78	0.10	0.18	8.05	46.15
Bsgn (16-29)	9.69	0.95	105.6	641.11	0.16	0.24	0.19	0.10	10.60	17.43
Cg (29-70+)	9.63	0.76	55.0	370.41	0.09	0.13	0.34	0	8.00	24.27
Mean	9.53	0.91	164.20	330.48	0.22	0.59	0.21	0.19	9.76	37.13
SD	0.16	0.23	101.13	233.51	0.13	0.50	0.10	0.22	2.14	19.91
P17 - Albic Solonetz (Arenic, Differentic, Endic, Hypernatric)										
An (0-6)	10.3	3.91	33.6	5.58	0.12	0.92	0.49	3.45	25.70	24.28
2An (6-15)	10	2.18	60.0	14.93	0.10	0.70	0.29	0.90	20.40	28.23
E1 (15-50)	10.3	3.58	9.1	4.35	0.07	0.95	0.44	5.35	30.34	27.77
E2 (50-90)	10.3	3.16	7.6	15.14	0.07	0.79	0.44	3.10	28.40	27.96
Btn (90+)	10.2	3.93	7.8	4.42	0.10	1.09	0.69	2.48	35.04	33.91
Mean	10.22	3.35	23.62	8.88	0.09	0.89	0.47	3.06	27.98	28.43
SD	0.13	0.73	23.12	5.64	0.02	0.15	0.14	1.61	5.44	3.46
P18 - Albic Nudinatric Protosalic Stagnic Gleyic Solonetz (Arenic, Differentic, Endic. Ochric, Hypernatric)										
Agn1 (0-16)	10.3	8.46	100.4	19.98	1.12	4.94	0.29	7.65	41.70	110.47
A2g (16-27)	9.85	2.01	-	-	-	-	-	-	-	103.72
Cg (27-60)	10	2.01	62.4	13.10	0.08	0.45	0.44	2.50	18.10	37.21
Btg1 (60-90)	10	0.96	231.4	84.52	0.29	1.12	0.15	0.58	8.90	41.80
Btg2 (90-106)	10.05	1.16	211.3	69.19	0.50	1.42	0.17	0.45	12.50	48.10
Btg3 (106-128)	10.07	1.76	696.4	510.62	1.05	1.72	-	0.50	15.80	39.68
Mean	10.05	2.73	260.38	139.48	0.61	1.93	0.26	2.34	19.40	63.50
SD	0.15	2.84	254.05	209.73	0.46	1.75	0.13	3.09	12.94	34.03
P19 - Stagnic Gleyic Entic Podzol (Arenic, Epic, Eutric, Sideralic)										
A1 (0-5)	8.55	4.37	304.0	114.34	0.19	0.96	0.82	0.45	15.35	36.99
A2 (5-10)	7.44	0.51	44.6	43.14	0.03	0.07	0.29	0.00	1.90	20.56
Bsc1 (10-28)	7.03	0.10	92.9	497.35	0.17	0.05	0.05	0	0.60	32.06
Bsc2 (28-48)	6.56	0.11	4.5	4.21	0.01	0.01	0.05	0	0.30	32.78
Bsc3 (48-70)	5.95	0.15	0.4	3.27	0.00	0.00	0.05	0	0.10	31.76
Mean	7.11	1.05	89.28	132.46	0.08	0.22	0.25	0.09	3.65	30.83
SD	0.98	1.86	125.72	208.92	0.09	0.42	0.34	0.20	6.58	6.11
P20 - Eutric Sideralic Brunic Arenosol (Ochric, Protoargic, Claric, Protospodic)										
AE (0-36)	7.26	0.21	33.22	28.19	0	0.00	0.09	0	0	33.17
E (36-53)	8.45	0.21	84.32	14.11	0	0.00	0.09	0	1.4	33.47
Bh (53-96)	8.6	0.48	67.92	42.46	0.03	0.04	0.09	0	3.3	32.90
Bsk (96-107)	8.93	0.59	44.71	52.54	0.03	0.14	0.09	0	5.3	42.83

Mean	8.10	0.36	57.54	34.32	0.02	0.05	0.09	0	2.50	35.21
SD	0.79	0.17	22.96	16.77	0.01	0.06	0.00	0	2.31	4.27

Note: SD - Standard deviation.

Concerning the Fe and Al contents from oxides, the Podzols of the *Salinas* and the *Vazantes* presented higher Fe (Fe_d and Fe_o) than the Podzol of the *Baías* (Table 5). On the other hand, the Podzol of the *Baías* and the Arenosol of the *Cordilheiras* presented higher Al (Al_d and Al_o) and Al_o/Al_d contents. The *Baías* also presented higher Fe_o/Fe_d, because reduction conditions favor the solubilization of Fe^{2+}.

Table 5 – Fe and Al extracted by Dithionite-Citrate-Bicarbonate (Fe_d and Al_d) and Ammonium Oxalate (Feo and Alo) of Podzols and one Arenosol (P20) of the Pantanal of Nhecolândia.

Profile	Horizon	Depth cm	Fe_d	Fe_o	Al_d	Al_o
			---------- g kg^{-1} ----------			
			Salina			
19	1A	0-5	5.70	2.5	0	2.13
	A2	5-10	8.37	4.71	0	0.99
	Bsc1	10-28	16.93	7.26	0	1.46
	Bsc2	28-48	9.72	1.82	0	1.56
	Bsc3	48-70+	1.90	1.19	0	1.61
			Cordilheira			
20	A	0-36	0.59	0.34	0	1.61
	AE	36-53	0.29	0.14	0.27	1.79
	E	53-96	0.49	0.05	0.23	1.42
	Bt	96-107	0.17	0.17	0.05	2.03
	Btnqx	107-110	0.88	0.34	0.17	3.07
			Baía			
21	A	0-5	1.64	1.39	0.43	2.55
	E	5-13	0.37	0.49	0.15	2.69
	Bh	13-29	0.31	0.48	0.09	3.12
	C	29-60	0.05	0.13	0.01	2.50
			Vazante			
29	A	0-14	1.49	1.17	0.65	1.02
	2A	14-23	0.90	0.76	0.16	0.31
	2AE	23-29	0.59	0.32	0.07	0.07
	2E	29/48-48/65	0.25	0.07	0.00	0.07
	2Bsm1	45/53-53-63	19.89	3.03	0.11	0.02
	2Bsm2	65/67-73/76	11.55	6.32	0.02	0.25
	2Cg1	76-94	3.92	1.02	0.05	0.08
	2Cg2	94+	0.97	0.49	0.07	0.22

2.4.4 Soil classification

The soil classes, as defined by the WRB/FAO international classification system and observed, included: Arenosol (22 soil profiles), Podzol (3), Gleysol (2), Planosol (1), and

Solonetz (2). According to the SiBCS, these soils were classified as follows: Neossolo Quartzarênico (21 soil profiles), Espodossolo (3), Planossolo (4), and Gleissolo (2) (Table 1).

The Arenosols (Figure 6a, f, and g) are sandy soils with minimum pedological development (IUSS Working Group WRB, 2014). This class was found in all soil profiles described under *Murundus* and *Campos* but is also the main soil on *Cordilheiras*. Some Baía and Vazante soil profiles were also classified as Arenosols. The main qualifiers associated with the Arenosols were Brunic (18 soil profiles), Sideralic (18), Gleyic (5), Dystric (13), and Eutric (8). The Brunic and Sideralic qualifiers occur at the *Cordilheiras*, *Baías*, *Murundus*, *Campos*, and *Vazantes*, indicating, respectively, little pedogenetic alteration and low pCEC. The Gleyic qualifier occur in the *Vazantes*, *Baías*, and *Cordilheiras* soils, which indicates reducing conditions due to waterlogging. Most of the Arenosols were Dystric, presenting higher exchangeable Al than base cations in their exchange complex. On the other hand, Eutric Arenosols were found in the *Cordilheiras* and *Baías* soils.

The Podzols (Figure 6b) are soils with subsurface accumulation of organic matter and/or Fe and Al oxides in subsurface (IUSS Working Group WRB, 2014, supplementary material). They occurred at the *Salinas* (P19), *Baías* (P21) and *Vazantes* (P29) landscape units, and the main qualifiers associated were Albic (1 soil profile), Entic (1), and Ortsteinic (1). Some Arenosols in the *Cordilheiras* (P20) and *Baías* (P24) presented a Protospodic qualifier, due to evidence of podzolization. The Albic Podzols occurred at the *Baías* and *Vazantes*, and it indicates the presence of albic horizon, a horizon from which organic matter and/or Fe oxides have been removed. The Entic Podzol occurred at the *Salinas* and indicates a soil with no albic material. The Ortsteinic Podzol occur at the *Vazantes* and it showed cementation in a subsurface horizon.

The Gleysols (Figure 6c) are soils affected by the variations of the groundwater level and show gleyic properties, due to Fe reduction in an anaerobic condition (IUSS Working Group WRB, 2014). The Gleysols occurred at the *Salinas* and presented the Reductigleyic (2 soil profiles) and Eutric (2) qualifiers, which indicate gleyic properties and base cations accumulation, respectively. Both Gleysols presented hypocarbonatic character, according to the SiBCS.

The Planosol (Figure 6d) are soils characterized for having an abrupt texture difference in a subsurface horizon (IUSS Working Group WRB, 2014). We found one Planosol profile at the baía landscape unit, which presented the Histic qualifier, due to the occurrence of a histic horizon, and the Gleyic, Albic and Eutric qualifiers, defined above. The Solonetz (Figure 6e, 2 soil profiles) are also soils characterized by having a distinctly high clay content in a subsurface

horizon as the Planosols, but they differ by having high content of exchangeable Na. Solonetz soil profiles presented Albic qualifier. One Solonetz (soil profile 18) presented hypocarbonatic character, according to the SiBCS.

Figure 6 – Main representative soil classes (WRB/FAO) of the Pantanal of Nhecolândia: a) Arenosol (soil profile 23) at the *Cordilheiras*; b) Podzol (soil profile 29) at *Vazantes*; c) Gleysol (soil profile 1) at the *Salinas*; d) Planosol (soil profile 4) at the *Baías*; e) Solonetz (17) at the *Salinas*; f) Arenosol (28) at the *Murundus*, g) Arenosol (11) at the *Campos*.

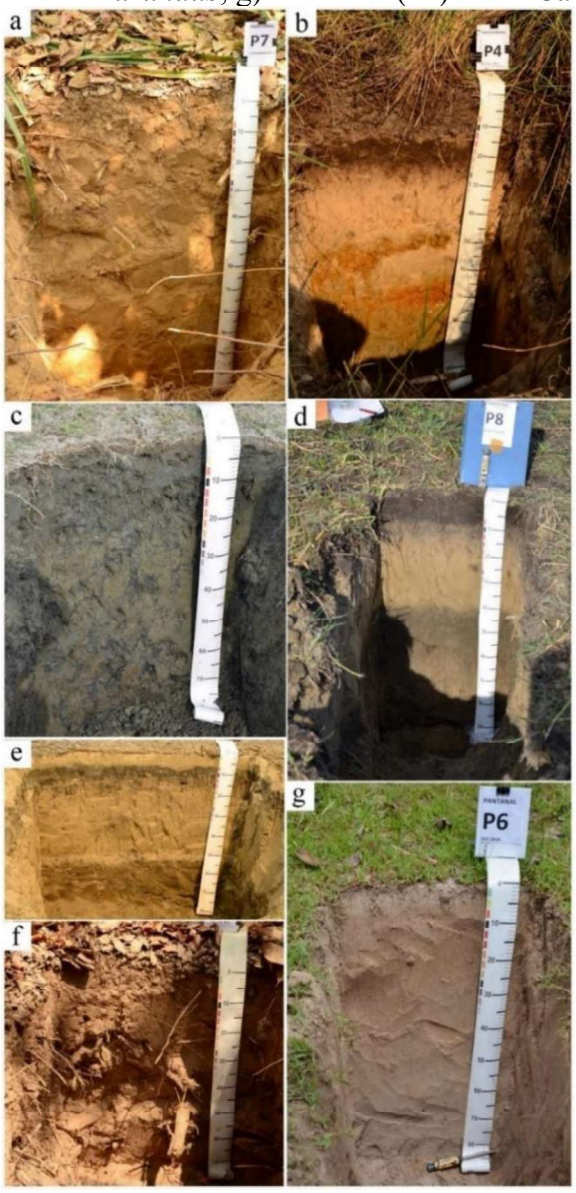

Source: The author.

2.5 DISCUSSION

The Pantanal represents a very complex landscape, whose distribution and functioning of its subsystems are entirely associated with hydrological and pedogeomorphological processes. In an attempt of classify the habitats of the Pantanal, Nunes da Cunha and Junk (2011) proposed a classification system considering the interplay of climate, hydrology, physical and chemical properties of water and soil, and floristic as key factors for understanding the landscape structure and functioning. The Nhecolândia subregion is part of this complex mosaic, with a peculiarity of having high-salinity lakes and soils, while the rest of the Pantanal have low to intermediate content of mineral salts and a pH of 5-7.

The Taquari megafan has two giant sandy lobes, Nhecolândia lakes region corresponds to the oldest one (Zani; Luis Assine; Mcglue, 2012). The lakes region has a regionally flat relief with little negligible slope. Different vegetational formations vary according to subtly watertable variations, with tree predominating in the flood-free areas and the grasslands on the lower areas, affected by seasonal inundation. As a product of pedogenetic processes acting over the unconsolidated sediments of the Pantanal Geological Formation, soils are mainly sandy, with the Arenosols/Neossolos Quartzarênicos (WRB/SiBCS, respectively) being the most frequent soil classes, occurring at most of the landscape units (Figure 7), regardless of the vegetation cover. This implies the water table is more important than texture in controlling the plant communities (Ferreira-Júnior *et al*., 2016a).

Figure 7 – Diagram of the topographic variation, main soil classes, and vegetation types of the Nhecolândia landscape units.

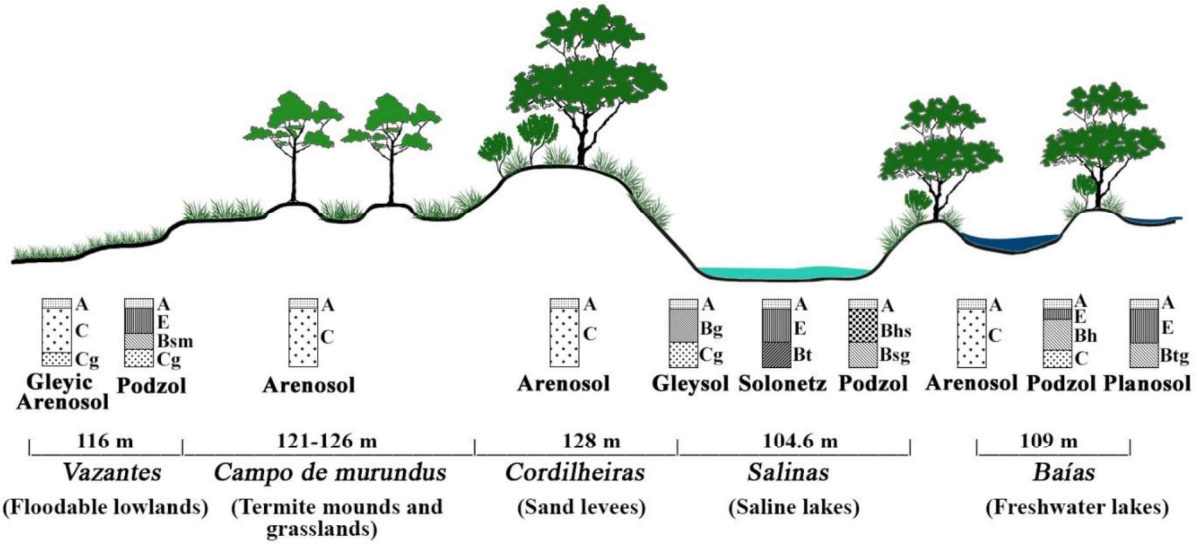

Source: The author.

2.5.1 The lakes: *Salinas* and *Baías*

The lakes are the most distinctive features of the Nhecolândia landscape. They have been widely studied in order to understand their characteristics, formation, and hydrological processes. A negative hydric balance is widespread in the Pantanal, which has average annual precipitation and potential evaporation of 1,100 and 1,400 mm on average, respectively (Alho 2008). However, beyond evaporation, the hydrogeochemical differences between *Salinas* and *Baías* are largely attributed to pedological and geomorphological factors (Barbiero *et al*., 2002, 2008; Bergier *et al*., 2014; Costa-Silva *et al*., 2024; Freitas et al., 2019; Furian *et al*., 2013; Furquim *et al*., 2008, 2010a, 2010b, 2017b; Merdy *et al*., 2022).

The salinity of the *Salinas* is related to the presence of adjacent *Cordilheiras*, which serves as barriers to surface water flow, and low permeability subsurface horizons that limit groundwater inflow (Barbiero *et al*., 2008, Furian *et al*., 2013, Merdy *et al*., 2022). In the case of the *Baías*, they may or may not be surrounded by *Cordilheiras*, but they are connected to the surface water and groundwater dynamic. The absence of the low permeability subsurface horizon favors the leaching of labile elements through deep drainage or groundwater flushing, so the ionic concentration effect in the *Baías* is not as pronounced as it is in the *Salinas* (Barbiero *et al*., 2008; Costa-Silva *et al*., 2024, Freitas *et al*., 2019).

The *Salinas* and *Baías* were the most pedodiverse environments in the Nhecolândia landscape, with the *Salinas* presenting a higher clay content. This is favored by clay formation through two processes: the transformation of micas into smectites, such as ferribeidellite, in the upper zone of the *Salinas*), and saponite or stevensite, in the lower zone (Furquim *et al*., 2008); and neoformation of micas, through precipitation from Si and K enriched waters (Furquim *et al*., 2010a). This last process is enabled by salt precipitation from nutrient-rich soil solutions combined with the presence of Si-rich amorphous material, which has been verified by many authors in the Nhecolândia soils (Barbiero *et al*., 2008; Dias *et al*., 2020; Furquim *et al*., 2010a; 2010b).

Salt accumulation in the *Salinas* favored soil pH values higher than 9, with some horizons reaching 10.3 in the Solonetz profiles. Although Solonetz (sodic soils) are more common in the southern portion of the Pantanal (Amaral Filho, 1986), at Nhecolândia, however, they were observed associated with alkaline-saline lakes (Furquim; Vidoca, 2021). The Solonetz derives from saline soils through the solonization process, which evolves the leaching of the most soluble salts and the permanence of Na^+, and/or the precipitation of Ca^{2+} and Mg^{2+} minerals, with an increase of Na^+ in soil (Furquim *et al*., 2017; Schaetzl; Anderson, 2005).

Besides salt accumulation, podzolization was also observed, with a significant increase in oxalate-extractable Fe content in the spodic horizon. However, dithionite-extractable Fe levels were higher than oxalate-extractable Fe, indicating the presence of crystalline Fe oxides. In the *Salinas*, Fe prevails over Al in forming metal-organic complexes, likely due to reducing conditions, as also observed by Menezes (2021) for Podzols in the Nhecolândia.

Soil sampling was done in the dry season and the *Salinas* were totally dry and bare. In the center of some *Salinas*, vegetation was absent, whereas in the border of some there was a grassy cover of Poaceae. In general, in most *Salinas* predominate algae and cyanobacteria mats (Bergier; Krusche; Guérin, 2014; Guerreiro *et al*., 2019). Studies have highlighted that the saline-alkaline lakes of Nhecolândia functions as CO_2 and N_2O net sink, and a CH_4 net source, with variations that depends on the magnitude of phytoplankton bloom (Barbiero *et al*., 2018; Bergier; Krusche; Guérin, 2014). Full conservation of the *Salinas* is also important for the cattle ranchers, since these environments provide a natural source of salts and minerals to supplement the cattle diet, favoring a cattle-raising sustainable beef production (Guerreiro *et al*., 2019).

In the *Baías* environments, the prolonged period of water saturation, enhances organic matter accumulation and Fe solubilization. The organic matter influence is evidenced by the dark colors, higher TOC content on surface horizons, and presence of a histic horizon, as reported by Schiavo *et al*. (2012). The contents of Fe and Al extracted with oxalate were higher, with Al being the highest, indicating a predominance of Al-organic complexes in the spodic horizon, and Fe^{2+} leaching, also observed by Schiavo *et al*. (2012).

The acidity in the soils of the *Baías* is explained by the leaching of the sandy substrate and the organic matter influence. The predominant vegetation on the *Baías* is aquatic macrophytes. According to Bergier *et al*. (2014), the *Baías* contribute to high CO_2 and CH_4 emissions to the atmosphere, when comparing with the *Salinas*, due to differences in the aquatic biota and microbiota, with a low efficiency of CO_2 sink and high potential emissions of CH_4 under anaerobic conditions.

2.5.2 The inundating lowlands: *Vazantes*

The *Vazantes* correspond to a low landscape segment, where the water flows during high floodings. Considered as a transitional environment, both aquatic and terrestrial plant species occur, and all soils showed a dense herbaceous cover. Despite the dark brown color, only a few soil profiles had organic matter accumulation at the surface, due to the low carbon

fixation of these sandy, acid soils. These results are in agreement with that of Cardoso *et al*. (2016), who reported low nutrient status and low organic matter content of the *Vazantes*.

The Arenosols and Podzol profiles presented mottles and/or cementation due to iron mobilization, caused by the water table oscillations. Cunha (1980) also found abundant mottling in the soils of the *Vazantes*. These features are common in soils that have alternating periods of oxidation and reduction. Under oxidizing conditions, the reduced Fe and Mn oxidize into low crystalline Fe oxyhydroxides, which assign reddish colors to soils (Schaetzl; Anderson, 2005). The spodic horizon presented higher Fe extracted by dithionite, although Fe extracted by oxalate presented significant levels comparing with Al, which indicates an intense oxidation-reduction condition and Fe accumulation. Besides, the lower TOC contents corroborate with this, once it favors the crystallization of Fe oxides, as demonstrated by Schwertmann (1966). Schiavo *et al*., (2012) also reported a more significant participation of Fe in the podzolization process in the *Vazantes* soils.

The very low pH value of the Podzol of the *Vazantes* indicates the occurrence of ferrolysis process, which is related to the above-mentioned seasonal cycles of oxidation and reduction of Fe, due to water table fluctuation. During the Fe oxidation at the bottom soil, H^+ cations are released and attack the octahedral layers of the clay minerals, releasing silicic acid and Al^{3+} (Brinkman, 1970; Schaetzl; Anderson, 2005). Couto and Oliveira (2010) also found soils with high content of Al^{3+} under hydromorphic conditions in Pantanal, related to ferrolysis process.

2.5.3 The sand levees: *Cordilheiras*

The *Cordilheiras* soils were classified as Arenosols, due to the major influence of a sandy substrate from the Pantanal Formation. Cunha (1980), Barbiero *et al*. (2008), and Cardoso *et al*. (2011) also found a dominance of sandy soils on the *Cordilheiras*. Despite the sandy texture, the *Cordilheiras* fertility is high in the surface horizons, due to the litter and faunal inputs, favoring nutrient cycling (Cardoso *et al*., 2011b, 2016; Cunha, 1980).

The Arenosol, classified as Planosol in the SiBCS presented an accumulation of Al extracted by oxalate in the Bt and Btnqx horizons, due to the translocation of Al-organic complexes. Associated with that, the Btnqx horizon also presented higher sodium content and $CaCO_3$, favoring higher pH values and amorphous silica. According to Barbiero *et al*. (2008), subsurface horizons of the *Salinas* presented cementation, due to high sodium content and

amorphous silica, which drastically decreases the water infiltration rate. In this case, the saline and alkaline groundwater of the *Salinas*, may be influencing the soils of *Cordilheiras*.

The well-drained *Cordilheiras* have Cerrado (Savannah) tree species adapted to free drainage, such as *Scheelea phalerata* (Mart.) Bur. and *Protium heptaphyllum*, which are considered key-species due to their abundance and importance for animal feeding (Junk *et al*., 2006; Pott *et al*., 2011). According to Cardoso *et al*. (2011b), these species were some of the most abundant found at the *Cordilheiras* covered by semideciduous forest and Cerradão (a forest type of the Cerrado biome) in the Nhecolândia.

The conversion of the forested areas into cultivated pasture poses a significant threat to the Pantanal's ecosystems (Silva *et al*., 1999). This land-use change has decreased soil quality, reducing base cations content, soil organic matter, and potential cation exchange capacity (Cardoso *et al*., 2011b). Additionally, intense cattle ranching in the *Cordilheiras* affects the vegetation structure and equilibrium by reducing understory biomass through trampling and grazing (Nunes da Cunha; Junk, 2009). Moreover, erosion around the *Salinas* has altered water geochemistry, leading to the transformation of Solonetz into Solodized Solonetz and Solods (Furquim *et al*., 2017). This degradation process has also been observed by local residents of the Nhecolândia, the Pantaneiros, who have linked the deterioration of the *Salinas* to the deforestation of the *Cordilheiras* (Silva; Passos, 2018). Furthermore, Fernandes *et al*. (2009) estimated that deforestation of a hectare of cerradão and cerrado vegetation in the *Cordilheiras* results in CO_2 emissions of 181.6 Mg and 85.7 Mg, respectively.

2.5.4 The fields and the termite mounds: *Campos* and *Murundus*

In both *Murundus* and *Campos*, Arenosols predominate. As typical Cerrado phytophysiognomy, the local occurrence of the Murundu mound is widely associated with Latosols (Ferralsols in the WRB classification system), which are more structured and clayey soils than the surrounding Gleysols (Corrêa, 1989; Paulino *et al*., 2015; Schaefer, 2001). Although widespread in the Pantanal, studies about the *Murundus* soils have been restricted to the north sector (Bordignon *et al*., 2007; Oliveira Junior *et al*., 2017), with only a mention to the occurrence of soils influenced by ants and termites in the Nhecolândia subregion in the study of Cunha (1980).

The Arenosols of the *Murundus* showed more clay content due to the termite activity, than Arenosols of the adjacent *Campos*. Fruett *et al*. (2023) observed that the clay content of the *Murundus* were higher than that of the surrounding soils without the termite influence,

indicating particle selection by termites during mound building. In addition, TOC content was also higher in the *Murundus* than the *Campos*, due to the intense biological activity, as reported elsewhere by Fruett *et al*. (2023) and Sarcinelli *et al*. (2009). Termites ingest soil organic matter and return it as faecal and buccal pellets, creating stable aggregates and favoring the preservation of soil organic matter (Sarcinelli *et al*., 2009). The acidity observed at the *Murundus* soils is consistent with the normal pH of mineral soils, selectively uptake by termites.

The formation of the *Murundus* is the result of a biological process of mound construction, followed by degradation, erosion, and formation of a pediment around the termite nest, originating the mound (Oliveira-Filho, 1992; Paulino *et al*., 2015). The interaction of the biota (earthworms, termites, ants, and others) with the soil is called bioturbation. This pedogenetic process is responsible for causing many alterations on soil properties, such as particle-size distribution, increasing aggregation, porosity, and organic content, which favored water holding capacity and reducing runoff (Wilkinson; Richards; Humphreys, 2009). The termites' activity in the *Murundus* also contributes to increase soil microbial (fungi and bacteria) richness, as observed by Chen *et al*. (2023) and Couto *et al*. (2023).

Soils of the *Campos* soils were similar to the *Murundus*. According to Oliveira-Filho (1992), the termites collect the subsoil to build the *Murundus*. The main differences between *Campos* and *Murundus* are related to biological activity and groundwater influence. One soil of the *Campos* presented evidence of groundwater oscillations (few mottles in subsurface). The little differentiation of *Campos* soils is due to high leaching index and groundwater stability and similar hydric regime (Cunha, 1980).

The plant species identified in the *Murundus* and in the *Campos* are typical of the Cerrado, with grasslands alternated with tree and shrub species, also called "campo cerrado" or "parque cerrado" (Savanna parkland) (Cunha, 1980; Ribeiro and Walter, 1998). In general, the smaller mounds (< 0.8 m diameter) have only herbs and smaller shrubs while the larger ones have higher shrubs and tall trees. On the other hand, the *Campos* are entirely covered with grassy vegetation, able to stand prolonged floods (Oliveira-Filho, 1992).

2.6 CONCLUSIONS

In the Nhecolândia Pantanal, slight topographical variations in a flat surface can create very contrasting environments in terms of soil, vegetation, and hydrological regimes. The variations in the hydrological regime affect the functioning of the ecosystem and create diverse

pedohabitats for fauna and flora. In Nhecolândia Pantanal, there is a predominance of sandy soils (Arenosols) in all environments, except in the *Salinas,* the most pedodiverse of all.

Despite the sandy texture, each environment differed in some aspect: the *Salinas* stand out with greater clay and base cation contents; the *Baías* and *Murundus* with higher organic carbon content; *Vazantes* presented more acidic soils; and the *Campos* the more dystrophic extremes.

The marked role of biological activity in the Arenosols of *Murundus* leads to increasing clay and soil carbon contents, through pedoturbation, and this represents the first detailed soil study of *Murundus* soil for the Pantanal of Nhecolândia.

Given the overall uniformity of texture (sandy) and subdued topography, even small differences in clay and sand contents, inundation regime, and morphological and mineralogical attributes of subsurface horizons can lead to significant ecosystem variations. Further studies on these environments and the interactions with biota are fundamental for better planning and management of soil use and conservation, understanding climatic changes trends, and assessing impacts on ecosystem functioning.

2.7 REFERENCES

AB'SÁBER, A. N. **Brasil, paisagens de exceção: o litoral e o Pantanal mato-grossense, patrimônios básicos**. 4. ed. Cotia: Ateliê Editorial, 2011.

ALHO, C. J. R. Biodiversity of the Pantanal: response to seasonal flooding regime and to environmental degradation. **Brazilian Journal of Biology**, [s. l.], v. 68, n. 4, p. 957–966, 2008.

ALHO, C. J. R. The Pantanal. In: FRASER, L. H.; KEDDY, P. A. (org.). **The World's Largest Wetlands**. Cambridge: Cambridge University Press, 2005. p. 203–271.

AMARAL FILHO, Z. P. do. Solos do Pantanal Mato-grossense. Simpósio sobre Recursos Naturais e Sócio-econômicos do Pantanal, 1, 1984, **Anais...** Corumbá. EMBRAPA-DDT, 1984. p. 91–104.

ASSINE, M. L. Brazilian Pantanal: A Large Pristine Tropical Wetland. In: VIEIRA, B. C.; S., RODRIGUES, A. A.; SANTOS, L. J. C. (org.). **Landscapes and Landforms of Brazil**. [S. l.]: Springer Dordrecht, 2015. p. 135–146.

ASSINE, M. L. *et al*. The Quaternary alluvial systems tract of the Pantanal Basin, Brazil. **Brazilian Journal of Geology**, [s. l.], v. 45, n. 3, p. 475–489, 2015.

BARBIERO, L. *et al*. Biogeochemical diversity, O2-supersaturation and hot moments of GHG emissions from shallow alkaline lakes in the Pantanal of Nhecolândia, Brazil. **Science of The Total Environment**, [s. l.], v. 619–620, p. 1420–1430, 2018.

BARBIERO, L. *et al*. Geochemistry of water and ground water in the Nhecolândia, Pantanal of Mato Grosso, Brazil: variability and associated processes. **Wetlands**, [s. l.], v. 22, n. 3, p. 528–540, 2002.

BARBIERO, L. *et al*. Soil morphological control on saline and freshwater lake hydrogeochemistry in the Pantanal of Nhecolândia, Brazil. **Geoderma**, [s. l.], v. 148, n. 1, p. 91–106, 2008a.

BERGIER, I.; KRUSCHE, A.; GUÉRIN, F. Alkaline Lake Dynamics in the Nhecolândia Landscape. In: BERGIER, I.; ASSINE, M. L. (org.). **Dynamics of the Pantanal Wetland in South America**. Switzerland: Springer International Publishing, 2014. p. 145–161.

BOIN, M. N. *et al*. Pantanal: The Brazilian Wetlands. In: SALGADO, A. A. R.; SANTOS, L. J. C.; PAISANI, J. C. (org.). **The Physical Geography of Brazil**. [S. l.]: Springer Cham, 2019. p. 75–91.

BORDIGNON, L. *et al*. Ilhas Vegetacionais no Pantanal Matogrossense: um teste da Teoria de Biogeografia de Ilhas. **Revista Brasileira de Biociências**, [s. l.], v. 5, n. S1, p. 387–389, 2007.

BRASIL. Projeto RADAMBRASIL. **Folha SE.21 Corumbá e parte da Folha SE.20: geologia, geomorfologia, pedologia, vegetação e uso potencial da terra**. Rio de Janeiro: [s. n.], 1982.

BRINKMAN, R. Ferrolysis, a hydromorphic soil forming process. **Geoderma**, [s. l.], p. 199–206, 1970.

CALHEIROS, D. F.; FONSECA JÚNIOR, W.C. **Perspectivas de estudos ecológicos sobre o Pantanal**. Corumbá: EMBRAPA-CPAP, 1996.

CARDOSO, E. L. *et al*. Qualidade química e física do solo sob vegetação arbórea nativa e pastagens no Pantanal Sul-Mato-Grossense. **Revista Brasileira de Ciência do Solo**, [s. l.], v. 35, n. 2, p. 613–622, 2011.

CARDOSO, E. L. *et al*. Relação entre solos e unidades da paisagem no ecossistema Pantanal. **Pesquisa Agropecuária Brasileira**, [s. l.], v. 51, n. 9, p. 1231–1240, 2016.

CHEN, C. *et al*. Effect of termite mounds on soil microbial communities and microbial processes: Implications for soil carbon and nitrogen cycling. **Geoderma**, [s. l.], v. 431, p. 116368, 2023.

CORRÊA, G. F. **Les microreliefs '*Murundus*' et leur environnment pédologique dans l'ouetat du Minas Gerais, région du Plateau Central Brésilien**. 1989. - Université de Nancy I, [s. l.], 1989.

COSTA-SILVA, A. R. *et al*. Soils surrounding saline-alkaline lakes of Nhecolândia, Pantanal, Brazil: Toposequences, mineralogy and chemistry. **Geoderma Regional**, [s. l.], v. 36, p. e00746, 2024.

COUTO, E. G. *et al*. Soils of Pantanal: The Largest Continental Wetland. In: Schaefer, C.E.G.R. (eds). **The Soils of Brazil**. Switzerland: Springer, Cham, 2023, p. 239-267.

COUTO, E. G.; OLIVEIRA, Virlei Álvaro. The Soil Diversity of the Pantanal. In: JUNK, W. J. *et al*. (org.). **The Pantanal: Ecology, biodiversity and sustainable management of a large neotropical seasonal wetland**. Moscow: Pensoft Publishers, 2010. p. 71–102.

CUNHA, N. G. da. **Considerações sobre os solos da sub-região da Nhecolândia, Pantanal Mato-grossense**. Corumbá: EMBRAPA, 1980.

DE OLIVEIRA, E. C.; PLA-PUEYO, S.; HACKNEY, C. R. Natural and anthropogenic influences on the Nhecolândia wetlands, SE Pantanal, Brazil. **Geological Society**, [s. l.], v. 488, n. 1, p. 167–180, 2019.

DIAS, I. A. *et al*. The Occurrence of Authigenic Clay Minerals in Alkaline-Saline Lakes, Pantanal Wetland (Nhecolândia Region, Brazil). **Minerals**, [s. l.], v. 10, n. 8, p. 718, 2020.

EITEN, George. The cerrado vegetation of Brazil. **The Botanical Review**, [s. l.], v. 38, n. 2, p. 201–341, 1972.

FERNANDES, A. H. B. Marozzi *et al*. **Estoques de Carbono do Estrato Arbóreo de Cerrados no Pantanal da Nhecolândia**. Corumbá: Embrapa Pantanal, 2009.

FERREIRA-JÚNIOR, W. G. *et al*. Flood regime and water table determines tree distribution in a forest-savanna gradient in the Brazilian Pantanal. **Anais da Academia Brasileira de Ciências**, [s. l.], v. 88, n. suppl 1, p. 719–731, 2016.

FREITAS, J. G. *et al*. Interaction between lakes' surface water and groundwater in the Pantanal wetland, Brazil. **Environmental Earth Sciences**, [s. l.], v. 78, n. 5, p. 139, 2019.

FRUETT, T. *et al*. Selectivity of soil constituents by termites in the construction of Brazilian termite mounds. **Scientia Agricola**, [s. l.], v. 80, 2023.

FURIAN, S. *et al*. Chemical diversity and spatial variability in myriad lakes in Nhecolândia in the Pantanal wetlands of Brazil. **Limnology and Oceanography**, [s. l.], v. 58, n. 6, p. 2249–2261, 2013.

FURQUIM, S. A. C. *et al*. Mineralogy and Genesis of Smectites in an Alkaline-Saline Environment of Pantanal Wetland, Brazil. **Clays and Clay Minerals**, [s. l.], v. 56, n. 5, p. 579–595, 2008.

FURQUIM, S. A. C. *et al*. Neoformation of micas in soils surrounding an alkaline-saline lake of Pantanal wetland, Brazil. **Geoderma**, [s. l.], v. 158, n. 3–4, p. 331–342, 2010a.

FURQUIM, S. A. C. *et al*. Salt-affected soils evolution and fluvial dynamics in the Pantanal wetland, Brazil. **Geoderma**, [s. l.], v. 286, p. 139–152, 2017.

FURQUIM, S. A. C. *et al*. Soil mineral genesis and distribution in a saline lake landscape of the Pantanal Wetland, Brazil. **Geoderma**, [s. l.], v. 154, n. 3–4, p. 518–528, 2010b.

FURQUIM, S. A. C.; VIDOCA, T. T. Salt-Affected Soils of Pantanal Wetland. In: TALEISNIK, Edith; LAVADO, Raúl S. (org.). **Saline and Alkaline Soils in Latin America**. Cham: Springer International Publishing, 2021. p. 229–254.

GARCIA, E. A. C. O **Clima no Pantanal Mato-grossense**. Corumbá: EMBRAPA, 1984.

GODOI, H. de O; MARTINS, E. G.; MELLO, J. C. R. de. **Programa Levantamentos Geológicos Básicos do Brasil - PLGB. Corumbá – Folha SE.21-Y-D, Aldeia Tomázia, Folha SF.21-V-B, Porto Murtinho, Folha SF.21-V-D, Estado de Mato Grosso do Sul**. Escala 1:250.000. Brasília: [s. n.], 2001.

GRADELLA, F. S. **Aspectos da dinâmica hidroclimática da lagoa salina do meio na fazenda Nhumirim e seu entorno, Pantanal da Nhecolândia, MS - Brasil**. 2008. 1–76 f. Mestrado - Universidade Federal de Mato Grosso do Sul, Aquidauana-MS, 2008.

GRADELLA, F.; QUÉNOL, H.; SAKAMOTO, A. Variation du niveau phréatique d'une saline dans le Pantanal en relation avec les précipitations et les inondations provoquées par le fleuve Paraguai (Brésil). **AIC 2009 Cluj**. Romênia: [s. n.], 2009. p. 223–228.

GUERREIRO, R. L. *et al*. The soda lakes of Nhecolândia: A conservation opportunity for the Pantanal wetlands. **Perspectives in Ecology and Conservation**, [s. l.], v. 17, n. 1, p. 9–18, 2019.

GUIMARÃES CÉSAR, E.; TREVELIN, C.; SARTORI MANOEL, P. **Pantanal paisagens, flora e fauna**. São Paulo: Cultura Acadêmica, 2014. v. 1 Disponível em: Acesso em: 25 mar. 2024.

IUSS WORKING GROUP WRB. **International soil classification system for naming soils and creating legends for soil maps**. 4. ed. Vienna, Austria: International Union of Soil Sciences (IUSS), 2022.

IUSS WORKING GROUP WRB. **International soil classification system for naming soils and creating legends for soil maps**. Rome: [s. n.], 2014.

IVORY, S. J *et al*. Vegetation, rainfall, and pulsing hydrology in the Pantanal, the world's largest tropical wetland. **Environmental Research Letters**, [s. l.], v. 14, n. 12, p. 124017, 2019.

JENNY, Hans. **Factors of soil formation: a system of quantitative pedology**. New York: Dover Publications, 1941.

JUNK, W. J. *et al*. Biodiversity and its conservation in the Pantanal of Mato Grosso, Brazil. **Aquatic Sciences**, [s. l.], v. 68, n. 3, p. 278–309, 2006.

JUNK, W. J. *et al*. Brazilian wetlands: their definition, delineation, and classification for research, sustainable management, and protection. **Aquatic Conservation: Marine and Freshwater Ecosystems**, [s. l.], v. 24, n. 1, p. 5–22, 2014.

LATRUBESSE, E. M.; STEVAUX, J. C.; DOS SANTOS, M. L.; ASSINE, M. L. Grandes sistemas fluviais: geologia, geomorfologia e paleoidrologia. In: SOUZA, C. R. de G.;

SEGUIO, K.; OLIVEIRA, A. M. dos S.; OLIVEIRA, P. E. de. (ed.). **Quaternário do Brasil**. Ribeirão Preto: Holos Editora, 2005. p. 276-297.

LEMOS, R. C.; SANTOS, R. D. **Manual de descrição e coleta de solo no campo**. 2. ed. Campinas: Sociedade Brasileira de Ciência do Solo, 1996.

MCGLUE, M. M. *et al*. Holocene stratigraphic evolution of saline lakes in Nhecolândia, southern Pantanal wetlands (Brazil). **Quaternary Research**, [s. l.], v. 88, n. 3, p. 472–490, 2017.

MCKEAGUE, J.A.; DAY, J. H. Dithionite and oxalate extractable fe and ai as aids in differentiating various classes of soils. **Canadian Journal of Soil Science**, [s. l.], v. 46, p. 13–22, 1966.

MENEZES, A. R. de. **Solos com feições espódicas do Pantanal Sul-MatoGrossense: Antagonismos às condições pedogenéticas**. 2021. 1–97 f. Tese (Doutorado) - Universidade Federal Rural do Rio de Janeiro, Seropédica, 2021.

MERDY, P. *et al*. Processes and rates of formation defined by modelling in alkaline to acidic soil systems in Brazilian Pantanal wetland. **Catena**, [s. l.], v. 210, p. 105876, 2022.

NUNES DA CUNHA, C.; JUNK, W. J. A preliminary classification of habitats of the Pantanal of Mato Grosso and Mato Grosso do Sul, and its relation to national and international wetland classification systems. In: JUNK, W.J. *et al*. (org.). **The Pantanal: Ecology, biodiversity and sustainable management of a large neotropical seasonal wetland**. Moscow: Pensoft Publishers, 2009. p. 127–141.

OLIVEIRA JUNIOR, J. C. de *et al*. Origin of mounds in the Pantanal wetlands: An integrated approach between geomorphology, pedogenesis, ecology and soil micromorphology. **PLOS ONE**, [s. l.], v. 12, n. 7, p. e0179197, 2017.

OLIVEIRA-FILHO, A.T. de. Floodplain "*Murundus*" of Central Brazil: evidence for the termite-origin hypothesis. **Journal of Tropical Ecolology**, [s. l.], v. 8, p. 1–19, 1992.

PADOVANI, C. R. **Dinâmica Espaço-Temporal das Inundações do Pantanal.** 2010. 1–175 f. Tese (Doutorado) - Escola Superior de Agricultura "Luiz de Queiroz", Piracicaba, 2010.

POTT, A. Pastagens das sub-regiões dos Paiaguás e Nhecolândia do Pantanal Mato-grossense. Corumbá: EMBRAPA, 1981.

POTT, A. *et al*. Plant diversity of the Pantanal wetland. **Brazilian Journal of Biology**, [s. l.], v. 71, n. 1, p. 265–273, 2011.

POTT, A.; POTT. Features and conservation of the Brazilian Pantanal wetland. **Wetlands Ecology and Management**, [s. l.], v. 12, p. 547–552, 2004. Disponível em: Acesso em: 1 out. 2023.

POTT, V.J.; POTT, A. **Plantas Aquáticas do Pantanal**. Corumbá, MS: EMBRAPA, 2000.

POTT, A.; POTT, V.J. **Plantas do Pantanal**. Corumbá, MS: EMBRAPA, 1994.

RASBOLD, G. G. *et al*. Holocene limnological changes in saline and freshwater lakes, Lower Nhecolândia, Pantanal, Brazil. **Hydrobiologia**, [s. l.], v. 851, n. 7, p. 1723–1739, 2024.

R CORE TEAM. R: **A language and environment for statistical computing**. Viena: R Foundation for Statistical Computing, 2024.

RIBEIRO, J. F.; WALTER, B. M. T. Fitofisionomias do bioma cerrado. In: SANO, S. M.; ALMEIDA, S. P. de (org.). **Cerrado: ambiente e flora.** Planaltina: EMBRAPA-CPAC, 1998. p. 89–166.

SANTOS, H. G. dos *et al*. **Sistema Brasileiro de Classificação de Solos**. 5. ed. Brasília: EMBRAPA, 2018.

SARCINELLI, T. S. *et al*. Chemical, physical and micromorphological properties of termite mounds and adjacent soils along a toposequence in Zona da Mata, Minas Gerais State, Brazil. **Catena**, [s. l.], v. 76, n. 2, p. 107–113, 2009.

SCHAEFER, C. E. R. Brazilian latosols and their B horizon microstructure as long-term biotic constructs. **Soil Research**, [s. l.], v. 39, n. 5, p. 909, 2001.

SCHAETZL, R.J.; ANDERSON, S. **Soils: Genesis and Geomorphology**. New York: Cambridge University Press, 2005.

SCHIAVO, Jolimar Antonio *et al*. Characterization and classification of soils in the Taquari river basin - Pantanal region, state of Mato Grosso do Sul, Brazil. **Revista Brasileira de Ciência do Solo**, [s. l.], v. 36, n. 3, p. 697–708, 2012.

SCHWERTMANN, U. Inhibitory Effect of Soil Organic Matter on the Crystallization of Amorphous Ferric Hydroxide. **Nature**, [s. l.], v. 212, n. 5062, p. 645–646, 1966.

SILVA, M P. da *et al*. Conversion of forests and woodlands to cultivated pastures in the wetland of Brazil. **Ecotropicos**, [s. l.], v. 12, n. 2, p. 101–108, 1999.

SILVA, A.E. *et al*. **Manual de métodos de análise de solo**. 3. ed. Brasília: EMBRAPA, 2017.

SILVA, J. dos S. V. da.; ABDON, M. de M. Delimitação do Pantanal Brasileiro e suas Sub-Regiões. **Pesq. agropec. bras,** [s. l.], v. 33, p. 1703–1711, 1998.

SILVA, M. H. S.; PASSOS, M. M. Discourse analysis of the authors/actors from the Nhecolândia Pantanal. **Mercator**, [s. l.], v. 17, n. 07, p. 1–16, 2018.

USSAMI, N.; SHIRAIWA, S.; DOMINGUEZ, J. M. L. Basement reactivation in a sub-Andean foreland flexural bulge: The Pantanal wetland, SW Brazil. **Tectonics**, [s. l.], v. 18, n. 1, p. 25–39, 1999.

VALVERDE, O. Fundamentos Geográficos do Planejamento do Município de Corumbá. **Revista Brasileira de Geografia**, [s. l.], v. 34, n. 1, p. 49–144, 1972.

WILKINSON, M. T.; RICHARDS, P. J.; HUMPHREYS, G. S. Breaking ground: Pedological, geological, and ecological implications of soil bioturbation. **Earth-Science Reviews**, [s. l.], v. 97, n. 1–4, p. 257–272, 2009.

YEOMANS, J. C.; BREMNER, J. M. A rapid and precise method for routine determination of organic carbon in soil. **Communications in Soil Science and Plant Analysis**, [s. l.], v. 19, n. 13, p. 1467–1476, 1988.

ZANI, H.; ASSINE, M. L.; MCGLUE, M. M. Remote sensing analysis of depositional landforms in alluvial settings: Method development and application to the Taquari megafan, Pantanal (Brazil). **Geomorphology**, [s. l.], 2012. Disponível em: Acesso em: 26 mar. 2024.

ZAVATTINI, J. A. A distribuição das chuvas e a circulação atmosférica no estado de Mato Grosso do Sul. In: ZAVATTINI, J. A. **As chuvas e as massas de ar no estado de Mato Grosso do Sul**: estudos geográficos com vista à regionalização climática. São Paulo: Cultura Acadêmica, 2009. p. 59–92.

3 CHAPTER 2: Soil-plant relationships in the Pantanal of Nhecolândia, western Brazil: a phytosociological and machine learning application study

3.1 ABSTRACT

Variations in the soil characteristics significantly influence the composition and distribution of plant communities, emphasizing the importance of soil-plant relationship studies for the understanding ecosystem dynamics and predicting environmental changes. This study aimed to characterize the floristic composition and phytosociological structure across six landscape units in the Pantanal of Nhecolândia, evaluating how soil properties affect species richness and composition. In the herbaceous vegetations (*Baías*, *Salinas*, *Campos*, and *Vazantes*) we randomly distributed 1 m² plots and evaluated the plant community structures using Braun-Blanquet cover scale method. In the woody vegetation (*Cordilheiras* and *Murundus*) 100 m² plots were randomly established at least 20 m apart from each other, and all individuals presenting DBH ≥ 15 cm (diameter at breast height at 1.30 m from the soil) were sampled. Composite soil samples (0-20 cm depth) were analyzed for physical and chemical properties. Venn diagram and Jaccard index were applied to verify floristic connection and similarity. Individual-based rarefaction and extrapolation curves were applied to analyze differences in species richness. Species composition variability was analyzed using nonmetric multidimensional scaling method (NMDS). Shannon-Wienner diversity index and Pielou's evenness index were also calculated. Vegetation structure was verified through the importance value index (IVI). Soil variables were summarized using statistical analyses. The effects of the soil attributes on species richness and composition were evaluated using the Random Forest (RF) regression algorithm. The model performances were evaluated though validation metrics and comparison to a null model (mean value of the response variables). All statistical analyses were performed using R software. Across the units, 130 species from 106 genera and 49 families were recorded, with Poaceae, Fabaceae, and Asteraceae being dominant. From all identified species, 73.07% occurred exclusively in one unit, with no species common to all units. There was greater composition similarity between *Cordilheiras* and *Murundus* (32%), and between *Baías* and *Vazantes* (18). *Cordilheiras* had the richest, most diverse, and most uniform landscape among the woody ones, and the *Vazantes* among the herbaceous ones. Soil acidity and nutrient-poor conditions prevailed, except in the eutrophic *Salinas* soils. *Murundus* and *Baías* showed high organic carbon contents, due to biological activity and water saturation, respectively. RF model outperformed the null model, showing soil affects species richness

(35%) and composition (83%). High Na levels in *Salinas* reduced species richness and composition, while P and K positively influenced *Cordilheiras* and *Murundus*. Conservation of vegetation, especially in the sandy *Cordilheiras* is vital for maintaining nutrient cycling and biodiversity amidst deforestation and soil degradation threats.

Keywords: Wetland. Phytosociology. Edaphic Factors. Random Forest.

3.2 INTRODUCTION

The Pantanal, a unique wetland in the Brazilian territory, was considered a National Heritage by the Brazilian Constitution in 1988, a Biosphere Reserve by UNESCO in 2000, and a Wetland Ecosystem of Extreme Importance for Biodiversity Conservation by the Ramsar Convention (Alho, 2005b; Boin *et al*., 2019). The Pantanal is the sixth out of eleven largest wetlands of the world (Keddy *et al*., 2009) and the second most preserved Brazilian biome (MapBiomas, 2024). As a large wetland, the Pantanal offers many ecosystem services, such as biological diversity maintenance, carbon storage, flood control, aquifer recharge, fish production, among others (Alho, 2008; Keddy *et al*., 2009). The vegetation of the Pantanal is considered a floristic complex of grasslands, palmlands, and forests from the phytogeographic provinces of Cerrado, Amazonia, Caatinga, Chaco and Atlantic Forest (Cole, 1960; Pott *et al*., 2011). The vegetation structure and composition in the Pantanal are mainly defined by the flooding dynamic, coupled with soil type and topography, once few changes in elevation have significant importance for the environmental conditions in floodplain habitats (Alho, 2008; Ivory *et al*., 2019; Junk *et al*., 2006; Schessl, 1999).

The Pantanal climate is marked by a hot and dry season and a rainy season. The flooding coincides with the rainy season in the northern portion of the Pantanal, but there is a lag of three to four months between the rainy season and flooding in the southern portion, due to the slow propagation of the flooding (Assine, 2015; Junk *et al*., 2014). The flooding in Pantanal is caused by a change in the slope of the rivers when entering the plain, where they lose energy and tend to overflow (Boin *et al*., 2019). The flooding pulse is the main factor conditioning the trophic relationships of the aquatic and terrestrial communities in Pantanal (Ivory *et al*., 2019), once the species abundance is related to the seasonal offer of ecological resources, such as feeding and reproductive niches (Alho, 2008). These changes in the landscape allow the formation of a mixture of permanent and temporary flooded habitats, which contributes to the richness of vegetation and productivity of the system, and consequently for an abundant fauna (Alho, 2008).

The inundation regime is the great limiting factor of the Pantanal vegetation richness and productivity of the system (Crispim *et al*., 2006; Ivory *et al*., 2019). This occurs because soil can determine nutrient-acquisition and use strategies among plant species and life form (Abrahão *et al*., 2019). Hess *et al*. (2007) reported that chemical composition of materials extracted from aerial parts of the of the Elionurus muticus was influenced by seasonal climatic and hydrological variations, indicating how sensible some species can be to soil moisture

changes. Ratter *et al*. (1988) identified an influence of soil nutrients, mainly Ca^{2+}, in the dry forests of the sand levees in the northern Pantanal, similarly to that in the deciduous and semideciduous forest from Central Brazil. According to Zeilhofer and Schessl (2000), the water regime and soil texture are the main factors responsible for vegetation distribution in the Pantanal of Poconé (one of the Pantanal's subregions). Vourlitis *et al*. (2015) observed that the differences in available Ca^{2+} and Mg^{2+} contents, between forest and savanna soils of the north Pantanal were due in part to variations in the clay content, which is correlated with a higher soil cation exchange capacity. Studies about the earthmounds (*Murundus*) of the north Pantanal have pointed out the importance of the groundwater regime for the differentiation between the cerrado vegetation over the mounds and the grasslands community in the surrounding wet area (Ferreira-Júnior *et al*., 2016b; Ponce; Da Cunha, 1993).

In the Pantanal of Nhecolândia, characterized by its sandy substrate and a myriad of freshwater and saline lakes, the predominance of sandy soils, combined with little topographic variations, allows a widespread inundation, which directly influences the distribution of different habitats and phytophysiognomies (Bacani *et al*., 2010; Cardoso *et al*., 2016; Cunha, 1980). In the Nhecolândia region, little variations in the topography (of centimeters in altitude) cause significant environmental changes: from lakes to non-floodable higher areas, is possible to find many physiognomic units of the *Cerrado*, with formations dominated by grasses, such as *campo limpo* and *campo cerrado*, and woodlands such as *cerrado* and *cerradão* (Ferreira-Júnior *et al*., 2016b; Silva; Abdon, 1998).

In Cerrado areas, many studies have observed that the interactions between soil and vegetation are fundamental for understanding the physiognomic and floristic variations and distribution (Eiten, 1972b; Oliveira-Filho *et al*., 1989; Ratter *et al*., 2010). Vegetational predictions studies based on environmental factors are important tools for helping the development of strategies and actions for biodiversity conservation (Valladares *et al*., 2015). Different from traditional statistical techniques, such as linear regression models, regression machine learning models are capable to deal with complex interactions using a highly dimensional and non-linear data, being more realistic to the confusing, real-world conditions (Prasad; Iverson; Liaw, 2006; Thessen, 2016).

The Pantanal has been used for cattle grazing for two hundred years (Pott, 1988). This economic activity has been practiced almost exclusively by the Pantaneiros (inhabitants of the Pantanal), due to the availability of extensive grassy savannah vegetation that serves as natural pasture. However, in recent decades, the external economic pressure to expand cattle production has intensified the deforestation of the *Cordilheiras*, which have been converted into planted

pastures (Junk et al., 2006; Silva; Passos, 2018). Associated with this, fire is used as a technique for adding nutrients to soil, which do not persist due to the sandy texture, being vulnerable for leaching, and significantly limiting the adaptation of new forage species (Cunha, 1985). Overgrazing of planted pastures has led to pasture degradation, with a tendency for woody vegetation to return (Cunha, 1985; Pott, 1988). Additionally, after grazing, the soils of the Cordilheiras are leached, loosing nutrients and organic carbon, and reducing the microorganisms' populations (Cardoso et al., 2009, 2011; Cunha, 1985). Besides affecting the soil quality of the Cordilheiras (Cardoso et al., 2011), nearby ecosystems, such as the Salinas, have also been affected, with transformations in water geochemistry altering soil dynamics (Furquim et al., 2017).

Despite the importance of abiotic factors for the vegetation distribution, studies focusing on the relationship between soil attributes and the vegetation in the Pantanal of Nhecolândia are still limited. For that reason, we aimed to characterize the floristic composition and phytosociological structure of different landscape units of the Pantanal of Nhecolândia, and to evaluate how species richness and composition are affected by soil physical and chemical attributes, by mean of a novel approach.

3.3 MATERIALS AND METHODS

3.3.1 Study area

The study was performed on the Nhecolândia, the second largest Pantanal sub-region, covering an area of 26.921 km², and is in the southern portion of the Taquari megafan (Silva; Abdon, 1998). It is placed in the municipalities of Corumbá, Aquidauana and Rio Verde de Mato Grosso, in Mato Grosso do Sul, ranging from the latitudes 18°12'52.76"S and 19°40'12.46"S, and the longitudes 54°52'39.21"W and 57°13'24.67"W (Figure 1). The Nhecolândia is characterized by a mean annual air temperature of 26 ºC and the mean annual rainfall of 1206 mm (Garcia, 1984). The rainy season occurs between November and March, while the period of strong water deficit ranges from August to October (Garcia, 1984). The flooding season occurs from March to May (Garcia, 1984),and is mainly caused by local precipitation or groundwater elevation (Gradella; Quénol; Sakamoto, 2009; Padovani, 2010).

The sedimentary lithology of the Pantanal consists of poorly consolidated fine- to coarse-grained sandstones, which form the Pantanal Formation (Godoi; Martins; Mello, 2001). The Nhecolândia is an abandoned alluvial fan lobe of the Taquari megafan, characterized by

flat relief and low slope gradients, with more than 10,000 shallow lakes and extensive sandy dunes (Assine *et al*., 2015; Zani; Assine; Mcglue, 2012). The Podzols and Arenosols are the main soil classes of the Nhecolândia, which are characterized by nutrient-poor and leaching susceptible soils (Couto, Oliveira, 2010; Cunha, 1980).

Figure 1 – Location map of the sampling area and the Nhecolândia landscape units: a) Saline-alkaline lakes – *Salinas*; b) Freshwater lakes – *Baías*; c) Seasonal floodable lowlands – *Vazantes*; d) Sandy ridges – *Cordilheira*; e) Termite mounds – *Murundus*; f) Occasionally flooded grasslands – *Campo*.

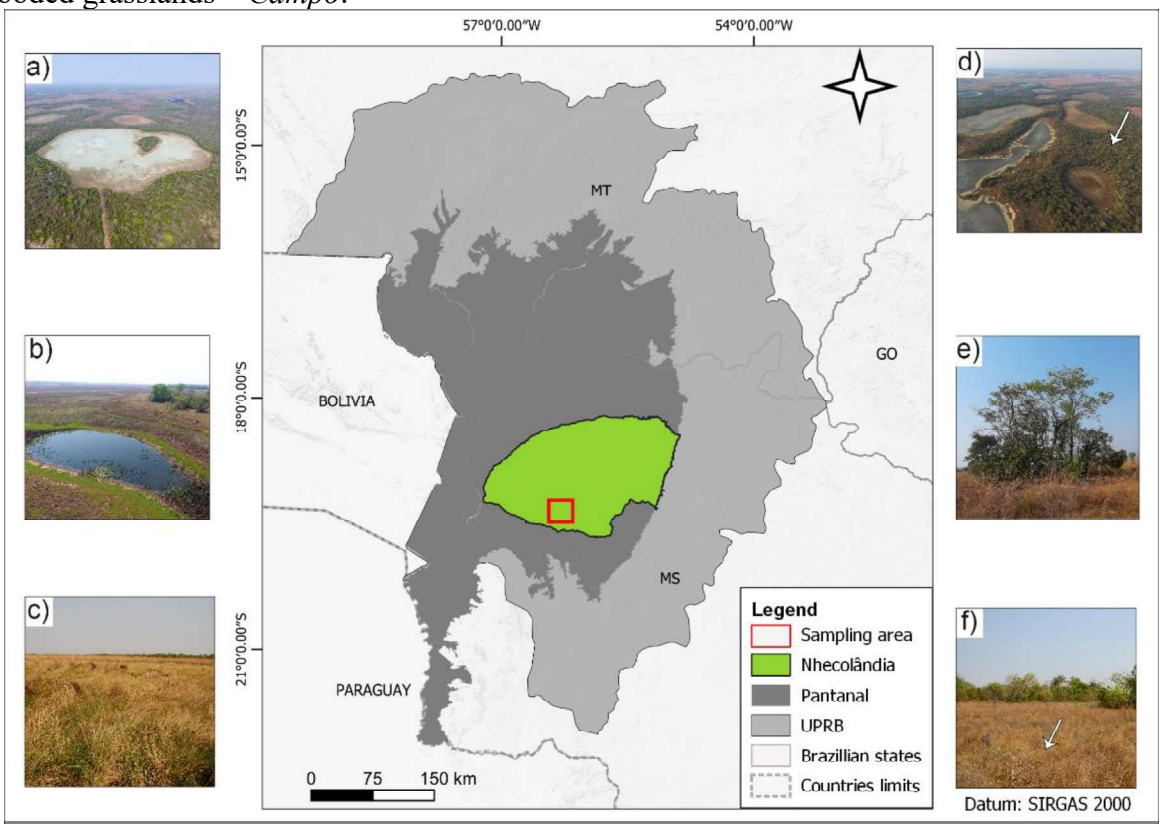

Source: The author.

3.3.2 Selection of the landscape units

Here, we selected six different landscape units (Figure1) based on the description of the phytophysiognomies of Nhecolândia, proposed by (Silva; Abdon, 1998) and the regional nomenclatures corroborated by Ab'Sáber (2011), Calheiros and Fonseca Júnior (1996) and Valverde (1972).

3.3.2.1 *Salinas*

The *Salinas* are shallow alkaline, saline or oligosaline lakes surrounded by the *Cordilheiras*. Their water depth does not exceed 2 m during austral summer (Guerreiro *et al*., 2019). The morphology of these lakes was molded by deflation in the arid early Holocene (Guerreiro *et al*., 2019; McGlue *et al*., 2017) and their salinity is explained by the accumulation of salts in the surface waters, due to the high evaporation, and the recharge limited by groundwater, which isolate the lakes from the seasonal flood channels (Barbiero *et al*., 2002; Furian *et al*., 2013b; McGlue *et al*., 2017). Due to the high salinity, the aquatic ecosystems of the *Salinas* are dominated by well-adapted extremophile life, such as cyanobacteria, giant mimiviruses, and aerobic and anaerobic microorganisms (Guerreiro *et al*., 2019).

3.3.2.2 *Baías*

The *Baías* are freshwater lakes, with varied size and depth, which can be temporary or permanent, and are influenced by the seasonal flood channels. The *Baías* are not isolated by the low-permeability soil horizon as the *Salinas*, so they have a hydrological regime that favors the connection between groundwater-surface water (Furian *et al*., 2013b). Aquatic vegetation is very common and diverse at the *Baías*, presenting 337 algae species and 248 species of aquatic macrophytes or hydrophytes (Junk *et al*., 2006).

3.3.2.3 *Vazantes*

The *Vazantes* are natural drains, which connect the *Baías* during the flooding season. They are wide and low areas, with characteristics of an intermittent fluvial watercourse (Calheiros; Fonseca Júnior, 1996). Seasonal floodings from December to April transform the *Vazantes* into palustrine grasslands, altering floristic composition: mesophytic and xerophytic plants give way to hygrophytic and aquatic species (Pott, 1984; Rabellato *et al*., 2005). So, this environment is considered as an aquatic-terrestrial transition zone, also called as floodable fields. During short inundation periods there are fields dominated with thickets of grass on hydromorphic soils, and during long inundation periods occur the predominance of tall grass (Alho, 2005b).

3.3.2.4 *Cordilheiras*

The *Cordilheiras* are narrow sandy elevations (circa of 2 m above ground) that surround the *Salinas*. They are covered with woody vegetation, that consist of a variety of species typically found in the cerrado or cerradão vegetation, characteristic of the Cerrado biome; deciduous forest, originating from the Chiquitania region in Bolivia and the Caatinga of the northeastern Brazil; and semideciduous forest, derived from the Atlantic Forest (Pott *et al*., 2011). The *Cordilheiras* do not inundate during the floods, serving as important habitats for little flood adapted plants and refuges for terrestrial animals (Junk *et al*., 2006). The origin of the *Cordilheiras* is associated with deflation of sand from the Nhecolândia fan lobe, which allow the formation of the depressions (lakes) and the complex marginal sand levees (*Cordilheiras*) (McGlue *et al*., 2017).

3.3.2.5 *Murundus*

The *Murundus* (earthmounds) corresponds to small, rounded elevations of land (0.5-20 m in diameter, and 0.2 – 2.0 m high), formed by termite nests and covered with woody cerrado plants (Oliveira-Filho, 1992; Ribeiro; Walter, 1998). The formation of the *Murundus* is associated with a localized and repeated nest-building by many generations of termite colonies, followed by continuous nest erosion, which led to the formation of a “pediment” around the mounds (Oliveira-Filho, 1992). During the wet season, the *Murundus* are true islands, protected against the inundation.

3.3.2.6 *Campos*

The *Campos* (or occasionally flooded grassland) are flat areas that surround the *Murundus* and are mainly composed by herbaceous vegetation, as grasses and herbs, with rare occurrence of sparce shrubs (Ribeiro; Walter, 1998).

3.3.3 Data collection

The plant and soil sampling occurred during September 2021, in the dry season. In each of the different landscape units, different plot sizes were used for each predominant life form of vascular plants. In the herbaceous vegetation from *Baías*, *Campos*, and *Salinas*, we

randomly distributed 40 plots (1 × 1 m) in each environment. In the herbaceous vegetation from the *Vazantes*, we distributed 60 plots (1 × 1 m). Plant community structures were evaluated by the cover scale proposed by Braun-Blanquet (1979). In addition, 72 plots (10 × 10 m) were established to woody vegetation, i.e. 36 plots along *Cordilheiras* and 36 plots along the *Murundus*. In the woody vegetation, each plot was at least 20 m apart from each other, and all individuals presenting circumference at 1.30 m from the soil (Diameter at Breast Height - DBH ≥ 15 cm, Moro and Martins 2011) were sampled. Finally, the identifications were made by consulting specialists and the literature. Taxonomic classification followed APG IV (Angiosperm Phylogeny Group 2016). The nomenclature of the species and respective abbreviations of the authors were standardized according to the List of Species of Flora of Brazil (2020).

The soil physical and chemical properties were determined for each plot, by means of a composite sample of three surface soil subsamples (0–20 cm depth) collected. Before the laboratory analyses, samples were air-dried and sifted through a 2 mm mesh sieve. Analyses were conducted at the Laboratory of Soil Analysis of the Federal University of Viçosa, following standards methods adapted from (Silva *et al*., 2017). Granulometric analysis was performed using the pipette method: coarse sand (2 – 0.02 mm), fine sand (0.2 – 0.5 mm), silt (0.05 – 0.002 mm), and clay (< 0.002 mm). The soil pH was determined in water. The available P, exchangeable Na^+ and K^+, and the micronutrients (Fe, Cu, Mn and Zn) were extracted with Mehlich-1 method (HCl 0.05 mol L^{-1} and H_2SO_4 0.0125 mol L^{-1}), and quantified by photocolorimetry (P), flame photometry (Na and K) and atomic absorption spectroscopy (micronutrients). The exchangeable cations (Ca^{2+}, Mg^{2+} and Al^{3+}) were extracted by KCl 1 mol L^{-1} and determined by atomic absorption spectroscopy (Ca^{2+} and Mg^{2+}) and titration with 0.025 mol L^{-1} NaOH solution (Al^{3+}). The potential acidity (H+Al) was obtained by a 0.5 mol L^{-1} calcium acetate solution buffered at pH and determined by titration with 0.025 mol L^{-1} NaOH solution. The remaining phosphorous (P-Rem) was determined with a 0,01 mol L^{-1} $CaCl_2$ solution and by photocolorimetry. Total organic carbon (TOC) was obtained by the wet-combustion method (Yeomans; Bremner, 1988). Effective cation exchange capacity (eCEC) was calculated by determining the sum of cations (Ca^{2+}, Mg^{2+}, Na^+, K^+, and Al^{3+}). The potential cation exchange capacity (pCEC) was estimated using the bases sum (BS) and potential acidity ($H^+ + Al^{3+}$). We determined the percentage of bases saturation (PBS), Al saturation index (Al_{sat}), and Na saturation index (NaSI).

3.3.4 Data analyses

All statistical analyses were performed in the R software (R Core Team, 2024). To assess the floristic connection between the landscape units, based on the presence and absence of species, a Venn diagram was made using the VennDiagram package (Chen; Boutros, 2011). The floristic similarity between environments was calculated using the Jaccard index (Magurran, 2004). We used individual-based rarefaction and extrapolation curves with the first Hill number (species richness, q = 0) to analyze differences in species richness among landscape units (Chao *et al*., 2014; Colwell *et al*., 2012) using the 'iNEXT' package (Hsieh; Ma; Chao, 2016).

To analyze the variability of species composition, the nonmetric multidimensional scaling method (NMDS) was used based on Jaccard index (presence-absence data) (Legendre; Legendre, 2012) of the 'vegan' package (Oksanen *et al*., 2018). For the *Cordilheiras* and *Murundus*, the vegetation structure was verified from the importance value index (IVI) given by the sum of the relative density (RD), relative dominance (RDo) and relative frequency (RF) of each species (Curtis; McIntosh, 1951). For the *Vazantes*, *Baías*, *Salinas*, and *Campos*, the importance Value Index (IVI) of each species was calculated by the sum of its relative frequency and relative cover (Braun-Blanquet, 1979). Shannon-Wienner diversity index and Pielou's evenness index were calculated for each landscape unit (Magurran, 2004).

Soil variables were summarized by using Principal Component Analysis (PCA) on the correlation matrix using the FactoMineR package (Husson *et al*., 2019). The PCA was performed after standardization of soil variables. Descriptive analysis was applied to the variables most important in explaining the soil variances, as indicated by the PCA. Spearman correlation (r) was applied to assess the degree of correlation between edaphic variables.

Finally, we tested the main effects of different soil attributes and their interactions on species richness and composition (first axis of the NMDS) using a machine learning (ML) approach, due to its ability to model highly dimensional and non-linear data with complex interactions (Thessen, 2016). We applied a method adapted from Fernandes-Filho *et al*. (2024) and choose the decision tree algorithm, Random Forest (RF), as the regression technique, due to its high performance on predictive analyses on Ecology (Cutler *et al*., 2007; Prasad; Iverson; Liaw, 2006; Thessen, 2016). The predictor variables corresponded to the physico-chemical soil attributes, as edaphic variables, and the landscape units, as an environmental variable. Variables with strong ($r > 0.9$) Spearman correlation were removed from the prediction. We split the dataset into training (80%) and test (20%) sets and applied the K-fold cross-validation method

to enhance the training performance of the RF. We optimized the number of variables used in the training through the mtry hyperparameter. The best mtry number was the one with the least mean absolute error (MAE). Modelling performances were measured using MAE, root mean squared error (RMSE) and the coefficient of determination (R2). The test results were compared to a null model, represented by the mean value of the response variables, to evaluate the model performance. Finally, we applied our model to the hole dataset to verify the model predictive performance. All processing was done using the caret package (Kuhn, 2019).

3.4 RESULTS

3.4.1 Species richness and composition

Overall, 130 species belonging to 106 genera and 49 families were sampled across all six landscape units (Appendix D and E). Most families occurred with one or two species. Most species belonged to three dominant families, namely Poaceae (16 genera, 19 species), Fabaceae (9 genera, 12 species) and Asteraceae (8 genera, 8 species), followed by Malvaceae (5 genera, 6 species), Cyperaceae (5 genera, 5 species) and Rubiaceae (4 genera, 5 species). These families comprised 44.34% of all genera and 42.30% of all species.

From all identified species, 95 (73.07%) occurred exclusively in one landscape unit and 30 (23.07%) were common to two (Figure 2A). There was no species common to the six landscape units. Floristic similarities according to Jaccard index indicated greater similarity between *Cordilheiras* and *Murundus* (32%), and *Baías* and *Vazantes* (18%) (Figure 2A). Species richness showed marked differences between the landscape units, as demonstrated by the sampled-based rarefaction and extrapolation curves (Figure 2B). The landscape units with higher species richness were *Cordilheiras* (48), followed by *Murundus* (46), which corresponded to the woody vegetation. Among the landscape units with herbaceous vegetation, the *Vazantes* presented the highest species richness (28), and the *Salinas* the lowest (10).

The NMDS indicated that the species composition of the woody environments (*Cordilheiras* and *Murundus*) is more similar between them and differ from that of the herbaceous environments (*Salinas, Baías, Vazantes*, and *Campos*) (Figure 3). The *Cordilheiras* presented the highest Shannon's diversity index and Pielou's evenness index, followed by the *Murundus*, which indicate high species diversity and a more equitable distribution of the individuals (Table 1). The *Baías* and *Vazantes* were very similar in relation to diversity and

evenness, and the *Salinas* and *Campos* showed the lowest values, indicating higher dominance of species.

Figure 2 – A) Venn diagram of exclusive and shared species among the six landscape units in the Pantanal of Nhecolândia, Brazil. *Sj* = Jaccard index; B) Sample-based rarefaction (solid line) and extrapolation curves (dashed lines) of species richness.

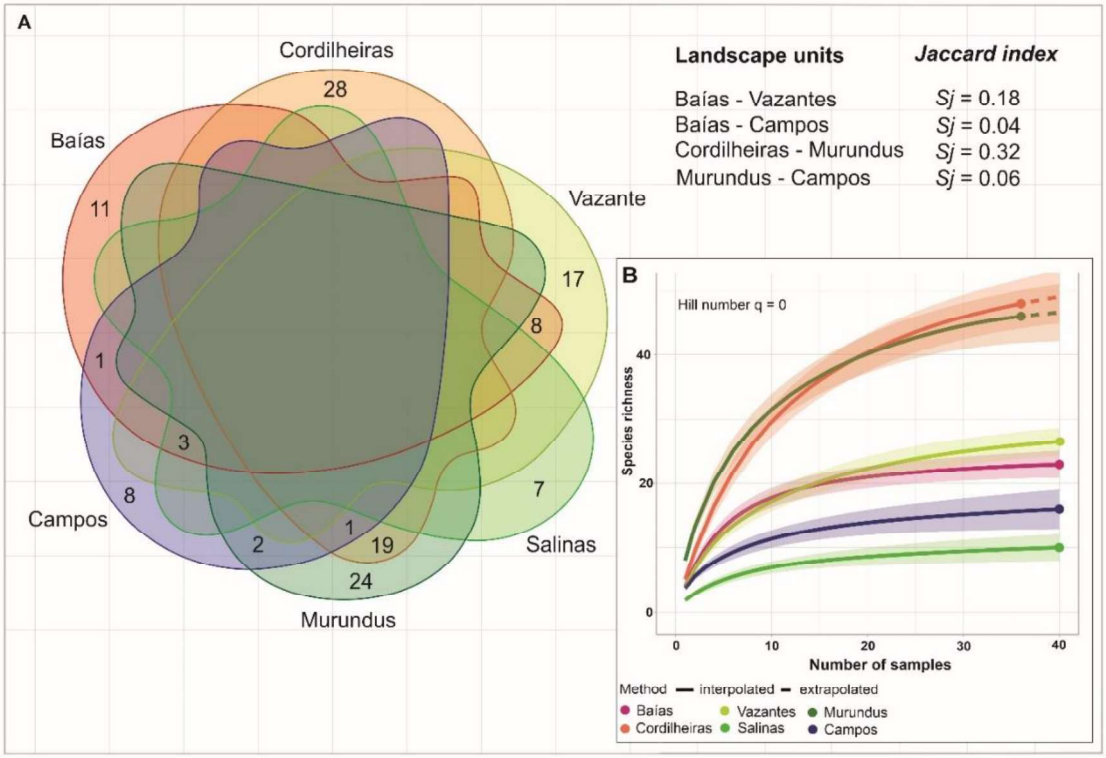

Source: The author.
Note: The curves present the mean values, and the bands the standard deviation with 95% confidence intervals. Whenever the 95% confidence intervals did not overlap, species numbers differed significantly at $p < 0.05$ (Colwell *et al.*, 2012).

Figure 3 – Arrangement diagram of the NMDS analysis of the six landscape units in the Pantanal of Nhecolândia, Brazil.

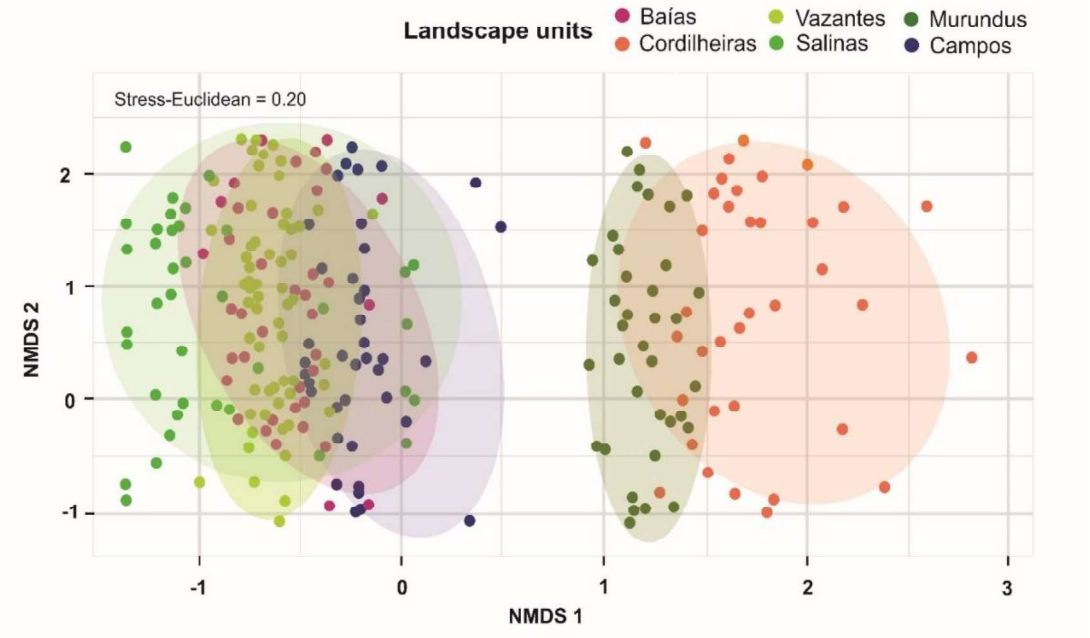

Source: The author.

Table 1: Species richness (S), Shannon's diversity index (H') and Pielou's evenness index (J') for each landscape unit of the Pantanal of Nhecolândia, Brazil.

Landscape unit	S	H'	J'
Cordilheiras	48	3.42	0.88
Murundus	46	2.99	0.78
Salinas	10	1.30	0.56
Baías	23	2.21	0.70
Vazantes	28	2.34	0.70
Campos	15	1.56	0.58

3.4.2 Community structure

In the woody vegetation, the 10 species with the highest IVI in each landscape units, represented approximately 52.41 and 64.9% of the total IVI of the *Cordilheiras* and *Murundus*, respectively. Among those 10 species, *Curatella americana* L. and *Pouteria torta* (Mart.) Radlk. were the most common species in both landscape units (with IVIs of 3.91 and 3.71%, respectively, in the *Cordilheiras*, and of 10.59 and 5.57%, respectively in the *Murundus* (Appendix D). In the *Cordilheiras*, *Attalea phalerata Mart. ex Spreng.* showed the highest IVI (12.48%) due to the higher relative dominance value, and *Protium heptaphyllum (Aubl.) Marchand* presented the second highest IVI (6.05%), due to the higher relative density and relative frequency. In the *Murundus*, *Mouriri elliptica Mart.* showed the higher IVI (16.66%), due to its higher values of relative density, dominance, and frequency. *Curatella americana* showed the second highest IVI of the *Murundus* (10.59%), due to its higher values of relative frequency.

In the herbaceous vegetation, the 10 species with the highest IVI in each landscape unit represented, approximately, 82.5, 73.3 and 95.5% of the total IVI for the *Vazantes*, *Baías*, and *Campos*, respectively. In each of these environments, the species with the highest IVI, respectively, were *Bulbostylis* sp. (17.7%), *Typha domingensis* Pers. (13%), and *Elionurus cf. muticus* (Spreng.) Kuntze (35.2%). In the *Salinas* there were only 10 species, of which *Paspalum vaginatum* Sw. and *Cynodon dactylon* (L.) Pers. presented the highest IVI (49.4 and 17.1%, respectively), corresponding to 66.6% of the total IVI, due to the higher relative values of cover and frequency (Appendix E). Considering those 10 species, *Bulbostylis* sp. was the most common species in the *Salinas*, *Baías*, and *Campos* (with IVIs of 7.17%, 2.76%, and 5.42%, respectively), while the *Poaceae 1* occurred in the *Salinas*, *Vazantes*, and *Campos* (with IVIs of 0.74%, 3.73%, and 17.67%, respectively).

3.4.3 Differences in soil attributes among landscape units

In general, the Spearman correlation values (Figure 4) allowed to distinguish three main soil groups: (i) the clayey, alkaline-sodic, and nutrient-rich soils; (ii) the sandy, acidic, and nutrient-poor soils; and the clayey, acidic, nutrient-rich soils (iii). The first soil group is evidenced by moderate to strong positive correlation values ($r \geq 0.4$) among silt, clay, $_{p}$CEC, Zn, Mg, TOC, Na, NaSI, Ca^{2+}, Mn, K, BS, and PBS. The second soil group is highlighted by moderate to strong negative correlation values ($r \leq 0.4$) among these attributes and CS, Al_{sat}, and P-Rem. The moderate positive correlation between CS and Al_{sat} highlights this. Moderate to strong positive correlations among H+Al and silt, clay, $_{p}$CEC, Zn, Mg, TOC, Cu, Fe, and Al^{3+} indicated the third soil group.

The PCA explained 62.1% of the total data variance, of which 36.9% corresponded to the first dimension and 25.2% to the second one (Figure 5). The *Salinas* soils are the most contrasting group incomparable with the other soils groups. They were more influenced by water pH, Na, K, BS, PBS, P, $_{p}$CEC, and clay, which presented the highest mean values (Figure 6). This indicates salt accumulation and neoformation of clay minerals, due to high evaporation and the disconnection with the surficial drainage.

Figure 4 – Spearman correlation matrix of the soil physico-chemical attributes of the Pantanal of Nhecolândia.

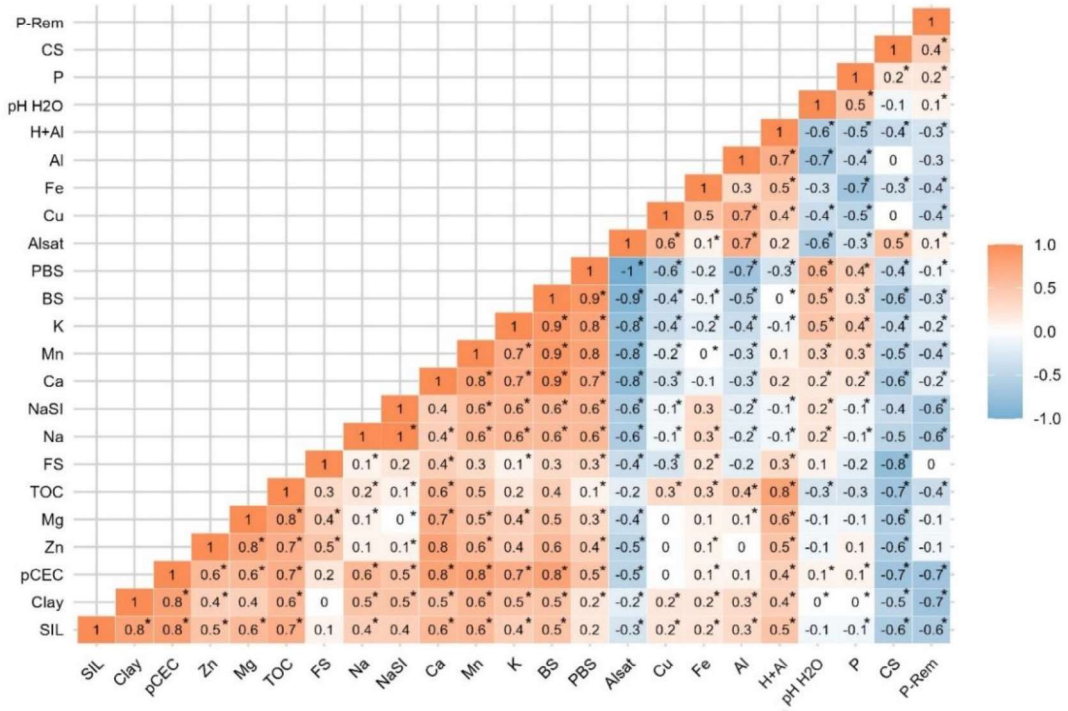

Source: The author.
Note: * $p \leq 0.05$.

Figure 5 – Principal component analysis of the soil physical and chemical attributes of the landscape units of the Pantanal of Nhecolândia, Brazil.

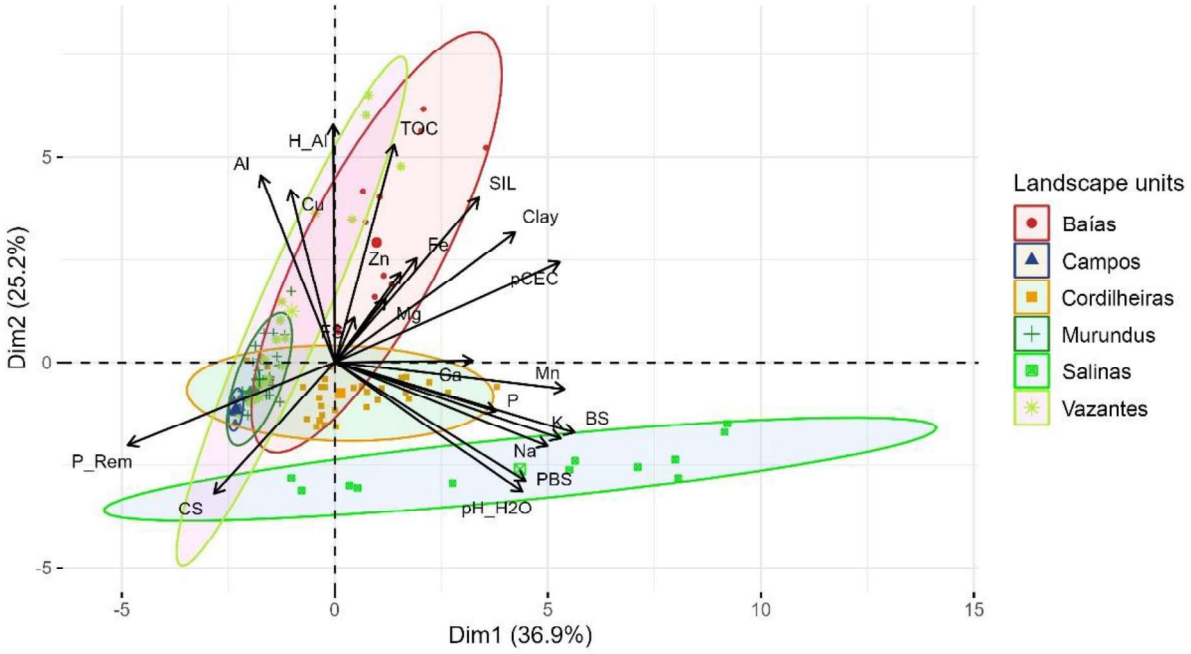

Source: The author.

The variance of the *Cordilheiras* soils was mainly explained by Ca^{2+}, P, and Mn contents (Figure 5), due to nutrient cycling from the organic matter input. However, TOC contents are not significant due lower clay content (Figure 6). The *Baías* soils were more influenced by silt, clay, TOC, and H+Al, and the *Vazantes* soils by TOC, H + Al, and Al^{3+} (Figure 5), Their acidity is evidenced by the highest H+Al values (Figure 6). Soils of the *Murundus* and *Campos* were more influenced by coarse sand and P-Rem (Figure 5), evidencing lower nutrient adsorption capacity. However, the *Murundus* soils presented more significant values of BS, TOC and H+Al, than the surrounding *Campos* soils, due to the influence of nutrients and organic matter from litter decomposition and biological activity (Figure 6).

Figure 6 – Basic statistics of the main soil physical and chemical attributes of the landscape units of the Pantanal of Nhecolândia, Brazil.

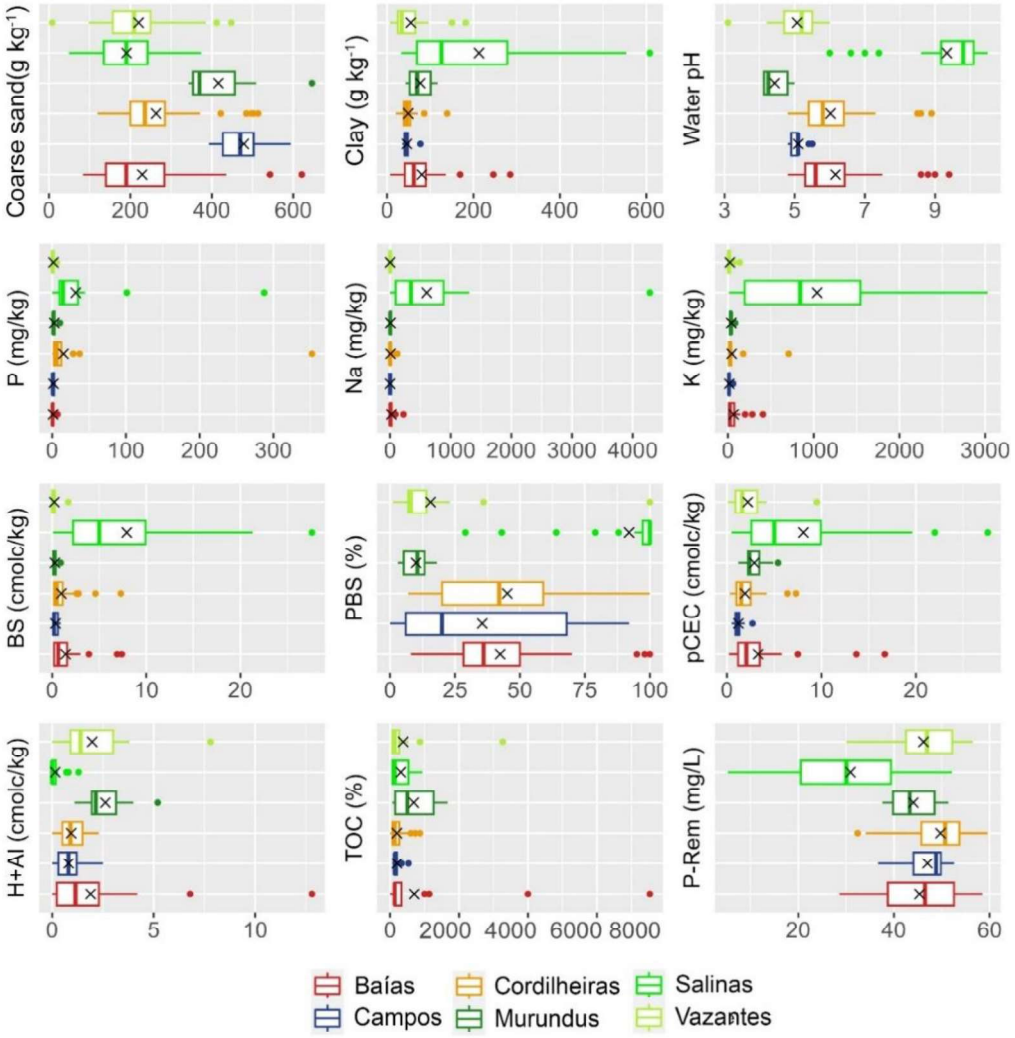

Source: The author.

3.4.4 Effects of soil attributes on species richness and composition

For the species richness, the RF model showed that test performance was almost nearly equal to that observed during cross-validation in the training step, as indicated by the slightly lower MAE and R^2, and slightly higher RMSE (Table 2). For the species composition, the RF model showed superior test performance than the training step, as indicated by the higher R^2 and lower RMSE and MAE. Compared to the null model, RF model's error corresponded to 65 and 17% of the null model's error for species richness and composition, respectively. This indicates a reduction of 35 and 83% in predictive error when applying the RF model for species richness and composition predictions, respectively.

Table 2 – Comparison of the Random Forest (RF) model's performance in the training and test steps, and that of the null model, in predicting species richness and composition.

Model	RMSE	MAE	R^2
Species richness			
RF – training step	1.819	1.295	0.501
RF – test step	1.971	1.286	0.492
Null model	2.744	1.975	-
Species composition			
RF – training step	0.281	0.191	0.920
RF – test step	0.262	0.142	0.936
Null model	1.008	0.823	-

Source: The author

In relation to the residuals of the RF model regression at the test step, we observed that they were higher (> MAE of the test) as higher the species richness value observed (Figure 7). For the species composition, few residuals were higher than the MAE, indicating a better performance of the model. Regarding the RF model residuals considering the whole dataset (Figure 8), we observed that the RF model had more difficulty on predicting the relationship between soil and species richness of the *Murundus* and between soil and composition species of the *Cordilheiras*. This occurred because these landscape units presented the highest values of species richness and composition, respectively, and, in general, regression models have difficulty of predicting extreme values (distant from the average) (Ribeiro; Moniz, 2020).

Figure 7 – Prediction errors (residuals) of species richness (A) and composition (B) at the test step, based on soil attributes using the RF regression model.

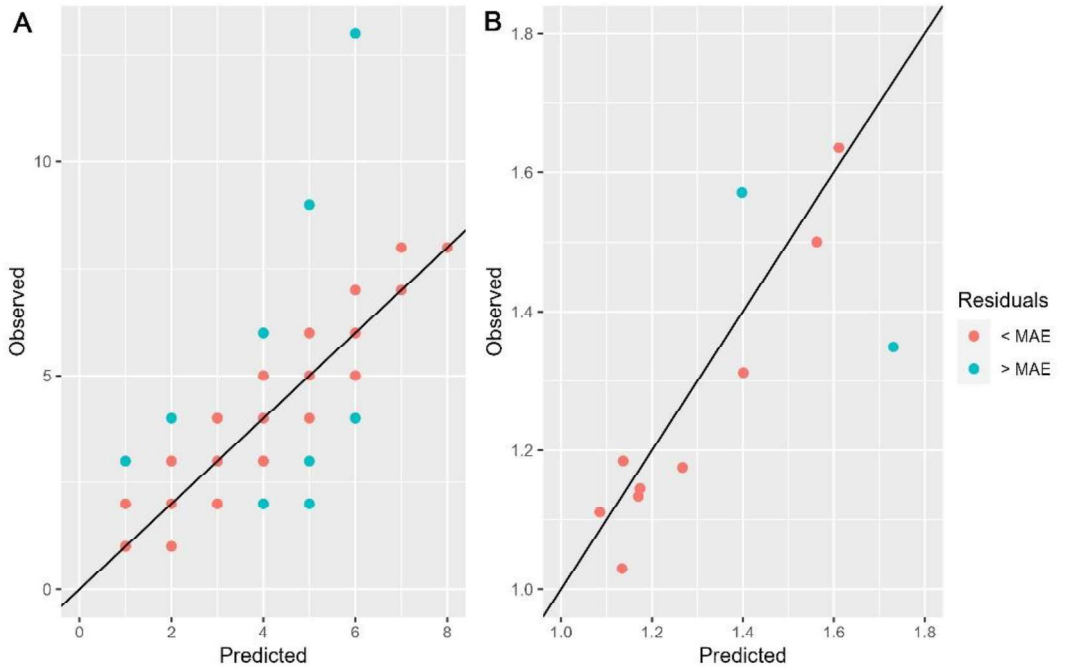

Source: The author.

Figure 8: Random Forest model prediction errors (residuals) of species richness (A) and composition (B) based on soil attributes of the six landscape units of the Pantanal of Nhecolândia, Brazil.

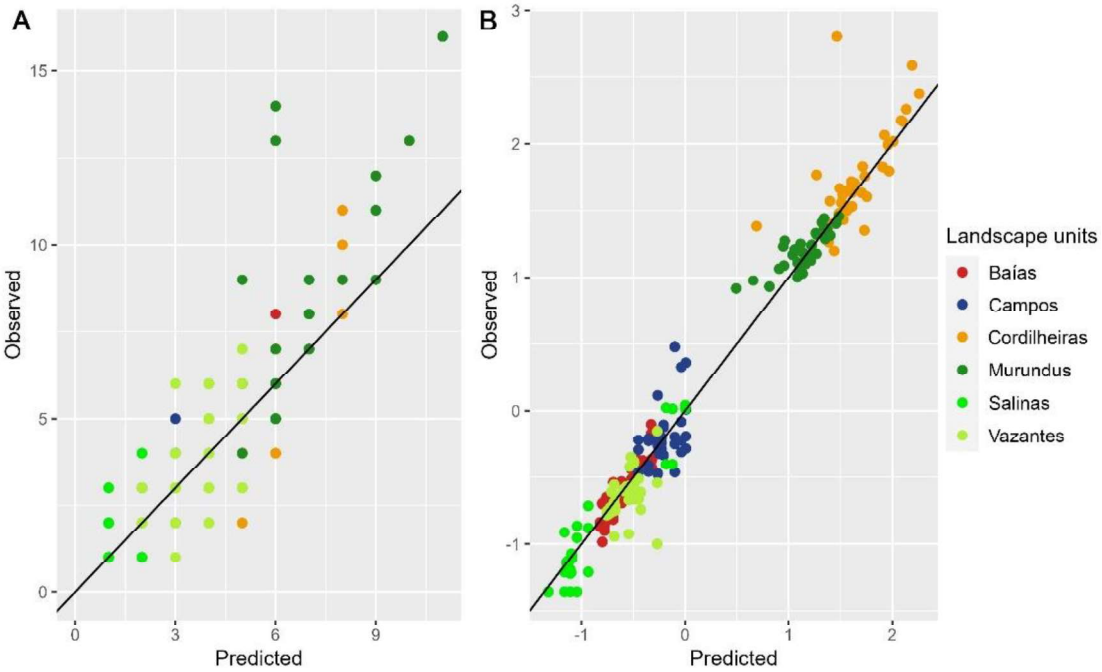

Source: The author.

Regarding the number of variables needed to predict the effect of soil on species richness and composition, out of 13 variables, 5 and 8 were required to stabilize the

performance of the RF model. The variables with more than 50% of importance for species richness were P, Na, water pH, and H+Al, while for species composition they were Na, P, and K (Figure 9).

Figure 9 – Soil physico-chemical attributes with important effects on species richness and composition of the landscape units of Pantanal of Nhecolândia, Brazil.

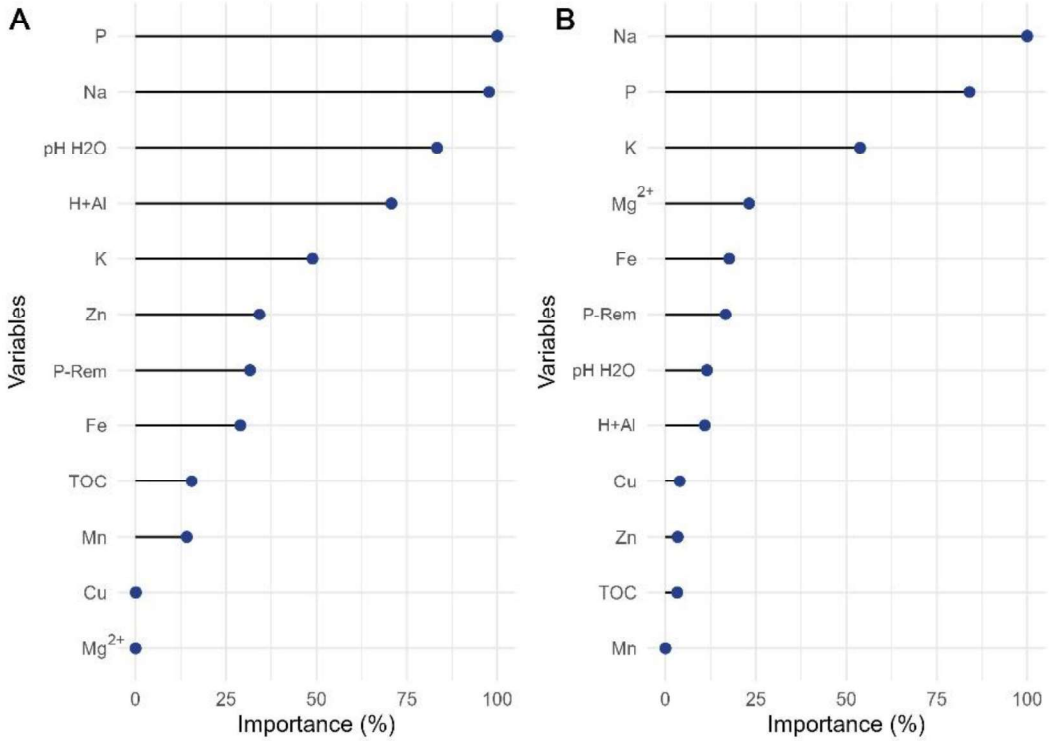

Source: The author.

3.5 DISCUSSION

3.5.1 Community diversity and structure

The most important families identified in our study corroborate the findings of Pott *et al*. (1986), who also highlighted Poaceae as the most numerous families, followed by Fabaceae and Asteraceae in the flora of Nhecolândia region. These families are also the most common of the Cerrado biome (Mantovani; Martins, 1993; Mendonça *et al*., 2008; Munhoz; Felfili, 2007; Warming, 1908). In the evolution history of the lowland flora of the Neotropics, Asteraceae and Poaceae dominated during the dry phase that occurred around 50 to 40 ka (Ledru *et al*., 1996). According to Burnham and Graham (1999), Fabaceae was dominant in both modern and Miocene neotropical floras, but plant diversity was much higher in the Miocene. In the Pantanal, Cerrado species predominate (30%), surpassed only by wide-ranging species (50%), most of

which are herbaceous species (Pott et al., 2011; Pott; da Silva, 2015). This is related to the fact that the Cerrado phytogeographic province covers a wide area surrounding the Pantanal (Adámoli, 1984), and that both regions have climatic similarities, presenting a marked dry season (Alvares *et al*., 2013).

In Nhecolândia, the non-floodable environments exhibited similar floristic composition and structure, with higher species diversity and richness compared to the floodable areas, where herbaceous species predominate. In the herbaceous environments, the Jaccard index was lower than 25%, indicating low similarity (Mueller-Dombois; Ellenberg, 1974). This suggests a high beta diversity among the herbaceous environments, with few similar species and a dominance of species adapted to specific limiting conditions. During the floodings, water affects the lower parts of Nhecolândia, where herbaceous vegetation predominates. Most of the herbaceous species are hemicryptophytes and geophytes, being more resistant to the adverse conditions such as drought and fire (Abdon *et al*., 1998). We observed that species richness and diversity increase as flooding period decreases, corroborating with the findings of Pinder and Rosso (1998) for the southeastern Pantanal.

Among the landscape units, the flooding-free *Cordilheiras* presented the richest and most heterogeneous floristic composition. The high number of species sampled in Nhecolândia's *Cordilheiras* corroborates with other studies conducted in the same subregion (Abdon *et al*., 1998; Pott *et al*., 1986; Ratter *et al*., 1988; Silva *et al*., 2000). *Attalea phalerata* Mart. ex Spreng. (commonly called as Acuri palm), identified as the most important species in the *Cordilheiras*, is commonly found in areas where Cerradão changes to deciduous forest, and serves as an indicator of eutrophic conditions (Abdon *et al*., 1998; Ferreira-Júnior *et al*., 2016b; Ratter *et al*., 1988). Most of the *Cordilheiras* are located surrounding the *Salinas*, where saline or alkaline soils predominate (Costa-Silva *et al*., 2024; Furquim *et al*., 2017). In agreement with Abdon *et al*. (1998), other typical Cerradão species, like *Protium heptaphyllum* (Aubl.) Marchand, was observed in the *Cordilheiras*.

The *Murundus* were the second most heterogenous environment of the Nhecolândia and showed significant similarity to the *Cordilheiras* in terms of floristic composition and structure. In the mounds, typical Cerrado species, such as Ipê roxo and Ipê amarelo (both *Tabebuia* spp.), and Lixeira (*Curatella americana*), form clumps of trees on the termite nests, where sediments accumulate vertically, resulting in flooding scape (Cole, 1960). In our study, Mouriri elliptica and *C. americana* were the most important species in *Murundus*. In the *Murundus* of Pantanal, C. americana has been identified as the most common species (Bordignon *et al*., 2007; Ferreira-Júnior *et al*., 2016b; Marimon *et al*., 2012; Morais *et al*., 2013)

and its occurrence is more related to water table levels than to other soil characteristics, due to its tolerance of inundation (Oliveira-Filho, 1992; Ratter *et al*., 1988). Among the species recorded by Abdon (1998), we also identified the occurrence of *Qualea parviflora* and *Rourea induta*, with lesser importance in our study.

In the *Campos*, surrounding the *Murundus*, the floristic composition was more homogenous, being predominated by Poaceae species, mainly *Elyonurus cf. muticus* (Spreng.) Kuntze. (capim-carona), common in the grassy-woody savana of the Pantanal (Abdon *et al*., 1998; Pott *et al*., 2011). According to Comastri Filho (1984), *E. muticus* are considered an invasive species and a forage plant of low nutritional value. Among the floodable environments, the *Campos* was one of the less diverse, presenting the second lesser values of the Shannon diversity and Pielou's evenness indexes. *E. muticus* occurs in sandy poor soils, only occasionally flooded, and it tends to dominate in the so-called caronal environment (Hess *et al*., 2007; Pott *et al*., 2011). *Stilpnopappus pantanalensis* H. Rob, considered an endemic species indicative of degraded fields (Santos *et al*., 2019) was found among the 10 more important species of the *Campos*.

Among the herbaceous environments, the *Vazantes* was the most heterogenous, due to the dynamism of these environments. In Nhecolândia, the species richness of the *Vazantes* was higher than that reported in seasonally flooded grassland communities of the northern Pantanal (Silva, 2020). Poaceae species were predominant, with *Schizachyrium tenerum* Nees, *Andropogon hypogynus* Hack., and *Paspalum acuminatum* Raddi showing the highest importance values. Notably, *A. hypogynus* Hack. and *Eichhornia azurea* (Sw.) Kunth, two of the 10 most important species, were also reported by Silva (2020) in a tall tussock grassland and a shortgrass floodplain, respectively, with the latter species only occurring during the flooding period.

Following, the *Baías* ranked second among the herbaceous environments in terms of species richness and diversity. In this environment, aquatic plants predominate, with most being amphibious or emergent, due to water level variations throughout the year. During the dry season, which coincided with our period of fieldwork, the *Baías* are the last environment to dry, with some remaining permanently saturated. The *Typha domingensis* Pers. (an emergent aquatic) was the most prominent species in the *Baías*. According to Pott *et al*. (2011), this species occurs in permanent or temporary ponds and increases in disturbed flooded areas. *Eichhornia azurea* (Sw.) Kunth (a rooted floating species), the second most important species, is very common in permanent water bodies of the Pantanal (Pott; Rego; Pott, 1986; Schessl, 1999). *Caperonia castaneifolia* (L.) A. St.-Hil. grows in both aquatic or dry phases, exhibiting

significant dimorphism during the hydrological cycle: large leaves and shoots in the aquatic phase, and short leaves and creeping shoots in the dry season (Schessl, 1999). Among the ten most important species, *Paspalidium paludivagum* (Hitchc. & Chase) Parodi, a species tolerant to salinity, was also found in the *Baías*. This emergent herb is common in the less saline lakes (Pott; Rego; Pott, 1986; Pott; Pott, 2000).

On the other hand, the *Salinas* presented the lower species richness and diversity. The high salinity found in their water and surrounding soils, act as an important filter, because few species are adapted to this condition (Pott; da Silva, 2015). *Paspalum vaginatum* Sw., a common salinity indicator found around the *Salinas* (Pott *et al*., 2011; Pott; Rego; Pott, 1986), was the most important species found, reaching the highest IVI among all the landscape units. The *Cynodon dactylon* (L.) Pers. corresponds to a xerophilous species and was the second most important species found in the *Salinas*. According to (Pott, 1981), xerophilous plants are considered invasive and indicative of pasture degradation, once is during the dry period the overgrazing occurs (Pott, 1981). *C. dactylon* (L.) poses a high nutritional value, and requires clayey and fertile soils to develop, being proper to be cultivated in the *Salinas* at the dry season, when soil is not saturated by water (Comastri Filho, 1984; Leite; Machado, 1999; Pott, 1981).

3.5.2 Soil-vegetation relationships

Sandy, acidic, and nutrient-poor soils predominate in the Pantanal of Nhecolândia, being mainly found in the *Vazantes* and *Campos* landscapes. The richest soils were found surrounding the *Salinas*. Clay and nutrients (Ca^{2+}, Mg^{2+}, K, Na, and P) accumulate in this environment due to neoformation of clay minerals caused by the concentration of solutes and evaporation and salt precipitation processes (Dias *et al*., 2020; Furquim, *et al*., 2010). The soils of the *Cordilheiras* also showed significant base cations content, due to nutrient cycling and subsurface richness, corroborating with Cardoso *et al*. (2016), who also studied the *Cordilheiras* covered by a semideciduous forest at Nhecolândia. The *Murundus* soils were the most acidic, mainly due to the pedobiological turnover of subsurface acid substrates brought from the intense termite activity. Soil organic carbon of the *Baías* was high, due to low microbial decomposition caused by extended periods of water saturation (Tiedje *et al*., 1984). This correlates with the higher soil organic matter found at the *Baías* of Nhecolândia and flooding-affected phytophysiognomies at Barão de Melgaço, during the inundation period (Mello *et al*., 2015).

Available P and exchangeable Na^+ were the main soil attributes affecting species richness and composition at the Nhecolândia landscapes. The P is a macronutrient, essential to plant growth, and the Na is considered benefic for stimulating plant development (Dechen; Nachtigall, 2007). Excess Na^+ is a great problem for plant development in saline soils, altering the nutrient absorption, reducing the root system, and affecting soil structure, which reduces the water infiltration, gas changes, and root growing (Freire; Freire, 2007). This justifies the lower species richness and composition of the natural saline ecosystems of the Nhecolândia *Salinas*, which presented species tolerant to high salinity conditions (halophytes). These species have the capacity of regulating the amount of salt in the shoot while retaining enough water for osmotic adjustments (Lonard; Judd; Stalter, 2015).

In the *Cordilheiras* and *Murundus* soils, landscape units with higher species richness and similar species composition, the available phosphorus varied from low to adequate levels depending on variation in clay content (Sobral *et al*., 2015), indicating a positive influence on vegetation development. In these environments, the organic matter deriving from the vegetation cover is incorporated into the soil through microbial decomposition, which helps increase nutrients in soils (Meurer, 2007). Exchangeable potassium (K^+) was also an important attribute affecting species richness and composition, as this element is involved in various metabolic processes vital to photosynthesis (Dechen; Nachtigall, 2007). *A. phalerata* is typically found in richer, clayey soils (Negrelle, 2015; Pott; Pott, 1994), but it was identified as the most important species in the *Cordilheiras*, where nutrient-rich soils, despite the sandy texture, plays a significant role.

The *Cordilheiras* soils presented the second-highest percentage of base saturation. However, they exhibited a wide range of values, indicating high variability. This results corroborates with Duarte (2007), which indicated that sandy soils with high nutrient content are able to support deciduous forests communities in Barão de Melgaço Pantanal. According to Salis *et al*. (2006), this wide variation in soil base cations in the *Cordilheiras* may be due to anthropogenic disturbances. This areas have been used as planted pasture areas and overgrazing has led to pasture degradation, favoring nutrient leaching and reducing organic carbon content of the soils (Cardoso *et al*., 2009, 2011; Cunha, 1985; Junk *et al*., 2006; Pott, 1988; Silva; Passos, 2018).

Soil water pH and potential acidity (H+Al) also significantly influenced species richness. Aluminum (Al^{3+}) is the main toxic element in tropical soils, affecting root development and, consequently, the plant growth (Meurer, 2007). The acidic soils located at the *Vazantes*, *Baías*, and *Campos* are primarily influenced by leaching, favored by the sandy

texture. These environments showed lower species richness, indicating a negatively effect of the acidity on vegetation. The acidic soils of the *Murundus* are an exception, because the acidity is the result of the humification, the process of humus formation though microbial decomposition, which is rich in organic acids (Sposito, 2008). So, the species richness and composition of the *Murundus* is mainly favored by the nutrients added from the decomposed organic matter.

As observed here and in other studies (Cardoso, 2012; Cardoso *et al*., 2016; Cunha, 1980) sandy soils are widespread in the Nhecolândia landscape units, which contributes to low soil nutrient retention capacity. In this situation, only rustic species, tolerant of such conditions, survive, and some of them dominate due to the low competitiveness of the environment (Cunha, 1980). Most of the sandy soils of the Nhecolândia are affected by flooding during the inundation period, which favors the nutrient leaching and is an additional limiting factor for plant development (Pott; Rego; Pott, 1986).

3.6 CONCLUSIONS

The investigation on soil-vegetation relationships in the Pantanal of Nhecolândia allowed to establish the following conclusions:

1. The floristic composition of the communities of the six landscape units follows a moisture gradient, with the most floodable areas exhibiting lower species richness and composition variability, except for the occasionally flooded *Campos*, where *Elionurus cf. muticus* (Spreng.) Kuntze dominated.

2. Most soils in the Nhecolândia were sandy, acidic and nutrient-poor, except the clayey and nutrient-rich soils of the *Salinas*, due to salt-precipitation and clay minerals neoformation in a closed system controlled by low permeable subsoils.

3. The *Salinas* species richness and composition were negatively affected by Na excess. The P and K contents on the soils of the *Cordilheiras* and *Murundus* positively contribute to the high species richness and composition, and they are the result of the organic matter input from the vegetation cover of these environments. High acidity (lower water pH and high H+Al), promoted by sandy texture and leaching, negatively contributed to species richness and composition of the *Baías*, *Campos*, and *Vazantes* communities.

4. Poaceae, Fabaceae, and Asteraceae were the most numerous families in the wetlands of Nhecolândia region, indicating a predominance of herbaceous plants.

5. According to the RF model prediction, the most important (> 50%) soil attributes affecting the species richness were P, Na, water pH, H+Al, and K; and affecting species composition were Na, P, and K.

6. The RF model showed a predictive capacity 35 and 83% better than the null model (mean value) for the prediction of the soil effect on species richness and compositions.

7. In the sandy domain of Nhecolândia, especially in the species-rich environment of the *Cordilheiras* where deforestation and soil degradation are increasing, the conservation of the vegetation cover is essential for maintaining nutrient cycling balance and, consequently, the biodiversity.

3.7 REFERENCES

ABDON, M. de M. *et al*. Utilização de dados analógicos do LANDSAT-TM na discriminação da vegetação de parte da sub-região da Nhecolândia no Pantanal. **Pesq. agropec. bras.**, [s. l.], v. 33, p. 1799–1813, 1998.

ABRAHÃO, A. *et al*. Soil types select for plants with matching nutrient-acquisition and -use traits in hyperdiverse and severely nutrient-impoverished *Campos* rupestres and cerrado in Central Brazil. **Journal of Ecology**, [s. l.], v. 107, n. 3, p. 1302–1316, 2019.

AB'SÁBER, A. N. **Brasil, paisagens de exceção: o litoral e o Pantanal mato-grossense, patrimônios básicos**. 4. ed. Cotia: Ateliê Editorial, 2011.

ADÁMOLI, J. Fitogeografia do Pantanal. In: Simpósio sobre Recursos Naturais e Sócio-econômicos do Pantanal, 1, 1984, Corumbá. **Anais...** EMBRAPA-DDT, 1984b. p. 105–6.

ALHO, C. J. R. Biodiversity of the Pantanal: response to seasonal flooding regime and to environmental degradation. **Brazilian Journal of Biology**, [s. l.], v. 68, n. 4, p. 957–966, 2008.

ALHO, C. J. R. The Pantanal. In: FRASER, L. H.; KEDDY, P. A. (org.). **The World's Largest Wetlands**. Cambridge: Cambridge University Press, 2005. p. 203–271.

ALVARES, C. A. *et al*. Köppen's climate classification map for Brazil. **Meteorologische Zeitschrift**, [s. l.], v. 22, n. 6, p. 711–728, 2013.

ASSINE, M. L. Brazilian Pantanal: A Large Pristine Tropical Wetland. In: VIEIRA, B. C.; S., RODRIGUES, A. A.; SANTOS, L. J. C. (org.). **Landscapes and Landforms of Brazil**. [S. l.]: Springer Dordrecht, 2015. p. 135–146.

ASSINE, M. L. *et al*. The Quaternary alluvial systems tract of the Pantanal Basin, Brazil. **Brazilian Journal of Geology**, [s. l.], v. 45, n. 3, p. 475–489, 2015.

BACANI, V. M. *et al*. Caracterização das diferenças microclimáticas e pedomorfológicas do entorno de uma lagoa salina no pantanal da Nhecolândia, MS. **Geografia**, [s. l.], v. 35, n. 1, p. 149–163, 2010.

BARBIERO, L. *et al*. Biogeochemical diversity, O2-supersaturation and hot moments of GHG emissions from shallow alkaline lakes in the Pantanal of Nhecolândia, Brazil. **Science of The Total Environment**, [s. l.], v. 619–620, p. 1420–1430, 2018.

BOIN, M. N. *et al*. Pantanal: The Brazilian Wetlands. In: SALGADO, A. A. R.; SANTOS, L. J. C.; PAISANI, J. C. (org.). **The Physical Geography of Brazil**. [S. l.]: Springer Cham, 2019. p. 75–91.

BORDIGNON, L. *et al*. Ilhas Vegetacionais no Pantanal Matogrossense: um teste da Teoria de Biogeografia de Ilhas. **Revista Brasileira de Biociências**, [s. l.], v. 5, n. S1, p. 387–389, 2007.

BRAUN-BLANQUET, J. **Fitosociología, bases para el estudio de las comunidades vegetales**. Madrid: Ed. Blume, 1979.

BURNHAM, R. J.; GRAHAM, A. The History of Neotropical Vegetation: New Developments and Status. **Annals of the Missouri Botanical Garden**, [s. l.], v. 86, n. 2, p. 546–589, 1999.

CALHEIROS, D. F.; FONSECA JÚNIOR, W.C. **Perspectivas de estudos ecológicos sobre o Pantanal**. Corumbá: EMBRAPA-CPAP, 1996.

CARDOSO, E. L. *et al*. Atributos biológicos indicadores da qualidade do solo em pastagem cultivada e nativa no Pantanal. **Pesq. agropec. bras.**, [s. l.], v. 44, n. 6, p. 631–637, 2009.

CARDOSO, E. L. *et al*. Qualidade química e física do solo sob vegetação arbórea nativa e pastagens no Pantanal Sul-Mato-Grossense. **Revista Brasileira de Ciência do Solo**, [s. l.], v. 35, n. 2, p. 613–622, 2011.

CARDOSO, E. L. *et al*. Relação entre solos e unidades da paisagem no ecossistema Pantanal. **Pesquisa Agropecuária Brasileira**, [s. l.], v. 51, n. 9, p. 1231–1240, 2016.

CARDOSO, E. L. C. **X Reunião Brasileira de Classificação de Solos**. Pantanal e Cerrado. Guia de Campo. Corumbá-MS: SBCS: EMBRAPA-UFRPE, 2012.

CHAO, A. *et al*. Rarefaction and extrapolation with Hill numbers: a framework for sampling and estimation in species diversity studies. **Ecological Monographs**, [s. l.], v. 84, n. 1, p. 45–67, 2014.

CHEN, Hanbo; BOUTROS, Paul C. **VennDiagram**: a package for the generation of highly-customizable Venn and Euler diagrams in R. [s. l.], 2011. Available in: http://www.biomedcentral.com/1471-2105/12/35. Acessed in: 17 sep. 2024.

COLE, M. M. Cerrado, Caatinga and Pantanal: The Distribution and Origin of the Savanna Vegetation of Brazil. **The Geographical Journal**, [s. l.], v. 126, n. 2, p. 168–179, 1960.

COLWELL, R. K. *et al*. Models and estimators linking individual-based and sample-based rarefaction, extrapolation and comparison of assemblages. **Journal of Plant Ecology**, [s. l.], v. 5, n. 1, p. 3–21, 2012.

COUTO, E. G.; OLIVEIRA, Virlei Álvaro. The Soil Diversity of the Pantanal. In: JUNK, W. J. *et al*. (org.). **The Pantanal: Ecology, biodiversity and sustainable management of a large neotropical seasonal wetland**. Moscow: Pensoft Publishers, 2010. p. 71–102.

COMASTRI FILHO, J. A. Pastagens nativas e cultivadas no Pantanal mato-grossense. Corumbá: EMBRAPA/UEPAE de Corumbá, 1984.

COSTA-SILVA, A. R. *et al*. Soils surrounding saline-alkaline lakes of Nhecolândia, Pantanal, Brazil: Toposequences, mineralogy and chemistry. **Geoderma Regional**, [s. l.], v. 36, p. e00746, 2024.

CRISPIM, S. M. A. *et al*. **Efeito da cheia fluvial na dinâmica das pastagens, Pantanal da Nhecolândia, MS**. 1. ed. Corumbá: Embrapa Pantanal, 2006.

CUNHA, N. G. da. **Considerações sobre os solos da sub-região da Nhecolândia, Pantanal Mato-grossense**. Corumbá: [s. n.], 1980.

CUNHA, N. G. da. **Dinâmica de nutrientes em solos arenosos o Pantanal mato-grossense**. Corumbá: Embrapa/CPAP, 1985.

CURTIS, J. T.; MCINTOSH, R. P. An Upland Forest Continuum in the Prairie-Forest Border Region of Wisconsin. **Ecology**, [s. l.], v. 32, n. 3, p. 476–496, 1951.

CUTLER, D. Richard *et al*. Random forests for classification in Ecology. **Ecology**, [s. l.], v. 88, n. 11, p. 2783–2792, 2007.

DECHEN, A. R.; NACHTIGALL, G. R. Elementos requeridos à nutrição de plantas. In: NOVAIS, Roberto Ferreira *et al*. (org.). **Fertilidade do Solo**. Viçosa - MG: Sociedade Brasileira de Ciência do Solo, 2007. p. 91–132.

DIAS, I. A. *et al*. The Occurrence of Authigenic Clay Minerals in Alkaline-Saline Lakes, Pantanal Wetland (Nhecolândia Region, Brazil). **Minerals**, [s. l.], v. 10, n. 8, p. 718, 2020.

DUARTE, T. G. **Florística, fitossociologia e relações solo-vegetação em floresta estacional decidual em Barão de Melgaço, Pantanal de Mato Grosso**. 2007. 1–144 f. Tese - Universidade Federal de Viçosa, Viçosa-MG, 2007.

EITEN, G. The cerrado vegetation of Brazil. **The Botanical Review**, [s. l.], v. 38, n. 2, p. 201–341, 1972.

FERNANDES-FILHO, E. I. *et al*. Methods and Challenges in Digital Soil Mapping: Applied Modelling with R Examples. In: CARVALHO JUNIOR, W. de; *et al*. (eds.). **Pedometrics in Brazil**. Switzerland: Springer Cham, 2024. p. 263–283.

FERREIRA-JÚNIOR, W. G. *et al*. Flood regime and water table determines tree distribution in a forest-savanna gradient in the Brazilian Pantanal. **Anais da Academia Brasileira de Ciências**, [s. l.], v. 88, n. suppl 1, p. 719–731, 2016.

FREIRE, M. B. G. dos S.; FREIRE, F. J. Fertilidade do solo e seu manejo em solos afetados por sais. In: NOVAIS, R. F. *et al*. (org.). **Fertilidade do Solo**. Viçosa-MG: Sociedade Brasileira de Ciência do Solo, 2007. p. 929–954.

FURIAN, S. *et al*. Chemical diversity and spatial variability in myriad lakes in Nhecolândia in the Pantanal wetlands of Brazil. **Limnology and Oceanography**, [s. l.], v. 58, n. 6, p. 2249–2261, 2013.

FURQUIM, S. A. C. *et al*. Salt-affected soils evolution and fluvial dynamics in the Pantanal wetland, Brazil. **Geoderma**, [s. l.], v. 286, p. 139–152, 2017.

FURQUIM, S. A. C. *et al*. Soil mineral genesis and distribution in a saline lake landscape of the Pantanal Wetland, Brazil. **Geoderma**, [s. l.], v. 154, n. 3–4, p. 518–528, 2010b.

FURQUIM, S. A. C.; VIDOCA, T. T. Salt-Affected Soils of Pantanal Wetland. In: TALEISNIK, Edith; LAVADO, R. S. (org.). **Saline and Alkaline Soils in Latin America**. Cham: Springer International Publishing, 2021. p. 229–254.

GARCIA, E. A. C. O **Clima no Pantanal Mato-grossense**. Corumbá: EMBRAPA, 1984.

GODOI, H. de O; MARTINS, E. G.; MELLO, J. C. R. de. **Programa Levantamentos Geológicos Básicos do Brasil - PLGB. Corumbá – Folha SE.21-Y-D, Aldeia Tomázia, Folha SF.21-V-B, Porto Murtinho, Folha SF.21-V-D, Estado de Mato Grosso do Sul**. Escala 1:250.000. Brasília: [s. n.], 2001

GRADELLA, F.; QUÉNOL, H.; SAKAMOTO, A. Variation du niveau phréatique d'une saline dans le Pantanal en relation avec les précipitations et les inondations provoquées par le fleuve Paraguai (Brésil). **AIC 2009 Cluj**. Romênia: [s. n.], 2009. p. 223–228.

GUERREIRO, R. L. *et al*. The soda lakes of Nhecolândia: A conservation opportunity for the Pantanal wetlands. **Perspectives in Ecology and Conservation**, [s. l.], v. 17, n. 1, p. 9–18, 2019.

HESS, S. C. *et al*. Evaluation of seasonal changes in chemical composition and antibacterial activity of *Elyonurus muticus* (sprengel) O. Kuntze (Gramineae). **Química Nova**, [s. l.], v. 30, n. 2, p. 370–373, 2007.

HSIEH, T. C.; MA, K. H.; CHAO, Anne. iNEXT: an R package for rarefaction and extrapolation of species diversity. **Methods in Ecology and Evolution**, [s. l.], v. 7, n. 12, p. 1451–1456, 2016.

HUSSON, F. *et al*. **"FactoMineR" package multivariate**: exploratory data analysis and data mining. [S. l.], 2019.

IVORY, Sarah J *et al*. Vegetation, rainfall, and pulsing hydrology in the Pantanal, the world's largest tropical wetland. **Environmental Research Letters**, [s. l.], v. 14, n. 12, p. 124017, 2019.

JUNK, Wolfgang J. *et al*. Biodiversity and its conservation in the Pantanal of Mato Grosso, Brazil. **Aquatic Sciences**, [s. l.], v. 68, n. 3, p. 278–309, 2006.

JUNK, W. J. *et al*. Brazilian wetlands: their definition, delineation, and classification for research, sustainable management, and protection. **Aquatic Conservation: Marine and Freshwater Ecosystems**, [s. l.], v. 24, n. 1, p. 5–22, 2014.

KEDDY, P. A. *et al*. Wet and Wonderful: The World's Largest Wetlands Are Conservation Priorities. **BioScience**, [s. l.], v. 59, n. 1, p. 39–51, 2009.

KUHN, M. **Caret**: Classification and regression training. [S. l.], 2019.

LEDRU, M. *et al*. The last 50,000 years in the Neotropics (Southern Brazil): evolution of vegetation and climate. **Palaeogeography, Palaeoclimatology, Palaeoecology**, [s. l.], v. 123, p. 239–257, 1996.

LEGENDRE, P.; LEGENDRE, L. **Numerical Ecology**. Amsterdam: Elsevier Science, 2012.

LEITE, G. G.; MACHADO, F. O. C. **Capim "Coast-cross" (*Cynodon dactylon* (L.) Pers)**. Planaltina-DF: Embrapa, 1999.

LONARD, R. I.; JUDD, F. W.; STALTER, R. Biological Flora of Coastal Dunes and Wetlands: *Paspalum vaginatum* Sw. **Journal of Coastal Research**, [s. l.], v. 31, n. 1, p. 213, 2015.

MAGURRAN, Anne E. **Measuring biological diversity**. Oxford: Blackwell Science, 2004.

MANTOVANI, Waldir; MARTINS, Fernando Roberto. Florística do cerrado na Reserva Biológica de Moji Guaçu, SP. **Acta bot. bras.**, [s. l.], v. 7, n. 1, p. 33–60, 1993.

MAPBIOMAS. Projeto MapBiomas - Mapeamento Anual de Cobertura e Uso da Terra no Brasil - Coleção 9. [S. l.], 2024.

MARIMON, B. S. *et al*. Florística dos *Campos* de *Murundus* do Pantanal do Araguaia, Mato Grosso, Brasil. **Acta Botanica Brasilica**, [s. l.], v. 26, n. 1, p. 181–196, 2012.

MCGLUE, M. M. *et al*. Holocene stratigraphic evolution of saline lakes in Nhecolândia, southern Pantanal wetlands (Brazil). **Quaternary Research**, [s. l.], v. 88, n. 3, p. 472–490, 2017.

MELLO, J. M. *et al*. Dinâmica dos atributos físico-químicos e variação sazonal dos estoques de carbono no solo em diferentes fitofisionomias do Pantanal Norte Mato-Grossense. **Revista Árvore**, [s. l.], v. 39, n. 2, p. 325–336, 2015.

MENDONÇA, R. C. de *et al*. Flora Vascular do Bioma Cerrado: Checklist com 12.356 espécies. In: SANO, S. M.; ALMEIDA, S. P. de; RIBEIRO, J. F. (org.). **Cerrado**: Ecologia e Flora. Brasília: Embrapa Informação Tecnológica, 2008. v. 2, p. 421–442.

MEURER, Egon J. Fatores que influenciam o crescimento e o desenvolvimento de plantas. In: NOVAIS, R. F. *et al*. (org.). **Fertilidade do Solo**. Viçosa-MG: Sociedade Brasileira de Ciência do Solo, 2007. p. 65–90.

MORAIS, R. F. de *et al*. Composição florística e estrutura da comunidade vegetal em diferentes fitofisionomias do Pantanal de Poconé, Mato Grosso. **Rodriguésia**, [s. l.], v. 64, n. 4, p. 775–790, 2013.

MUELLER-DOMBOIS, D.; ELLENBERG, H. **Aims and methods of vegetation ecology**. John Wiley, [s. l.], p. 1–547, 1974.

MUNHOZ, C. B. R.; FELFILI, J. M. Florística do estrato herbáceo-subarbustivo de um campo limpo úmido em Brasília, Brasil. **Biota Neotropica**, [s. l.], v. 7, n. 3, p. 205–215, 2007.

NEGRELLE, R. R. B. *Attalea phalerata* Mart. Ex Spreng.: Aspectos botânicos, ecológicos, etnobotânicos e agronômicos. **Ciência Florestal**, [s. l.], v. 25, n. 4, p. 1061–1066, 2015.

OKSANEN, J. *et al*. **Vegan**: community ecology package. [S. l.]: R package version 2.5-2, 2018.

OLIVEIRA-FILHO, A. T. de *et al*. Environmental factors affecting physiognomic and floristic variation in an area of cerrado in central Brazil. **Journal of Tropical Ecology**, [s. l.], v. 5, n. 4, p. 413–431, 1989.

OLIVEIRA-FILHO, A.T. de. Floodplain "*Murundus*" of Central Brazil: evidence for the termite-origin hypothesis. **Journal of Tropical Ecology**, [s. l.], v. 8, p. 1–19, 1992.

PADOVANI, C. R. **Dinâmica Espaço-Temporal das Inundações do Pantanal.** 2010. 1–175 f. Tese (Doutorado) - Escola Superior de Agricultura "Luiz de Queiroz", Piracicaba, 2010.

PINDER, L.; ROSSO, S. Classification and ordination of plant formations in the Pantanal of Brazil. **Plant Ecology**, [s. l.], v. 136, p. 151–165, 1998.

PONCE, V. M.; DA CUNHA, C. N. Vegetated earthmounds in tropical savannas of Central Brazil: a synthesis. **Journal of Biogeography**, [s. l.], v. 20, n. 2, p. 219–225, 1993.

POTT, Vali J. *et al*. **Flora da fazenda Nhumirim, Nhecolândia, Pantanal. Relação preliminar**. Corumbá: EMBRAPA/CPAP, 1986.

POTT, Arnildo. **Pastagens das sub-regiões dos Paiaguás e da Nhecolândia do Pantanal mato-grossense**. Corumbá: Embrapa, 1981.

POTT, Arnildo. **Pastagens no Pantanal**. Corumbá: Embrapa/CPAP, 1988.

POTT, A. *et al*. Plant diversity of the Pantanal wetland. **Brazilian Journal of Biology**, [s. l.], v. 71, n. 1, p. 265–273, 2011.

POTT, Arnildo; DA SILVA, João Santos Vila. Terrestrial and Aquatic Vegetation Diversity of the Pantanal Wetland. In: [S. l.: s. n.], 2015. p. 111–131.

POTT, A., DA SILVA, J.S.V. (2015). Terrestrial and Aquatic Vegetation Diversity of the Pantanal Wetland. In: BERGIER, I., ASSINE, M. (eds) **Dynamics of the Pantanal Wetland in South America**. The Handbook of Environmental Chemistry, vol 37. Springer, Cham.

POTT, A.; POTT, V. J. Features and conservation of the Brazilian Pantanal wetland. **Wetlands Ecology and Management**, [s. l.], v. 12, p. 547–552, 2004.

POTT, V.J.; POTT, A. **Plantas Aquáticas do Pantanal**. Corumbá, MS: EMBRAPA, 2000.

POTT, A.; POTT, V.J. **Plantas do Pantanal**. Corumbá, MS: EMBRAPA, 1994.

POTT, V. J.; REGO, S. C. de A.; POTT, A. **Plantas uliginosas e aquáticas do Pantanal Arenoso**. Corumbá: EMBRAPA/CPAP, 1986.

PRASAD, A. M.; IVERSON, L. R.; LIAW, A. Newer Classification and Regression Tree Techniques: Bagging and Random Forests for Ecological Prediction. **Ecosystems**, [s. l.], v. 9, n. 2, p. 181–199, 2006.

R CORE TEAM. **R**: A language and environment for statistical computing. Viena: R Foundation for Statistical Computing, 2024.

RATTER, J. A. *et al*. Analysis of the floristic composition of the Brazilian cerrado vegetation II: Comparison of the woody vegetation of 98 areas. **Edinburgh Journal of Botany**, [s. l.], v. 53, n. 2, p. 153–180, 2010.

RATTER, J. A. *et al*. Observations on woody vegetation types in the Pantanal and at Corumbá, Brazil. **Notes RGB Edinb**., [s. l.], v. 45, n. 3, p. 503–525, 1988.

RIBEIRO, R. P.; MONIZ, Nuno. Imbalanced regression and extreme value prediction. **Machine Learning**, [s. l.], v. 109, n. 9–10, p. 1803–1835, 2020.

RIBEIRO, J. F.; WALTER, B. M. T. Fitofisionomias do bioma cerrado. In: SANO, S. M.; ALMEIDA, S. P. de (org.). **Cerrado**: ambiente e flora. Planaltina: EMBRAPA-CPAC, 1998. p. 89–166.

SALIS, S. M. *et al*. Distribuição e abundância de espécies arbóreas em cerradões no Pantanal, Estado do Mato Grosso do Sul, Brasil. **Revista Brasileira de Botânica**, [s. l.], v. 29, n. 3, 2006.

SANTOS, S. A. *et al*. **Guia para identificação das pastagens nativas do Pantanal**. Corumbá-MS: Embrapa Pantanal, 2019.

SCHESSL, M. Floristic Composition and Structure of Floodplain Vegetation in the Northern Pantanal of Mato Grosso, Brazil. **Phyton**, [s. l.], v. 39, n. 2, p. 303–336, 1999.

SILVA, M. P. da *et al*. Fitossociologia e estrutura de cerradão e mata semidecídua do Pantanal da Nhecolândia, MS. In: Simpósio sobre Recursos Naturais e Sócio-econômicos do Pantanal, 3, Corumbá, **Anais...** Corumbá-MS: [s. n.], 2000. p. 1–23.

SILVA, F. H. B. da. **Florística e biomassa da vegetação de *Campos* sazonalmente inundáveis do Pantanal de Mato Grosso**. 2020. 1–140 f. Tese de doutorado - Universidade Federal do Rio Grande do Sul, Porto Alegre, 2020.

SILVA, A.E. *et al*. **Manual de métodos de análise de solo**. 3. ed. Brasília: EMBRAPA, 2017.

SILVA, J. dos S. V. da; ABDON, M. de M. Delimitação do Pantanal Brasileiro e suas Sub-Regiões. **Pesq. agropec. bras**, [s. l.], v. 33, p. 1703–1711, 1998.

SILVA, M. H. S.; PASSOS, M. M. Discourse analysis of the authors/actors from the Nhecolândia Pantanal. **Mercator**, [s. l.], v. 17, n. 07, p. 1–16, 2018.

SOBRAL, L. F. *et al*. **Guia Prático para Interpretação de Resultados de Análises de Solo**. Aracajú: Embrapa Tabuleiros Costeiros, 2015.

SPOSITO, G. The Chemistry of Soils. 2. ed. [S. l.]: Oxford University Press, 2008.

TRICART, J. El Pantanal: um ejemplo del impacto geomorfológico sobre el ambiente. **Inform. Geogr.**, Chile, v. 29, p. 81-97, 19982.

THESSEN, A. Adoption of Machine Learning Techniques in Ecology and Earth Science. **One Ecosystem**, [s. l.], v. 1, p. e8621, 2016.

TIEDJE, J. M. *et al*. Anaerobic processes in soil. **Plant and Soil**, [s. l.], p. 197–212, 1984.

USSAMI, N.; SHIRAIWA, S.; DOMINGUEZ, J. M. L. Basement reactivation in a sub-Andean foreland flexural bulge: The Pantanal wetland, SW Brazil. **Tectonics**, [s. l.], v. 18, n. 1, p. 25–39, 1999.

VALLADARES, Fernando *et al*. Species coexistence in a changing world. **Frontiers in Plant Science**, [s. l.], v. 6, 2015.

VALVERDE, O. Fundamentos Geográficos do Planejamento do Município de Corumbá. **Revista Brasileira de Geografia**, [s. l.], v. 34, n. 1, p. 49–144, 1972.

VOURLITIS, George L *et al*. Variations in aboveground vegetation structure along a nutrient availability gradient in the Brazilian pantanal. **Plant and Soil**, [s. l.], v. 389, n. 1–2, p. 307–321, 2015.

WARMING, Eugênio. Lagoa Santa: **Contribuição para a Geographia Phytobiologica**. Belo Horizonte: Imprensa oficial do estado de Minas Gerais, 1908.

YEOMANS, J. C.; BREMNER, J. M. A rapid and precise method for routine determination of organic carbon in soil. **Communications in Soil Science and Plant Analysis**, [s. l.], v. 19, n. 13, p. 1467–1476, 1988.

ZANI, H.; ASSINE, M. L.; MCGLUE, M. M. Remote sensing analysis of depositional landforms in alluvial settings: Method development and application to the Taquari megafan, Pantanal (Brazil). **Geomorphology**, v. 161–162, p. 82-92, 2012.

ZAVATTINI, J. A. A distribuição das chuvas e a circulação atmosférica no estado de Mato Grosso do Sul. In: As chuvas e as massas de ar no estado de Mato Grosso do Sul: Estudos Geográficos com vista à regionalização climática. [S. l.]: **Cultura Acadêmica**, 2009. p. 59–92.

ZEILHOFER, P.; SCHESSL, M. Relationship between Vegetation and Environmental Conditions in the Northern Pantanal of Mato Grosso, Brazil. **Journal of Biogeography**, [s. l.], v. 27, n. 1, p. 159–168, 2000.

4 CHAPTER 3: Soil genesis and landscape evolution in the Nhecolândia Pantanal wetland, central Brazil

4.1 ABSTRACT

The Pantanal landscape is marked by relict landforms shaped by neotectonic activity and changes in climate and inundation regimes, reflecting a complex evolutionary history. This study evaluated soil-forming processes and landscape evolution in the Pantanal of Nhecolândia using a pedological and geochronological approach. Six landscape units were analyzed: saline lakes (*Salinas*), freshwater lakes (*Baías*), sand levees (*Cordilheiras*), floodable lowlands (*Vazantes*), termite mounds fields (*Murundus*), and occasionally flooded grasslands (*Campos*). Twelve soil profiles were characterized for (macro and micro) morphology, granulometry, chemistry, mineralogy, and geochemistry, with classification based on Brazilian and international classification systems. Stable carbon isotopes and dating techniques were used to assess landscape evolution. The Nhecolândia soils are predominantly sandy, acidic, kaolinitic, and nutrient-poor, due to sandy parent material. Pedological differences are driven by climate, relief, and biological activity. In *Salinas*, salinization, sodification, and calcification processes dominated, forming nutrient-rich soils with 2:1 minerals under high evaporation and an endorheic system. Soil variation in the *Salinas* is linked to progressive drainage of the lakes, evidenced by hydroxy-Al interlayered minerals formation under increasing leaching. *Baías* exhibited Arenosols and Planosols, influenced by paludization, and solodization, suggesting they evolved from former *Salinas*. *Cordilheiras* and *Murundus* Arenosols are enriched by organic matter from litter and termite activity, with Planosols showing salinization, calcification, sodification, and amorphous silica cementation, from alkaline groundwater. *Campos* and *Vazantes* soils are acidic and nutrient-poor due to intense leaching, with *Vazantes* Podzol, showing ferrolysis and crystalline Fe oxides. Minimum ages for *Salinas* and *Baías* are ~6,110 and ~6,585 years BP, while *Vazantes* range from ~4,680-8,970 years BP. C3 plants dominate in the *Baías* and lower *Vazantes* since the Middle Holocene, with *Salinas* and upper *Vazantes* transitioning from savannah-like C3 vegetation to C4 grasslands in Late Holocene due to hydrological shifts. Ongoing hydrological and climatic changes promoted generalized leaching and acidification in the floodable environments, altering soil-landscape dynamics.

Keywords: Pedogenesis. Salinization. Solodization. Ferrolysis. Paleoenvironment.

4.2 INTRODUCTION

The Pantanal is one of the world's largest continental wetlands (Keddy *et al*., 2009), located in the Upper Paraguay River Basin and covering approximately 140,000 km² (38% of the basin area) (Silva; Abdon, 1998). Although it means "swamp" in Portuguese, the Pantanal has very contrasting wet and dry seasons (Garcia, 1984), with a complex hydrological dynamic, influenced by the varying inundation regime and geomorphological features (Assine *et al*., 2015; Tricart, 1982). The water dynamics in the Pantanal clearly affect vegetation and soils, creating various habitats throughout the year and, consequently, supporting high pedobiodiversity (Alho, 2008; Alho; Silva, 2012; Couto; Oliveira, 2010; Ivory *et al*., 2019). The Pantanal landscape contains many relict landforms due to neotectonic activity and historical changes in the climate and inundation regimes (Bezerra *et al*., 2019; Oliveira *et al*., 2018; Soares; Soares; Assine, 2003). For instance, the abandoned southern alluvial fan of the Taquari megafan, known as the Nhecolândia subregion, is notable for its more than 10,000 closed lakes, which exhibit significant variations in shape and water geochemistry, as well as its unconsolidated sandy sheets (Barbiero *et al*., 2002; Oliveira *et al*., 2018).

The Pantanal provides numerous ecosystemic services, such as supporting biological diversity, offering feeding and reproductive niches, carbon storage, controlling floods, recharging aquifer, and sustaining fish production (Alho, 2005a, 2008; Freitas *et al.*, 2019; Guerreiro *et al*., 2019). Additionally, cattle ranching in Pantanal, the main economic activity of the region, is considered one of the most important significant examples of sustainable natural resources use in the global South, balancing environmental protection with the production of over 3.8 million cattle (Chiaravalloti *et al*., 2023). However, this cattle production system is threatened by more intensive cattle production on the surrounding plateaus, which leads to deforestation, biodiversity loss, and soil degradation in these elevated areas and in the Pantanal lowland, which directly impacts the hydrological regime (Alho, 2005a; Guerra *et al*., 2020a, 2020b). In the case of the Taquari megafan, the sediment supply of its channel has increased in the last 30 years due to pasture expansion and intensive agriculture (Assine, 2005). Climate change predictions point to a combined scenario of reduced rainfall, higher temperatures and increased deforestation (Guerra *et al*., 2020a; Marengo; Alves; Torres, 2016), which heighten the Pantanal's fragility and risk of desertification, especially in the sandy Nhecolândia subregion (Soares; Soares; Assine, 2003).

Understanding the evolutionary history of the Pantanal has posed a challenge for scientists due to its complexity. Since the early studies, up to the present day, a variety of

techniques has been employed, including remote and proximal sensing (Tricart, 1982; Macedo *et al*., 2014; Oliveira *et al*., 2018; Taioli *et al*., 2021), lake sediment analysis (McGlue *et al*., 2012, 2017; Metcalfe *et al*., 2014), examination of alluvial and floodplain strata (Assine, 2005; Gradella *et al*., 2011), study of terrestrial carbonates (Bertaux *et al*., 2002), analysis of microfossils (Bezerra *et al*., 2019; Kuerten *et al*., 2013; Rasbold *et al*., 2019), carbon stable isotope data (Rasbold *et al*., 2024; Victoria *et al*., 1995) and soil investigations (De Queiroz *et al*., 2017; Ferreira-Júnior *et al*., 2016; Merdy *et al*., 2022; Nascimento *et al*., 2015, 2024; Oliveira Junior *et al*., 2017, 2019), to gather hydroclimatic and paleoecological information that can elucidate the Pantanal's Quaternary history. Integrated landscape studies in the Pantanal are essential for understanding the dynamics and evolution of the landscape components, providing valuable tools for effective land planning and management.

Pedological studies in Pantanal of Nhecolândia have been focused on describing the soils attributes and classification (Cardoso, 2012; Cunha, 1980), soil landscape relationships (Barbiero *et al*., 2008; Cardoso *et al*., 2011, 2016), mineralogical composition (Andrade *et al*., 2020; Barbiero *et al*., 2016; Dias *et al*., 2020; Furquim *et al*., 2008; Furquim *et al*., 2010), and soil genesis with a primary focus on the formation and evolution of the alkaline-saline lakes (Bacani *et al*., 2010; Costa-Silva *et al*., 2024; Furian *et al*., 2013; Furquim *et al*., 2017). Soils, as products of interactions among landscape components (Jenny, 1941) exhibit morphological, mineralogical, physical, and chemical characteristics shaped by pedogenetic processes that are closely linked to the climatic conditions over time (Gelybó *et al*., 2018). The lacustrine system of the Nhecolândia is an intriguing example of how the soil-geomorphology interaction may govern pedological and biological processes over time (Barbiero *et al*., 2002; McGlue *et al*., 2017; Rasbold *et al*., 2019, 2024).

Besides the myriad lakes, the Nhecolândia subregion also stands out by its heterogenous landscape (Nunes da Cunha; Junk, 2009) formed over a uniform and poor sandy substrate that has been remobilized and altered by many fluvial, aeolian, and pedological processes as a result of changes in the climate, sedimentation, and hydrological regimes (McGlue *et al*., 2017; Soares; Soares; Assine, 2003). To date, few studies (Cardoso *et al*., 2016; Cunha, 1980; Reis, 2017) have sought to evaluate soil genesis and interactions among the different landscape units of the Pantanal of Nhecolândia. In this context, we aimed to assess the soil-forming processes and the evolution of the Nhecolândia landscape units through an integrated pedological and chronological approach.

4.3 MATERIAL AND METHODS

4.3.1 Study area

The Brazilian Pantanal is located in the Upper Paraguay River Basin (UPRB), in the states of Mato Grosso and Mato Grosso do Sul. The Pantanal covers an area of 138.183 km2 and was sub-divided into 11 sub-regions according to differences related to flood regime, relief, soil and vegetation (Silva; Abdon, 1998). The Nhecolândia is the second largest Pantanal sub-region, covering an area of 26.921 km², and is in the southern portion of the Taquari megafan (Silva; Abdon, 1998). It is placed in the municipalities of Corumbá, Aquidauana, and Rio Verde de Mato Grosso, in Mato Grosso do Sul, ranging from the latitudes 18°12'52.76"S and 19°40'12.46"S, and the longitudes 54°52'39.21"W and 57°13'24.67"W (Figure 1).

The climate of the Pantanal is classified as Aw, according to the Köppen system, indicating a tropical continental climate with dry winter (Alvares *et al*., 2013). In the Nhecolândia, the mean annual air temperature is 26 ºC, and the mean annual rainfall is 1,206 mm (Garcia, 1984). The rainy season occurs between November and March, while the period of strong water deficit ranges from August to October (Garcia, 1984). The flooding season occurs from March to May (Garcia, 1984) and is mainly caused by local precipitation or groundwater elevation (Gradella; Quénol; Sakamoto, 2009; Padovani, 2010).

The sedimentary lithology of the Pantanal consists of poorly consolidated fine- to coarse-grained sandstones, which form the Pantanal Formation (Godoi; Martins; Mello, 2001). The Pantanal is an active sedimentary basin, formed by the uplift of the Andes and epeirogenic movements across central Brazil during the Cenozoic era (Assine, 2015; Ussami; Shiraiwa; Dominguez, 1999). The depression of the UPRB evolved into the Pantanal basin due to fluvial dissection, subsidence, and sedimentation processes during the Quaternary (Ab'Sáber, 2011; Assine, 2015). The upper areas of the UPRB, ranging from 200 to 1200 m above sea level, are remnants of the uplift of the Sul-Americana surface during the early Cenozoic, before the formation of the Pantanal depression, which ranges from 80 to 150 m above sea level (Alho, 2005b; Assine, 2015). The Nhecolândia is an abandoned alluvial fan lobe of the Taquari megafan, characterized by flat relief and low slope gradients, with more than 10,000 shallow lakes and extensive sandy dunes (Assine *et al*., 2015; Zani; Luis Assine; Mcglue, 2012).

The Pantanal has a heterogenous landscape, shaped by the flooding regime. The landscape units of Nhecolândia, with typical regional designations, were based on the works of Ab'Sáber (2011), Brasil (1982), Calheiros and Fonseca Júnior (1996), and Valverde (1972).

The lakes can be differentiated into *Baías* and *Salinas*. The *Baías* (Figure 1a) are freshwater lakes, with varied size and depth, which can be temporary or permanent, and are influenced by the seasonal flooding, presenting a surface-groundwater connection (Furian *et al*., 2013). The *Salinas* (Figure 1b) are shallow saline or oligosaline lakes, differentiated by their functional biogeochemistry into cyanobacteria lake and bacterial lake, respectively. They are permanently isolated from the surface and subsurface drainage network by a low permeable loamy subsurface horizon (Furian *et al*., 2013). The sand levees surrounding the *Salinas* are called *Cordilheiras* (Figure 1c) and they are characterized by narrow elevations covered by cerrado or cerradão (vegetation types of the Cerrado biome).

The *Vazantes* (Figure 1d), also called floodable lowlands, are natural channels of intermitent rivers that connect the *Baías* during the high floods. They are wide and low areas, considered to be an aquatic-terrestrial transition zone (Calheiros; Fonseca Júnior, 1996). The *Murundus* (termite mounds; Figure 1e) are recognized as biogenic landforms created by the long-term pedoturbation by termites (Couto; Oliveira, 2010). They are widely distributed round elevations (0.5-20 m in diameter, and 0.2 – 2.0 m high) covered by woody cerrado trees and shrubs (Eiten, 1972; Ribeiro; Walter, 1998). The *Campos* (Figure 1f), grassy areas surrounding the *Murundus*, are covered by herbaceous vegetation and occasionally flooded during inundation season.

The Pantanal is a unique combination of the Brazilian biomes Cerrado (Savanna), Atlantic Forest, Amazon, and some fragments of Caatinga (Brazilian steppe vegetation). According to Pott *et al*. (2011), the Pantanal is considered a mosaic of formations, with gallery forests, palmlands, grasslands, savannas, grasslands and well-drained ridges. In the Pantanal depression there are 1863 phanerogam plant species listed and 250 species of aquatic plants (Alho, 2008). The fauna is biodiverse and composed by many species of birds, mammals, reptiles, amphibious, and fishes, which reflect the heterogeneity of the Pantanal environment (Guimarães *et al*., 2014).

The economic activities in Pantanal are associated with traditional cattle ranching, based on the native pasture, and tourism, and the main threat to the Pantanal conservation is associated with the erosion caused by the land use of the surrounding highlands (Pott; Pott, 2004).

Figure 1 – Location map of the study area and the Nhecolândia landscape units: a) Freshwater lake – *Baías*; b) Saline-alkaline lakes – *Salinas*; c) Sandy ridges – *Cordilheira*; d) Seasonal floodable lowlands – *Vazantes*; e) Termite mounds – *Murundus*; f) Occasionally flooded grasslands – *Campo*.

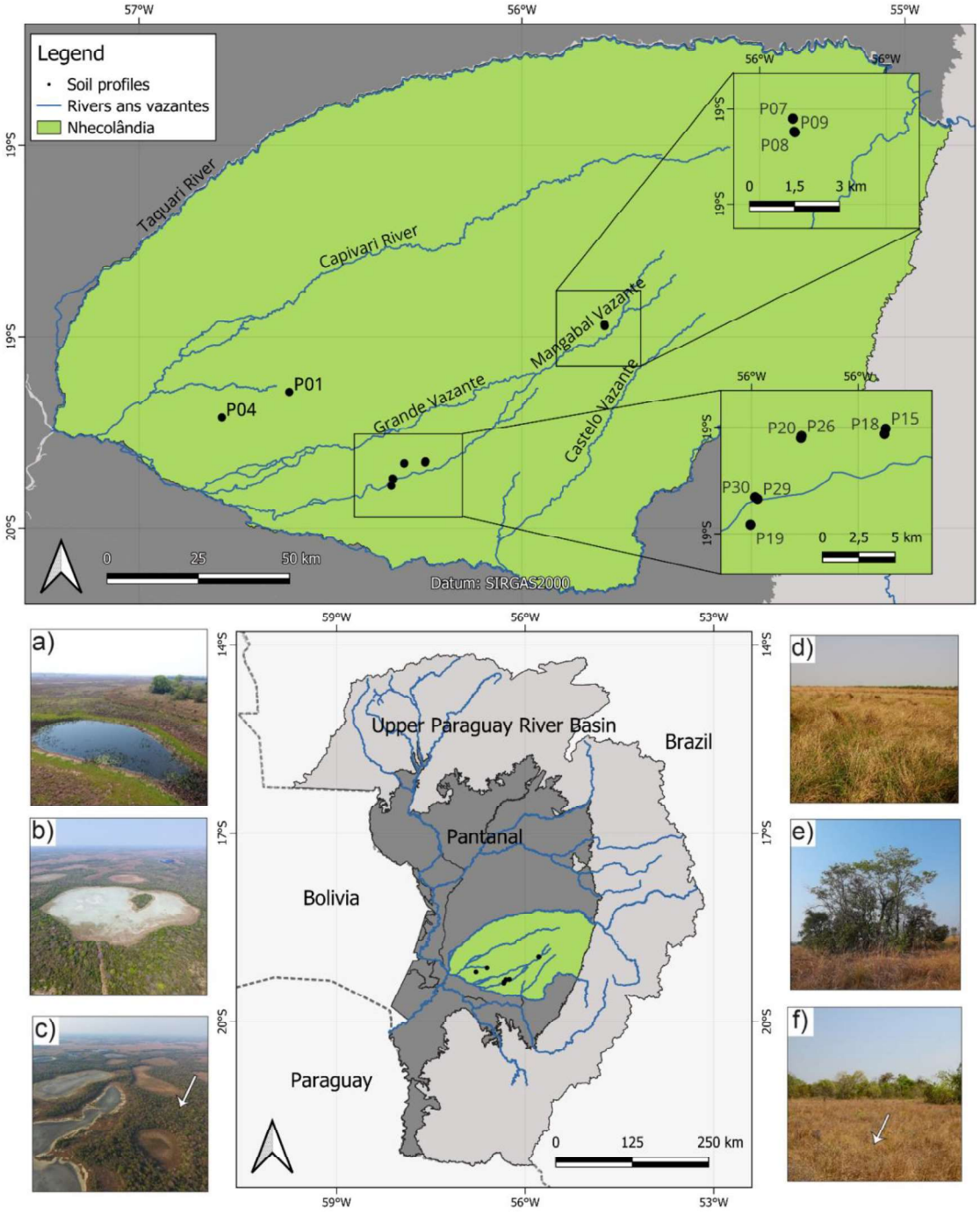

Source: The author.

4.3.2 Soil survey, description and classification

Samples of twelve representative soil profiles were collected for each of the six landscape units of the Pantanal of Nhecolândia. The field work occurred during the dry periods of August, November and December 2016, November 2017, September 2019, and September 2021. Soil descriptions followed Lemos and Santos (1996), and the classification was based on the Brazilian Soil Classification System (Santos *et al*., 2018) and the World Reference Base for Soil Resources (IUSS Working Group WRB, 2022). The vegetation was described according to Pott and Pott (1994, 2000).

4.3.3 Soil physical and chemical analyses

Soil samples were air dried, crushed and passed through a 2 mm sieve, and submitted to physical and chemical analyses by official methods (Teixeira *et al*., 2017) in the Routine Soil Fertility Laboratory of the Soil Department of the Federal University of Viçosa, Brazil. The standard pipette method was used for granulometric analysis, obtaining coarse sand (2 - 0.2 mm), fine sand (0.2 - 0.05 mm), silt (0.05 - 0.002 mm) and clay (<0.002 mm) fractions.

Soil pH was determined in water (active acidity) and 1 mol L^{-1} KCl 1:2.5 soil:solution. The available P, exchangeable Na^{+} and K^{+}, and the micronutrients (Fe, Cu, Mn and Zn) were extracted with Mehlich-1 method (HCl 0.05 mol L^{-1} and H_2SO_4 0.0125 mol L^{-1}), and quantified by photocolorimetry (P), flame photometry (Na^{+} and K^{+}) and atomic absorption spectroscopy (micronutrients). The exchangeable Ca^{2+}, Mg^{2+}, and Al^{3+} (exchangeable acidity) were extracted by KCl 1 mol L^{-1} and determined by atomic absorption spectroscopy (Ca^{2+} and Mg^{2+}) and titration with 0.025 mol L^{-1} NaOH solution (Al^{3+}). The H+Al (potential acidity) was obtained by a 0.5 mol L^{-1} calcium acetate solution buffered at pH and determined by titration with 0.025 mol L^{-1} NaOH solution. The remaining phosphorous (P-Rem) was determined with a 0.01 mol L^{-1} $CaCl_2$ solution and by photocolorimetry. Total organic carbon (TOC) was obtained by the wet-combustion method (Yeomans; Bremner, 1988). Effective cation exchange capacity ($_eCEC$) was calculated by determining the sum of cations (Ca^{2+}, Mg^{2+}, Na^{+}, K^{+}, and Al^{3+}). The potential cation exchange capacity ($_pCEC$) was estimated using the bases sum (BS) and potential acidity (H+Al). We determined the percentage of bases saturation (PBS), Al saturation index (Alsat), and Na saturation index (NaSI).

Soil profiles presenting high water pH values (>8) were selected for measure the electrical conductivity (EC) and analyze the soluble salts and $CaCO_3$ equivalent (CCE). Soil

solution was extracted by the saturated paste method. For some samples, we used the 1:1 soil-water extractions. Soil EC was measured using a benchtop conductivity measurement equipment. Soluble Ca^{2+} and Mg^{2+} were determined by atomic absorption spectroscopy and soluble Na^{+} and K^{+} were determined by flame photometry. Chlorates were determined by titration using a 0.05 mol L^{-1} $AgNO_3$ solution and 5% K_2CrO_4 as indicator. CCE was determined by attacking the soil with an excess of 0.5 mol L^{-1} HCl with a 0.25 mol L^{-1} NaOH solution. This procedure is not adjusted for Mg, K, or Na carbonates or organic matter which may be present.

4.3.4 Micromorphological and microchemical analyses

Undisturbed soil blocks from selected soil profiles were sampled at varied depths, dried at 50°C, and impregnated with a 10:1 araldite resin. The impregnated samples were cut into slabs of 0.5 cm thickness using a diamond saw and polished with corundum abrasives of 500 and 2000 mesh. After ultrasonic cleaning, the polished blocks were mounted onto glass slides followed by polishing and hand-finishing to produce thin sections 0.2 cm thick, 5×2.5 cm size. Thin sections were examined under a petrographic microscope, and the descriptions followed the guidelines of Stoops (2020).

Representative images covering the entire thin sections were used for sand fraction measurements, which were done using the JMicroVision v.1.2.7 software. Equivalent diameter (ED) and the circularity index (K) (Cox, 1927) were calculated to determine the mean sand grain size and roundness, respectively. The sand size was classified according to Santos et al. (2015) based on the ED, as coarse sand (2-0.2 mm), fine sand (0.2-0.05 mm), silt (0.05-0.002 mm), and clay (<0.002). K values closer to 1 indicate a circular particle shape. So roundness was classified according to Stoops (2020) using the K values as angular (0-0.2), subangular (0.2-0.4), subrounded (0.4-0.7), and rounded to well rounded (0.7-1). Sorting was classified according to Stoops (2020) using the percentage of fractions as perfectly sorted (occurrence of one size fraction), well sorted (5-10% of sizes other than the dominant one), moderately sorted (10-30% of sizes other than the dominant one), poorly sorted (>30% of sizes other than the dominant one), and unsorted (occurrence of a variety of sizes).

Selected areas of the thin sections were further investigated under a ZEISS LEO-1430 VP scanning electron microscope coupled with an Oxford Energy Dispersive X-ray Detector (SEM/EDS). Microchemical analyses were acquired at a working distance of 100 to 20 µm and with an accelerating voltage of 20 kv.

4.3.5 Mineralogical analyses

Some representative samples of each soil profile were selected to mineralogical analyses, following the methods described in Teixeira *et al*. (2017). Saline, sodic and carbonatic soil samples were dispersed with Sodium Hexametaphosphate 0.058 mol L^{-1} buffered with Sodium Carbonate 0.075 mol L^{-1}, and the acid soil samples with Sodium Hydroxide 0.1 mol L^{-1}. The separation of the soil fractions was done using the principle of sedimentation of Stoke's law. Non-oriented silt and sand samples were analyzed through X-Ray Diffraction (DRX) technique for mineral identification, using a PANalytical/X'PertPro diffractometer with CoKα radiation in a 2–60° 2θ range. Oriented clay samples were analyzed using a Rigaku Miniflex 600 diffractometer equipped with a Cu tube (CuKα) and Ni filter. This diffractometer was operated at 40 kV and 15 mA, with a goniometer angular velocity of 1.2º2θ min^{-1}, and a sweep range from 4 to 70º2θ. In addition, some clay samples were treated with Mg saturation ($MgCl_2$), glycerol solvation and K saturation (KCl) at room temperature and heated at 350 and 550 °C for better identification of expansive (2:1) minerals. Fe and Al content of crystalline and amorphous oxides were extracted with dithionite-citrate-bicarbonate (Fe_d and Al_d) Mehra; Jackson, 1960) and ammonium oxalate (Fe_o and Al_o) (McKeague; Day, 1966), respectively, and determined by atomic absorption spectroscopy.

4.3.6 Geochemichal analysis

The alkaline fusion analysis was conducted according to Pansu and Gautheyrou (2003) and slightly modified by Guerra *et al*. (2013). Clay samples were weighed in graphite crucibles, where 0.25 g of the fusion reagent was previously added, followed by 60 mg of the sample. Finally, an additional 0.25 g of lithium metaborate was added to the sample to form a double layer of reagent. This procedure was performed in duplicate. The material was placed in a muffle furnace, and a heating program was applied, consisting of two stages as described by Guerra *et al*. (2013), starting at 450°C for 1 hour and finishing at 1000°C for 10 minutes. Soluble salt was not removed from the clay samples.

The fused soil beads were carefully transferred to 50 mL centrifuge tubes containing 25 mL of 10% v/v HNO_3 solution. To ensure complete dissolution, the samples were shaken on a horizontal rotary mixer at 90 rpm for 4 hours. Then, the volume was adjusted to 50 mL with deionized water. Before elemental analysis, the samples were diluted 10 times, with the final acidity corrected to 1% v/v with nitric acid. The precision of the measurements was ensured by

using a Certified Reference Material, San Joaquin soil (NIST 2709a). The quantification of major elements, Na, K, Ca, Mg, Fe, Ti, Mn, P, Si, and Al, and minor elements, Cu and Zn, was carried out by inductively coupled plasma optical emission spectrometry (ICP OES), using a dual-view spectrometer (Optima 7300 DV, Perkin Elmer, Shelton, CT, USA). The ICP OES was equipped with a PEEK Mira Mist nebulizer and a cyclonic spray chamber. Ki index (1.7 SiO2/Al2O3) was calculated to evaluate the soil weathering degree and mineralogical composition relationships.

4.3.7 Chronological and carbon stable isotope analyzes

A coal sample from a depth of 100 cm in a *Salina* (P18) and a soil sample from the surface horizon (P26 15 – 20 cm depth) of a Baía lake were collected for radiocarbon (14C) dating. This analysis provides the age of soil organic matter, indicating the minimum age of the soil and its development (Wang; Amundson; Trumbore, 1996). Dating was performed by the Beta Analytic laboratory using the AMS (Accelerator Mass Spectrometry) technique. Samples were grounded, sieved and passed through a complete pre-treatment (acid/alkali/acid) to remove soil carbonates and secondary organic acids (Beta Analytic, 2022). The radiocarbon age is obtained comparing the 14C/13C ratio of the sample with the one of the NBS (National Bureau of Standards) oxalic acid standard. In 14C, age is expressed in cal BP, which is used to mean before AD 1950. The cal BP was calculated using BetaCal4.20 method and SHCAL20 database (Ramsey, 2009; Hogg *et al*., 2020).

For the OSL (Optically Stimulated Luminescence) dating technique, light-proof aluminum core tubes (with 5 cm diameter and 50 cm long) were used to collect undisturbed samples at 5-15 (P18 A1 horizon), 60 (P26 E2 horizon), 80-90 (P29 Cg1 horizon), and 70-80 cm (P30 C3 horizon) of depth. Dating was performed by the Datação, Comércio e Prestação de Serviços LTDA (São Paulo – SP) laboratory using the SAR (Single Aliquot Regenerative-Dose) protocol (Murray; Wintle, 2000) (Chart 1). This protocol is a method of determination of the equivalent dose using an aliquot (3 mg) of the sample for calibration curve (Appendix F). In this case, there were used 15 aliquots for each sample, so 15 ages were found for each sample and were used in statistical methods for the construction of frequency diagrams to know the fluctuation of the ages found for each sample. Aliquots were accepted if the recycling and recuperation ratios were within 10% of the natural signal. The De and inferred ages were estimated using a weighted mean, through the Central Age Model (CAM).

Chart 1: The SAR protocol applied for OSL dating.

1. Preheat at 200-240°C for 10s;
2. Measure natural OSL (Blue-led stimulation at 125°C for 40s);
3. Irradiate with a test dose to correct sensitivity;
4. Preheat at 200-240°C for 10s;
5. Measure OSL;
6. Radiate with light;
7. Irradiate with regenerative dose = $D_{1;}$
8. Preheat 200-240°C for 10s;
9. Measure OSL (Blue-led stimulation at 125°C for 40s);
10. Return to 3, increasing the regenerative dose value;
11. Repeat for Dose Zero to verify regeneration of the OSL signal (recovery test);
12. Repeat dose D_1 to check recycling of the OSL signal (recycling test).

Source: *Datação, Comércio e Prestação de Serviços* LTDA report.

For the carbon stable isotope analysis, selected soil samples were milled and analyzed using an elemental CN analyzer coupled to an isotope ratio mass spectrometer (ANCA GSL 20-20, Sercon, Crewe, UK). The results are expressed in percent of dry weight, with an analytical precision of 0.1%. The ^{13}C results are expressed as $\delta^{13}C$ with respect to the VPDB standard using the following conventional notations:

$$\delta 13C\ (‰) = \left[\left(\frac{R1}{R2}\right) - 1\right] . 1000$$

where R1 and R2 are, respectively, the $^{13}C/^{12}C$ ratios in the sample and for the international standard.

4.4 RESULTS

4.4.1 Soil macromorphology

In general, soils of the *Salinas* presented redoximorphic features, with variations in the reduction and oxidation features. The three *Salinas* soils (P1, P18, and P19) showed darker surface horizons, where roots occur more abundant down to 20 cm depth (Table 1). The Gleysol and Solonetz (P1 and P18) showed a reduced grayish soil matrix. The Podzol (P19) exhibited reddish and yellowish zones of Fe concentration. Mottles were found in the B horizons of the

Gleysol, the A2 and E horizons of the Solonetz, and spodic B of the Podzol. Clay texture prevails in these soils, except for the Podzol, which presented a sandy texture. Prismatic structure predominates in the Gleysol and occurs in the surface horizon of the Solonetz, where a subangular blocky structure prevails. The Podzol was structureless.

The predominant color of the *Baías* soils (P4 and P26) was dark gray, indicating accumulation of organic matter and hydromorphism. The texture varied from sandy clay loam to sand (Table 1). All soil horizons were structureless, except for the Planosol (P4) B horizon, which exhibited a subangular blocky structure. Mottles occurred at the first 50 cm depth of the Planosol and in the C1 horizon of the Arenosol (P26), evidencing Fe oxidation. Roots occurred until 108 cm depth at the E horizon of the Planosol.

The soils of the *Vazantes* (P29 and P30) presented brown color, varying from reddish to dark brown (Table 1). They were predominantly structureless, due to the sandy texture. The spodic horizon of the Podzol (P29) was moderately to strongly cemented due to Fe concentration, presenting mottles at the E horizon. In both soil profiles, roots reached 65 cm depth.

The color of the *Cordilheiras* soils (Arenosols - P7, P15, and P20) varied from brown to yellowish/grayish brown colors (Table 1). They were also sandy and structureless. The deepest horizons of the P20 presented hard to extremely hard consistency, and a strong cementation. Roots occurred abundantly almost in the entire soil profiles, and mottles were found in the C1 horizon of the P7. Similarly, the *Murundus* (P8) and *Campos* (P9) soils were sandy and structureless and presented a predominant dark grayish brown color.

4.4.2 Soil physical and chemical characteristics

The first and second dimensions of the PCA explained 59.8% of the soil variance (Figure 2). Dim1 accounted for 40.8% of the variance, with its positive axis significantly associated with clay, silt, water pH, K, BS, Ca, and $_{p}$CEC. These attributes influenced the soils of the *Salinas* and some horizons of the *Baías* Planosol and *Cordilheiras* Arenosol. In contrast, the negative axis of Dim1 was mainly defined by FS and P-Rem, which affected the Arenosols of the *Baías*, *Cordilheiras*, *Murundus*, and *Campos*, as well as the *Baías* Planosol and the *Salinas* Podzol. Dim 2 explained 19% of the data variance, being strongly influenced by H+Al, Zn, and TOC. These soil attributes had a greater effect on some horizons of the Arenosol and Planosol of the *Baías*, and the Podzol of the *Vazantes*.

The higher mean values of clay, water pH, BS, P, and pCEC (Figure 3) were associated with the Solonetz and Gleysol of the *Salinas*, where salts accumulate. Water pH of the *Salinas* Podzol presented a wide range, reaching a minimum of 6, due to the occurrence of H+Al accumulation in the spodic B (Appendix B). The *Cordilheiras* Arenosols also had a significant P content. The *Vazantes* Podzol and *Baías* Arenosol showed the highest H+Al values, which are related to greater TOC content, indicating low rate of organic matter decomposition, under prolonged water saturation. The *Salinas* Gleysol and *Murundus* Arenosol also exhibited significant TOC values, attributed to water saturation and intense biological turnover by termites, respectively. The soils of the *Baías*, *Campos*, *Cordilheiras*, and the *Vazantes* Arenosol had the highest mean P-Rem values, suggesting very low P-Retention due to their sandy texture. Higher soluble Fe content was observed in the *Vazantes* and *Salinas* Podzols, as well as in the *Baías* soils, indicating low-oxygen conditions.

Table 1 – Macromorphological attributes and the classification (WRB/FAO and SiBCS) of the soils of Nhecolândia Pantanal.

Horizon (Depth)	Color		Texture	Horizon boundary	Structure	Consistence		Cementation	Plasticity	Stickiness	Mottles	Roots
cm	Moist					Dry	Moist					
					Salinas							
P1 – Reductigleyic Eutric Gleysol (Clayic, Alcalic, Sideralic, Humic, Protosodic, Sodic, Uterquic) GLEISSOLO HÁPLICO Sódico típico hipocarbonático êutrico												
An (0-11)	5Y 3/2	dark olive gray	Clay	C, S	MO, ME-CO, SB	HA	FR	NA	SPL	SST	NA	M, VF-F
ABgn (11-23)	5Y 4/1	dark gray	Clay	G, S	MO, FI-ME, PR	VHA	FR	NA	SPL	SST	NA	M, VF-F
Bgn1 (23-57)	5Y 4/2	olive gray	Clay	C, S	ST, FI-ME, PR	VHA	FR	NA	SPL	SST	FE, FI, D	C, VF-F
Bgn2 (57-88)	5Y 2/2	black	Clay	A, S	ST, FI-ME, PR	VHA	FR	NA	SPL	SST	FE, FI, D	C, VF-F
Cn (88-110)	2,5 Y 5/4	reddish brown	Sand	NA		LO	LO	NA	NPL	NST	NA	NA
P18 – Albic Nudinatric Protosalic Stagnic Gleyic Solonetz (Arenic, Differentic, Endic. Ochric, Hypernatric) PLANOSSOLO NÁTRICO Sálico mésico hipocarbonático												
Agn1 (0-16)	5Y 3/2	Dark olive gray	Clay	C, S	ST, FI, SB/MO, CO, PR/WE, VC, PL	VHA	FI	NA	VPL	NST	NA	VF-F
Agn2 (16-27)	5Y 4/1	Dark gray	Sandy clay loam	A, S	MO, ME-CO,SB	HA	FR	NA	SPL	NST	VF, FI, FA	VF-F
E (27-60)	5Y 4/2	Olive gray	Sand	C, S	WE, ME-CO, SB/SG	SO	VFR	NA	NPL	NST	VF, FI, FA	NA
Btn (60-90)	5Y 2/2	Black	Loamy sand	NA	WE, ME-CO, SB	SO	VFR	NA	NPL	NST	NA	NA
Btgn (90-106)	2,5 Y 5/4	Reddish brown	Sandy clay loam	NA	NA	NA	NA	NA	NA	NA	NA	NA
Btg (106-128)	5GY 3/2	Dark grayish green	Sandy clay loam	NA	NA	NA	NA	NA	NA	NA	NA	NA
P19 – Stagnic Gleyic Entic Podzol (Arenic, Epic, Eutric, Sideralic) ESPODOSSOLO FERRILÚVICO Hidromórfico arênico												
An1 (0-5)	10Y 4/2	Dark grayish green	Sand	C, S	SG	SO	VFR	NA	NPL	NST	NA	M, VF-F

An2 (5-10)	5Y 6/2	Light olive gray	Sand	A, S	SG	SO	VFR	NA	NPL	NST	NA	C, VF-F
Bsc1 (10-28)	5Y 5/2	Olive gray	Loamy sand	C, S	SG	LO	VFR	NA	NPL	NST	M, FI-ME, P	NA
Bsc2 (28-48)	10Y 3/2	Very dark grayish olive	Sand	C, S	SG	LO	VFR	NA	NPL	NST	M, FI-A, P	NA
Bsc3 (48-70+)	5GY 3/1	Very dark greenish gray	Loamy sand	NA	SG	LO	VFR	NA	NPL	NST	C, ME-C, FA	NA
Baías												
P4 – Eutric Albic Gleyic Histic Planosol (Arenic, Alcalic, Sideralic, Humic, Sodic) PLANOSSOLO HÁPLICO Eutrófico gleissólico solódico												
An (0-10)	5Y 3/1	Very dark gray	Sandy loam	C, S	SG	SO	VFR	NA	NPL	NST	FE, FI, FA	M, VF-F
AEn (10-17)	5Y 4/1	Dark gray	Loamy sand	C, S	SG	SO	VFR	NA	NPL	NST	FE, FI, FA	M, VF-F
E (17-44)	5Y 5/3	Olive	Sand	C, S	SG	LO	VFR	NA	NPL	NST	FE, FI, FA	C, VF-F
Eg1 (44-75)	5Y 3/1	Very dark gray	Sand	C, S	SG	SO	VFR	NA	NPL	NST	NA	FE, VF-F
Eg2 (75-108)	5Y 5/3	Olive	Sand	A, S	SG	SO	VFR	NA	NPL	NST	NA	FE, VF-F
Bt (108-130)	5Y 4/2	Olive gray	Sandy clay loam	NA	ME-CO, SB	VHA	VFR	NA	NPL	NST	NA	
P26 – Eutric Sideralic Brunic Gleyic Arenosol (Humic) NEOSSOLO QUARTZARÊNICO Hidromórfico organossólico												
H (0-21)	10YR 2/1	Black	Sandy clay loam	C, W	MA	SO	VFR	NA	NPL	NST	NA	C, VF-F
A (21-25)	10YR 3/1	Very dark gray	Loamy sand	C, W	SG	LO	VFR	NA	NPL	NST	NA	FE, VF-F
C1 (25-42)	10YR 4/3	Brown	Sand	C, W	SG	LO	VFR	NA	NPL	NST	C, ME-C, FA	NA
C2 (42-75)	10YR 4/3	Brown	Sand	C, W	SG	LO	VFR	NA	NPL	NST	NA	NA
Cg (75-105)	10YR 4/2	Dark grayish brown	Sand	NA	SG	LO	VFR	NA	NPL	NST	NA	NA
Vazantes												
P29 – Gleyic Histic Albic Ortsteinic Podzol (Arenic, Abruptic, Epic, Sideralic) ESPODOSSOLO FERRILÚVICO Hidromórfico arênico dúrico												
A (0-14)	5YR 2,5/1	Black	Loamy sand	A, S	SG	LO	VFR	NA	NPL	NST	NA	M

2A (14-230	5YR 2,5/1	Black	Loamy sand	C, S	SG	LO	VFR	NA	NPL	NST	NA	M
2AE (23-29)	10YR 3/2	Dark reddish brown	Sand	G, S	SG	LO	VFR	NA	NPL	NST	NA	C
2E (29/48-48/65)	7,5YR 5/4	Reddish brown	Sand	A, I	SG	LO	VFR	NA	NPL	NST	C, FI-ME, P	FE
2Bsm1 (45/53-53/63)	7,5YR 4/4	Brown	Loamy sand	A, I	SG	EHA	EFI	C	NPL	NST	NA	NA
2Bsm2 (65/67-73/76)	7,5YR 4/6	Strong brown	Loamy sand	C, W	SG	VA	VFR	C	NPL	NST	NA	NA
2Cg1 (76-94)	7,5YR 4/6	Strong brown	Sand	C, W	SG	LO	VFR	NA	NPL	NST	NA	NA
2Cg2 (94+)	10YR 4/2	Dark grayish brown	Loamy sand	NA	SG	LO	VFR	NA	NPL	NST	NA	NA
P30 – Dystric Sideralic Arenosol (Ochric) NEOSSOLO QUARTZARÊNICO Órtico típico												
A (0-6)	7,5 YR 2,5/2	Dark brown	Sand	C, S	SG	LO	FR	NA	NPL	NST	NA	M, VF-F
AC (6-12)	7,5YR 3/2	Dark brown	Sand	G, S	SG	LO	FR	NA	NPL	NST	NA	FE, VF-F
C1 (12-45)	7,5YR 3/2	Dark brown	Sand	G, S	SG	LO	FR	NA	NPL	NST	NA	FE, VF-F
C2 (45-69)	7,5YR 4/3	Brown	Sand	G, S	SG	LO	VFR	NA	NPL	NST	NA	FE, VF-F
C3 (69-90)	7,5YR 5/4	Brown	Sand	NA	SG	LO	VFR	NA	NPL	NST	NA	NA
Cordilheiras												
P7 – Eutric Sideralic Brunic Arenosol (Ochric, Rubic) NEOSSOLO QUARTZARÊNICO Órtico típico												
A (0-27)	10YR 4/3	Brown	Sand	D, S	SG	LO	FR	NA	NPL	NST	NA	M, VF-F
CA (27-44)	10YR 4/4	Brown	Sand	D, S	SG	LO	FR	NA	NPL	NST	NA	FE, VF-F
C1 (44-67)	10YR 4/4	Dark yellowish brown	Sand	D, S	SG	LO	FR	NA	NPL	NST	FI-ME, D	FE, VF-F
C2 (67-91)	10YR 5/8	Yellowish brown	Sand	D, S	SG	LO	FR	NA	NPL	NST	NA	FE, VF-F
C3 (91-115)	10YR 6/4	Light yellowish brown	Sand	NA	SG	LO	FR	NA	NPL	NST	NA	NA

P15 – Dystric Sideralic Brunic Arenosol (Ochric) NEOSSOLO QUARTZARÊNICO Órtico típico												
A1 (0-24)	10YR 3/2	Dark grayish brown	Sand	C, S	SG	SO	FR	NA	NPL	NST	NA	M, VF-CO
A2 (24-33)	10YR 4/2	Dark grayish brown	Sand	C, S	SG	SO	VFR	NA	NPL	NST	NA	M, VF-CO
CA (33-59)	10YR 4/2	Dark grayish brown	Sand	C, S	SG	SO	VFR	NA	NPL	NST	NA	M, VF-CO
C1 (59-106)	10YR 4/4	Dark yellowish brown	Sand	D, S	SG	SO	VFR	NA	NPL	NST	NA	C, F-ME
C2 (106-120)	10YR 3/4	Dark yellowish brown	Sand	NA	SG	SO	FR	NA	NPL	NST	NA	C, F-ME
P20 – Eutric Sideralic Brunic Arenosol (Ochric, Protoargic, Claric, Protospodic) PLANOSSOLO HÁPLICO Eutrófico solódico espessarênico												
A (0-36)	2,5 Y 4/3	Olive brown	Sand	C, S	SG	SO	VFR	NA	NPL	NST	NA	M, VF-CO
AE (36-53)	2,5 Y 6/3	Light yellowish brown	Sand	A, S	SG	SO	VFR	NA	NPL	NST	NA	M, VF-CO
E (53-96)	2,5 Y 7/3	Pale brown	Loamy sand	C, W	SG	LO	VFR	NA	NPL	NST	NA	M, VF-CO
Bt (96-107)	2,5 Y 4/2	Dark grayish brown	Loamy sand	C, S	SG	VHA	VFR	NA	NPL	NST	NA	FE, VF
Btnqx (107-110)	7,5 YR 4/2	Brown	Sand	NA	SG	VHA	VFR	C	NPL	NST	NA	FE, VF
Murundus												
P8 – Dystric Sideralic Brunic Arenosol (Ochric, Isopteric Claric) NEOSSOLO QUARTZARÊNICO Órtico típico												
A (0-5)	10YR 3/2	Dark grayish brown	Sand	C, S	SG	SO	vfr	NA	NPL	NST	NA	M, VF-VC
CA (5-16)	10YR 4/2	Dark grayish brown	Sand	D, S	SG	LO	vfr	NA	NPL	NST	NA	M, VF-VC
C1 (16-67)	10YR 4/2	Dark grayish brown	Loamy sand	D, S	SG	LO	VFR	NA	NPL	NST	NA	M, VF-VC

C2 (67-110)	10YR 5/2	Grayish brown	Loamy sand	NA	SG	LO	LO	NA	NPL	NST	NA	M, VF-VC
P9 – Eutric Sideralic Brunic Arenosol (Ochric) NEOSSOLO QUARTZARÊNICO Órtico típico												
C (0-3)		NA	Sand	A, S	SG	LO	LO	NA	NPL	NST	NA	M, VF-VC
2A (3-7)	10YR 3/2	Very dark grayish brown	Sand	C, S	SG	LO	FR	NA	NPL	NST	NA	M, VF-F
2CA (7-16)	10YR 4/2	Dark grayish brown	Sand	D, S	SG	LO	FR	NA	NPL	NST	FE, FI-ME, D	M, VF-F
2C1 (16-63)	10YR 4/3	Brown	Sand	D, S	SG	LO	VFR	NA	NPL	NST	NA	M, VF-F
2C2 (63-97)	10YR 5/4	Yellowish brown	Sand	NA	SG	LO	VFR	NA	NPL	NST	NA	M, VF-F

Source: The author.

Note: Horizon boundary: A – abrupt, C – clear, D – diffuse, G – gradual, S – smooth, I – irregular, W – wavy; Structure: WE – weak, MO – moderate, ST – strong, FI – fine, ME – medium, CO – coarse, VC – very coarse, MA – massive, PL – platy, PR – prismatic, SB – subangular blocky, SG – single grain; Consistency – dry: LO – loose, SO – soft, HA – hard, VHA – very hard, EHA – extremely hard; Consistence – moist: LO – loose, FR – friable, VFR – very friable, FR – firm, EFI – extremely firm; Cementation: C – cemented; Plasticity: NPL – non-plastic, SPL – slightly plastic, VPL – very plastic; Stickness: NST – non-sticky, SST - slightly sticky; Mottles: VF – very few, FE – few, C – common, M – many, FI – fine, ME – medium, A – coarse, FA – faint, D – distinct, P – prominent; Roots: FE – few, C – common, M – many, VF – very fine, F – fine, ME – medium, CO – coarse, VC – very coarse; NA – non-applicable.

Figure 2 – Principal component analysis of the physical and chemical attributes of the main soil classes across the six landscape units of the Nhecolândia, Pantanal.

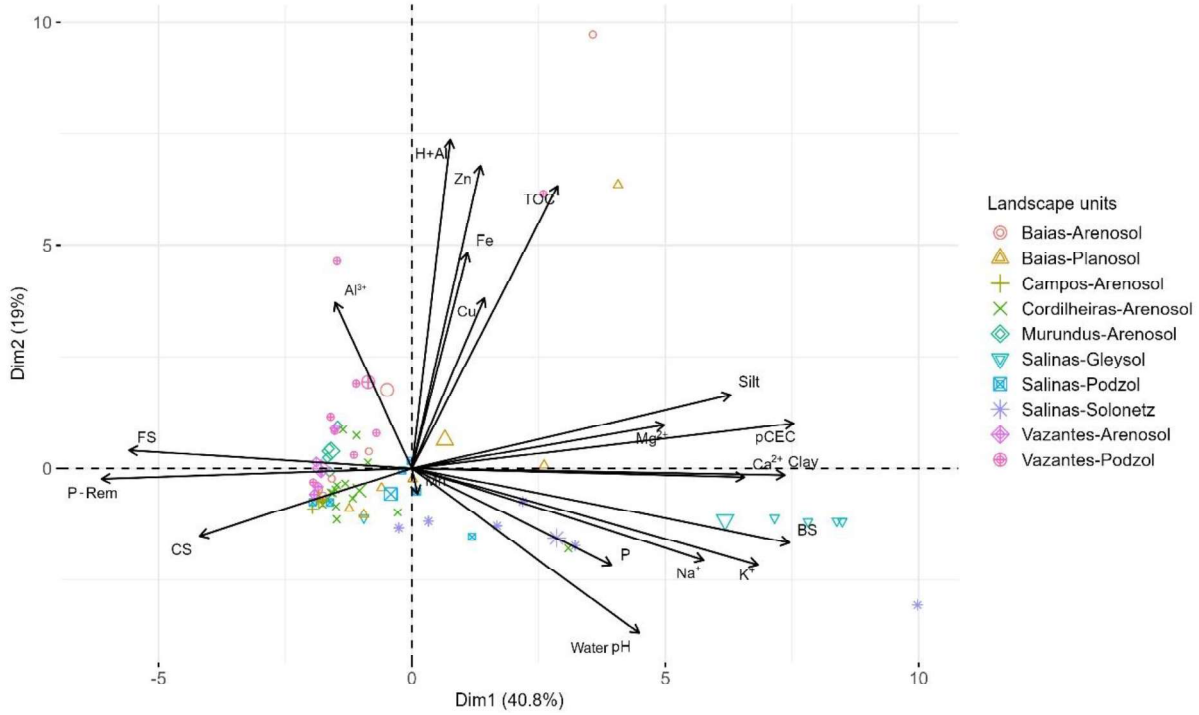

Source: The author.
Notes: Al – exchangeable acidity; BS – base sum; CS – coarse sand; Cu, Zn, Fe, and Mn – microelements; FS – fine sand; H+Al – potential acidity; Mg^{2+}, Ca^{2+}, Na^{+}, and K^{+} – exchangeable cations; $_{p}$CEC – potential cation exchange capacity; P – available P; P-Rem - remaining phosphorous; TOC – total organic carbon.

In the *Salinas*, the Solonetz (P18) presented the highest EC (mean of 2.74), reaching 8.46 dS m^{-1} at the surface horizon, mainly due to higher K^{+}, Na^{+}, carbonate, bicarbonate, and CCE contents (Table 2). The Gleysol (P01) water pH, soluble salts, and CCE contents were almost uniform across the profile, with little increase at depth. The Podzol (P19) presented significant values of CE, soluble salts, and CCE only at the surface. The Planosol of the *Baías* presented considerable contents of soluble salts at the surface, and an increase of CE and CCE at depth. The Arenosol of the *Cordilheiras* presented an increase of CE, soluble salts, and CCE at depth, reaching 42.83 g kg^{-1} of CCE at the Btnqx horizon.

Figure 3 – Descriptive statistics of selected soil physical and chemical attributes of the main soil classes across the six landscape units of the Nhecolândia, Pantanal.

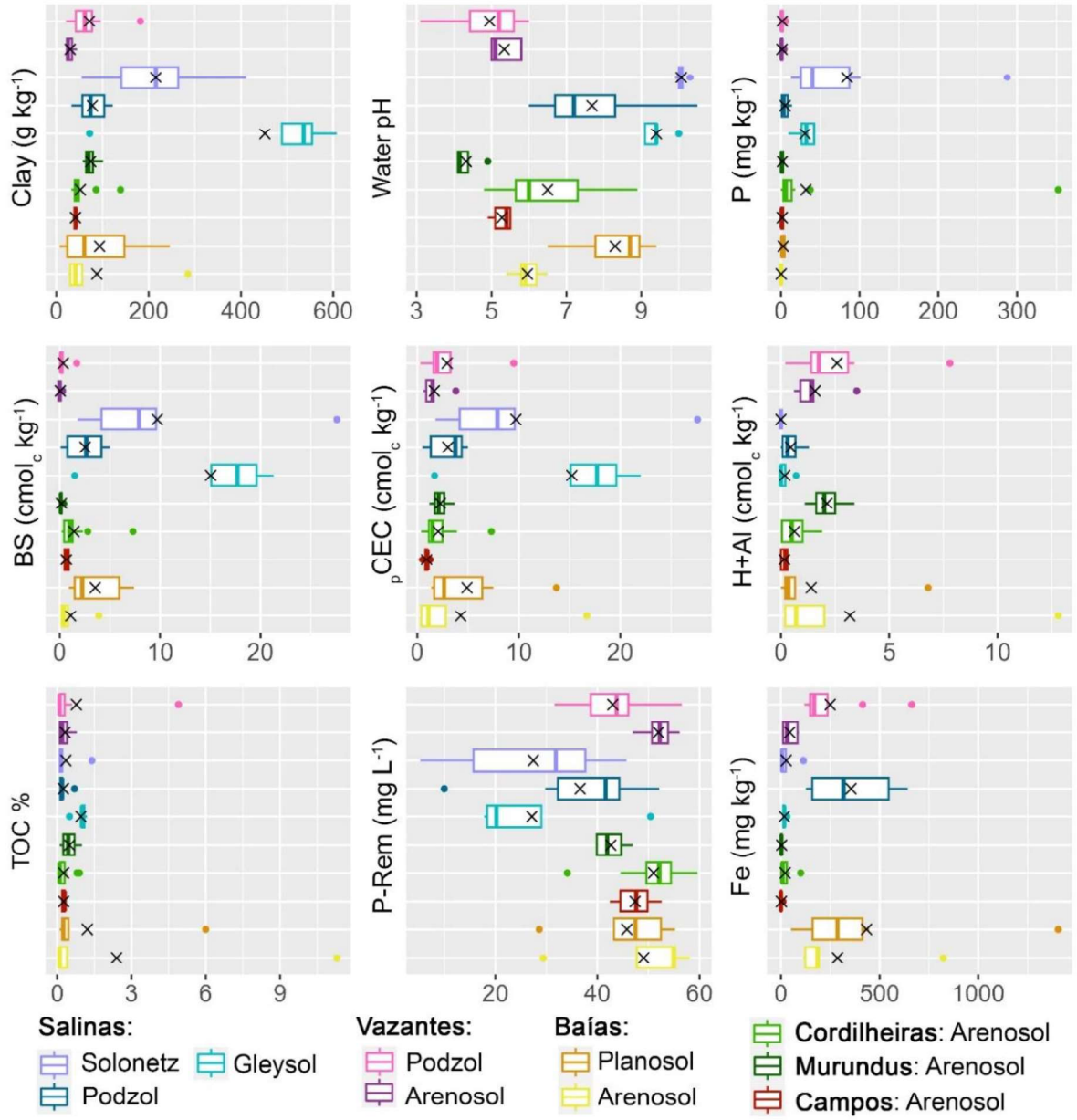

Source: The author.

Notes: BS – base sum; Fe – microelement; H+Al – potential acidity; $_{p}$CEC – potential cation exchange capacity; P – available P; P-Rem - remaining phosphorous; TOC – total organic carbon.

Table 2 – Water pH, CE, soluble salts, and CCE of soils of the *Salinas* (P1, P18, and P19) and selected soils of the *Baías* (P4) and *Cordilheiras* (P20).

Horizon/ Depth	Water pH	EC	Ca^{2+}	Mg^{2+}	K^{+}	Na^{+}	Cl^{-}	$CO3^{2-}$	HCO_3^{-}	CCE
cm		$dS\ m^{-1}$	---------- $cmol_c\ kg^{-1}$ ----------				--------- $cmol_c\ L^{-1}$ -------			$g\ kg^{-1}$
P1 – Reductigleyic Eutric Gleysol (Clayic, Alcalic, Sideralic, Humic, Protosodic, Uterquic)										
GLEISSOLO HÁPLICO Sódico Típico										
An (0-11)	9.09	0.89	461.1	594.91	0.40	0.95	0.20	0.20	10.75	77.82
ABgn (11-23)	9.12	1.19	252.7	145.12	0.38	1.30	0.19	0	12.90	49.04
Bgn1 (23-57)	9.35	0.70	267.8	285.43	0.22	0.73	1.95	0.38	8.45	96.51
Bgn2 (57-88)	9.43	0.80	351.7	522.71	0.27	0.86	0.95	0	10.70	94.96
Cn (88-110+)	9.09	0.95	54.9	127.68	0.07	0.17	-	0	10.80	18.85
Mean	9.35	0.89	267.84	285.43	0.27	0.86	0.57	0	10.75	77.82
SD	0.35	0.18	149.54	214.64	0.13	0.41	0.83	0.17	1.57	33.2
P18 – Albic Nudinatric Protosalic Stagnic Gleyic Solonetz (Arenic, Differentic, Endic. Ochric, Hypernatric)										
PLANOSSOLO NÁTRICO Sálico êndico										
Agn1 (0-16)	10.3	8.46	100.4	19.98	1.12	4.94	0.29	7.65	41.70	110.47
Agn2 (16-27)	9.85	2.01	-	-	-	-	-	-	-	103.72
E (27-60)	10	2.01	62.4	13.10	0.08	0.45	0.44	2.50	18.10	37.21
Btn (60-90)	10	0.96	231.4	84.52	0.29	1.12	0.15	0.58	8.90	41.8
Btgn (90-106)	10.05	1.16	211.3	69.19	0.50	1.42	0.17	0.45	12.50	48.1
Btg (106-128)	10.07	1.76	696.4	510.62	1.05	1.72	-	0.50	15.80	39.68
Mean	10.05	2.73	260.38	139.48	0.61	1.93	0.26	2.34	19.40	63.5
SD	0.15	2.84	254.05	209.73	0.46	1.75	0.13	3.09	12.94	34.03
P19 – Stagnic Gleyic Entic Podzol (Arenic, Epic, Eutric, Sideralic)										
ESPODOSSOLO FERRILÚVICO Hidromórfico arênico										
A1 (0-5)	8.55	4.37	304.0	114.34	0.19	0.96	0.82	0.45	15.35	36.99
A2 (5-10)	7.44	0.51	44.6	43.14	0.03	0.07	0.29	0	1.90	20.56
Bsc1 (10-28)	7.03	0.10	92.9	497.35	0.17	0.05	0.05	0	0.60	32.06
Bsc2 (28-48)	6.56	0.11	4.5	4.21	0.01	0.01	0.05	0	0.30	32.78
Bsc3 (48-70)	5.95	0.15	0.4	3.27	0	0	0.05	0	0.10	31.76
Mean	7.11	1.05	89.28	132.46	0.08	0.22	0.25	0.09	3.65	30.83
SD	0.98	1.86	125.72	208.92	0.09	0.42	0.34	0.20	6.58	6.11
P4 – Eutric Albic Gleyic Histic Planosol (Arenic, Alcalic, Sideralic, Humic, Sodic)										
PLANOSSOLO HÁPLICO Eutrófico gleissólico										
An (0-10)	6.54	0.81	107.31	112.80	0.20	0.49	0.10	0	3.65	19.59
AEn (10-17)	7.47	0.39	44.07	38.38	0.03	0.05	0.09	0	2.46	16.31
E (17-44)	8.60	0.38	83.00	61.18	0.03	0.06	0.09	0	3.30	11.29
Eg1 (44-75)	9.35	0.51	77.61	29.45	0.03	0.07	0.09	0	5.70	12.51
Eg2 (75-108)	8.75	0.43	75.12	51.73	0.13	0.02	0.05	0	5.00	23.15
Mean	8.14	0.50	77.42	58.71	0.09	0.14	0.08	0	4.02	16.57
SD	1.12	0.18	22.59	32.59	0.08	0.20	0.02	0	1.31	4.92
P20 – Eutric Sideralic Brunic Arenosol (Ochric, Protoargic, Claric, Protospodic)										
PLANOSSOLO HÁPLICO Eutrófico solódico espessarênico										
AE (0-36)	7.26	0.21	33.22	28.19	0	0.00	0.09	0	0	33.17
E (36-53)	8.45	0.21	84.32	14.11	0	0.00	0.09	0	1.4	33.47
Bh (53-96)	8.6	0.48	67.92	42.46	0.03	0.04	0.09	0	3.3	32.9
Bsqnx (96-107)	8.93	0.59	44.71	52.54	0.03	0.14	0.09	0	5.3	42.83
Mean	8.10	0.36	57.54	34.32	0.02	0.05	0.09	0	2.50	35.21
SD	0.79	0.17	22.96	16.77	0.01	0.06	0	0	2.31	4.27

Source: The author.

Note: CCE – Calcium carbonate equivalent; Cl^-, CO_3^{2-}, HCO_3^- – soluble anions; EC – electrical conductivity; Mg^{2+}, Ca^{2+}, Na^+, and K^+ – soluble cations; and SD – standard deviation.

4.4.3 Soil micromorphology and microchemistry

In relation to *Salinas* soils, we investigated the Agn2-E and Btgn horizons of the Solonetz (P18), and the surface duripan and A horizon of the Podzol (P19). In general, the coarse material of the Solonetz horizons was mostly subangular to well-rounded, poorly sorted, fine sand-sized quartz grains (Appendix G), and some K-feldspar grains. In the fine material, silicate clay and organic matter predominated, along with some iron oxides and calcite. These groundmass constituents contribute to the greenish gray and yellowish-brown colors, with some reddish color parts in the Btgn horizon. Both horizons of the Solonetz presented a close and single-double spaced porphyric coarse/fine (c/f) related distribution pattern with some parts chito-gefuric. Vughs, channels, and simple packing occurred in both horizons, with the Agn2-E horizon presenting some plane pores. The microstructure was vughy and bridged-pellicular grain in both horizons, and sub-angular blocky in the Agn2-E. Crystallitic b-fabric predominated, influenced by the mica and calcite fine material (Figure 4a). In the Agn2-E horizon, coatings of clay and organic matter were abundant (Figure 4a). In the Btgn horizon, typic silicious-ferruginous nodules were common, surrounded by Ca-rich clay coatings (Table 3 and Figure 5).

The Podzol surface duripan and A horizon presented subangular, subrounded, and rounded, poorly to moderately sorted, fine sand-sized quartz and K-feldspar grains (Appendix G and Figure 6). The duripan fine material presented yellowish-brown colors and was composed of amorphous silica, aluminosilicate clay, and manganese and iron oxides, with some calcite (Figure 4C). In the A horizon, the green color predominated due to cyanobacterial mats (Figure 4B). The duripan c/f related distribution pattern was single-spaced porphyric and some chitonic, while that of the A horizon was chito-gefuric, with some single-spaced porphyric. The porosity consisted of simple packing, with vughs and channels occurring at the duripan. The microstructure of the duripan was vughy and some pellicular grain, and of the A horizon was single-bridged-pellicular grains. Porostriated and undifferentiated b-fabric predominated, with some stipple-speckled fabric in the surface crust. Coatings, infillings, and nodules of clay and organic matter occurred in the duripan (Figure 4C). An impregnated Mn and Fe-rich nodule occurred in the duripan groundmass, with quartz and some Ti oxide grains (Figure 6 and Table 3).

Figure 4 – Microphotographs (PPL – plain polarized light; and XPL – crossed polarized light) of the *Salinas* soils of the Nhecolândia Pantanal. a) Agn2-E horizon transition of Solonetz (P18); b) A horizon of Podzol (P19); and c) overground duripan of the Podzol (P19).

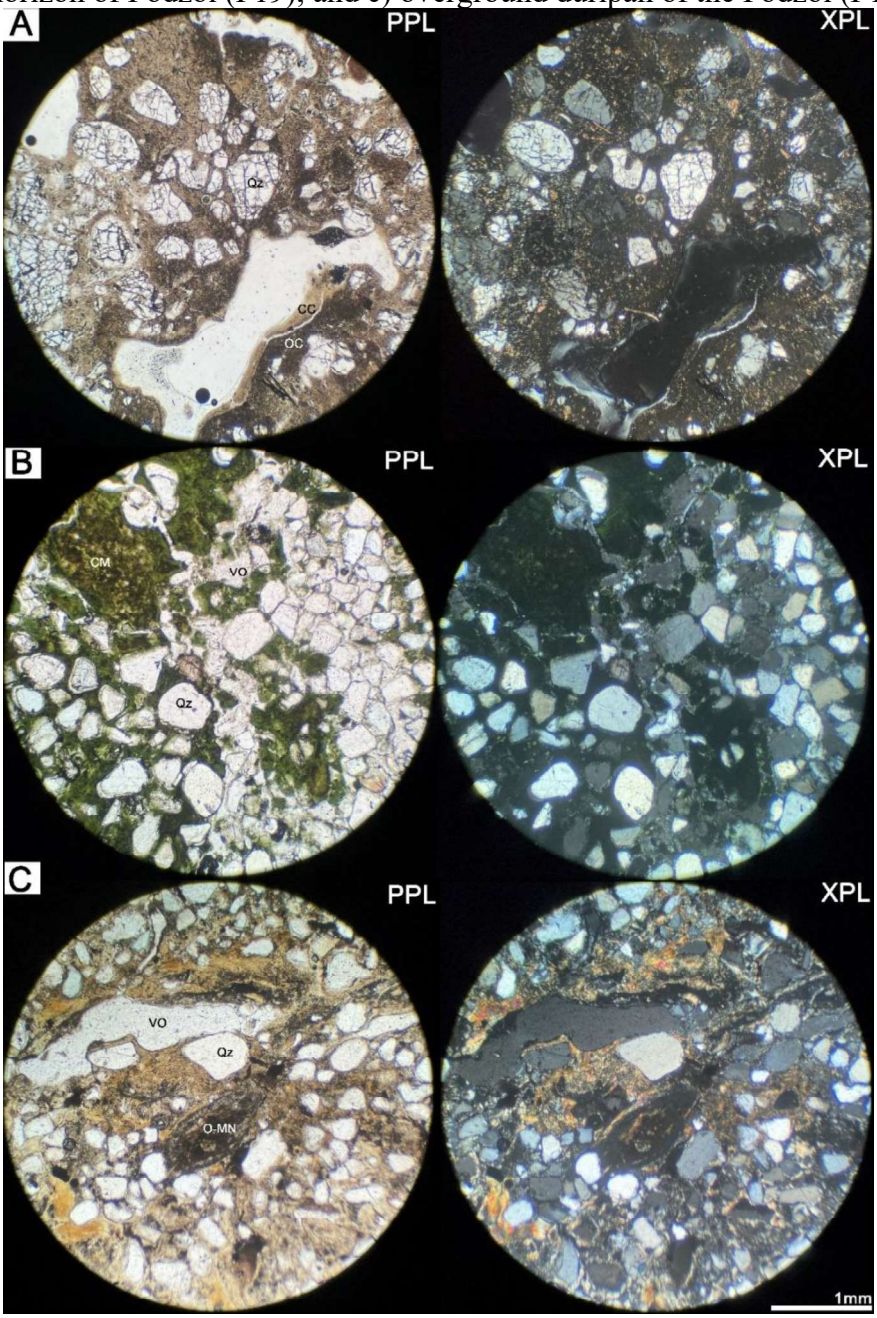

Source: The author.

Notes: Qz – quartz grains; VO – void; CC – clay coating; OC – organic material coating; CM – cyanobacterial material; O-MN – organic material nodule.

Figure 5 – SEM/EDS elemental maps of the Agn2-E horizon of the Solonetz (P18) located at a *Salina* at Nhecolândia Pantanal. a) indicate the nodule coating.

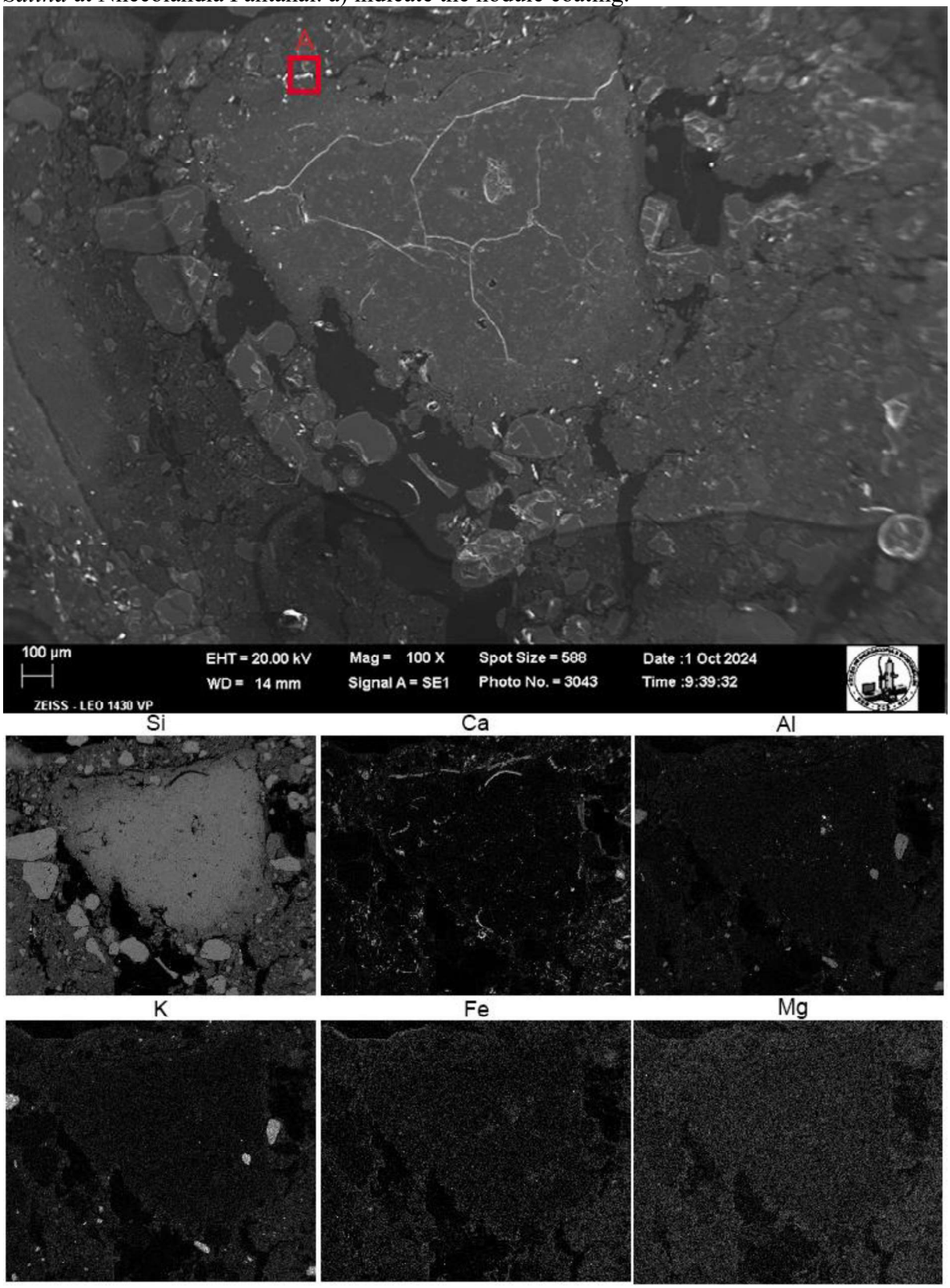

Source: The author.

Table 3 – Semiquantitative EDS analysis (wt% - weighted percentage) of selected soil thin sections of the six landscape units of the Nhecolândia Pantanal.

Sample	Na	Mg	Al	Si	P	S	Cl	K	Ca	Ti	Mn	Fe	Cu	Zn
	wt.%													
P18 (Agn2-E)	0.51	1.26	3.58	82.08	0	0.37	0.56	2.55	5.68	0.33	0.75	2.22	0.05	0.05
P18 (A)	0.68	1.31	52.33	10.08	0.57	1.03	3.47	0.87	23.67	0.68	2.71	1.93	0.35	0.32
P19	0.45	0.38	5.51	79.27	0	0.14	0.15	2.80	0.34	1.20	4.24	5.39	0.05	0.07
Duricrust														
P19 (A)	0.32	0.40	0.44	0.57	0.51	0.25	0.21	0.12	0.08	96.34	0.18	0.19	0.12	0.26
P19 (B)	1.11	0.40	8.73	32.53	0.53	0.26	0.26	4.29	0.49	3.67	31.70	15.52	0.33	0.17
P26 C3	0.38	0.38	4.48	84.23	0	0.18	0.29	2.72	0.33	0.22	1.35	5.26	0.09	0.11
P26 (A)	0	0.20	0.43	1.15	0.25	0.15	0.09	0.14	0.05	53.67	2.54	40.92	0.14	0.26
P26 (B)	0.25	0.63	1.82	6.57	0.98	0.22	0.70	0.52	2.31	0.31	24.72	60.51	0.25	0.63
P29 E-Bsm1	0.27	0.32	0.96	43.34	0.03	0.18	0.16	0.22	0.11	0.06	0.11	54.13	0.05	0.05
P29 (A)	10.79	3.47	1.22	70.59	0	0.39	-	0.31	11.80	0.11	0.06	0.91	0.14	0.21
P29 (B)	0.34	0.13	0.37	7.86	0.16	0.21	0.04	0.13	0.17	0.08	0.09	90.05	0.19	0.20

Source: The author.

Note: P18 (A) – nodule coating at figure 5; P19 (A) – Ti oxide at figure 6; P19 (B) – nodule matrix at figure 6; P26 (A) – Ti and Fe oxides at figure 7; P26 (B) matrix of Fe and Mn nodule at figure 7; P29 (A) – Si nodule; P29 (B) – soil matrix at figure 8.

Figure 6 – SEM/EDS elemental maps of a Fe/Mn nodule from the duricrust of the Podzol (P19) located at a *Salina* at Nhecolândia Pantanal. Higher chemical element levels correspond to lighter shades of gray. a) indicate the Ti oxide; b) indicate the nodule matrix, with dispersed grains of K-Feldspar.

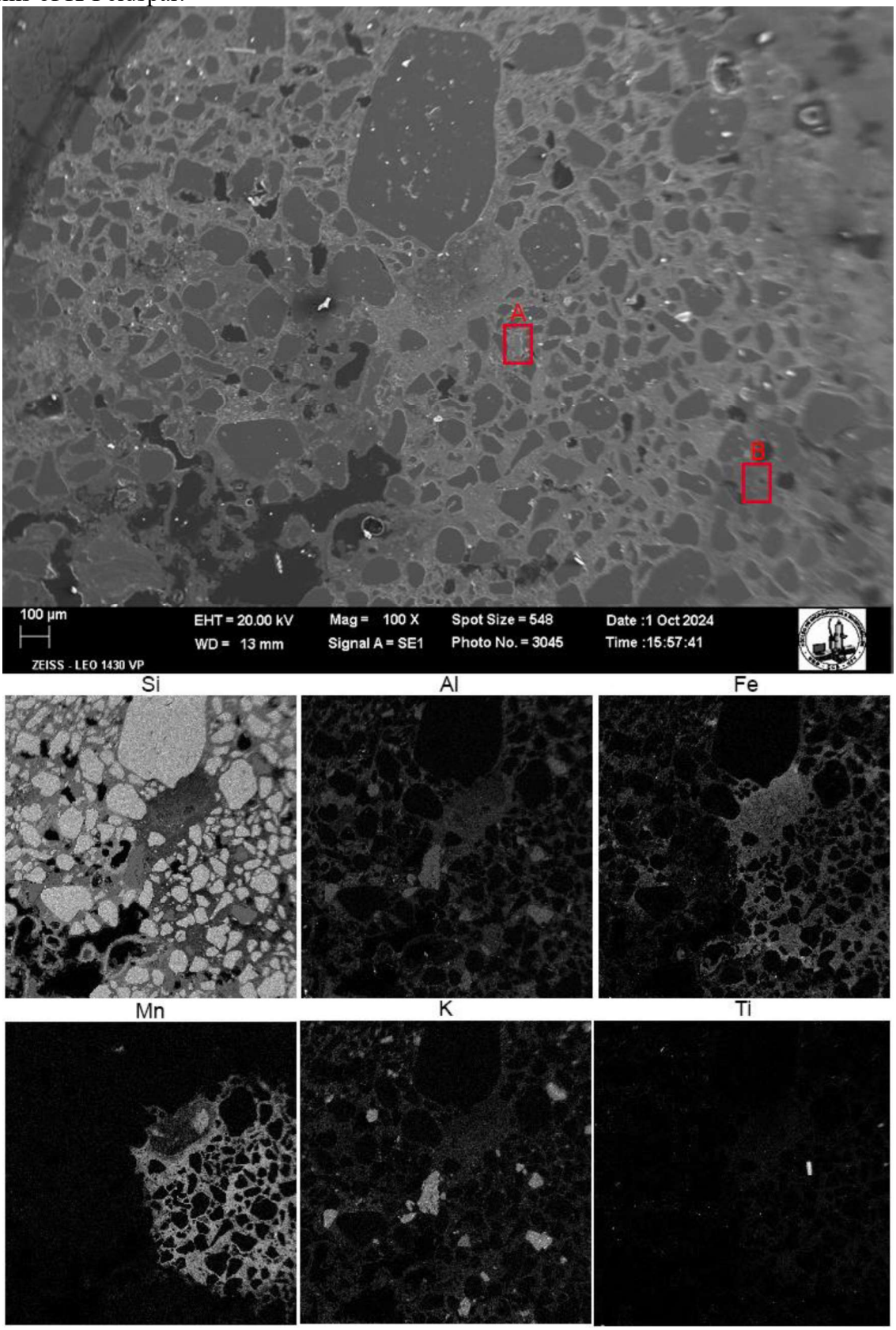

Source: The author.

In the Cg horizon of the *Baías* Arenosol (P26), the coarse material was composed of subangular, subrounded, and rounded, poorly sorted, fine sand-sized quartz grains (Appendix G), and some K-feldspar, plagioclase and Ti oxides (Figure 7 and Table3). The fine material was mainly composed of silicate clay, organic matter, and Fe and Mn oxides (Figure 7 and Table 3). The c/f related distribution was closed and single spaced porphyric, with some coarse monic and chitonic (Figure 8a). It presented simple packing porosity, along with single-pellicular grain. The b-fabric was undifferentiated, with few striated parts. Manganese and iron oxides nodules were common pedofeatures.

In the Podzol (P29) of the *Vazantes*, the 2E-2Bsm1 and 2Cg1-2Cg2 horizons presented subangular to rounded, poorly sorted, fine sand-sized quartz grains (Appendix G), with some K-feldspar and tourmaline (Figure 8b). The fine material of the 2E-2Bsm1 horizons was composed of silicate clay with gray colors and some iron oxides with red and yellowish-brown colors, which predominated in the Bsm1 horizon. Both 2E-2Bsm1 horizons exhibited coarse monic, chito-gefuric, and few single-spaced porphyric c/f related distribution pattern, mainly associated with Fe oxides in the Bsm1 (Figure 8b). The 2Cg1-2Cg2 horizons contained silicate clay with gray colors and some concentrations of iron oxides with reddish and yellowish-brown colors. The c/f related distribution pattern was coarse monic, chito-gefuric, and single spaced porphyric in the Fe oxides impregnations. All horizons of the P29 exhibited simple packing, vughs and few channels pores, as well as a single-bridged-pellicular grain and vughy microstructure (Figure 9). Orthic Fe and/or Mn nodules occur in the E-Bsm1, as well as Si nodules, enriched with Ca and Na, as observed in the SEM/EDS. (Figure 10 and Table 3).

The coarse material of the Btnqx horizon of the *Cordilheiras* Arenosol (P20) is composed of subangular, subrounded, and rounded, moderately sorted, fine sand-sized quartz grains (Appendix G). The fine material was mainly composed of silicate clay, iron oxides, and organic matter. The c/f related distribution patterns were chito-gefuric, and closed and single-spaced porphyric. Simple packing, vughs, chambers, and channels pores were present. The microstructure was characterized as vughy and bridged pellicular grain, and the b-fabric was undifferentiated. Some clay and organic matter infillings occurred (Figure 9a).

In the A horizon of the *Murundus* Arenosol (P8), the coarse material was composed of subangular, subrounded, and rounded, poorly sorted, fine sand-sized quartz grains (Appendix G). The fine material was composed of organic matter with brown and red colors, and very few iron oxides with red colors. The c/f related distribution pattern was coarse monic, with some chitonic and closed fine enaulic patterns. The porosity was characterized by complex packing, with some voughs and channels. The microstructure was single grain and crumb, with a weakly

developed and unaccommodated pedality due to the contribution of organic material. The pedofeatures found were clay coatings, organo-mineral aggregates, and impregnated orthic iron oxides nodules (Figure 9b).

Figure 7 – SEM/EDS elemental maps of the Arenosol (P26) located at a *Baía* at Nhecolândia Pantanal. a) Ti and Fe oxides; and b) matrix of Fe and Mn nodules and larger areas of Fe deposition.

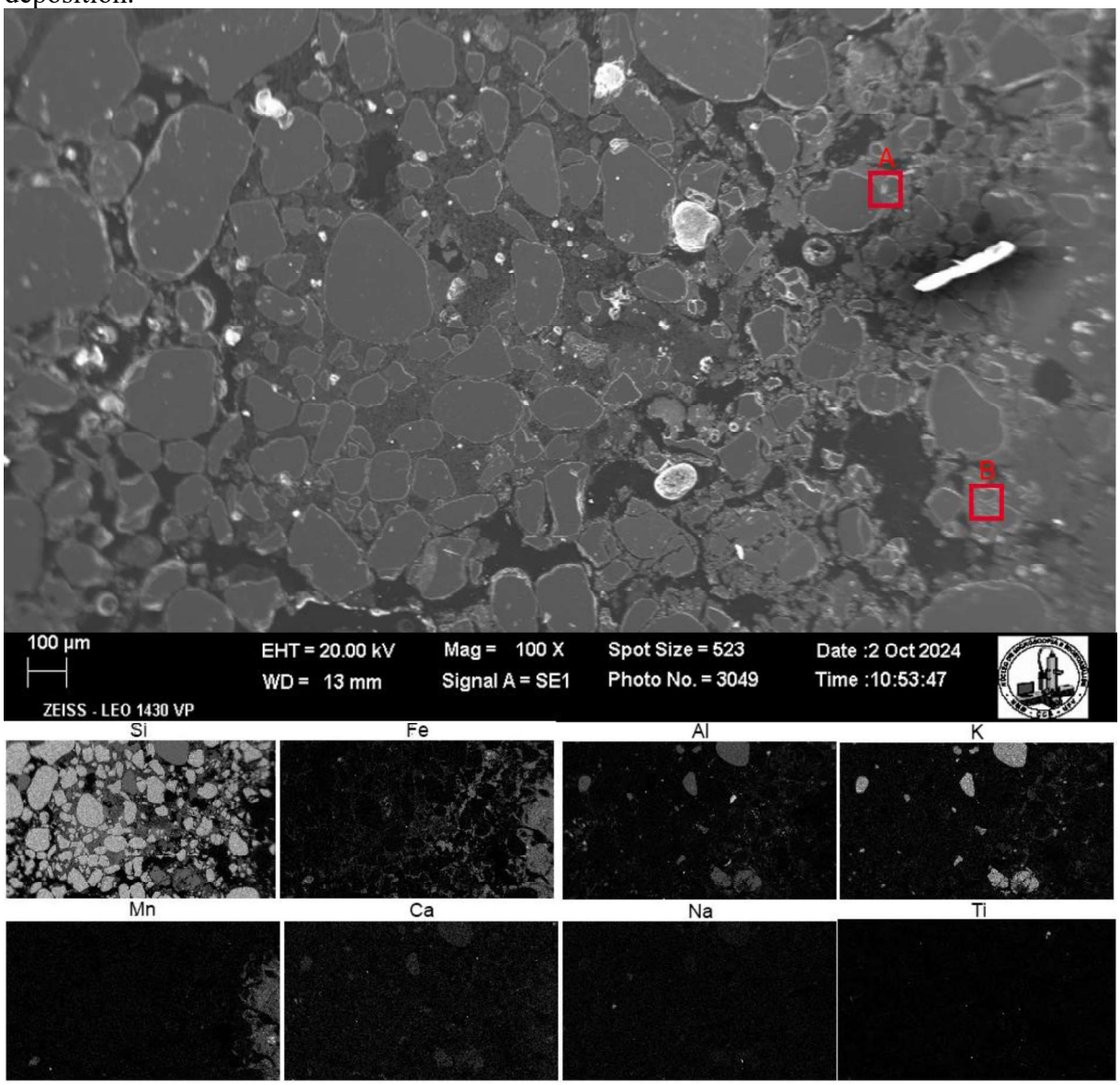

Source: The author.

Figure 8 – Microphotographs (PPL – plain polarized light; and XPL – crossed polarized light) of: a) Cg horizon of the *Baías* Arenosol (P26); b) E-Bsm1 horizon transition of the *Vazantes* Podzol (P29).

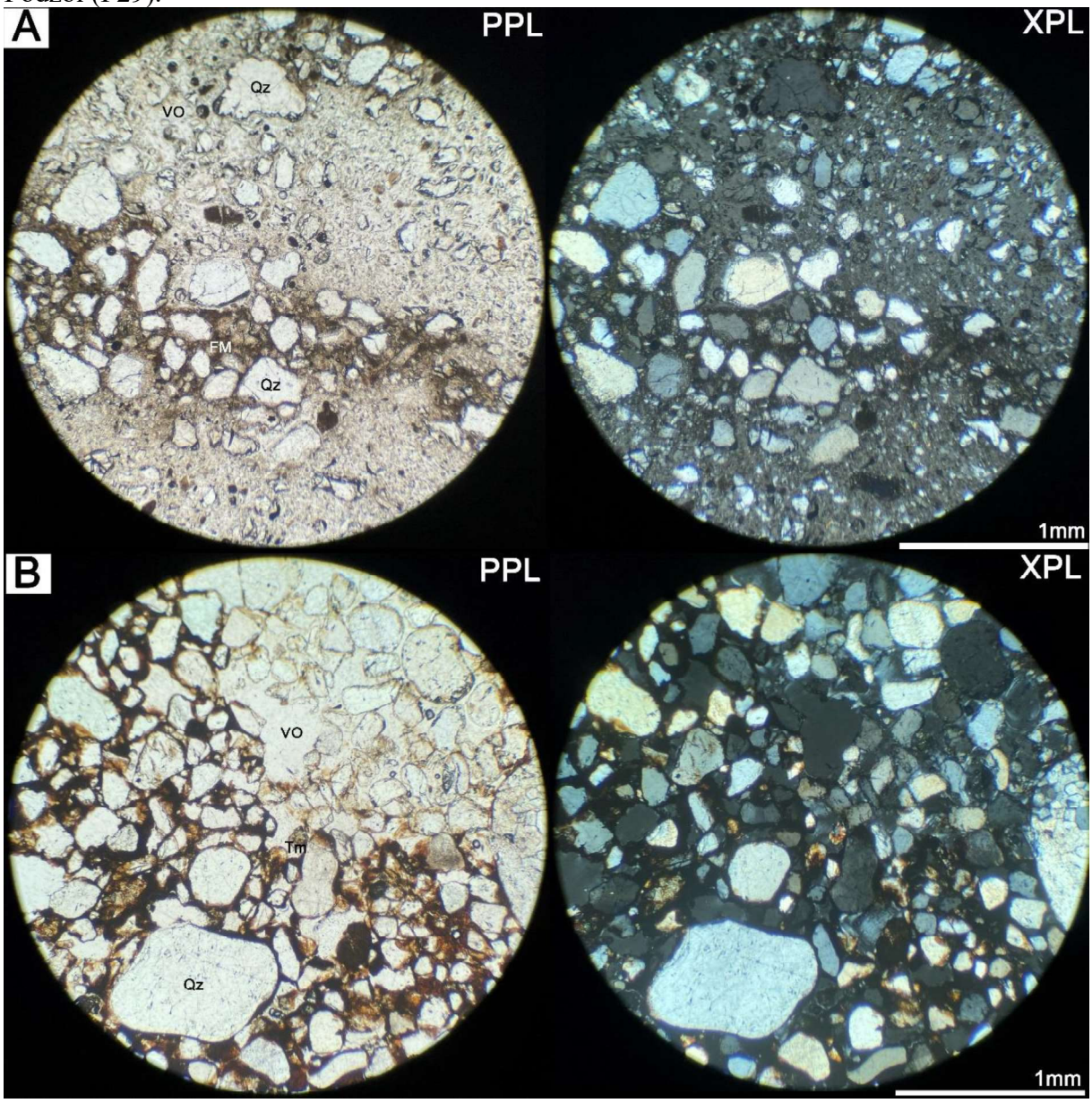

Source: The author.
Notes: FM – fine material; Qz – quartz grains; VO – void; Tm – tourmaline.

Figure 9 – Microphotographs (PPL – plain polarized light; and XPL – crossed polarized light) of: a) Btnqx horizon of a *Cordilheiras* Arenosol (P20); and b) A horizon of a *Murundus* Arenosol (P8).

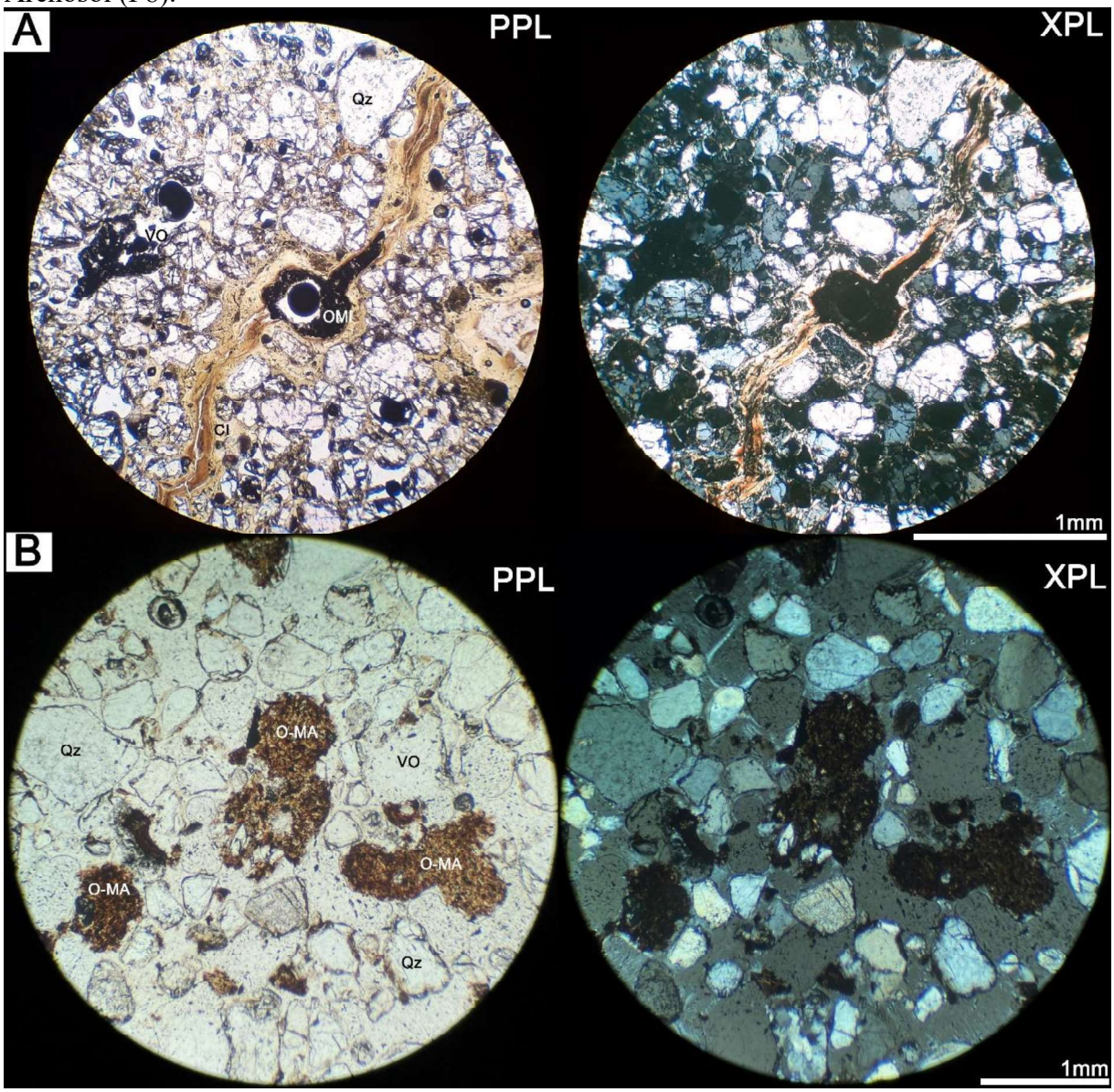

Source: The author.

Notes: Qz – quartz grains; VO – void; Tm – tourmaline; OMI – organic matter infillings; CI – clay infillings; O-MA – organic matter aggregate.

Figure 10 – SEM/EDS elemental maps of the 2E-2Bsm1 horizon Podzol (P29) located at a *Vazante* at Nhecolândia Pantanal. a) Fe-cemented with an inclusion of silica/Na nodule; b) soil matrix.

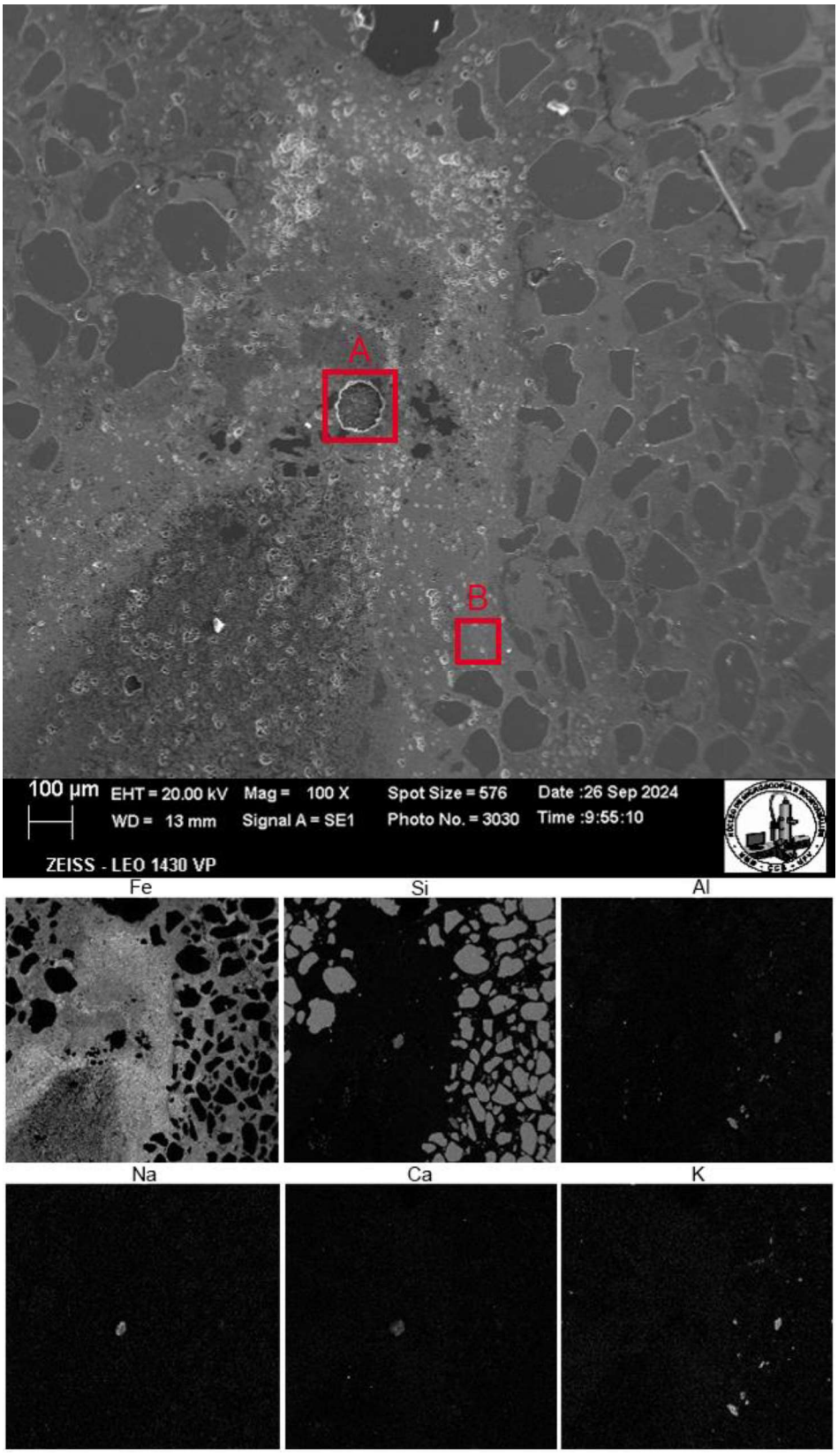

Source: The author.

4.4.4 Soil geochemistry and mineralogy

In general, the correlation matrix of soil geochemistry, crystalline (Fe_d and Al_d) and amorphous (Fe_o and Al_o) Fe and Al oxides, and water pH reveals two main soil groups in Nhecolândia region (Figure 11). The first soil group comprises acidic and kaolinitic soils, as indicated by the strong negative correlation between water pH and SiO_2 and TiO_2, alongside a strong positive correlation between SiO_2, Al_2O_3, and TiO_2. The second soil group consists of alkaline soils, enriched with salts and 2:1 minerals, evidenced by the strong positive correlation between water pH and K_2O, CaO, MgO, MnO, Na_2O, P_2O_5, as well as correlations among these oxides.

Figure 11 – Correlation matrix of geochemistry, Fe and Al oxides, and water pH of the soils Nhecolândia. Significant correlations ($p < 0.05$) are highlighted.

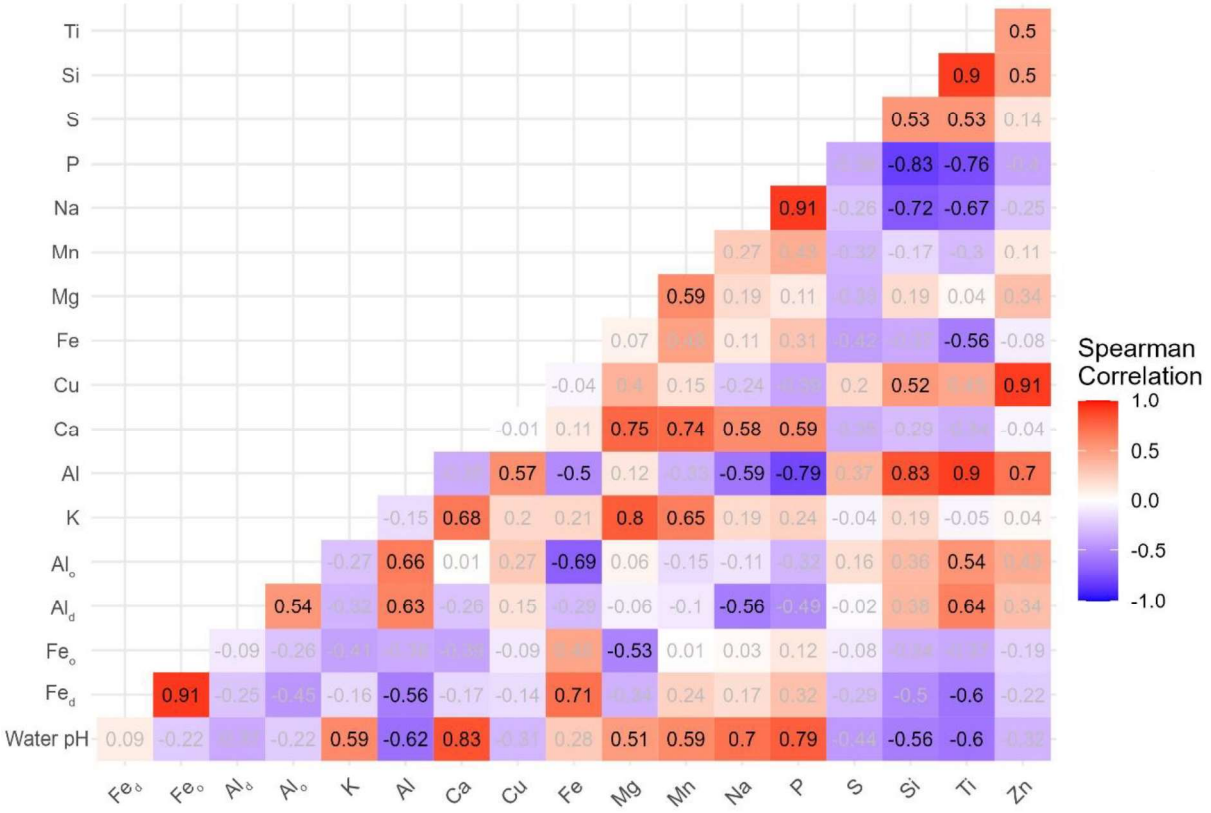

Source: The author.

Due to the homogeneity of the parent material, we analyzed the coarse fraction mineralogy of selected soil samples. The coarse and fine sand fractions from the *Salinas* Podzol (P19 Bsc1 horizon), *Baías* Planosol (P4 Bt horizon), and *Campos* Arenosol (P9 2C1 horizon) were predominantly quartz and K-feldspar (data not shown). Similarly, the silt fraction (Figure 12) across the six landscape units was mainly quartz and K-feldspar. However, calcite was

identified in the silt fraction of the *Salinas* Gleysol (P1 Bgn2 horizon), and goethite in the *Vazantes* Podzol (P29 2Bsm1 horizon).

Figure 12 – Mineralogical composition of the silt fraction of the *Salinas* (blue), *Baías* (orange), *Vazantes* (pink), *Cordilheiras* (light green), *Murundus* (dark green), and *Campos* (red) in the Nhecolândia Pantanal. Peaks d values in nm. Cc – calcite; Gt – goethite; It – illite; K-feld – k-feldspar; Ko – kaolinite; Qz – quartz.

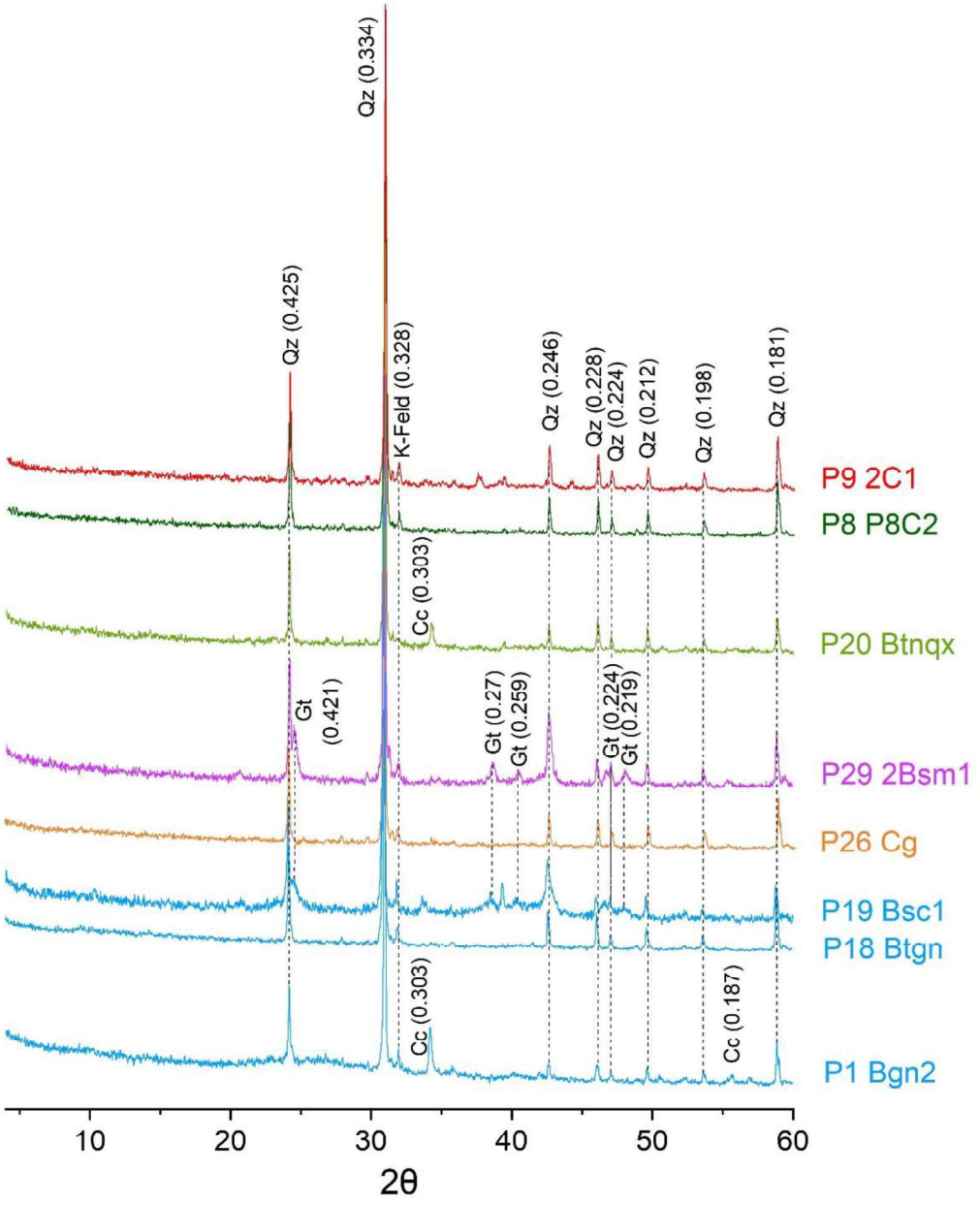

Source: The author.

The soil clay fraction of all landscape units contained kaolinite (Figures 13, 16, 17 and 19) and quartz. Kaolinite was identified by the disappearance of the 0.71 nm peak after K treatment at 550 ºC. Illite was present in the clay fraction of all *Salinas* soils, except for the Podzol (P19 Bsc1) (Figure 13), and was detected by the persistence of the 1.0 nm peak after

heating to 550 ºC (Figure 14a). Calcite was observed in the Bgn1 and Bgn2 horizons of the Gleysol (P1) and the Btgn1 horizon of the Solonetz (P18) (Figure 12), consistent with higher water pH, CCE, and total Ca contents (Tables 2 and 4). The clay fraction of the Gleysol horizons was more "illitic" than kaolinitic (Figure 14a), as indicated by high total K (Table 4), a trend also observed in the Agn2 horizon of the *Solonetz*. High total Fe indicated more Fe substitution in the illite structure of the Gleysol horizons (Table 4). The Agn2 horizon of the Solonetz exhibited a 0.757 nm d(001)-spacing peak, suggesting the presence of hydrated, poorly crystalline kaolinite (Figure 13). The Btgn horizon of the Solonetz presented more kaolinite and microcline than illite (Figure 14b), supported by high total Al content (Table 4). Poorly crystalline hydroxy-interlayered vermiculite (HIV) was also detected in this horizon, which also explains the higher Al contents. This was characterized by the lack of expansion of the 1.44 nm d(001)-spacing after ethylene-glycol solvation, partial collapse to 1.24 nm with K saturation, and full collapse to 1.02 nm after 550 ºC heating.

Figure 13 – Mineralogical composition of the clay fraction of the *Salinas* soils: Gleysol – P1 Bgn1 and Bgn2; Solonetz – P18 Agn2 and Btgn; and Podzol – P19 Bsc1. Peaks d values in nm. Cc – calcite; Gt – goethite; It – illite; K-feld – k-feldspar; Ko – kaolinite; Mc – microcline; Qz – quartz; and 2:1 – 2:1 phyllosilicate.

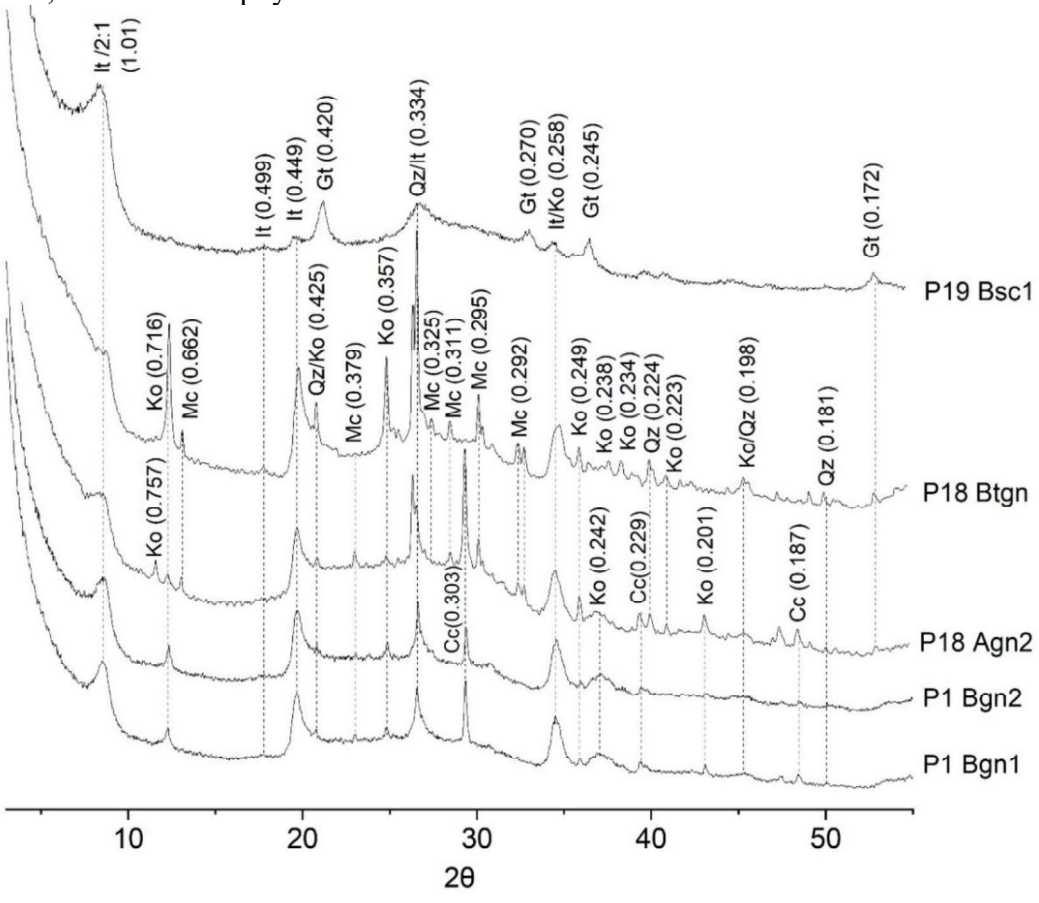

Source: The author.

Figure 14 – Mg saturation, K saturation, and heating treatments of the clay fraction of the: a) *Salinas* Gleysol (P1 Bgn1); and b) *Salinas* Solonetz (P18 Btgn). Peaks d values in nm. HIV: hydroxy-interlayered vermiculite; It – illite; Ko – kaolinite; and Qz – quartz.

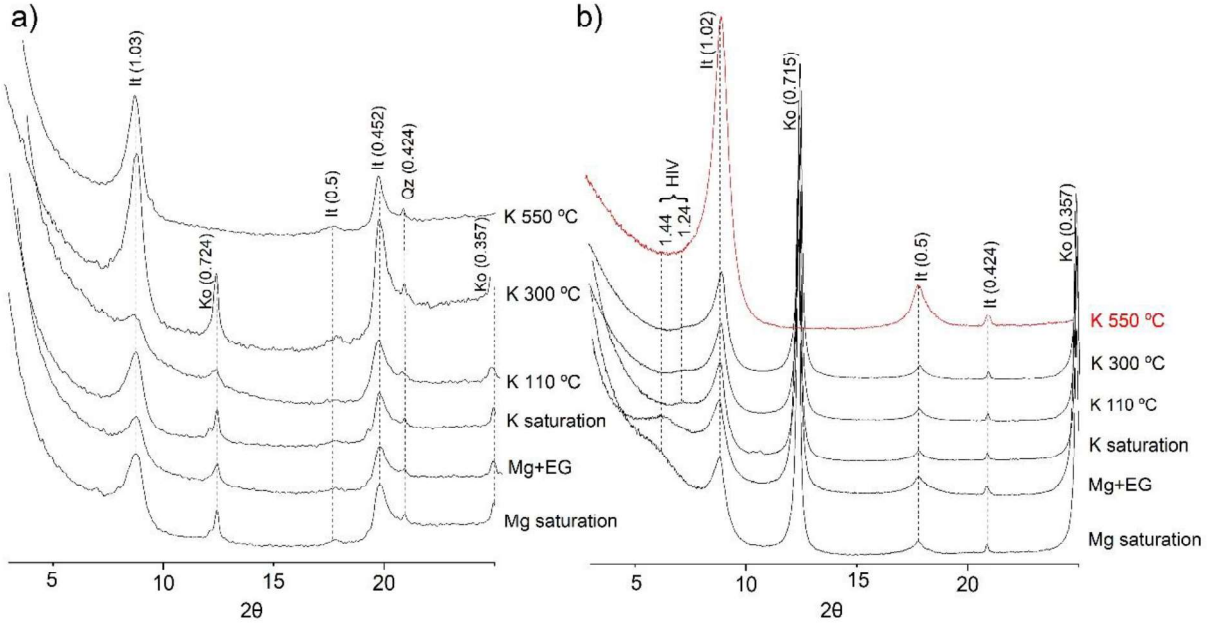

Source: The author.

Table 4 – Total content of geochemical composition of the soils of the six landscape units of Nhecolândia Pantanal.

Sample	K	Al	Ca	Fe	Mg	Mn	Na	P	S	Si	Ti	Zn	Cu
	%											-ppm-	
Salinas													
P1 Bgn1	2.69	2.34	2.52	4.92	1.27	0.83	6.38	6.83	0.02	17.13	0.11	38.54	42.08
P1 Bgn2	2.19	1.77	1.95	4.52	1.17	0.81	8.44	8.77	0.00	14.56	0.07	13.73	11.26
P18 Agn2	3.08	1.23	2.48	1.82	0.69	0.52	10.43	11.45	0.02	11.72	0.04	1.44	15.83
P18 Btgn	1.69	4.78	0.70	3.25	0.66	0.25	11.06	12.39	0.02	11.25	0.23	28.77	20.36
P19 A1	2.20	1.15	0.13	9.53	0.77	0.37	6.84	6.65	0.04	15.75	0.05	6.55	28.84
P19 A2	0.71	0.24	0.16	3.84	0.25	0.15	16.96	20.31	0.02	4.50	0.01	28.94	27.54
P19 Bsc1	0.63	0.12	0.13	7.22	0.14	0.17	15.37	18.05	0.02	3.77	0.00	0	1.58
Baías													
P4 Bt	1.91	2.96	0.68	5.88	0.71	0.25	9.73	10.40	0.01	12.66	0.15	37.91	32.95
P26 Cg	2.21	8.18	0.08	4.49	0.29	0.11	0.64	0.13	0.03	24.11	1.39	19.49	24.74
Vazantes													
P29 2Bsm1	0.25	1.22	0.05	5.79	0.02	0.08	0.47	0.17	0.00	4.64	0.02	4.01	9.70
P29 2Cg2	0.95	12.72	0.03	4.14	0.38	0.02	0.75	0.06	0.02	21.34	1.08	31.20	32.12
Cordilheiras													
P15 C1	1.54	8.88	0.20	4.70	0.32	1.03	1.14	0.24	0.02	21.12	1.12	55.32	27.99
P20 Bsnqx	0.93	2.78	1.58	1.57	0.46	0.08	14.20	16.72	0.00	8.18	0.18	14.21	11.39
Murundus													
P8 A	0.60	8.75	0.10	1.35	0.18	0.02	1.05	0.09	0.04	20.53	1.24	19.14	18.40
P8 C2	0.64	8.67	0.07	1.52	0.15	0.02	0.71	0.07	0.03	23.97	1.75	15.12	25.14

							Campos						
P9 2C1	0.44	13.72	0.08	1.59	0.28	0.00	1.76	0.08	0.02	20.04	0.87	46.39	26.05

The clay fraction of the Bsc1 horizon in the Podzol (P19) was dominated by goethite (Figure 12), consistent with its high total Fe (Table 4) and Fe_d (Table 5) contents. Among the 2:1 aluminosilicate, an interstratified mineral composed of HIV, vermiculite, and smectite predominated (Figure 14). This mineral was identified by the progressive collapse of the 1.12 nm d(001)-spacing peak after K saturation: to 1.2 nm (HIV); to 1.05 nm (vermiculite); and finally to 0.997 nm (smectite). Full collapse to 0.997 nm occurred only after heating to 550 ºC.

Figure 15 – Mg saturation, K saturation, and heating treatments of the clay fraction of the: *Salinas* Podzol (P19 Bsc1). Peaks d values in nm. Sm – smectite; HIV: hydroxy-interlayered vermiculite; Ko – kaolinite; Qz – quartz; and Vm – vermiculite.

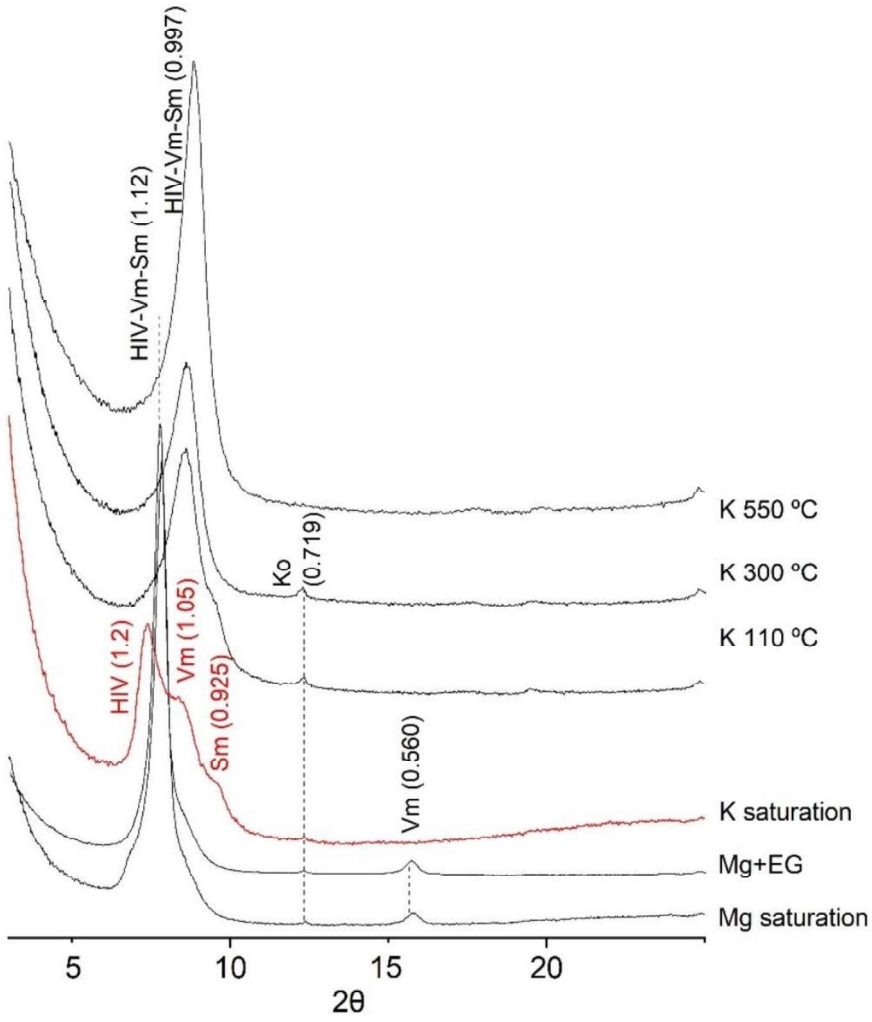

Source: The author.

Table 5 – Fe and Al oxides extracted by Dithionite-Citrate-Bicarbonate (Fe_d and Al_d) and by Ammonium Oxalate (Fe_o and Al_d) from the clay fraction of selected soil samples from the six landscape units of Nhecolândia Pantanal.

Sample	Fe_d	Fe_o	Fe_o/Fe_d	Al_d	Al_o	Al_o/Al_d
	g kg^{-1}					
Salinas						
P1 Bgn1	7.75	12.21	1.58	0.32	0.25	7.75
P1 Bgn2	9.26	12.79	1.38	0.32	0.32	9.26
P18 Agn2	4.79	11.39	2.38	0.18	0.45	4.79
P18 Btn	5.70	11.85	2.08	1.58	0.93	5.70
P19 A2	32.20	89.19	2.77	0.00	0.34	32.20
P19 Bsc1	96.51	339.99	3.52	0.09	0.10	96.51
Baías						
P4 Bt	10.32	17.34	1.68	0.74	0.28	10.32
P26 C3	4.16	8.00	1.92	0.81	0.12	4.16
Vazantes						
P29 2Bsm1	457.24	134.16	0.29	1.35	0.21	457.24
P29 2Cg2	15.68	8.20	0.52	0.98	0.33	15.68
Cordilheiras						
P15 C1	16.65	77.98	4.68	2.16	1.44	16.65
P20 Btnqx	3.91	8.42	2.15	1.18	0.70	3.91
Murundus						
P8 A	4.34	14.34	3.30	1.11	1.01	4.34
P8 C2	5.85	32.06	5.48	1.03	1.02	5.85
Campos						
P9 2C1	1.24	3.15	2.54	0.78	1.23	1.24

In the *Baías* Arenosol (P26 Cg), the clay fraction (Figure 15a) was dominated by kaolinite, but also presented illite, HIV, microcline, plagioclase, and quartz. These minerals also occurred in the *Cordilheiras* Arenosol (P20 Btnqx) (Figure 16b). The HIV was detected by the lack of expansion of the 1.46 nm d(001)-spacing peak with ethilene-glycol solvation, partial collapse to 1.2 nm with K saturation, and full collapse to approximately 1 nm after heating 550 ºC.

Figure 16 – Mg saturation, K saturation, and heating treatments of the clay fraction of the Arenosols of the: a) *Baías* (P26 Cg), and b) *Cordilheiras* (P20 Btnqx). Peaks d values in nm. HIV: hydroxy-interlayered vermiculite; It – illite; K-feld – K-feldspar; Ko – kaolinite; Pg – plagioclase; and Qz – quartz.

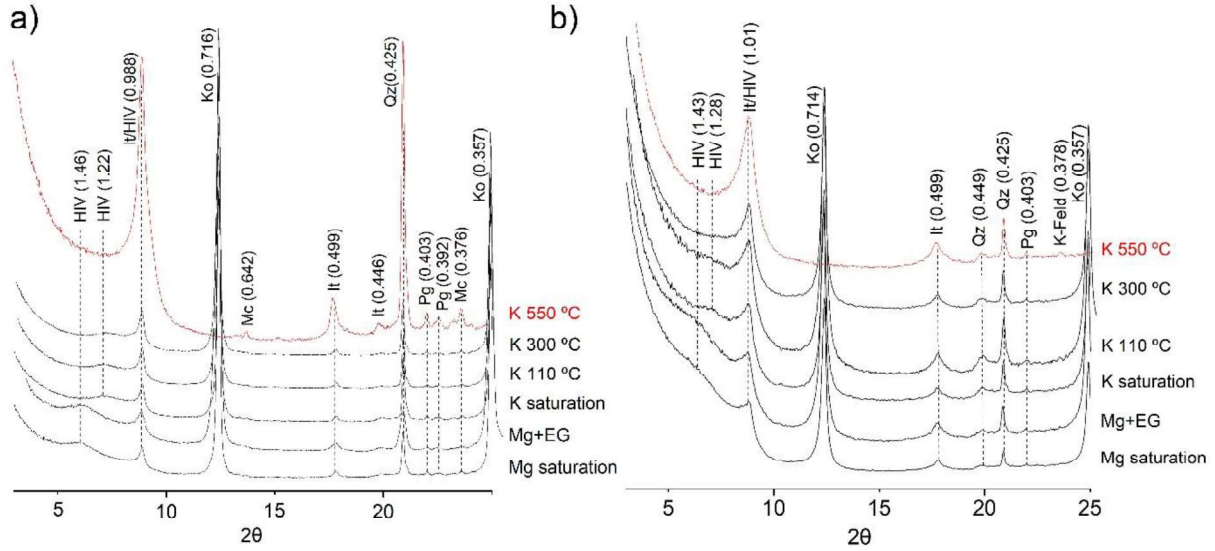

Source: The author.

The 2Bsm1 horizon of the *Vazantes* Podzol (P29) was dominated by goethite and hematite in the clay fraction (Figure 17), consistent with its high Fe_d (Table 5) and total Fe (Table 4) contents. In contrast, the 2Cg2 horizon lacked iron oxides, aligning with its low total Fe (Table 4) and Fe_d contents (Table 5). Instead, an intense kaolinite peak was observed (Figure 4). The 2Cg2 horizon also contained illite and an interstratified mineral (HIV or HIS). This mineral exhibited a 1.49 d(001)-spacing peak that expanded to 1.69 nm with ethylene-glycol solvation, confirming smectite. Partial collapse to 1.53 and 1.25 nm after K saturation at 25 ºC indicated HIV and HIS, respectively (Velde; Meunier, 2008). Upon heating to 300 ºC, the 1.25 nm peak persisted but disappeared at 550 ºC (Figure 18). These findings were supported by higher total K, Mg, and Na, contents in the 2Cg2 horizon, compared to the 2Bsm1 horizon.

The soils of the *Murundus* and *Campos* (P8 C2 and P9 2C1 horizons, respectively) exhibited similar clay mineralogy (Figure 19). K-feldspar and plagioclase were identified, which explain the significant total K and Al contents. Anatase was confirmed by elevated total Ti content, with the *Murundus* soil displaying the highest value among all analyzed samples.

Figure 17 – Mineralogical composition of the clay fraction of the Podzol located at the *Vazantes* landscape unit (P29), in Nhecolândia Pantanal. Peaks d values in nm. Gt – goethite; HIS/HIV – hydroxy-interlayered smectite/vermiculite; Hm- hematite; It – illite; K-feld – k-feldspar; Ko – kaolinite; Pg – plagioclase; Qz – quartz.

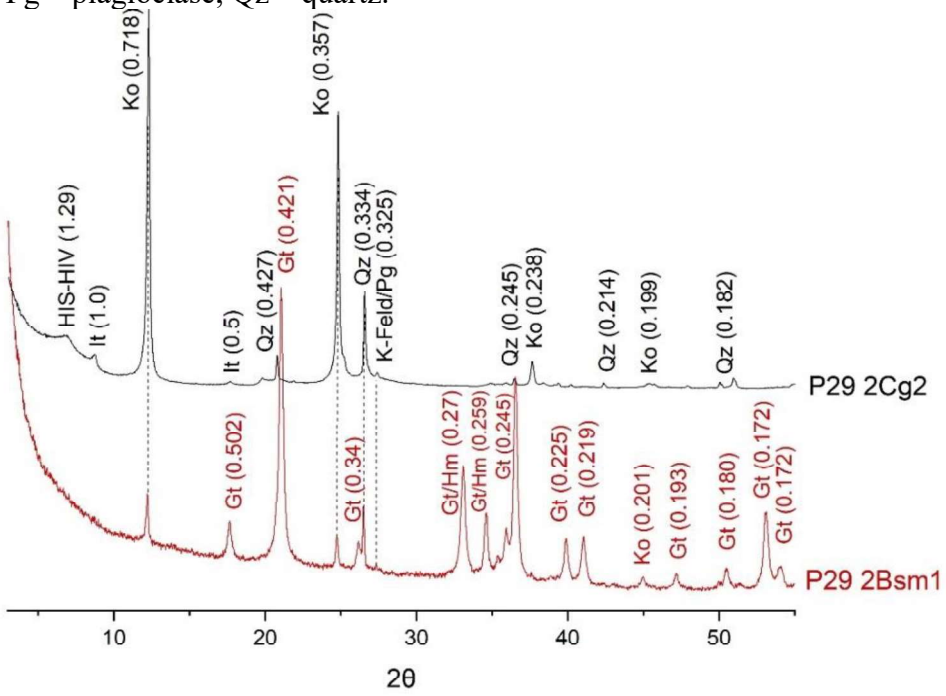

Source: The author.

Figure 18 – Saturation and heating treatments of the 2Cg2 clay fraction of the Podzol located at the *Vazantes* landscape unit, in Nhecolândia Pantanal. HIS/HIV – hydroxy-interlayered smectite/vermiculite; It – illite; Ko – kaolinite; Pg – plagioclase; Qz – quartz.

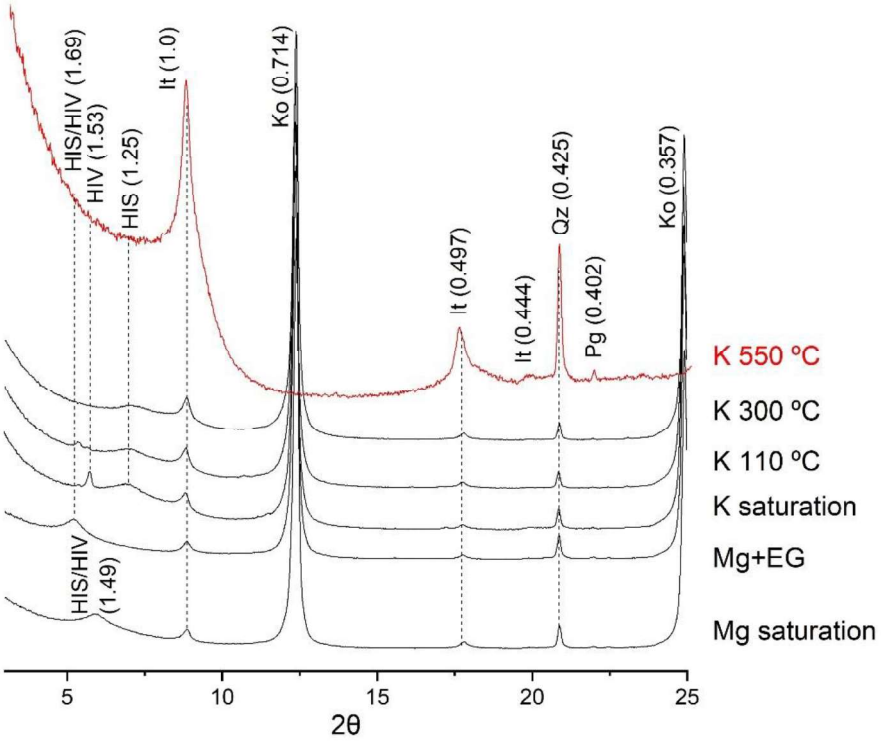

Source: The author.

Figure 19 – Mineralogical composition of the soils of *Murundus* (P8 C2) and *Campos* (P9 2C1) at Nhecolândia Pantanal.

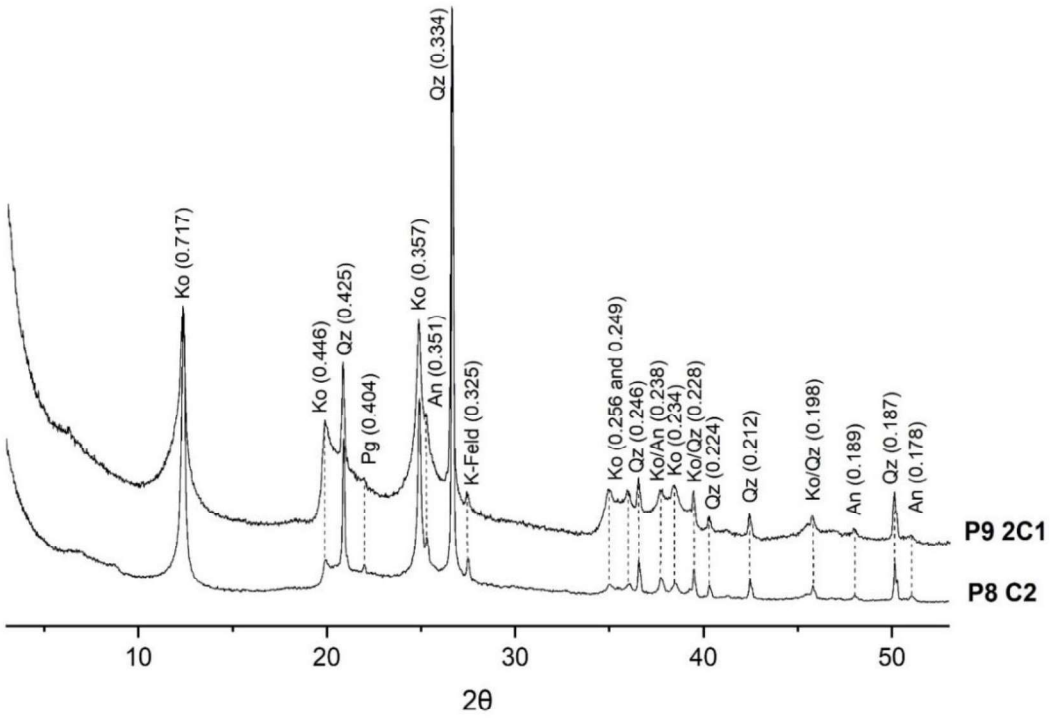

Source: The author.

4.4.5 Soil classification

In the Pantanal of Nhecolândia, five and four soil classes prevail according to the international (WRB/FAO) and Brazilian (SiBCS) soil classification systems, respectively (Table 1). Although many soils were influenced by groundwater and hydromorphic, only P1 qualified as Gleysol, specifically classified as Reductigleyic Eutric Gleysol (Clayic, Alcalic, Sideralic, Humic, Protosodic, Sodic, Uterquic) (GLEISSOLO HÁPLICO Sódico "hipocarbonático" êutrico). Gleysols are defined as "having a layer ≥ 25 cm thick and starting ≤ 40 cm from the mineral soil surface, that has gleyic properties throughout and reducing conditions in some parts of all sublayers" (IUSS Working Group WRB, 2022, p. 93). The qualifier eutric indicates base saturation higher than 50%, while reductigleyic denotes the absence of oximorphic features at depth. In the SiBCS, we suggest the hypocarbonatic qualifier for the Gleysol, as it contains CCE values between 50 and 150 g kg-1 (Santos *et al*., 2018). In the WRB/FAO system, this qualifier applies only to Solonchacks, but we also suggest it for Gleysols.

The P18 soil profile was classified as Albic Nudinatric Protosalic Stagnic Gleyic Solonetz (Arenic, Differentic, Endic, Ochric, Hypernatric) (PLANOSSOLO NÁTRICO Sálico

êndico). The Solonetz is characterized by a natric horizon, defined as a layer with high Na+ and clay contents (IUSS Working Group WRB, 2022). These soils typically exhibit columnar or prismatic structures. This Solonetz displayed high electrical conductivity (Table 2) and a natric horizon at the surface, qualifying it as protosalic and nudinatric, respectively. Other soil profiles in Nhecolândia also showed significant Na+ amounts, such as the Gleysol and the *Baías* Planosol, thus receiving the sodic supplementary qualifier. Although the *Salinas* Podzol had a high NaSI in the surface horizon, it did not meet the criteria for sodic, as the layer was not ≥ 20 cm thick.

The *Salinas* Podzol (P19) was classified as Stagnic Gleyic Entic Podzol (Arenic, Epic, Eutric, Sideralic) (ESPODOSSOLO FERRILÚVICO Hidromórfico "salino" "sódico" arênico), while the *Vazantes* Podzol (P29) was identified as a Gleyic Histic Albic Ortsteinic Podzol (Arenic, Abruptic, Epic, Sideralic) (ESPODOSSOLO FERRILÚVICO Hidromórfico arênico dúrico). Both Podzols displayed increased Fe at depth (mainly Fed), indicating strong podzolization predominantly involving Fe mobility (Table 6). The gleyic qualifier in both profiles indicate groundwater influence. In the SiBCS system, we recommend adding the saline and sodic qualifers to the *Salinas* Podzol, as it exhibits unusual high CCE (Table 2) and NaSI (Appendix C) in the surface horizon. However, in the WRB/FAO system, this surface horizon did not meet the thickness criteria for the sodic or natric qualifiers, and was therefore classified only as eutric. The *Salinas* Podzol, lacking albic material (E horizon), was qualified as entic and it exhibited stagnic properties, suggesting reducing conditions due to surface water. The *Vazantes* Podzol showed a cemented spodic horizon (ortstein) and a histic surface horizon (humic A horizon in the SiBCS).

The Baía Planosol (P4) was classified as an Eutric Albic Gleyic Histic Planosol (Arenic, Alcalic, Sideralic, Humic, Sodic) (PLANOSSOLO HÁPLICO Eutrófico gleissólico). The *Cordilheiras* Arenosol (P20) was classified as an Eutric Sideralic Brunic Arenosol (Ochric, Protoargic, Claric, Protospodic) in the WRB/FAO system but as a Planosol (PLANOSSOLO HÁPLICO Eutrófico solódico espessarênico) in the SiBCS. In the Brazilian classification, this profile displayed an abrupt textural change from the E to Bt horizon, which otherwise did not meet WRB/FAO criteria. Both the Planosol and Arenosol received the eutric qualifier due to high base saturation. The *Baías* Planosol was assigned the sodic supplementary qualifier because of increased Na+ at depth, while the Cordilheira Arenosol did not receive this qualifier, as its Na+ accumulation occurred below 100 cm depth. Additionally, the *Cordilheiras* Arenosol received the protospodic supplementary qualifier due to an increase in the Alo content at depth (Table 6), although did not meet the criteria for spodic horizon.

The *Baías* Arenosol (P26) was classified as Eutric Sideralic Brunic Gleyic Arenosol ("Histic") (NEOSSOLO QUARTZARÊNICO Hidromórfico organossólico), being the only Arenosol profile to show groundwater influence and a histic horizon due to organic matter accumulation. The *Vazantes* Arenosol (P30) was classified as Dystric Sideralic Arenosol (Ochric) (NEOSSOLO QUARTZARÊNICO Órtico típico), due to its lower pCEC. The P7 and P15 profiles of the *Cordilheiras* were classified as Eutric Sideralic Brunic Arenosol (Ochric) (NEOSSOLO QUARTZARÊNICO Órtico típico). The *Murundus* soil was classified as a Dystric Sideralic Brunic Arenosol (Ochric, Isopteric, Claric), and of the *Campos* soil was Eutric Sideralic Brunic Arenosol (Ochric) (both NEOSSOLO QUARTZARÊNICO Órtico típico), with the distinction that the *Murundus* profile showed intense biological activity, while the *Campos* profiles had higher base saturation.

Table 6 – Fe and Al extracted by Dithionite-Citrate-Bicarbonate (Fe_d and Al_d) and Ammonium Oxalate (Feo and Alo) of the total soil fractions of two Podzols (P19 and 29) and one Planosol (P20) of the Pantanal of Nhecolândia.

Profile	Horizon	Depth	Fe_d	Fe_o	Al_d	Al_o
		cm	---------- g kg^{-1} ----------			
			Salina			
19	1A	0-5	5.70	2.5	0	2.13
	A2	5-10	8.37	4.71	0	0.99
	Bsc1	10-28	16.93	7.26	0	1.46
	Bsc2	28-48	9.72	1.82	0	1.56
	Bsc3	48-70+	1.90	1.19	0	1.61
			Cordilheira			
20	A	0-36	0.59	0.34	0	1.61
	AE	36-53	0.29	0.14	0.27	1.79
	E	53-96	0.49	0.05	0.23	1.42
	Bt	96-107	0.17	0.17	0.05	2.03
	Btnqx	107-110	0.88	0.34	0.17	3.07
			Vazante			
29	Oo	0-14	1.49	1.17	0.65	1.02
	AO	14-23	0.90	0.76	0.16	0.31
	AE	23-29	0.59	0.32	0.07	0.07
	E	29/48-48/65	0.25	0.07	0	0.07
	Bsm1	45/53-53-63	19.89	3.03	0.11	0.02
	Bsm2	65/67-73/76	11.55	6.32	0.02	0.25
	Cg1	76-94	3.92	1.02	0.05	0.08
	Cg2	94+	0.97	0.49	0.07	0.22

Source: The author.

4.4.6 Stable carbon isotopes and dating

The $\delta^{13}C$ of the deepest horizon (106-128 cm) of the Solonetz (P18) profile showed a signal of -23.4‰, indicating a contribution of C3 plants (Figure 19). The ^{14}C dating of this horizon was 6,110 ± 30 cal years BP (Table 7 and Figure 19). From this depth to the surface the carbon isotopic signals increase, varying from -15.53 to -11.92 ‰, indicating increasing contribution of C4 plants with time. Carbon isotopic enrichment higher than 3 to 4 ‰ probably indicates a change in plant community during pedogenesis (Martinelli *et al.*, 2009). The age of the Solonetz surface horizon (5-15 cm) was 2,115 ± 165 years.

The $\delta^{13}C$ signals of the *Baías* Arenosol (P26) did not show a significant variation along the profile. From the 105 cm depth to surface, there was an insignificant decreasing from -25.43 to -27.25 ‰, indicating the predominance of C3 plants, which we postulate is an aquatic vegetation. OSL dating at 60 cm depth of the *Baías* Arenosol was 6,585 ± 670 years (Table 8) and the ^{14}C dating at 15-20 cm depth was 420 ± 30 cal years BP (Table 7 and figure 19), which is influenced by migration of organic matter.

The *Vazantes* Podzol (P29) also did not present any significant variation of the $\delta^{13}C$ signals along the soil, varying from -22.93‰ at 94 cm depth to -24.42‰ at surface, which indicate a predominance of C3 plants. The OSL dating at 73/76 – 94 cm depth showed the oldest age of 8,970 ± 785 years (Table 8 and Figure 19). In contrast, the *Vazantes* Arenosol (P30) showed a carbon isotopic signal of -21.72‰ at a depth of 90 cm, indicating the contribution of C3 plants, increasing to -14.34 at the soil surface. This great $\delta^{13}C$ change indicates an environmental change from C3 to C4 dominated plants communities. OSL dating of quartz grains in 70-80 cm depth indicates an age of 4,680 ± 360 years BP (Table 8 and Figure L).

The mean $\delta^{13}C$ signals of the *Cordilheiras* Arenosols (P7 and P14) were, respectively, -24.11 and -23.77‰, indicating a major contribution from C3 plants. Both soils showed increasing $\delta^{13}C$ signal with depth, that was only significant (~4 ‰) at P7. A carbon isotopic value of -22.6 at P14, indicate a mixed C3/C4 plant community. The mean $\delta^{13}C$ of the *Murundus* Arenosol (P8) was -26.84‰, also indicating a major contribution from C3 plants, with no significant enrichment at depth. In turn the $\delta^{13}C$ of the *Campos* Arenosol varied from -19.15 to -22.58 ‰, with a mean of -20.7 ‰, showing a mixture of C3/C4 plants.

Figure 19 – $\delta^{13}C$ signals and dating results (^{14}C and OSL) of selected soils from landscape units in the Nhecolândia Pantanal. Radiocarbon ages are given in years before 1950 (BP), while OSL ages represent average years.

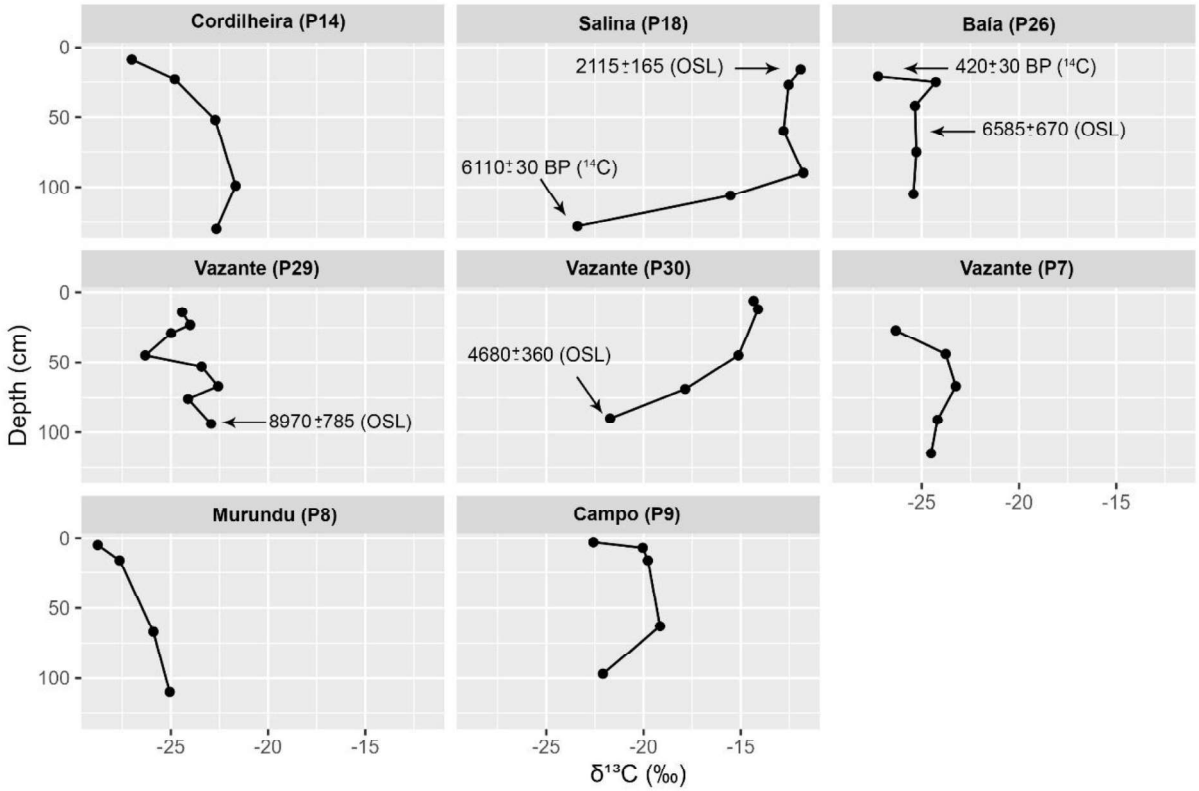

Source: The author.

Table 7 – ^{14}C calibrated ages for samples collected at a Salina (P18 Btg2) and a Baía (P26 H) lakes.

ID	**Depth (cm)**	**Lab code**	**$\delta^{13}C$ (‰)**	**Age (^{14}C yr BP)**	**Error (±)**	**95.4% Probability (cal yr BP)**	**Material**
P18 Btg	106-128	Beta-613499	-22	6110 ±30	30	7015-6795	Charcoal
P26 H	0-20	Beta-613500	-25.8	420 ± 30	30	502-437	Peat

Table 8: OSL age estimates for the quartz sands from the *Salinas* (P18), *Baías* (P26), and *Vazantes* (P29 and P30) of the Nhecolândia Pantanal.

Soil profile (cm)	Depth (cm)	Sample	Aliquots used/total	Over-dispersion (%)	Equivalent dose - D_e (Gy)	Age (yr)
P18 A1	5-15	5596	15/15	0 ± 38%	4.18 ± 0.18	2115 ± 165
P26 E2	60	5597	15/15	29 ± 6%	9.64 ± 0.83	6585 ± 670
P29 2Cg1	80-90	5598	15/15	20 ± 4%	11.77 ± 0.79	8970 ± 785
P30 C3	70-80	5599	15/15	9 ± 2%	7.55 ± 0.39	4680 ± 360

4.5 DISCUSSION

4.5.1 Pedogenesis at the Nhecolândia landscape units: soil forming factors and processes

4.5.1.1 The importance of the parent material

Except for the *Salinas* soils, which are more clay-rich and alkaline-sodic, the soils across Nhecolândia's landscape units are predominantly sandy, acidic, and dystrophic, as highlighted by previous pedological studies in the region (Cardoso *et al*., 2016; Cunha, 1980, 1985; Reis, 2017). This predominance reflects a strong influence of the pre-weathered sediments nutrient-poor substrates. Arenosols were the most common soil class, with quartz dominating the sand fraction and kaolinite consistently present in the clay fraction of all samples. This mineral composition suggests that Nhecolândia's sediments originate from the highly weathered and nutrient-poor sources where a Ferralsols cover (Latossolos Vermelho-Escuros álicos and Latossolos Vermelho-Escuros distróficos) (Furquim *et al*., 2010). Overlain the the quarzitic sandstones of the high plateaux of Maracaju-Campo Grande Plateau (Brasil, 1982). Additionally, micromorphological and mineralogical analyses indicated the presence of weathering-resistant Ti oxides in the sand (SEM/EDS results) and clay (DRX results) fractions of the *Salinas* and *Murundus* soils, respectively, supporting the presence of highly weathered parent material in the Nhecolândia region, corroborating with Rasbold *et al*. (2024), who also found common Ti minerals in the sediments of a *Salinas* lake at Nhecolândia.

Although the Nhecolândia is part of the abandoned lobe of the Taquari megafan, its soils lack the stratified layers that would qualify them as having a fluvial character. Previous studies (Assine, 2004; McGlue *et al*., 2017; Soares; Soares; Assine, 2003) have identified a complex mix of eolian and fluvial sediments in the Nhecolândia wetlands. This sediment composition results from extensive aeolian remobilization, transport, and redeposition of sorted sand, followed by alluvial reworking that facilitated mixing with sands transported by rivers. The subangular to well-rounded, poorly to moderately sorted fine sand grains observed in the micromorphological analysis support these findings.

4.5.1.2 The importance of the organisms

Apart from a homogenous parent material, the variability of Nhecolândia soils is influenced by factors such as vegetation and soil fauna. The Arenosols of the *Cordilheiras* and *Murundus* show significant organic carbon content at surface, due to organic material input from the arboreous vegetation cover. Nascimento *et al*. (2024) reported that leaf litter in the Nhecolândia *Cordilheiras* and *Murundus* had higher organic carbon content compared to the forested areas of the Pantanal subregions of Abobral and Miranda. In Nhecolândia, these areas exhibit similar floristic composition (see Chapter 2), characteristic of semideciduous forest, cerradão and cerrado phytophysiognomies. In environments influenced by water table fluctuations, woody species typically occupy higher, well-drained ground, either caused by abiotic (hydrological/geomorphological) or biotic factors (termite mounds) (Ferreira-Júnior *et al*., 2016; Ponce; Da Cunha, 1993).

In the *Cordilheiras*, despite the sandy texture, the significant cation exchange capacity and relatively high contents of P and TOC indicate a dependence on organic complexes for nutrient retention in these soils (Cunha, 1980, 1985). The formation of a weakly developed A horizon in the *Cordilheiras* reflects the incipient but still significant input of organic matter through the pedogenetic process addition. This is very important for nutrient cycling in the sandy environments of Pantanal (Cunha, 1985). Cardoso *et al*. (2011) identified a decrease in soil chemical quality after the replacement of native tree vegetation in the *Cordilheiras* by pasture, with losses of soil organic matter, particularly in the 0–10 cm layer.

Except for the P20, the Arenosols of the *Cordilheiras* (P7 and P15) were acidic (pH ≤ 6.2), which corroborates with the studies of Costa-Silva *et al*. (2024) and Merdy *et al*. (2022), who described a light brown sand layer (pH = 6.8) and a deep, slightly acidic water table (pH = 7) occurring in the *Cordilheiras*. Below the pale brown sand layer, these authors encountered a silcrete-type horizon in the transition to a deep greenish-brown sand layer, the site of amorphous silica precipitation driven by supersaturation promoted by evaporation in the capillary fringe (Barbiero *et al*., 2002; 2008; Costa-Silva *et al*., 2024). Deep in the P20, which we classified as a Planosol (Planossolo Háplico) in the Brazilian classification system (SiBCS), we found an Btnqx horizon with increasing clay content, high pH values, concentrations of $CaCO_3$, and exchangeable Na. Cementation was found, although total Si was not so high (~8%). There was also an increase of Al_o content in the Btnqx horizon, though not significant enough to form spodic horizons. In addition, clay and organic matter infillings confirm the lessivage and podzolization processes. Kaolinite, illite, and hidroxy-interlayered vermiculite were found

in the clay fraction of this horizon supporting the findings of Furquim *et al*. (2008) which also found 2:1 phyllosilicate minerals in the upper zone of the *Salinas*, close to the *Cordilheiras*.

The formation of this subsurface alkaline, sodic, cemented horizon in the *Cordilheiras* would be explained by influence of the perched water table of the *Salinas*. However, the P20 is located around a *Baía* lake (P26), not a *Salina* lake. According to Barbiero *et al*. (2008), the alkaline and low permeable subsurface horizons occur both in *Salinas* and *Baías* lakes, being discontinuous in this last one due to degradation by freshwater flux, in contrast to the saline-alkaline conditions of the *Salinas*. This would explain the occurrence of the Btnqx horizon around the *Baía*, but no evidence of the cemented horizon was found in P26, at least not until our observation's depth. Recent studies indicate that any changes in drainage condition allow ion leaching from the system and, consequently, reduction of saline-lakes' alkalinity, showing that hydraulic connection in some Nhecolândia lakes is converting *Salinas* into *Baías* (Costa-Silva *et al*., 2024; Furquim *et al*., 2017; Merdy et al., 2022).

In the *Murundus*, we observed evidence of bioturbation and pedalization driven by termite activity. The increase in clay content with soil depth results from termites selecting fine organic and mineral particles to construct their nests, which are cemented with salivary secretions (Howse, 1992; Jouquet; Lepage; Velde, 2002). After ingesting these particles (geophagy), their digestive system physically and chemically alters the organic matter, promoting humification and forming stable organo-mineral complexes with clay (Brauman, 2000). Microphotographs revealed an enaulic c/f related distribution pattern, showing individual aggregates formed by organic-mineral complexes derived from topsoil materials (Humphreys, 1993). Brazilian Latosols exhibit a microgranular microstructure, a long-term biotic product primarily shaped by termites (Fruett *et al*., 2023; Schaefer, 2001). The high acidity of the *Murundus* soils is therefore attributed to organic acids released during the humification process, intensified by the termite activity (Brauman, 2000).

Studying the mounds of the North Pantanal, Oliveira Junior *et al*. (2017) postulated a formation by erosion and rounding of the *Cordilheiras* during erosive Holocene floodings events, followed by termites colonization seeking refuge from inundation. This may explain the similarities between the *Cordilheiras* and *Murundus* Arenosols. However, the slightly higher TOC contents and, especially, the higher clay content and its variations along the soil profile in the *Murundus* highlight the role of termites in mound development through a continuous process of erosion and reconstruction (Nascimento *et al*., 2015; Oliveira-Filho, 1992). Comparisons with surrounding *Campos* Arenosols, currently covered with grasses, further support termite activity's role in the *Murundus*, as indicated by the higher TOC content (See

Chapter 2), consistent with findings by Nascimento *et al*. (2015). Soil eroded from the *Murundus* accumulates in the *Campos*, as evidenced by surface discontinuities and elevated exchangeable Ca and Mg contents in the surface horizons, compared with the *Murundus*. In this soil, there were no evidences of redoximorphic features, as commonly occur around the *Murundus* (Oliveira-Filho, 1992), once this area is only occasionally inundated, and Fe is leached.

4.5.1.3 The importance of the hydrological regime, influenced by climate and topography

The Arenosol of the *Vazantes* closely resembles that of the *Campos* but showed higher surface soluble Fe, likely due to leaching from the elevated areas. Despite seasonal flooding, no gleization was observed, likely because its slightly higher topographical position and sandy texture, which limits microbial activity and oxidation (Schaetzl; Anderson, 2005). In contrast, the *Vazantes* Podzol exhibited alternating redox conditions caused by groundwater fluctuations, driving processes such as paludization, podzolization, and gleization. Paludization is marked by a histic or humic A horizon, according to WRB/FAO and SiBCS classification, respectively, formed under water saturation, and low organic matter decomposition (Tiedje *et al*., 1984). OM-Fe-complexes eluviated from the upper areas, laterally migrates to form subsurface organic-rich surface horizons, which translocate in the profile to deeper horizons, creating the combined albic (E) and spodic horizons (Bsm1, Bsm2). This was evidenced by higher contents of Fe_o than Al_o, though organic matter was lower. Glei horizons below the spodic horizon suggests permanent reducing conditions near the water table, where Fe mobility and oxidation-reduction cycles promote red-orange mottling and cementation (Schaetzl; Anderson, 2005). Additionally, the 2Bsm1 horizon also contains well-crystallized goethite and hematite, confirmed by high Fe_d and total Fe contents, as previously reported by Schiavo *et al*. (2012) in the seasonally flooded Podzols in this region.

The glei horizons (2Cg1 and 2Cg2) of the *Vazantes* Podzol exhibited very low pH values (4.2 and 3.5, respectively), indicating ferrolysis. Under reducing conditions, Fe^{2+} ions replace base cations and Al^{3+} on clay exchange sites. Upon oxidation, the adsorbed Fe^{2+} oxidizes to Fe^{3+}, releasing H^+ and increasing acidity, as reflected in the higher Al^{3+} and H+Al levels compared to the overlying spodic horizons. This process degrades clay minerals, particularly 2:1 clays with higher CEC, while kaolinite dominates in the 2Cg2 horizon, confirmed by low Ki values (Schaetzl; Anderson, 2005). However, illite and hydroxy-

interlayered smectite and vermiculite minerals persist, for being stabilized by high Si, Al, and Mg concentrations under restricted drainage (Dixon; Weed, 1989).

In the *Baías* soils, prolonged water saturation promotes paludization, particularly in the Arenosol, where a histic epipedon forms, contributing to increase the acidity. The Planosol, however, exhibits a very dark gray A horizon with high TOC content. Both profiles showed lessivage and gleization in the deeper, being more pronounced in the Planosol due to higher clay content. In this soil profile, clay illuviation occurred at ~44 cm (Eg1) and ~100 cm (Bt) depth, reflecting seasonal water table fluctuations. In addition, pH, base cation saturation, Na saturation, $CaCO_3$, and HCO^{3-} increase with depth, indicating sodification and calcification from salt leaching. This suggests increased leaching, favoring solodization and possibly transforming the *Salinas* into *Baías*. Furquim *et al*. (2017) and Reis (2017) reported similar process in Nhecolândia soils, driven by freshwater influx from the *Cordilheiras* and intense leaching.

Salinization, sodification, calcification and neoformation were the primary soil-forming processes observed in the *Salinas* of the Nhecolândia, as corroborated by several studies (Bacani *et al*., 2010; Barbiero *et al*., 2008, 2002, 2016; Costa-Silva *et al*., 2024; Dias *et al*., 2020; Freitas *et al*., 2019; Furian *et al*., 2013; Furquim *et al*., 2008, 2010, 2010; Merdy *et al*., 2022). High water pH values, elevated electrical conductivity, concentrations of soluble salts, calcium carbonates, and high exchangeable Na were observed in the upper horizons of the Gleysol, Solonetz and Podzol, evidencing these processes. Calcite in the Gleysol (P1) and Solonetz (P18) was confirmed by mineralogy and micropedology, with its presence in the silt fraction of the Gleysol suggesting microaggration. In the Solonetz, calcite composed the soil micromass, as evidenced by the crystallitic b-fabric, and coated silicious-ferruginous nodule, attributed to amorphous silica precipitation. Amorphous silica is abundant in the *Salinas* environment (Barbiero *et al*., 2008) and Ca chemisorption occur, as well as other metallic cations, due to its more reactive negative surface (Dixon; Weed, 1989). The corroded surface and discontinuous boundary of the nodule indicated degradation, driven by increased silica solubility at pH > 9 (Dixon; Weed, 1989).

The formation of the *Salinas* is driven by hydrological disconnection from the surrounding landscape, caused by a low-permeability greenish sandy loam horizon acting as a barrier (Barbiero *et al*., 2008; Costa-Silva *et al*., 2024; Furian *et al*., 2013). We identified this greenish horizon only at the Solonetz profile, at 128 cm depth. Barbiero *et al*., (2008) and Furquim *et al*., (2008) found this horizon reaching, respectively, 6 m and 3.2 m depth at a *Salina*. During the dry season, evaporation exceeds precipitation, lowering the water table and

isolating the *Salinas* from the fresh groundwater system. This promotes the precipitation of amorphous silica, calcite, and clay minerals along the *Salinas* shore, due to evaporation from the capillary zone, usually forming a trona crust. On the *Salinas* Podzol shore, a duripan (or silcrete) was identified, composed of indurated amorphous silica (Opal-A) mixed with Mn, Fe, Al, and Ti oxides, as confirmed by microchemical analysis. Silcretes in lacustrine environments often contain diverse matrix minerals influenced by lake sediment chemistry (Dixon; Weed, 1989; Nash; Ullyott, 2007). During the wet season, water levels rise above the greenish horizon, enabling flow towards the *Salinas*. In the *Baías*, the same process occurs, but the discontinuous greenish (indurated) layer results in less pronounced evaporation effects.

In the *Salinas* clay fraction, authigenic 2:1 phyllosilicate minerals, including illite, vermiculite, smectites, and interstratified minerals were predominant, as also observed by many studies (Dias *et al*., 2020; Furquim *et al*., 2008; Furquim *et al*., 2010a; 2010b). Although typically found as primary minerals, micas, such as illite, glauconite and Fe-illite were found as secondary minerals in the alkaline environment of the Nhecolândia *Salinas* (Furquim *et al*., 2010). Their formation likely occurs through precipitation from a soil solution enriched with exchangeable cations, elevated K^+ activity, abundant silica, and high pH, or via illitization (Dixon; Weed, 1989). This process involves the transformation of smectites into illites, by adding K in the interlayer and Al in the tetrahedral layer of smectites, typically in high-temperature conditions (Dixon; Weed, 1989). However, the absence of interstratified micas in the *Salinas* soils suggests that mica neoformation is more plausible than illitization, as also suggested by Furquim *et al*. (2008).

In the *Salinas* Gleysol, clay content was the highest among all soils and illite dominated in the clay fraction, indicating a more closed soil system, favorable for bisialitization. In contrast, the abundance of kaolinite relative to 2:1 minerals in the Solonetz, coupled with lessivage and abrupt textural change, suggested less intense bisialitization, due partial desilification. Kaolinite was widespread across all landscape units, with its allochthonous origin and degradation in alkaline *Salinas* soils confirmed by Furquim *et al*. (2010). This aligns with the predominance of kaolinite in more acidic environments, such as the *Baías*, *Cordilheiras*, *Vazantes*, *Murundus*, and *Campos*, as indicated by their lower Ki values.

The presence of hydroxy-interlayered minerals (HIM) in *Salinas* soils suggests some degree of acidification. HIM is formed by chloritization, a process where hydroxy-Al polymers are added to the interlayers of smectites, resembling a chlorite structure (Dixon; Weed, 1989). These minerals are not distinct species but rather interstratified minerals of different Al

polymerization degrees (Velde; Meunier, 2008). Their formation is promoted by moderately acidic conditions, low organic matter, and wetting-drying cycles (Dixon; Weed, 1989; Velde; Meunier, 2008). The occurrence of HIM in the Solonetz and Podzol of the *Salinas* is an indicative of early soil leaching and acidification. Changes in the *Salinas* biogeochemistry may alter the equilibrium of the greenhouse gases emissions, affecting the atmosphere regional balance (Barbiero *et al*., 2018). In addition, the *Salinas* are accessed for the *pantaneiros* (Pantanal ranchers) as they provide salts and minerals to supplement cattle diet, favoring a more sustainable beef production (Guerreiro *et al*., 2019).

Despite being the most acidic soil of the *Salinas* environment, the pH values of the Podzol were not as low as expected for the spodic horizons (pH < 5.5) by the WBR/FAO classification system. Fe_o contents in the spodic horizons were higher than Al_o, except in the deepest horizon where Al_o content slightly exceeded Fe_o, indicating podzolization. The presence of goethite in the spodic horizon, reflected by elevated Fe_d contents, suggests Fe accumulation through redoximorphic processes linked to water level fluctuations, as also observed in the *Vazantes* Podzol. Similar conditions were reported by Menezes *et al*. (2022) for the *Salinas* Podzol of Nhecolândia.

4.5.2 Landscape evolution model of the Pantanal of Nhecolândia

The history of the Pantanal landscape has been shaped by climatic changes since the Last Glacial Maximum (LGM) period of the late Pleistocene. Research in the Laguna La Gaiba, on the Bolivian margin of the Pantanal (Fornace *et al*., 2016; Metcalfe *et al*., 2014; Whitney *et al*., 2011), identified two major climatic shifts during the last glacial-interglacial transition. Between ~45 and 19.5 kyr BP, the climate was much colder and drier than today, indicated by sparse tree cover and reduced lake levels. After 19.5 kyr BP, the expansion of tropical trees signaled post-glacial warming, though the climate remained drier than the present until ~12 kyr BP. Subsequently, wetter conditions prevailed, with rising lake levels and increased flooding in the Pantanal. However, in the early to middle Holocene (10-3 kyr BP), pollen data suggest intensified drought conditions, but less severe than those of the LGM. According to McGlue *et al*. (2012), regular flooding in the Laguna La Gaiba only began after ~2.6 kyr BP.

In Nhecolândia, the formation of the saline and freshwater lakes began during the Mid Holocene under dry conditions, when deflation process shaped variable depth lakes and the marginal *Cordilheiras* (McGlue *et al*., 2017). A shift in sediment composition from sandy to silt-rich deposits around ~3,080 years BP, in the Late Holocene, indicated the beginning of a

more permanent lacustrine system, which stabilized by ~1,300 years BP (McGlue *et al*., 2017; Rasbold *et al*., 2024). After this period, intensified precipitation altered the drainage patterns of some lakes, leading to their geochemical differentiation and the formation of the *Baías* (Rasbold *et al*., 2024). This aligns with studies suggesting that the *Baías* represent former *Salinas*, evolved from saline condition to freshwater, due to connections with ephemeral, shallow channels carrying acidic waters, a draining process still ongoing today (Barbiero *et al*., 2002; Furquim *et al*., 2017).

The oldest soil dating was identified between 80-90 cm depth in the *Vazantes* Podzol (P29), corresponding to ~8,970 years BP, during the Early-Middle Holocene. The average δ13C signal indicated a dominant contribution of C3 plants, with no significant variation along the profile. This reflects the local heterogeneity of the herbaceous community, which includes a mix of C3 and C4 plants among grasses and aquatic macrophytes of the Poaceae and Cyperaceae families (Appendix E). In seasonally flooded environments of Pantanal, vegetation composition changes according to hydrological dynamics, with C4 grasses predominating in the terrestrial phase and C3 grasses in the aquatic phase (Silva, 2020), so that δ13C would be basically dependent on the water table fluctuations, locally.

Similarly, in the *Campos* and *Baías* Arenosol (P9 and P26, respectively), C3 plants were dominant. However, the *Campos* Arenosol showed δ13C enrichment, suggesting a more mixed community and an influence of the surrounded C3 arboreal vegetation of the *Murundus*, whereas the *Baías* Arenosol was dominated by aquatic macrophytes due to more perennial water saturation (See appendix of chapter 2). In the *Baías* Arenosol, the absence of significant shifts in the δ13C signal, combined with dating of ~6,585 years BP, indicates local environmental stability since middle Holocene. The organic matter of the histic horizon dated to ~420 years BP also showed C3 carbon isotopic signal, confirming the dominance of aquatic macrophytes.

In the *Vazantes* Arenosol (P30), a shift from C3 to C4 plants was observed at 90 cm depth, dated to 4,680 ± 360 years BP. Similarly, in the *Salinas* Solonetz (P18), a transition from C3 to C4 plants occurred at 100 cm depth, with charcoal collected at the same depth dated to ~6,110 years BP. The δ13C signal of the charcoal indicated a C3 plant origin, suggesting an autochthonous origin. The drier Mid Holocene climate favored the occurrence of fire in the non-flooded South American seasonally dry tropical forests (Power *et al*., 2016). However, this observation contrasts with the stability noted in the *Vazantes* Podzol and *Baías* Arenosol, which also dated back to the Mid Holocene.

Overall, we interpret that, during the drier Mid Holocene, while weaker seasonal floodings occurred, the bottom-land topographical position of the *Vazantes* Podzol and *Baías* Arenosol favored prolonged water saturation, leading to dominance of C3 grasses and aquatic macrophytes – conditions that have persisted, little changed, until today (Figure 20). In contrast, the *Vazantes* Arenosol, located slightly higher than the *Vazantes* Podzol, experienced less persistent flooding during this period, allowing C3 plants to dominate over the C4 grasses. From the starting of Late Holocene to the present, with changing drainage, C4 grasses started to prevail. In the *Salinas* Solonetz, the proximity to the *Cordilheiras* suggests an influence of C3 plants during the Mid Holocene, shifting to a C4 grasses-dominated cover in the Late Holocene. Rasbold *et al*. (2024) identified Arecaceae and Bromeliaceae phytoliths, as well as woody dicotyledons where freshwater and saline lakes occur presently, indicating that it was possibly covered by cerrado vegetation during Mid to Late Holocene. In our case, this is only consistent with the *Salinas*, since the *Baías* did not present a shift in the δ13C signals, and C3 plants prevailed all time, as explained before.

In the *Cordilheiras* (P7 and P14) and *Murundus* (P8) landscape units C3 plants dominated, forming an arboreal community (Appendix D), which is less adapted to flooding conditions (Ferreira-Júnior *et al*., 2016). However, an enrichment of the δ13C signal along depth in the P14 and P8, that was more intense in the P14, suggests a past mixed C3-C4 community, with a more open canopy. Roots were found throughout the entire soil profile in the *Cordilheiras* and *Murundus*, likely lowing δ13C signals.

Figure 20 – Conceptual model of the Nhecolândia landscape evolution during Middle-Late Holocene. Image not to scale.

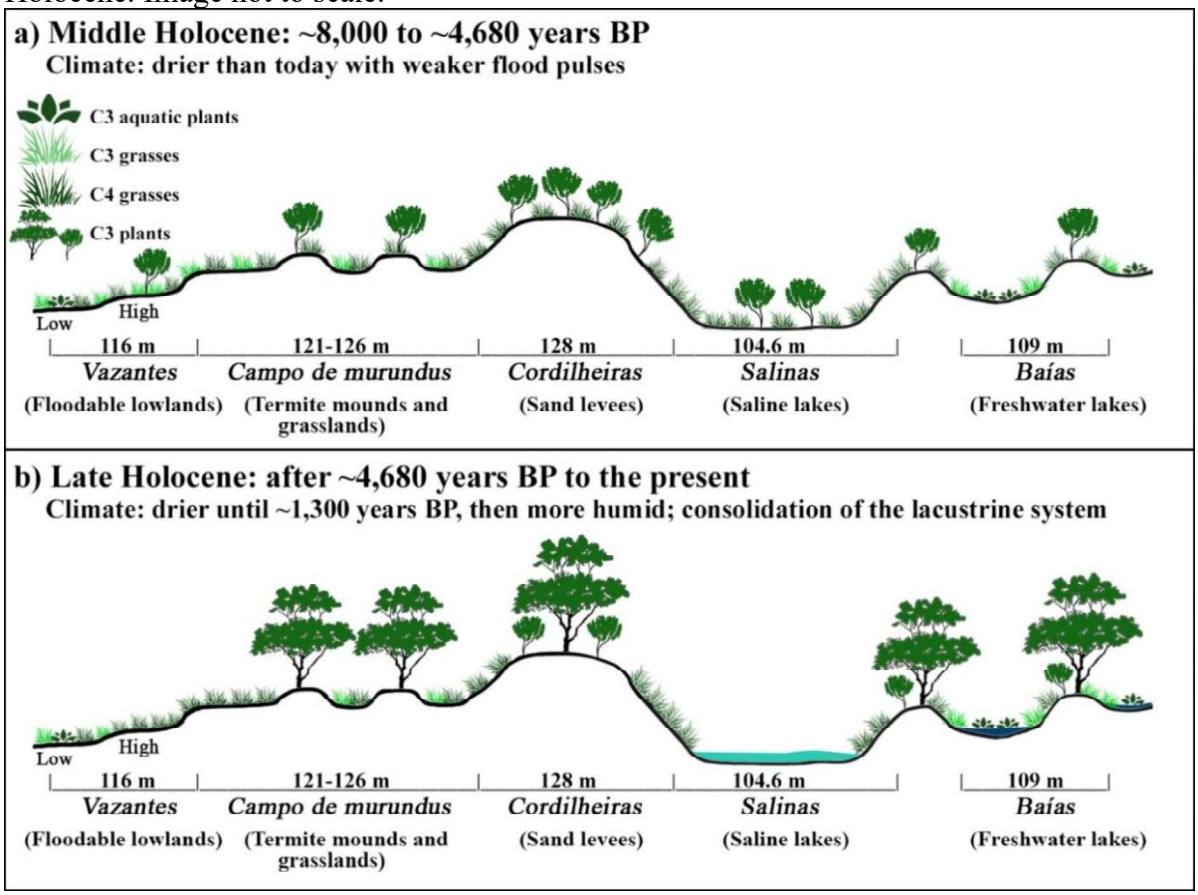

Source: The author, adapted from chapter 2.

4.6 CONCLUSIONS

The current Nhecolândia landscape is a complex evolving sandy wetland, shaped during the early-Mid Holocene under drier climatic conditions, driven by combined aeolian and fluvial processes, that became established at the beginning of the Late Holocene. During this period, the *Salinas* transitioned from a cerrado (savanna) to a grassy environment, while the higher *Vazantes* with mixed C3-C4 grass cover changed to a C4-dominated grassland. In contrast, lower areas, such as the *Baías* and lower *Vazantes*, remained dominated by hydrophilic and aquatic macrophytes due to a more persistent flooding regime.

In the *Salinas*, pedogenetic processes, such as salinization, sodification, calcification, gleization, and bissialitization occurred, resulting in the formation of less permeable clayey subsurface horizons, indicative of a closed hydrological system, especially in the Gleysols. In contrast, the *Baías* exhibited paludization and solodization, pointing to a more acidic and hydrologically open system. These findings suggest that hydrological dynamics within and

between Nhecolândia's landscape units are highly influenced by subtle differences in topography, soil characteristics, and internal drainage. Ongoing hydrological changes are increasing interconnectivity among lacustrine systems, promoting enhanced nutrient leaching and acidification in the *Salinas*, which are gradually evolving to *Baías*. These transformations have been previously documented and underscore the importance of these lakes for regional greenhouse gases regulation and sustainability of cattle ranching.

Non-floodable arboreal environments, such as *Cordilheiras* and *Murundus*, showed a δ13C signal enrichment with depth, which suggests a past mixed C3-C4 vegetation. In the *Cordilheiras*, the δ13C shift was more intense. Nutrient cycling in the predominantly sandy soils of the *Cordilheiras* is maintained by the cerrado and cerradão vegetation. Evidence of salinization, sodification, calcification, and silica-cemented horizons suggests a possible connection with alkaline groundwater, contradicting recent studies on the Cordilheira-lake system (Freitas *et al*., 2019; Merdy *et al*., 2022). Further hydrological, pedological, and chronological investigations are required to clarify these relationships.

In the *Murundus*, the termite activity plays a crucial role in pedogenesis, even in sandy environments, contributing to organic matter accumulation and soil structuring. Our findings provide rare evidence of pedoturbation in Nhecolândia soils, highlighting the need for more detailed pedological and chronological studies to explore the evolutionary origins of these environments. Changes in the hydrological dynamics or deforestation of Nhecolândia arboreal areas could severely disrupt its ecological equilibrium. The non-floodable environments function as vital refuges for local fauna and cattle during floods and ensure the connectivity among forest fragments throughout the Pantanal.

4.7 REFERENCES

AB'SÁBER, A. N. **Brasil, paisagens de exceção: o litoral e o Pantanal mato-grossense, patrimônios básicos**. 4. ed. Cotia: Ateliê Editorial, 2011.

ALHO, C. J. R. Biodiversity of the Pantanal: response to seasonal flooding regime and to environmental degradation. **Brazilian Journal of Biology**, [s. l.], v. 68, n. 4, p. 957–966, 2008.

ALHO, C. J. R. The Pantanal. In: FRASER, L. H.; KEDDY, P. A. (org.). **The World's Largest Wetlands**. Cambridge: Cambridge University Press, 2005. p. 203–271.

ALHO, C. J. R.; SILVA, J. S. V. Effects of Severe Floods and Droughts on Wildlife of the Pantanal Wetland (Brazil)—A Review. **Animals**, [s. l.], v. 2, n. 4, p. 591–610, 2012.

ALVARES, C. A. *et al*. Köppen's climate classification map for Brazil. **Meteorologische Zeitschrift**, [s. l.], v. 22, n. 6, p. 711–728, 2013.

ANDRADE, G. R. P. *et al*. Transformation of clay minerals in salt-affected soils, Pantanal wetland, Brazil. **Geoderma**, [s. l.], v. 371, p. 114-380, 2020.

ASSINE, M. L. Brazilian Pantanal: A Large Pristine Tropical Wetland. In: VIEIRA, B. C.; S., RODRIGUES, A. A.; SANTOS, L. J. C. (org.). **Landscapes and Landforms of Brazil**. [S. l.]: Springer Dordrecht, 2015. p. 135–146.

ASSINE, M. L. Quaternary of the Pantanal, west-central Brazil. **Quaternary International**, [s. l.], v. 114, n. 1, p. 23–34, 2004.

ASSINE, M. L. River avulsions on the Taquari megafan, Pantanal wetland, Brazil. **Geomorphology**, [s. l.], v. 70, n. 3–4, p. 357–371, 2005.

ASSINE, M. L. *et al*. The Quaternary alluvial systems tract of the Pantanal Basin, Brazil. **Brazilian Journal of Geology**, [s. l.], v. 45, n. 3, p. 475–489, 2015.

BACANI, V. M. *et al*. Caracterização das diferenças microclimáticas e pedomorfológicas do entorno de uma lagoa salina no pantanal da Nhecolândia, MS. **Geografia**, [s. l.], v. 35, n. 1, p. 149–163, 2010.

BARBIERO, L. *et al*. Biogeochemical diversity, O2-supersaturation and hot moments of GHG emissions from shallow alkaline lakes in the Pantanal of Nhecolândia, Brazil. **Science of The Total Environment**, [s. l.], v. 619–620, p. 1420–1430, 2018.

BARBIERO, L. *et al*. Geochemistry of water and ground water in the Nhecolândia, Pantanal of Mato Grosso, Brazil: variability and associated processes. **Wetlands**, [s. l.], v. 22, n. 3, p. 528–540, 2002.

BARBIERO, L *et al*. Organic Control of Dioctahedral and Trioctahedral Clay Formation in an Alkaline Soil System in the Pantanal Wetland of Nhecolândia, Brazil. PLOS ONE, [s. l.], v. 11, n. 7, p. e0159972, 2016.

BARBIERO, L. *et al*. Soil morphological control on saline and freshwater lake hydrogeochemistry in the Pantanal of Nhecolândia, Brazil. **Geoderma**, [s. l.], v. 148, n. 1, p. 91–106, 2008.

BERTAUX, J. *et al*. Paleoclimatic record of speleothems in a tropical region: study of laminated sequences from a Holocene stalagmite in Central–West Brazil. **Quaternary International**, [s. l.], v. 89, n. 1, p. 3–16, 2002.

BETA ANALYTIC. **Beta Analytic Standard Pretreatment Protocols**. [S. l.], 2022.

BEZERRA, M. A. de O. *et al*. Late Pleistocene/Holocene environmental history of the Southern Brazilian Pantanal wetlands. **Oecologia Australis**, [s. l.], v. 23, n. 04, p. 712–729, 2019.

BOIN, M. N. *et al*. Pantanal: The Brazilian Wetlands. In: SALGADO, A. A. R.; SANTOS, L. J. C.; PAISANI, J. C. (org.). **The Physical Geography of Brazil**. [S. l.]: Springer Cham, 2019. p. 75–91.

BRASIL. Folha **SE.21 Corumbá e parte da Folha SE.20**. Rio de Janeiro - RJ: Projeto RADAMBRASIL, 1982. v. 27

BRAUMAN, Alain. Effect of gut transit and mound deposit on soil organic matter transformations in the soil feeding termite: A review. **European Journal of Soil Biology**, [s. l.], v. 36, n. 3–4, p. 117–125, 2000.

CALHEIROS, D. F.; FONSECA JÚNIOR, W.C. **Perspectivas de estudos ecológicos sobre o Pantanal**. Corumbá: EMBRAPA-CPAP, 1996.

CARDOSO, E. L. *et al*. Qualidade química e física do solo sob vegetação arbórea nativa e pastagens no Pantanal Sul-Mato-Grossense. **Revista Brasileira de Ciência do Solo**, [s. l.], v. 35, n. 2, p. 613–622, 2011.

CARDOSO, E. L. *et al*. Relação entre solos e unidades da paisagem no ecossistema Pantanal. **Pesquisa Agropecuária Brasileira**, [s. l.], v. 51, n. 9, p. 1231–1240, 2016.

CARDOSO, E. L. C. **X Reunião Brasileira de Classificação de Solos**. Pantanal e Cerrado. Guia de Campo. Corumbá-MS: SBCS: EMBRAPA-UFRPE, 2012.

CHIARAVALLOTI, R. M. *et al*. Achieving conservation through cattle ranching: The case of the Brazilian Pantanal. **Conservation Science and Practice**, [s. l.], 2023.

COSTA-SILVA, A. R. *et al*. Soils surrounding saline-alkaline lakes of Nhecolândia, Pantanal, Brazil: Toposequences, mineralogy and chemistry. **Geoderma Regional**, [s. l.], v. 36, p. e00746, 2024.

COUTO, E. G.; OLIVEIRA, V. A. The Soil Diversity of the Pantanal. In: JUNK, W. J. *et al*. (org.). **The Pantanal: Ecology, biodiversity and sustainable management of a large neotropical seasonal wetland**. Moscow: Pensoft Publishers, 2010. p. 71–102.

COX, E. P. A method of assigning numerical and percentage values to the degree of roundness of sand grains. **Journal of Paleontology**, [s. l.], v. 1, n. 3, p. 179–183, 1927.

CUNHA, N. G. da. **Considerações sobre os solos da sub-região da Nhecolândia, Pantanal Mato-grossense**. Corumbá: [s. n.], 1980.

CUNHA, N. G. da. **Dinâmica de nutrientes em solos arenosos o Pantanal mato-grossense**. Corumbá: Embrapa/CPAP, 1985.

DE QUEIROZ, Roberta Franco Pereira *et al*. Geoambientes no Pantanal do Abobral, Mato Grosso do Sul, Brasil. **Boletim do Museu Paraense Emílio Goeldi - Ciências Naturais**, [s. l.], v. 12, n. 2, p. 277–291, 2017.

DIAS, I. A. *et al*. The Occurrence of Authigenic Clay Minerals in Alkaline-Saline Lakes, Pantanal Wetland (Nhecolândia Region, Brazil). **Minerals**, [s. l.], v. 10, n. 8, p. 718, 2020.

DIXON, J.B.; WEED, S.B. **Minerals in Soil Environments**. 2. ed. Madison: Soil Science Society of America, 1989.

EITEN, George. The cerrado vegetation of Brazil. **The Botanical Review**, [s. l.], v. 38, n. 2, p. 201–341, 1972.

FERREIRA-JÚNIOR, W. G. *et al*. Flood regime and water table determines tree distribution in a forest-savanna gradient in the Brazilian Pantanal. **Anais da Academia Brasileira de Ciências**, [s. l.], v. 88, n. suppl 1, p. 719–731, 2016.

FORNACE, K. L. *et al*. Late Quaternary environmental change in the interior South American tropics: new insight from leaf wax stable isotopes. **Earth and Planetary Science Letters**, [s. l.], v. 438, p. 75–85, 2016.

FREITAS, J. G. *et al*. Interaction between lakes' surface water and groundwater in the Pantanal wetland, Brazil. **Environmental Earth Sciences**, [s. l.], v. 78, n. 5, p. 139, 2019.

FRUETT, T. *et al*. Selectivity of soil constituents by termites in the construction of Brazilian termite mounds. **Scientia Agricola**, [s. l.], v. 80, 2023.

FURIAN, S. *et al*. Chemical diversity and spatial variability in myriad lakes in Nhecolândia in the Pantanal wetlands of Brazil. **Limnology and Oceanography**, [s. l.], v. 58, n. 6, p. 2249–2261, 2013.

FURQUIM, S. A. C. *et al*. Mineralogy and Genesis of Smectites in an Alkaline-Saline Environment of Pantanal Wetland, Brazil. **Clays and Clay Minerals**, [s. l.], v. 56, n. 5, p. 579–595, 2008.

FURQUIM, S. A. C. *et al*. Neoformation of micas in soils surrounding an alkaline-saline lake of Pantanal wetland, Brazil. **Geoderma**, [s. l.], v. 158, n. 3–4, p. 331–342, 2010a.

FURQUIM, Sheila A. C. *et al*. Salt-affected soils evolution and fluvial dynamics in the Pantanal wetland, Brazil. **Geoderma**, [s. l.], v. 286, p. 139–152, 2017.

FURQUIM, S.A.C. *et al*. Soil mineral genesis and distribution in a saline lake landscape of the Pantanal Wetland, Brazil. **Geoderma**, [s. l.], v. 154, n. 3–4, p. 518–528, 2010b.

GARCIA, E. A. C. O **Clima no Pantanal Mato-grossense**. Corumbá: EMBRAPA, 1984.

GELYBÓ, G. *et al*. Potential impacts of climate change on soil properties. **Agrokémia és Talajtan**, [s. l.], v. 67, n. 1, p. 121–141, 2018.

GODOI, H. de O; MARTINS, E. G.; MELLO, J. C. R. de. **Programa Levantamentos Geológicos Básicos do Brasil - PLGB. Corumbá – Folha SE.21-Y-D, Aldeia Tomázia, Folha SF.21-V-B, Porto Murtinho, Folha SF.21-V-D, Estado de Mato Grosso do Sul**. Escala 1:250.000. Brasília: [s. n.], 2001

GRADELLA, F. dos S. *et al*. Geomorphology and deposition events in Nhecolandia Pantanal Wetland. **Geografia**, [s. l.], v. 36, p. 107–117, 2011.

GRADELLA, F.; QUÉNOL, H.; SAKAMOTO, A. Variation du niveau phréatique d'une saline dans le Pantanal en relation avec les précipitations et les inondations provoquées par le fleuve Paraguai (Brésil). **AIC 2009 Cluj**. Romênia: [s. n.], 2009. p. 223–228.

GUERRA, A. *et al*. Drivers and projections of vegetation loss in the Pantanal and surrounding ecosystems. **Land Use Policy**, [s. l.], v. 91, p. 104388, 2020a.

GUERRA, M. B. B. *et al*. Post-fire study of the Brazilian Scientific Antarctic Station: Toxic element contamination and potential mobility on the surrounding environment. **Microchemical Journal**, [s. l.], v. 110, p. 21–27, 2013.

GUERRA, A. *et al*. The importance of Legal Reserves for protecting the Pantanal biome and preventing agricultural losses. **Journal of Environmental Management**, [s. l.], v. 260, p. 110128, 2020b.

GUERREIRO, Renato L. *et al*. The soda lakes of Nhecolândia: A conservation opportunity for the Pantanal wetlands. **Perspectives in Ecology and Conservation**, [s. l.], v. 17, n. 1, p. 9–18, 2019.

GUIMARÃES CÉSAR, E.; TREVELIN, C.; SARTORI MANOEL, P. **Pantanal paisagens, flora e fauna**. São Paulo: Cultura Acadêmica, 2014. v. 1 Disponível em: Acesso em: 25 mar. 2024.

HOGG, A. G *et al*. SHCal20 Southern Hemisphere Calibration, 0–55,000 Years cal BP. **Radiocarbon**, [s. l.], v. 62, n. 4, p. 759–778, 2020.

HOWSE, P.E. The chemical ecology of forest and savanna termites. In: FURLEY, P.A.; PROCTOR, J.; RATTER, J.A. (org.). **Nature and Dynamics of Forest-Savanna Boundaries**. London: Chapman & Hall, 1992. p. 485–498.

HUMPHREYS, G.S. Bioturbatlion, biofabrics and the biomantle: an example from the Sydney Basin. In: RINGROSE-VOASE, A.J.; HUMPHREYS, G.S. (org.). **Soil Micromorphology: Studies in Management and Genesis**. Amsterdam: Elsevier, 1993. v. 22, p. 421–436.

IUSS WORKING GROUP WRB. **International soil classification system for naming soils and creating legends for soil maps**. 4. ed. Vienna, Austria: International Union of Soil Sciences (IUSS), 2022.

IVORY, Sarah J *et al*. Vegetation, rainfall, and pulsing hydrology in the Pantanal, the world's largest tropical wetland. **Environmental Research Letters**, [s. l.], v. 14, n. 12, p. 124017, 2019.

NASH, D. J.; ULLYOTT, J. S. Silcrete. In: NASH, D. J.; McLAREN, S. J. (eds.) **Geochemical sediments and landscapes**. [S. l.]: Wiley, 2007. p. 95–148.

TRICART, J. El Pantanal: un ejemplo del impacto geomorfologico sobre el ambiente. **Investigaciones Geográficas**, Chile, n. 29, p. 81–97, 1982.

JENNY, H. **Factors of soil formation: a system of quantitative pedology**. New York: Dover Publications, 1941.

JOUQUET, P.; LEPAGE, M.; VELDE, B. Termite soil preferences and particle selections: strategies related to ecological requirements. **Insectes Sociaux**, [s. l.], v. 49, n. 1, p. 1–7, 2002.

KEDDY, P. A. *et al*. Wet and Wonderful: The World's Largest Wetlands Are Conservation Priorities. **BioScience**, [s. l.], v. 59, n. 1, p. 39–51, 2009.

KUERTEN, S. *et al*. Sponge spicules indicate Holocene environmental changes on the Nabileque River floodplain, southern Pantanal, Brazil. **Journal of Paleolimnology**, [s. l.], v. 49, n. 2, p. 171–183, 2013.

LEMOS, R. C.; SANTOS, R. D. Manual de descrição e coleta de solo no campo. 2. ed. Campinas: Sociedade Brasileira de Ciência do Solo, 1996.

MACEDO, H. de A. *et al*. Mudanças paleo-hidrológicas na planície do Rio Paraguai, Quaternário do Pantanal. **Revista Brasileira de Geomorfologia**, [s. l.], v. 15, n. 1, p. 75–85, 2014.

MARENGO, J. A.; ALVES, LM; TORRES, RR. Regional climate change scenarios in the Brazilian Pantanal watershed. **Climate Research**, [s. l.], v. 68, n. 2–3, p. 201–213, 2016.

MARTINELLI, L. A. *et al*. **Desvendando questões ambientais com isótopos estáveis**. São Paulo: Oficina de Textos, 2009.

MCGLUE, Michael M. *et al*. Holocene stratigraphic evolution of saline lakes in Nhecolândia, southern Pantanal wetlands (Brazil). **Quaternary Research**, [s. l.], v. 88, n. 3, p. 472–490, 2017.

MCGLUE, Michael M. *et al*. Lacustrine records of Holocene flood pulse dynamics in the Upper Paraguay River watershed (Pantanal wetlands, Brazil). **Quaternary Research**, [s. l.], v. 78, n. 2, p. 285–294, 2012.

MCKEAGUE, J.A.; DAY, J. H. Dithionite and oxalate extractable fe and ai as aids in differentiating various classes of soils. **Canadian Journal of Soil Science**, [s. l.], v. 46, p. 13–22, 1966.

MEHRA, O.P.; JACKSON, M. L. Iron oxide removal from soils and clays by a dithionite-citrate system buffered with sodium bicarbonate. **Clay and Clay Minerals**, [s. l.], v. 7, p. 317–327, 1960.

MENEZES, A. R. de *et al*. Soils with dark subsurface horizons in saline basins in the Brazilian Pantanal. **Revista Brasileira de Ciência do Solo**, [s. l.], v. 46, 2022.

MERDY, P. *et al*. Processes and rates of formation defined by modelling in alkaline to acidic soil systems in Brazilian Pantanal wetland. **Catena**, [s. l.], v. 210, p. 105876, 2022.

METCALFE, S. E. *et al*. Hydrology and climatology at Laguna La Gaiba, lowland Bolivia: complex responses to climatic forcings over the last 25 000 years. **Journal of Quaternary Science**, [s. l.], v. 29, n. 3, p. 289–300, 2014.

MURRAY, A.S.; WINTLE, A.G. Luminescence dating of quartz using an improved single-aliquot regenerative-dose protocol. **Radiation Measurements**, [s. l.], v. 32, n. 1, p. 57–73, 2000.

NASCIMENTO, A. F. *et al*. Pedogenesis in a Pleistocene fluvial system of the Northern Pantanal — Brazil. **Geoderma**, [s. l.], v. 255–256, p. 58–72, 2015.

NASCIMENTO, D. C. *et al*. Soil attributes and leaf litter composition in forest communities of the Brazilian Pantanal. **Anais da Academia Brasileira de Ciências**, [s. l.], v. 96, p. 2–16, 2024.

NUNES DA CUNHA, C. ; JUNK, Wolfgang J. A preliminary classification of habitats of the Pantanal of Mato Grosso and Mato Grosso do Sul, and its relation to national and international wetland classification systems. In: JUNK, W.J. *et al*. (org.). **The Pantanal**: Ecology, biodiversity and sustainable management of a large neotropical seasonal wetland. Moscow: Pensoft Publishers, 2009. p. 127–141.

OLIVEIRA, A. P. G. *et al*. The expression of neotectonics in the Pantanal da Nhecolândia, State of Mato Grosso do Sul - Brazil. **Anais da Academia Brasileira de Ciências**, [s. l.], v. 90, n. 2, p. 1293–1308, 2018a.

OLIVEIRA JUNIOR, J. C. de *et al*. Origin of mounds in the Pantanal wetlands: An integrated approach between geomorphology, pedogenesis, ecology and soil micromorphology. **PLOS ONE**, [s. l.], v. 12, n. 7, p. e0179197, 2017.

OLIVEIRA JUNIOR, J. C. *et al*. Salt-affected soils on elevated landforms of an alluvial megafan, northern Pantanal, Brazil. **Catena**, [s. l.], v. 172, p. 819–830, 2019.

OLIVEIRA-FILHO, A.T. de. Floodplain "*Murundus*" of Central Brazil: evidence for the termite-origin hypothesis. **Journal of Tropical Ecolology**, [s. l.], v. 8, p. 1–19, 1992.

PADOVANI, C. R. **Dinâmica Espaço-Temporal das Inundações do Pantanal.** 2010. 1–175 f. Tese (Doutorado) - Escola Superior de Agricultura "Luiz de Queiroz", Piracicaba, 2010.

PANSU, M.; GAUTHEYROU, J. **Handbook of Soil Analysis** — Mineralogical, Organic and Inorganic Methods. Dordrecht, The Netherlands: Springer, 2003.

PONCE, V. M.; NUNES DA CUNHA, C. Vegetated earthmounds in tropical savannas of Central Brazil: a synthesis. **Journal of Biogeography**, [s. l.], v. 20, n. 2, p. 219–225, 1993.

POTT, A.; POTT, V. J. Features and conservation of the Brazilian Pantanal wetland. **Wetlands Ecology and Management**, [s. l.], v. 12, p. 547–552, 2004. Disponível em: Acesso em: 1 out. 2023.

POTT, V.J.; POTT, A. **Plantas Aquáticas do Pantanal**. Corumbá, MS: EMBRAPA, 2000.

POTT, A.; POTT, V.J. **Plantas do Pantanal**. Corumbá, MS: EMBRAPA, 1994.

POWER, M. J. *et al*. Fire, climate and vegetation linkages in the Bolivian Chiquitano seasonally dry tropical forest. **Philosophical Transactions of the Royal Society B: Biological Sciences**, [s. l.], v. 371, n. 1696, p. 20150165, 2016.

RAMSEY, C. Bayesian Analysis of Radiocarbon Dates. **Radiocarbon**, [s. l.], v. 51, n. 1, p. 337–360, 2009.

RASBOLD, G. G. *et al*. Holocene limnological changes in saline and freshwater lakes, Lower Nhecolândia, Pantanal, Brazil. **Hydrobiologia**, [s. l.], v. 851, n. 7, p. 1723–1739, 2024.

RASBOLD, G. G. *et al*. Sponge spicule and phytolith evidence for Late Quaternary environmental changes in the tropical Pantanal wetlands of western Brazil. **Palaeogeography, Palaeoclimatology, Palaeoecology**, [s. l.], v. 518, p. 119–133, 2019.

REIS, J. S. **Caracterização e gênese de uma sequência de solos da região da Nhecolândia, Pantanal Sul-Mato-Grossense**. 2017. 1–99 f. Dissertação - Universidade Federal de Viçosa, Viçosa, 2017.

RIBEIRO, J. F.; WALTER, B. M. T. Fitofisionomias do bioma cerrado. In: SANO, S. M.; ALMEIDA, S. P. de (org.). **Cerrado**: ambiente e flora. Planaltina: EMBRAPA-CPAC, 1998. p. 89–166.

SANTOS, H. G. dos *et al*. **Sistema Brasileiro de Classificação de Solos**. 5. ed. Brasília: EMBRAPA, 2018.

SANTOS, R. D. *et al*. **Manual de descrição e coleta de solos no campo**. 7. ed. Viçosa. Sociedade Brasileira de Ciência do Solo, 2015. 102p.

SCHAEFER, C. E. R. Brazilian latosols and their B horizon microstructure as long-term biotic constructs. **Soil Research**, [s. l.], v. 39, n. 5, p. 909, 2001.

SCHAETZL, R. J.; ANDERSON, S. **Soils Genesis and Geomorphology**. New York: Cambridge University Press, 2005.

SCHIAVO, J. A. *et al*. Characterization and classification of soils in the Taquari river basin - Pantanal region, state of Mato Grosso do Sul, Brazil. **Revista Brasileira de Ciência do Solo**, [s. l.], v. 36, n. 3, p. 697–708, 2012.

SILVA, F. H. B. da. **Florística e biomassa da vegetação de *Campos* sazonalmente inundáveis do Pantanal de Mato Grosso**. 2020. 1–140 f. Tese de doutorado - Universidade Federal do Rio Grande do Sul, Porto Alegre, 2020.

SILVA, J. dos S. V. da; ABDON, M. de M. Delimitação do Pantanal Brasileiro e suas Sub-Regiões. **Pesq. agropec. bras**, [s. l.], v. 33, p. 1703–1711, 1998.

SOARES, A. P.; SOARES, P. C.; ASSINE, M. L. Areiais e lagoas do Pantanal, Brasil: herança paleoclimática? **Brazilian Journal of Geology**, [s. l.], v. 33, n. 2, p. 211–224, 2003.

STOOPS, G. **Guidelines for Analysis and Description of Soil and Regolith Thin Sections**. [S. l.]: Wiley, 2020.

TAIOLI, F. *et al*. How Ground Penetrating Radar helps to understand the Nhecolândia lakes landscape in the Brazilian Pantanal wetland. **Brazilian Journal of Geology**, [s. l.], v. 51, n. 2, 2021.

TEIXEIRA, P. C. *et al*. **Manual de métodos de análise de solo**. 3. ed. Brasília, DF: Embrapa, 2017.

TIEDJE, J. M. *et al*. Anaerobic processes in soil. **Plant and Soil**, [s. l.], p. 197–212, 1984.

VALVERDE, O. Fundamentos Geográficos do Planejamento do Município de Corumbá. **Revista Brasileira de Geografia**, [s. l.], v. 34, n. 1, p. 49–144, 1972.

VELDE, B.; MEUNIER, A. **The Origin of Clay Minerals in Soils and Weathered Rocks**. Berlin, Heidelberg: Springer Berlin Heidelberg, 2008.

VICTORIA, R. L. *et al*. Past vegetation changes in the Brazilian Pantanal arboreal–grassy savanna ecotone by using carbon isotopes in the soil organic matter. **Global Change Biology**, [s. l.], v. 1, n. 3, p. 165–171, 1995.

WANG, Y.; AMUNDSON, R.; TRUMBORE, S. Radiocarbon Dating of Soil Organic Matter. **Quaternary Research**, [s. l.], v. 45, n. 3, p. 282–288, 1996.

WHITNEY, B. S. *et al*. A 45kyr palaeoclimate record from the lowland interior of tropical South America. **Palaeogeography, Palaeoclimatology, Palaeoecology**, [s. l.], v. 307, n. 1–4, p. 177–192, 2011.

YEOMANS, J. C.; BREMNER, J. M. A rapid and precise method for routine determination of organic carbon in soil. Communications in Soil Science and Plant Analysis, [s. l.], v. 19, n. 13, p. 1467–1476, 1988.

ZANI, H.; ASSINE, M. L.; MCGLUE, M. M. Remote sensing analysis of depositional landforms in alluvial settings: Method development and application to the Taquari megafan, Pantanal (Brazil). **Geomorphology**, [s. l.], 2012. Disponível em: Acesso em: 26 mar. 2024.
ZAVATTINI, J. A. A distribuição das chuvas e a circulação atmosférica no estado de Mato Grosso do Sul. In: ZAVATTINI, J. A. **As chuvas e as massas de ar no estado de Mato Grosso do Sul**: estudos geográficos com vista à regionalização climática. São Paulo: Cultura Acadêmica, 2009. p. 59–92.

5 CHAPTER 4: Inundation monitoring of the Upper Paraguay River Basin from 2018 to 2021: applying a multi-source data and machine learning approach

5.1 ABSTRACT

The Upper Paraguay River Basin (UPRB), home to the Pantanal biome, the world's largest continuous continental wetland, is crucial water resource studies in South America. This study aimed to map the inundation frequency in the UPRB from 2018 to 2021 using Sentinel-1 SAR data combined with multi-source data and a machine learning approach. Seasonal periods were based on hydrometric station data. Water and non-water sample points were derived using Sentinel-1, MapBiomas Land Use and Land Cover (LULC) maps, and ArcGIS Pro tools. Dynamic covariates included Sentinel-1 VV and VH bands, while static covariates comprised spectral indices (from Sentinel-1 and Sentinel-2), and a digital elevation model (FABDEM). A Random Forest (RF) model, implemented in the R software with ten-fold cross-validation, was used for spatiotemporal modeling. Model performance was assessed using metrics from the 100-executions of the RF. Statistical analyses and Man-Kendall trend analysis were also applied. Results revealed misclassification during the dry season, as water backscatter was mainly confused with pasture and soybean crops. Flooding affected 11% and 1.25% of the area for 10% and 20% of the analyzed period, respectively, with only 0.57% flooded over 90% of the time. Paraguay Pantanal and Upper Cuiabá River sub-basins had more areas with permanent water. Trend analysis showed a moderate decline in wet season water extent, while dry season trends were not statistically significant. RF model achieved high accuracy, with VV, MNDWI, and VH being key covariates. These findings highlight the effectiveness of Sentinel-1 images and Random Forest for water mapping in complex environments, using a high dimensional, multi-source dataset.

Keywords: Flooding. Modelling. Pantanal. Radar. Classification.

5.2 INTRODUCTION

The Upper Paraguay River Basin (UPRB), spanning Brazil, Paraguay, and Bolivia, is an important region for water resource studies and supply in South America (Schulz *et al*., 2019). It forms part of the La Plata River Basin (LPRB), which covers an area of 3.1 million km², making it the second-largest drainage basin in South America and the fifth largest in the world (WWAP, 2007). The UPRB also encompasses a significant portion of the Guarani Aquifer, the largest transboundary freshwater aquifer in the world (WWAP, 2007). Moreover, it contains the entire Pantanal biome, the world's largest continuous continental wetland, recognized as a UNESCO Reserve of Biosphere, and a Ramsar Wetland of international importance (Furquim; Vidoca, 2021; Keddy *et al*., 2009).

The UPRB, with its unique natural characteristics and high environmental fragility, holds strategic importance for biodiversity conservation and the continuous provision of ecosystem services. In addition to the Pantanal, the region partially includes two other important Brazilian biomes: the Cerrado and the Amazon, contributing to a diverse phytogeographic mosaic (Pott *et al*., 2011). However, in recent decades, inappropriate land use for agriculture and cattle ranching, along with the anthropization has led to an increase of erosive and aggradation processes, which directly affects the Pantanal's flooding regime (WWF-Brasil; Instituto SOS Pantanal, 2015). Furthermore, global and regional climate changes are expected to significantly impact wetlands by altering their hydrological regimes (Erwin, 2009; Marengo; Alves; Torres, 2016). Such changes may directly affect inundation areas and consequently impact on the Pantanal's biological (Alho, 2008; Ferreira-Júnior *et al*., 2016; Ivory *et al*., 2019), pedological (Freitas *et al*., 2019; Furquim *et al*., 2017; Merdy *et al*., 2022), and human dynamics (Chiaravalloti *et al*., 2023; Guerreiro *et al*., 2019).

Numerous studies in the Pantanal have aimed to map and monitor flood dynamics, predominantly using optical satellite images such the MODIS time-series (Adami *et al*., 2008; Antunes; Esquerdo, 2015; Moraes; Pereira; Cardozo, 2013; Padovani, 2010), or Landsat time-series (MapBiomas, 2024). Optical images offer the advantage of long time-series availability: since 1972 for Landsat (Landsat Missions, 2024) and since 2000 for MODIS (NASA, 2024). However, their use can be limited by cloud cover and shadows.

Synthetic Aperture Radar (SAR), operating in the microwave range, overcome these limitations with near all-weather and day-night imaging capabilities, unaffected by atmospheric conditions (Martinis; Rieke, 2015). Additionally, open water areas are easily detected in radar data, which appear as low-intensity pixels contrasting with the high-intensity surrounding land

surface (Guo *et al*., 2022; Martinis; Rieke, 2015). Despite its advantages, past inundation studies in Pantanal using microwave images have relied on coarser-resolution radar data over short analysis periods (Costa; Telmer, 2007; Evans *et al*., 2010). Recently, Sentinel-1 SAR Satellite imagery has gained prominence in flood monitoring due to its high-resolution data, frequent revisit time, and open availability (Clement; Kilsby; Moore, 2018; Li *et al*., 2023; Zuo *et al*., 2024).

Multi-temporal analysis applied to large areas generates high-dimensional and complex datasets, demanding fast processing and accurate results. For this reason, machine learning algorithms have been widely applied in inundation studies due to their ability of pattern recognition and of making accurate predictions automatically (Karim *et al*., 2023). Among these, decision-tree-based algorithms, such as Random Forest, stand out for their high classification accuracy, fast prediction speed, and simple principles. These algorithms are particularly effective for binary classifications, such as distinguishing between water and non-water areas (Li *et al*., 2021, 2023).

Water plays a critical role in the biosphere, making it essential to monitor the inundation to understand the interplays between its spatiotemporal dynamics and climate changes. Such monitoring serves as a valuable tool for public managers to develop effective water management strategies (Karpatne *et al*., 2016). Given the strong relationship between the Pantanal ecosystem dynamics and the flooding regime, this study aimed to map the inundation frequency of the UPRB by applying a multi-temporal Sentinel-1 SAR data combined with multi-source data through a machine learning classification approach.

5.3 MATERIAL AND METHODS

5.3.1 Study area

The UPRB covers an area of 796,258 km² (Figure 1) and is divided into three main regions: Planalto, Pantanal, and Chaco regions. In Brazil, the UPRB comprises the Planalto and Pantanal regions, which together cover an area of 361,630 km², representing 45.4% of the basin's total area. The Planalto is a plateau, located in the northern and eastern portions of the UPRB, surrounding the Pantanal depression. The Brazilian UPRB is managed by the Brazilian National Water Agency (ANA, in Portuguese) and is subdivided into twelve sub-basins, which also serve as planning and management units (ANA, 2017).

The UPRB is bounded to the north by the Cuiabá ridge, to the east by the Maracajú and Taquari-Itiquira Plateaus, to the south by the Bodoquena Plateau, and to the west by the Urucum-Amolar Plateaus (Alho, 2005; Boin *et al*., 2019). The UPRB Planalto ranges in elevation from 200 to 1200 m above mean sea level (amsl), while the Pantanal basin lies significantly lower, at elevations between 80 to 150 m amsl. The Pantanal is an active sedimentary basin, formed by the uplift of the Andes and epeirogenic movements across central Brazil during the Cenozoic era (Assine, 2015; Ussami; Shiraiwa; Dominguez, 1999). Major faults caused subsidence in the central part of the basement uplift, known as a boutonnière, leading to the formation of the Pantanal basin (Ab'Sáber, 1988; Assine, 2015).

The surrounding plateaus of the UPRB are remnants of the ancient South American plain, primarily composed of Paleozoic sedimentary rocks and Precambrian crystalline rocks, while the Pantanal basin is composed of sand-clayey sediments derived from the erosion of the plateaus and deposited by fluvial fans and megafans (Assine, 2015). Soils in the UPRB are highly diverse, reflecting the region's varied geology, geomorphology, and hydrology. They include Arenosols, Acrisols, Cambisols, Ferralsols, Gleysols, Leptosols, Nitisols, Phaeozems, Podzols, Planosols, Plinthosols, Solonetz, and Vertisols (Amaral Filho, 1984; Brasil, 1982).

The rivers that form the Pantanal alluvial plains originate in the plateaus. The Paraguay River beings in the Parecis Plateau, in the northern UPRB, and flows southward, collecting water from several tributaries, including the Cabaçal, Sepotuba, Jauru, Taquari, Negro, Miranda, and Aquidauana rivers (Carvalho, 1984). Upon entering the Pantanal basin, the river slopes decrease significantly, from 0.6 m/km on the plateaus to 0.1-0.3 m/km in the plain, which diminishes its energy and leads to extensive inundation (Boin *et al*., 2019).

The climate of the Pantanal is classified as Aw according to the Köppen system, indicating a tropical continental climate with dry winter (Alvares *et al*., 2013). The mean annual temperature ranges from 19.9ºC in July (in Aquidauana) to 27.4ºC in December (in Corumbá), while mean precipitation varies from less than 100 mm during autumn-winter months to 250-300 mm during the spring-summer period (Tarifa, 1984). In the upper course of the rivers, flooding begins in January, driven by precipitation accumulated in the plateaus since the start of the rainy season. These floodwaters reach the southern region of Corumbá three months later, at the beginning of the drying period (Padovani, 2010).

The vegetation of the UPRB primarily consists of Pantanal vegetation, formed by the convergence of distinct phytogeographic provinces: Amazonia to the north, Cerrado (savannah) to the east, Meridional Forests to the south, and the Chaco region to the west, fostering high biodiversity (Pott *et al*., 2011). The main economic activities in the UPRB plateau include

agriculture, particularly soybean cultivation, and cattle ranching. In the Pantanal, the economy is driven by agriculture, cattle ranching, fishing, gold mining, and tourism (Alho, 2005; Alho *et al*., 2019).

Figure 1 – Location of the Upper Paraguay River basin, sub-basins limits, hypsometric information, and distribution of the fluviometric and pluviometric stations of the Brazilian National Water Agency in the area.

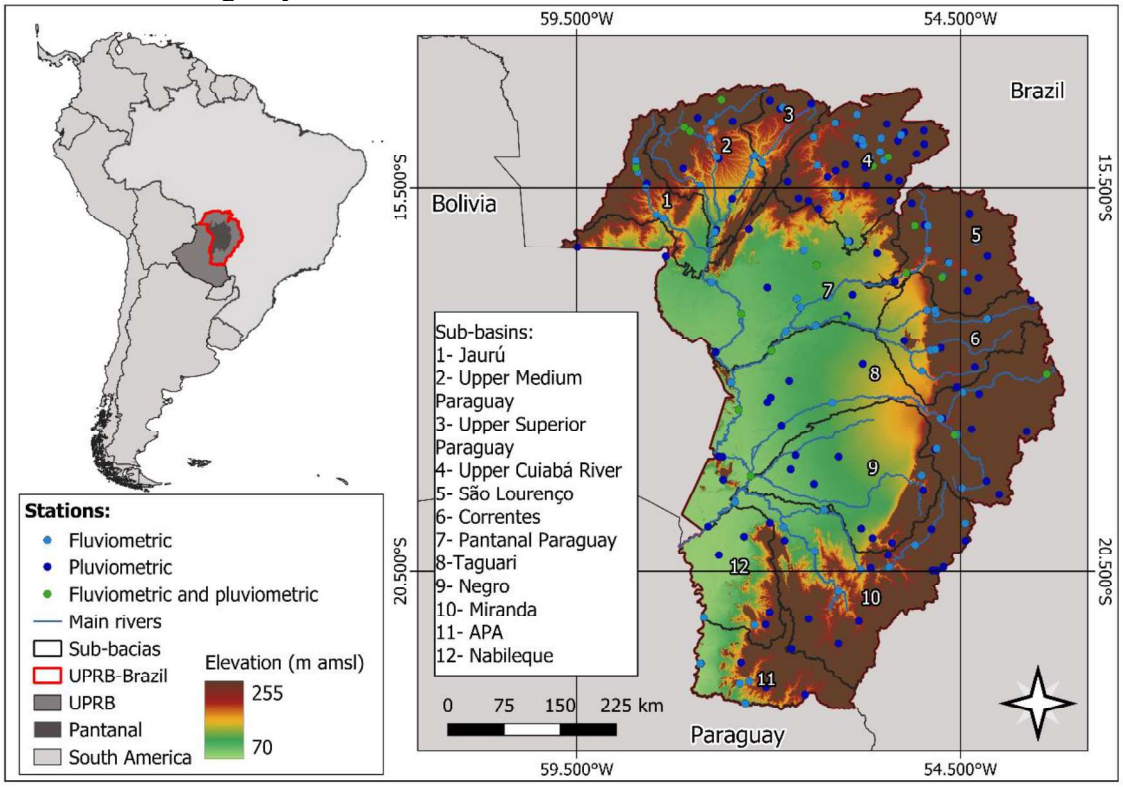

Source: The Author.

5.3.2 Data survey

The definition of the wet and dry periods in the study area was based on the analysis of rainfall and streamflow data from hydrometric stations provided by the (ANA, 2024), which were accessed using the hydroweb package in the R software. The wet and dry season were defined based on the median streamflow values to avoid the influence of outliers (Figure 2b). Throughout 2018 and 2021, the highest streamflow values occurred between February and March, which coincide with the rainy summer season (Figure 2a) while the lowest values were observed between August and September. Thus, the wet season was defined as the six months with higher streamflow values (from November to May), and the dry season as the six months with the lower streamflow values (from June to November).

Figure 2 – Mean monthly rainfall (a), and mean and median monthly streamflow (b) in the Upper Paraguay River Basin from 2018 to 2021.

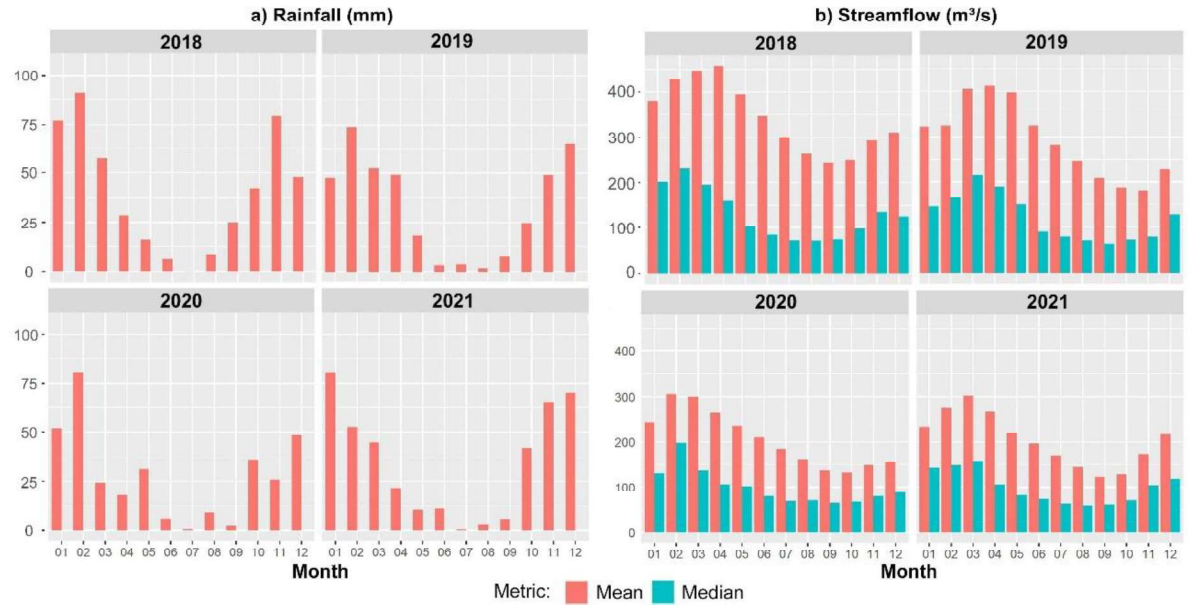

Source: (ANA, 2024).

To assess the inundation frequency in the study area, we used radar images from Sentinel-1 satellite, spectral indices from both Sentinel-1 and Sentinel-2 satellites, and a digital elevation model (FABDEM). The Sentinel-1 mission, provided by the European Space Agency, delivers high-resolution radar imagery (Torres *et al*., 2012). The Sentinel-1 products are freely available for download in the Google Earth Engine (GEE) platform (https://developers.google.com/earth-engine/datasets/catalog/sentinel).

We utilized the Ground Range Detected (GRD) scenes of the dual-polarization bands from the C-band Synthetic Aperture Radar instrument, which underwent calibration and orthorectification pre-processing. The dual-polarization bands include a vertical transmit/vertical receive (VV) signal and a vertical transmit/horizontal receive (VH) signal. These data have a spatial resolution of 10 m and a revisit time of six-day (Torres *et al*., 2012). However, due to the large size of the study area and the need to cover it in a single image, we downscaled the data to a spatial resolution of 30 m and a temporal resolution of 20 days. The analyzed period spanned from March 31, 2018, to November 30, 2021, and was selected to include dates that covered the entire study area and contain no missing pixel values. Additionally, we calculated three spectral indices using the radar bands (Table 1).

Sentinel-2 is a high-resolution, multispectral imaging mission with a global 5-day revisit frequency, provided by the European Space Agency, and freely available for download in the GEE platform (https://developers.google.com/earth-

engine/datasets/catalog/COPERNICUS_S2_SR_HARMONIZED). The Sentinel-2 data consists of orthorectified, atmospherically corrected surface reflectance images with a spatial resolution of 30 m. Due to cloud cover limitations, optical images were used as static variables. For each year, the wet season image was derived as the mean of the available Sentinel-2 images from January to April (with a maximum of 5% cloud cover), while the dry season image was the mean of the available images from August to September (with 0% of cloud cover). The Sentinel-2 bands (Table 2) were used here to calculate spectral indices, which helped to distinguish the water surface in both seasons (Table 1).

Table 1 – Sentinel-1 and Sentinel-2 Spectral indices

Spectral indices	Name	Equation	Source
		Sentinel-1	
VHVVD	VH-VV Difference	VH – VV	(Nasirzadehdizaji *et al.*, 2019)
VHVVR	VH-VV Ratio	VH/VV	(Alvarez-Mozos *et al.*, 2021)
NDPI	Normalized Difference Polarization Index	(VV – VH)/(VV + VH)	(Cao; Yan; Zheng, 2008)
		Sentinel-2	
NDWI	Normalized Difference Water Index	(B3 – B8) / (B3 + B8)	(McFeeters, 1996)
MNDWI	Modified Normalized Difference Water Index	(B3 – B11) / (B3 + B11)	(Xu, 2006)
RNDVI	Reversed Normalized Difference Vegetation Index	(B4 – B8)/(B4 + B8)	(Themistocleous *et al.*, 2020)
S2WI	Sentinel-2 Water Index	(B5 – B12)/(B5 + B12)	(Jiang *et al.*, 2021)
SWM	Sentinel Water Mask	(B2 + B3)/(B8 + B11)	(Milczarek; Robak; Gadawska, 2017)
WRI	Water Ratio Index	(B3 + B4)/(B8 + B11)	(Shen; Li, 2010)
LSWI	Land Surface Water Index	(B8 – B11)/(B8 + B11)	(Xiao *et al.*, 2004)
TWI	Triangle Water Index	(2.84 * (B5 – B6) / (B3 + B12)) + ((1.25 * (B3 – B2) – (B8 – B2)) / (B8 + 1.25 * B3 – 0.25 * B2))	(Niu *et al.*, 2022)
EVI	Enhanced Vegetation Index	g * (B8 – B4) / (B8 + C1 * B4 – C2 * B2 + L)	(Huete, 1997)
MSAVI	Modified Soil-Adjusted Vegetation Index	0.5 * (2.0 * B8 + 1 – (((2 * B8 + 1) * 2) – 8 * (B8 – B4)) * 0.5)	(Qi *et al.*, 1994)
NDVI	Normalized Difference Vegetation Index	(B8 – B4)/(B8 + B4)	(Rouse *et al.*, 1974)
IRECI	Inverted Red-Edge Chlorophyll Index	(B7 – B4) / (B5 / B6)	(Frampton *et al.*, 2013)
MCARI	Modified Chlorophyll Absorption in Reflectance Index	((B5 – B4) – 0.2 * (B5 – B3)) * (B5 / B4)	(Daughtry, 2000)
NBR	Normalized Burn Ratio	(B8 – B12) / (B8 + B12)	(Coffelt; Livingston, 2002)
NBR2	Normalized Burn Ratio 2	(B11 – B12) / (B11 + B12)	(Landsat Missions, 2023)

Source: (Montero *et al.*, 2023).

Table 2 – Sentinel 2 spectral bands wavelengths

Band	Description	Wavelength (nm)
B1	Aerosols	443.9
B2	Blue	496.6
B3	Green	560
B4	Red	664.5
B5	Red Edge 1	703.9
B6	Red Edge 2	740.2
B7	Red Edge 3	782.5
B8	Near Infrared	835.1
B8A	Near Infrared 2	864.8
B9	Water Vapour	945
B11	Short-wave Infrared 1	1613.7
B12	Short-wave Infrared 2	2202.4

Source: ESA 2015

The FABDEM was also considered a static variable, as it represents surface elevation. It was derived from the Copernicus GLO-30 DEM, a digital elevation model with a 30 m spatial resolution. The data is freely available for download at the University of Bristol website (https://data.bris.ac.uk/data/dataset/s5hqmjcdj8yo2ibzi9b4ew3sn). This model was processed using machine learning techniques to remove forest and buildings (Hawker *et al*., 2022).

5.3.3 Data processing

5.3.3.1 Global model development

The whole modeling process was summarized in figure 3. The first step of model training was to obtain point samples of water and non-water classes from the study area using ArcGIS Pro tools. Sampling was supported by the Land Use and Land Cover (LULC) Collection 9 data from MapBiomas (https://brasil.mapbiomas.org/downloads/), which helped confirm sampling over water surfaces. This ensured that floodable environments, such as floodable forests, wetlands, grasslands, pastures, and rice fields, were not mistakenly classified as non-water classes, as they are prone to seasonal inundation. We collected 300 water samples, and 300 non-water samples based on two Sentinel-1 images: one representing the wet season (2019/03/06 to 2019/03/26) and other representing the dry season (2019/11/21-2019-12-11).

Figure 3 – Flowchart of the main steps of the water modelling process.

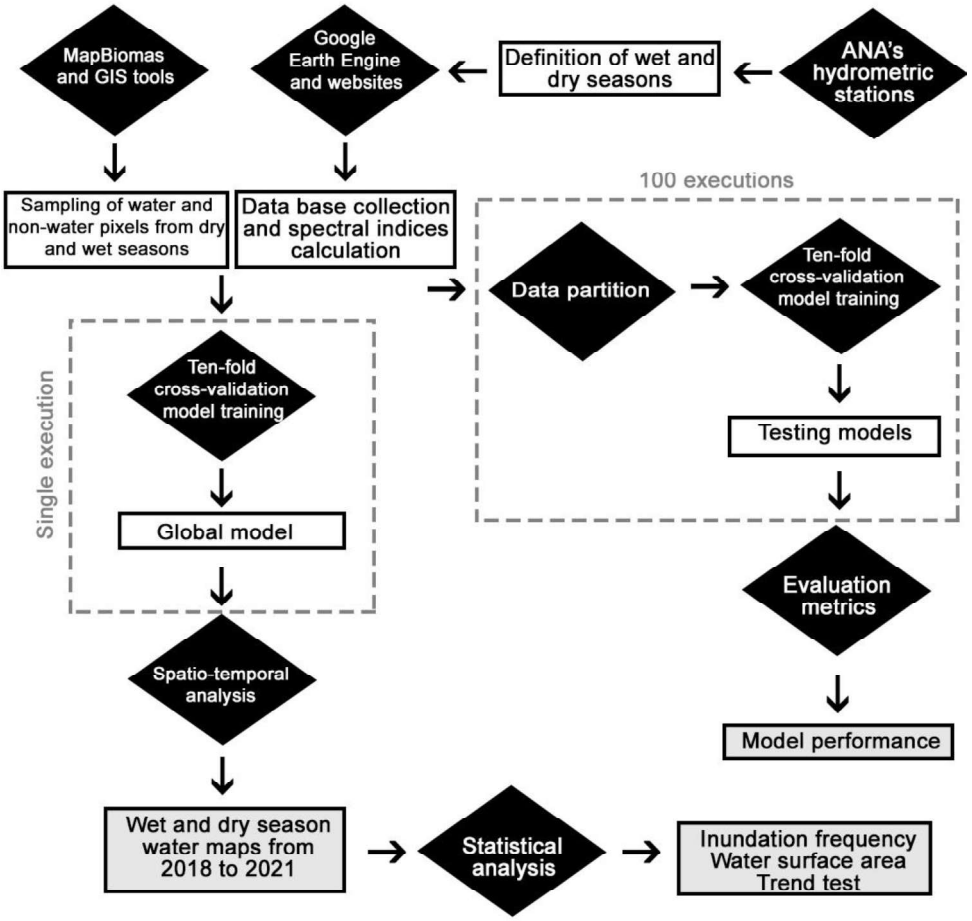

Source: The author.

The modelling process was performed using the R software (R Core Team, 2024). The point samples of the wet and dry seasons overlapped with their respective Sentinel-1 VH and VV bands of both wet (2019/03/06 to 2019/03/26) and dry season (2019/11/21-2019-12-11) to extract the corresponding pixel values, using the terra package. For this process, eight surrounding pixels were considered to calculate the mean value, to obtain a more representative sample. This process was repeated for each spectral index (from Sentinel-1 and Sentinel-2) and for the FABDEM. In the end, we obtained a data frame with 1,200 Y variables (the target variable) in the rows, represented by the water and non-water samples. The twenty-one X variables (the explanatory covariates) were in columns, represented by the Sentinel-1 VH and VV bands, the eighteen spectral indices (from Sentinel-1 and Sentinel-2), and the FABDEM.

The prediction methodology follows that of (Fernandes-Filho *et al*., 2024). Before model training, variables with a strong ($r > 0.95$) Spearman correlation were removed, using the findcorrelation function of the caret package. In addition, we applied the Recursive Feature Elimination (RFE) algorithm to select the best subset of covariates and improve model

performance, using the rfe function of the caret package. We used the Random Forest (RF) classification model because of its successful application on a water resources studies (Álvarez-Cabria; Barquín; Peñas, 2016; Li *et al*., 2023; Shaeri Karimi *et al*., 2019; Tulbure *et al*., 2016). We applied ten-fold cross-validation method to enhance the RF model training performance, using the caret package. We optimized the number of variables used in training using the mtry hyperparameter, which was selected as the one that resulted in the best kappa coefficient. At the end of this step, we obtained a global RF model.

5.3.3.2 Spatiotemporal analysis applying the global model

For the spatiotemporal analysis, the global RF model prediction used dynamic and static variables. The dynamic variables were the Sentinel-1 bands with a 20-day interval. The statics variables included reflectance indices (Sentinel-1 and Sentinel-2), corresponding to the wet or dry season, and FABDEM. Finally, we obtained 29 water maps of the wet season, and 32 for the dry season, covering the period from 2018 to 2021.

5.3.3.3 Model validation

To test the model's performance, we split the 1,200 point samples into training (80%) and test (20%). We used the same Sentinel-1 images from the global RF model: one representing the wet season (2019/03/06 to 2019/03/26) and other representing the dry season (2019/11/21-2019-12-11). The training samples were used to train and tune the RF model using ten-fold cross-validation. The mtry hyperparameter was also used, based on the best kappa coefficient. The tuned model was tested using the test samples, applying Kappa coefficient, Accuracy, and F1-Score metrics. This process was repeated 100 times to vary the training, tuning, and testing models (Fernandes-Filho *et al*., 2024). Thus, the overall performance of the RF model was represented by statistical measures of the evaluation metrics.

5.3.3.4 Post-processing

The 61 water maps of the UPRB, representing both wet and dry seasons, were overlapped to calculate the absolute frequency using the *mdsFuncs* package. A final map depicting the inundation frequency was then created. The inundation frequency classes, based

on (Padovani, 2010) for comparison, included the following ranges: 0%, 1 to 10%, 11-20%, 21-30%, 31-40%, 51-50%, 51-60%, 61-70%, 71-80%, 81-90%, 91-100%.

Additionally, we applied the non-parametric Mann-Kendall trend test using the *trend* package, considering only trends with a significance level of 5% ($p \leq 0.05$). Kendall's τ was calculated to assess trend strength: τ close to 1 indicates a strong increasing trend, τ close to -1 indicates a strong decreasing trend, and τ equal to 0 indicates no trend.

Finally, we extracted the water surface area mapped by the MapBiomas, from the Land Use and Land Cover Mapping of Collection 9 (https://brasil.mapbiomas.org/downloads/) for comparing with our results.

5.4 RESULTS

5.4.1 The spatiotemporal water modelling

In the predictor selection step, nine of twenty-one covariates (IRECI, NBR, NDVI, NDWI, NDPoll, RNDVI, SWM, TWI, and WRI) were eliminated due to strong correlations. Of the remaining twelve, only four (FABDEM, MNDWI, S2WI, and VH) were sufficient to stabilize the RF model performance. Among these, FABDEM proved to be the most important for water prediction in the UPRB (Figure 4). The evaluation metric Kappa, Accuracy and F1-Score demonstrated high values (0.989, 0.995, and 0.995, respectively).

Figure 4 – Importance of the explanatory covariates used in the global RF model.

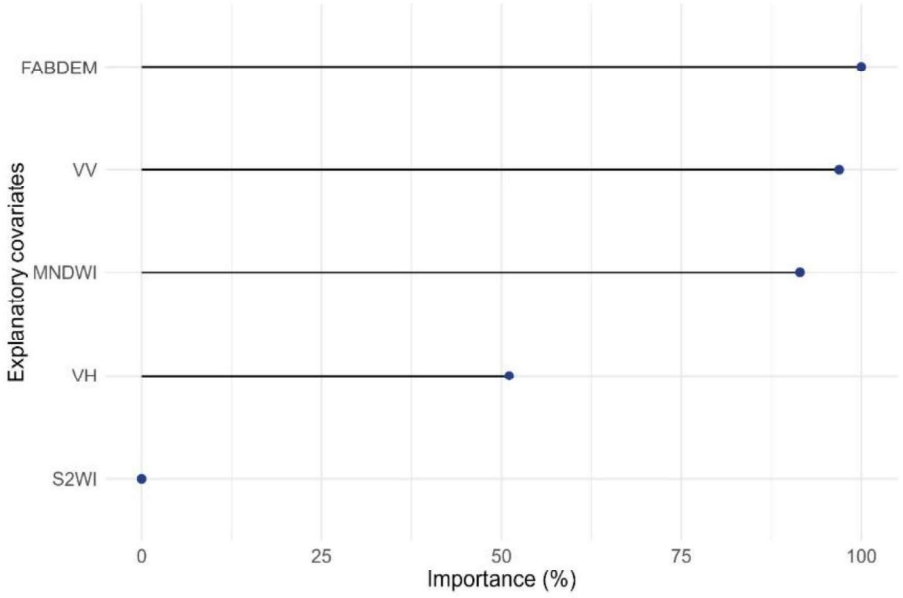

Source: The author.

Throughout most of the analyzed period, the dry season exhibited higher total water surface values than the wet season (Figure 5). This overestimation in the dry season was influenced by variations in the backscattering coefficient across different land uses and covers. For instance, during the dry period from 2021/10/01 to 2021-10-21 significant areas of pasture and soybean crops (Figure 6c) were misclassified as water (figure 6c) due to the lower (dark color) VV band backscatter (Figure 6a). In another dry season period (Figure 6e), the misclassification was minimal, attributed to changes in the VV band backscatter (Figure 6d). During the wet season, misclassification persisted but affected significantly fewer areas (Figure 6h).

Figure 5 – Total water surface area in the UPRB for the dry and wet season during 2018 and 2021.

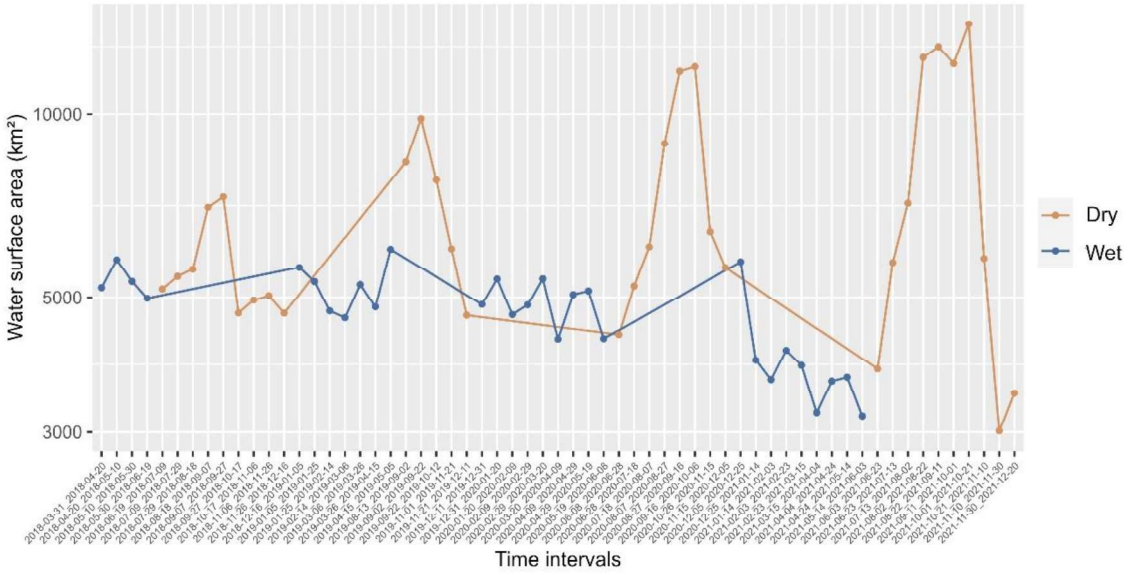

Source: The author.

Figure 6 – Images of the dry periods from 2021/10/01 to 2021/10/21 (a, b, and c), and from 2021/11/30 to 2021/12/20 (d, e, and f). Image of the wet season from 2020/12/05 to 2020/12/25. Sentinel-1 VV band (a, d, and g), surface water mapped (b, e, and h), and MapBiomas land use and cover data from 2021 (c and f), and from 2020 (i).

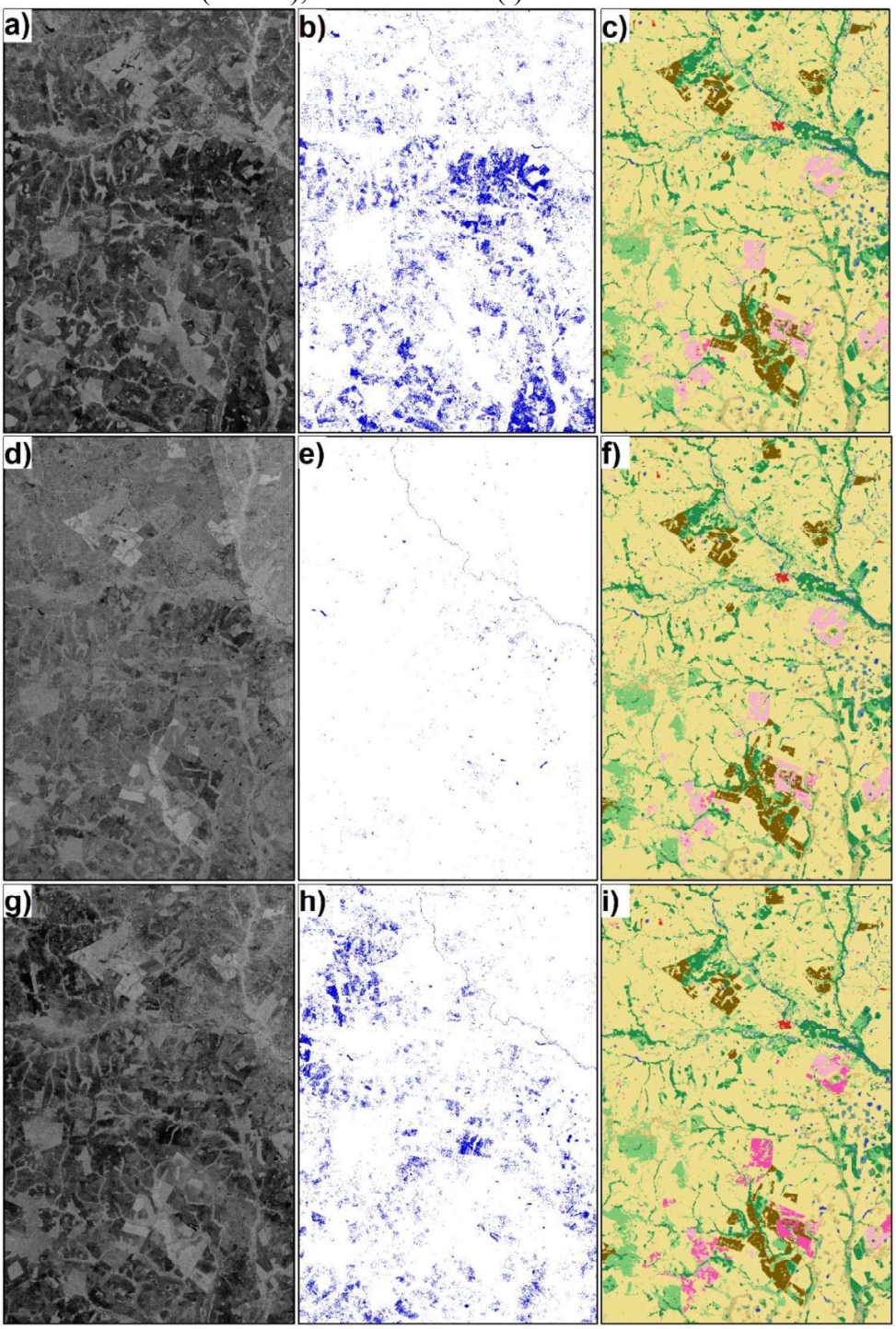

Source: The author.

Notes: a, d, and g) Gray scale – low backscattering coefficient (black) to high backscattering coefficient (light gray); b, e, and h) Water (blue) and non-water (white); c, f, and i) Urban area (red), soybean (light pink), other temporary crops (dark pink), forest plantation (brown), grassland (light brown) rocky outcrop (orange), savanna formation (light green), forest formation (dark green), pasture (yellow), wetland (light blue) and river or lake (dark blue).

Between 2018 to 2021, 86% of the total UPRB area (~318,784 km2) remained unaffected by flooding (Figure 6a and 6b). Flooding affected only 11% and 1.25% of the area for 10% and 20% of the analyzed period, respectively, while only 0.57% of the area was flooded for more than 90% of the time. Inundation frequencies between 30 and 90% were observed in less than 0.5% of the area. In the center part of the study area (Figure 6a), where some radar bands images overlapped, there were some anomalous pixels, which were misclassified as water during some part of the analyzed period, covering an area of approximately 853.6 km² (0.23% of the total UPRB area). The Paraguay Pantanal (sub-basin 7) and Upper Cuiabá River (4) had 1.34% and 1.28% of their areas with permanent water, respectively. The São Lourenço River (5), Miranda River (10), Upper Cuiabá River (4), Correntes River (6), and Jaurú River (1) had over 90% of their areas unaffected by floodings.

During the wet over the analyzed period, a statistically significant ($p < 0.05$) moderate to strong decreasing trend ($\tau < 0$) in the water surface area of the UPRB was observed (Figure 7). In contrast, no statistically significant trend was detected for the dry season. Among the sub-basins (Figure 8), only the Upper Cuiabá River (4), Jaurú River (1), Nabileque River (12), Negro River (9), Paraguay Pantanal (7), and Taquari River (8) presented statistically significant trends. A decreasing trend in wet season water surface area was observed in the Upper Cuiabá River (4), Jaurú River (1), Negro River (9), Paraguay Pantanal (7), and Taquari River (8), with the strongest decline being in the Pantanal Paraguay ($\tau = -0.76$). For the dry season, an increasing trend was noted in the Nabileque River (12), Negro River (9), and Taquari River (8), with the Negro River exhibiting the strongest trend ($\tau = 0.31$).

Figure 6 – Inundation frequency of the UPRB and its sub-basins.

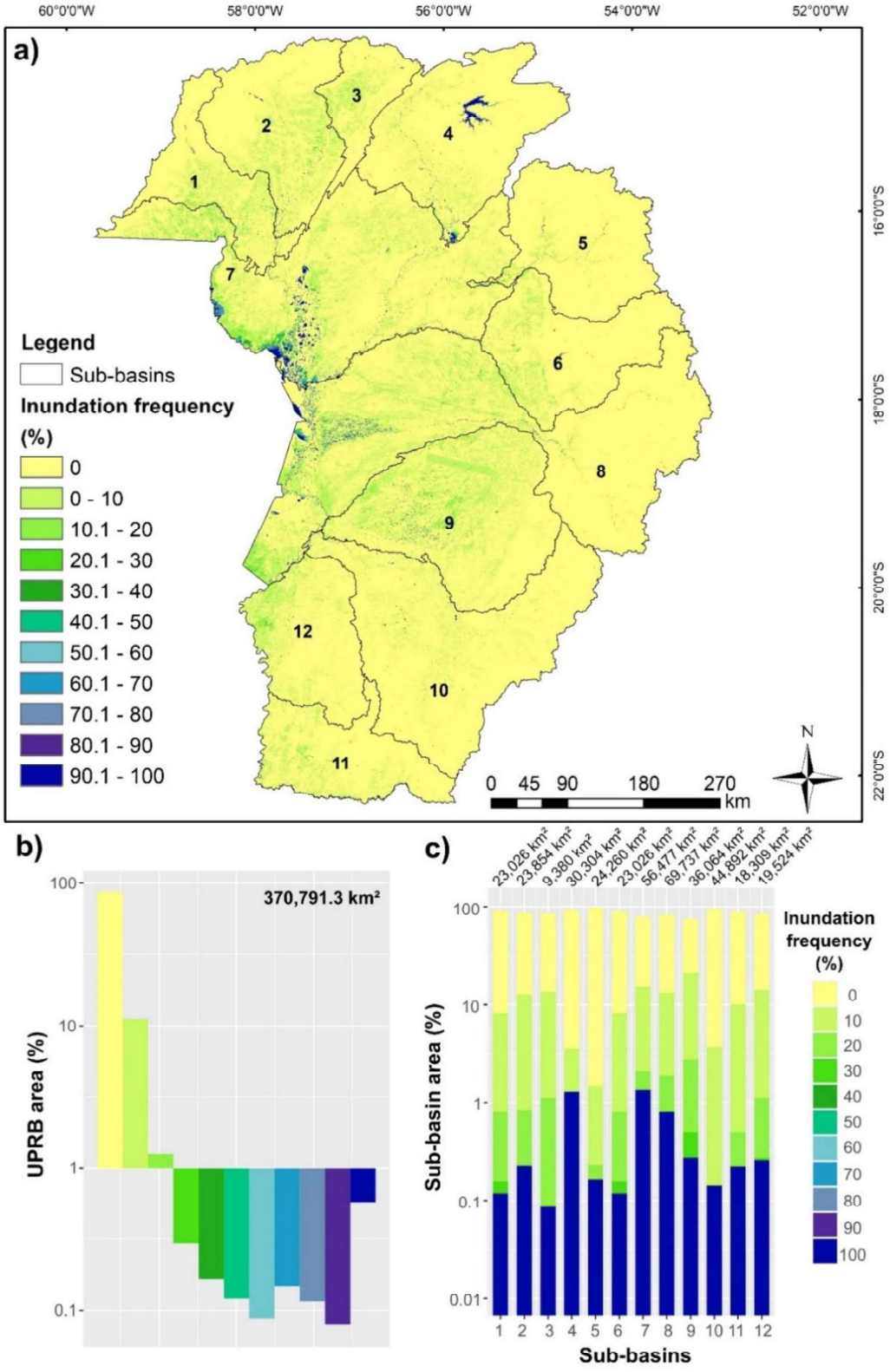

Source: The author.
Note: Sub-basins – 1) Jaurú River, 2) Upper Medium Paraguay, 3) Upper Superior Paraguay, 4) Upper Cuiabá River, 5) São Lourenço River, 6) Correntes River, 7) Paraguay Pantanal, 8) Taquari River, 9) Negro River, 10) Miranda River, 11) APA River, and 12) Nabileque River.

Figure 7 – Mann-Kendall test results for the Upper Paraguay River Basin.

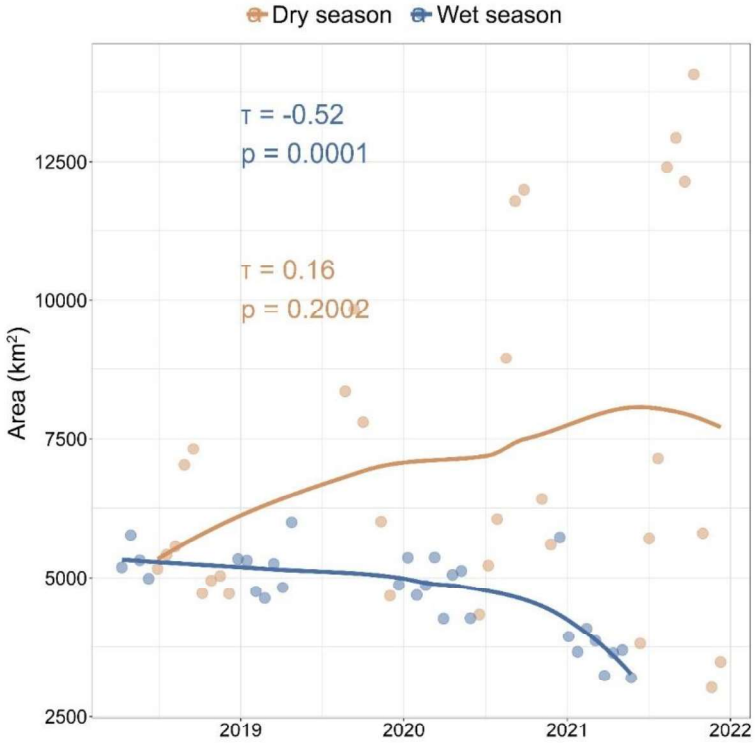

Source: The author.

Figure 8 – Mann-Kendall test results for the sub-basins of the Upper Paraguay River Basin.

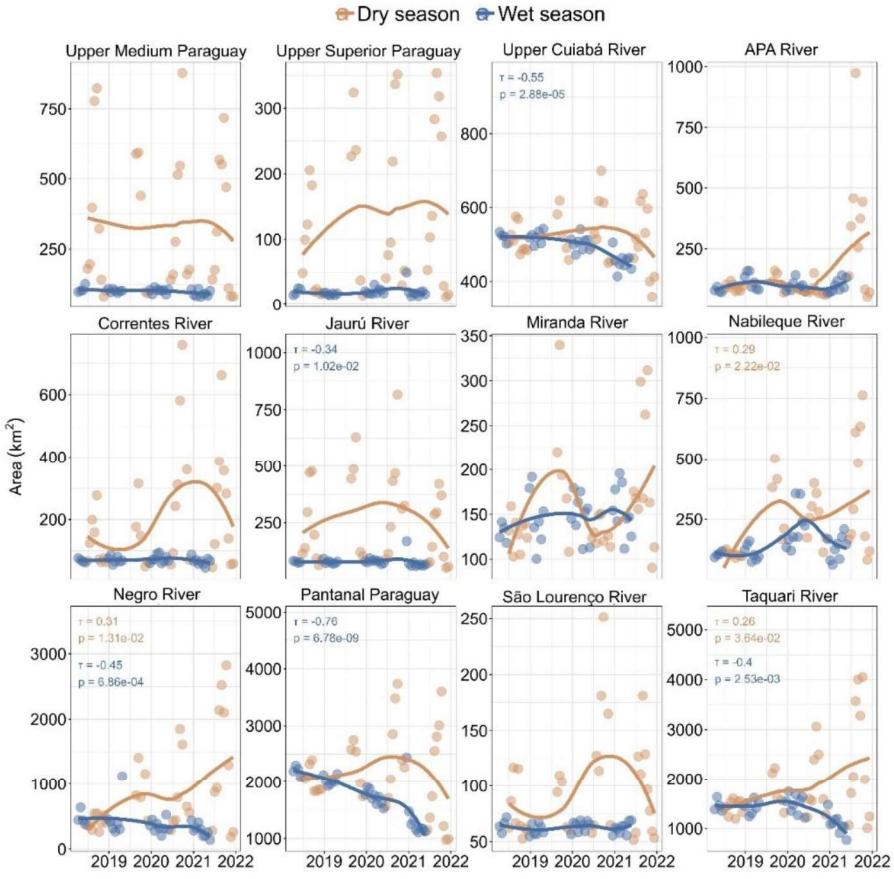

Source: The author.

Comparing our results with the MapBiomas water classification by year, during the analyzed period, we observed a difference of approximately 10,261 km² in 2018 (Table 1). In the other years, the MapBiomas water surface area remained higher than our results, except for 2021. Considering that the wet season water surface area was less influenced by the land use backscatter confusion, our results agree with a decreasing in the water surface area presented by the MapBiomas.

Table 3 – Comparison between the MapBiomas water class extent and our water extent for the UPRB during 2018 to 2021.

	MapBiomas Water Class	Water Modelling		
Year	Annual	Annual*	Wet season*	Dry Season*
		km²		
2018	15,738.63	5,477.61	5,365.342	5,539.981
2019	9,582.304	5,968.957	5,119.404	7,328.241
2020	6,378.683	6,091.081	4,805.519	7,537.339
2021	5,138.745	6,221.507	3,621.084	8,041.804

Notes: *Mean values during the corresponding period.

5.4.2 Evaluation of the Random Forest model performance

Across 100 runs, after eliminating the most correlated covariates, FABDEM, MNDWI, MSAVI, S2WI, VH and VV were the most frequently selected during the RF models optimization process. The optimal mtry hyperparameter varied from 2 to 100, with a median of 4, aligning with the best fit previously observed for the RF global model (Figure 9). Among the covariates, VV, MNDWI, and VH were more important than FABDEM for water prediction in the UPRB (Figure 10).

Figure 9 – The *mtry* hyperparameter variation over the 100 runs.

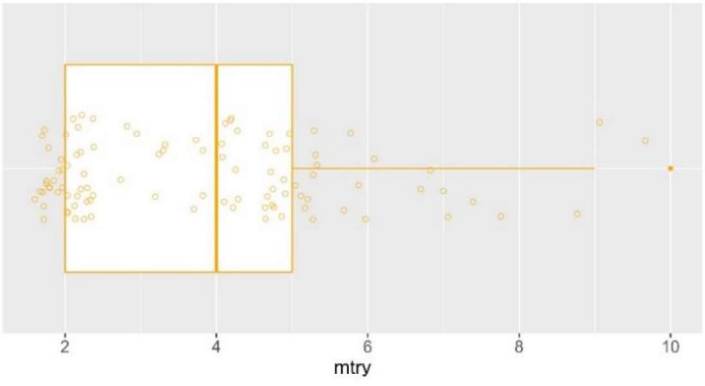

Source: The author.

Figure 10 – The most important explanatory covariates over the 100 runs.

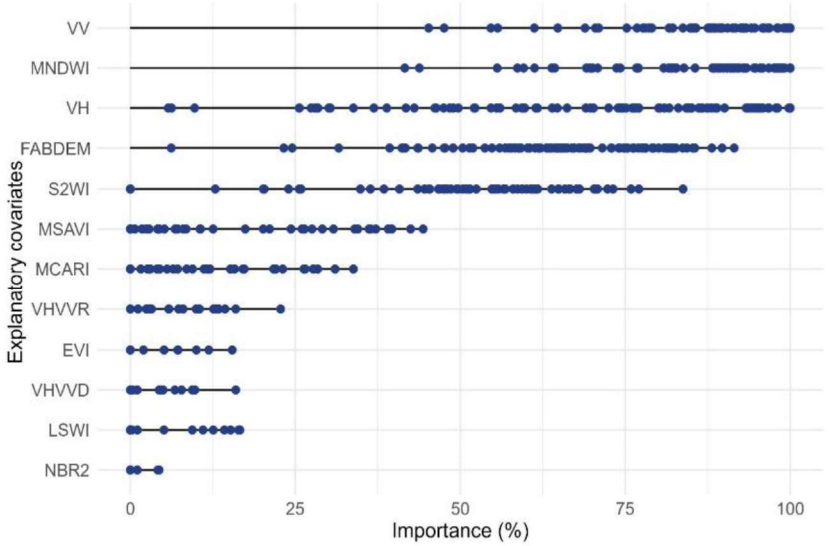

Source: The author.

The RF model demonstrated consistently high performance metrics (Figure 11). The mean and median values from the 100 runs during the test step were equal to or slightly higher than those observed in the training step. Among the evaluation metrics, Accuracy and F1-Score from the test step slightly outperformed (both with a mean of 0.99) the Kappa coefficient (0.98).

Figure 11 – Random Forest performances in 100 runs for water and non-water classes.

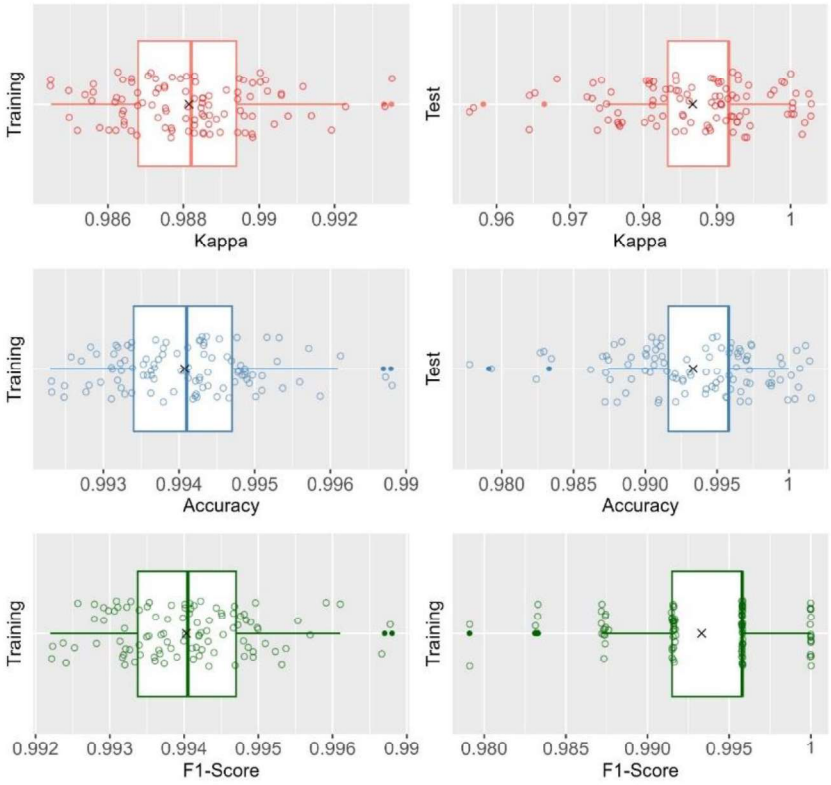

Source: The author.

5.5 DISCUSSION

5.5.1 The water modelling

In this study, the Sentinel-1 VV and VH bands showed great importance on water modelling. Radar images are particularly suitable for identifying flood-prone areas due to their ability to capture images both day and night (Anusha; Bharathi, 2020). According to (Clement; Kilsby; Moore, 2018; Twele *et al*., 2016), the VV band from Sentinel-1 showed slightly higher accuracy in mapping flood extents compared to the VH band. This aligns with our findings, where the VV band proved more important than the VH band in both the 100 test models and the global RF model.

Among the spectral indices, MNDWI was the most important for distinguishing water and the second most important among all covariates. MNDWI emphasizes the strong absorption of SWIR radiation by water bodies, making it more effective than other spectral indices, such as the NDWI (Clement; Kilsby; Moore, 2018). In the study of Clement, Kilsby and Moore (2018), MNDWI was used to validate the water extent extracted by the VV and VH bands, showing slightly higher accuracy when combined with the VV band. This highlights a strong relationship between the optical results and the Sentinel-1 images.

FABDEM proved to be a crucial covariate for water modelling due to the strong relationship between geomorphology and inundation dynamics in the UPRB (Ferreira-Júnior *et al*., 2016; Ivory *et al*., 2019). To address the similarity between mountain shadows and water bodies in radar images, (Li *et al*., 2023) incorporated terrain features from the SRTM-1 DEM into their modeling, achieving increased accuracy in flood detection across both high and low hill areas. Moreover, FABDEM is considered a more reliable DEM for representing bare terrain elevations (Bielski *et al*., 2024), further enhancing the detection of water bodies.

A limitation of using radar images for water modelling is the confusion between water and other land uses and covers. We observed an overestimation of the surface water area, mainly in the dry season, which can be associated with some crops phenological stages and their response to the radar bands backscatter. In a study conducted by (Clement; Kilsby; Moore, 2018), some agricultural fields that became partially inundated were more easily detected with VH band. (Marković *et al*., 2023) found that the VH band is more suitable for soybean harvest detection due to its higher sensitivity to structural changes in crops, showing a significant decrease in VH polarization values after the harvest. According to (Veloso *et al*., 2017), VH backscatter is primarily influenced by attenuated double-bounce and volume scattering

mechanisms, and VV backscatter is dominated by the direct contributions from the ground and canopy. After soybean harvest, VH backscatter decreases, while VV backscatter increases due to reduced attenuation from crop structure and significant surface scattering from the soil, respectively. For other crops, such as maize, soil tillage can smooth the soil surface, leading to a decrease in VV backscatter (Veloso *et al*., 2017).

The RF model's performance, measured over 100 test runs, was exceptionally high, indicating the model's strong ability to predict unseen data. In a flooding monitoring study by (Li *et al*., 2023), which applied various water extraction methods and a multi-data source approach (radar images, optical images, and DEM), RF showed slightly lower Accuracy and Kappa coefficient values compared to our results. Nevertheless, it was considered one of the best water extraction methods, second only to the Channel Attention U-Net model. Similarly, (Shaeri Karimi *et al*., 2019) used RF with topographic, climatic, and hydrologic covariates to model inundation patterns, achieving reasonable prediction metrics. Their findings further demonstrate that machine learning is a promising tool for reproducing long-term daily inundation extents to characterizing inundation regimes.

5.5.2 The water regime on the UPRB

The general distribution pattern of the inundation frequency in the UPRB indicates that permanently inundated areas are primarily located near the Paraguay River (90% of inundation frequency), within the Paraguay Pantanal sub-basin, in the western portion of the UPRB. Other significant permanently inundated areas include the Taquari megafan (also in the western portion), the artificial lakes located in the Upper Cuiabá River sub-basin (northern portion), corresponding to Manso Lake formed by the APM Manso Hydroelectric Power Plant, and the thousands of lakes in the Negro River sub-basin (southern portion), which encompassed the freshwater and alkaline-saline lakes of the Pantanal of Nhecolândia. In contrast, non-inundated areas and low inundation frequency classes (10% and 20%) predominated across the rest of the UPRB. These findings align with the results of Padovani (2010) for the Pantanal depression, except for the 30% frequency class, which was more significant in their study.

Historically, the Pantanal has exhibited significant interannual variability in its inundation area. According to Hamilton (2002) and Hamilton, Sippel and Melack (1996), from 1900 to 1964, this variability was considerable, though wet-dry cycles were less pronounced. Between 1964 and 1974, relatively dry conditions prevailed with limited inundation, whereas the period from 1974 to 1993 experienced more regular cycles of flooding and drying. This

variability, driven by fluctuations in precipitation, that caused severe floods or pronounced droughts, is influenced by regional-scale water balance and soil moisture, and large-scale phenomena associated with the Pacific and Atlantic Oceans, such as El Niño and the South America Monsoon System (Bergier, 2010).

Despite the short four-years analysis period, the decreasing trend in water surface observed during the wet season aligns with the reduction in water surface extent reported by the MapBiomas mapping. Analyzing the monthly precipitation trends from 1977 to 2006 using data from 12 rain gauge stations in Pantanal, (Cardozo; Marcuzzo, 2010; Marcuzzo *et al*., 2010) identified a moderate decrease in precipitation accompanied by pronounced interannual variability. Similarly, (Silio-Calzada *et al*., 2017), studying the floodplain dynamics of the Chacororé Lake (Western Pantanal), reported a decrease in the lake's surface area between September 1984 and September 2011. Moreover, future climate change scenarios for the Pantanal generally project temperature increases, rainfall reductions, and consequently, greater soil water deficiency due to higher evaporation by the end of the 21st century (Marengo; Alves; Torres, 2016; Marengo; Oliveira; Alves, 2015).

5.6 CONCLUSIONS

During the rainy season, optical imagery availability is severely limited by adverse weather conditions. In this study, Sentinel-1 imagery enabled monitoring at 20-days intervals, supplemented by multi-source data, to assess inundation in the UPRB from 2018 to 2021. Seasonal monitoring, particularly during dry season, is challenging due to difficulties distinguishing land uses such as pasture and soybean crops from water in the VH band backscatter. To address this issue, we propose including land use and cover as a covariate in the water modelling.

The Random Forest model demonstrated significant superiority in water extraction tasks, achieving high performance and proving well-suitable for binary classification using a high dimensional, multi-source dataset.

Areas with higher inundation frequency are concentrated in the western portion of the UPRB, near to the Paraguay River, and in the southern portion, where the Nhecolândia's lake occur, with a decreasing trend in water extent observed during the wet season. Given the importance of the flood pulses in the Pantanal ecosystem, monitoring inundation frequency is essential for forecasting the impacts of future climate changes.

5.7 REFERENCES

AB'SÁBER, A. N. O Pantanal Mato-Grossense e a Teoria dos Refúgios. **Revista Brasileira de Geografia**, [s. l.], v. 50, p. 9–57, 1988.

ADAMI, M. *et al*. Estudo da dinâmica espaço-temporal do bioma Pantanal por meio de imagens MODIS. **Pesquisa Agropecuária Brasileira**, [s. l.], v. 43, n. 10, p. 1371–1378, 2008.

ALHO, C. J. R. *et al*. Ameaças à biodiversidade do Pantanal brasileiro pelo uso e ocupação da terra. **Ambiente & Sociedade**, [s. l.], v. 22, 2019.

ALHO, C. J. R. Biodiversity of the Pantanal: response to seasonal flooding regime and to environmental degradation. Brazilian Journal of Biology, [s. l.], v. 68, n. 4, p. 957–966, 2008.

ALHO, C. J. R. The Pantanal. In: FRASER, L.H.; KEDDY, P.A. (org**.). The World's Largest Wetlands**: Ecology and Conservation. Cambridge: Cambridge University Press, 2005. p. 203–271.

ALVARES, C. Alcarde *et al*. Köppen's climate classification map for Brazil. **Meteorologische Zeitschrift**, [s. l.], v. 22, n. 6, p. 711–728, 2013.

ÁLVAREZ-CABRIA, M.; BARQUÍN, J.; PEÑAS, F. J. Modelling the spatial and seasonal variability of water quality for entire river networks: Relationships with natural and anthropogenic factors. **Science of The Total Environment**, [s. l.], v. 545–546, p. 152–162, 2016.

ALVAREZ-MOZOS, J. *et al*. **Correlation Between NDVI and Sentinel-1 Derived Features for Maize**. IEEE International Geoscience and Remote Sensing Symposium IGARSS. [S. l.]: IEEE, 2021. p. 6773–6776.

AMARAL FILHO, Z. P. do. Solos do Pantanal Mato-grossense. Simpósio sobre Recursos Naturais e Sócio-econômicos do Pantanal, 1, 1984, **Anais...** Corumbá. EMBRAPA-DDT, 1984. p. 91–104.

ANA. **Plano de Recursos Hídricos da Região Hidrográfica do Paraguai - PRH Paraguai, Produto Parical PP-02**. Brasília: Ana/SPR, ENGECORPS ENGENHARIA S.A., 2017.

ANA. **Portal HidroWeb**. [S. l.], 2024.

ANTUNES, J. F. G.; ESQUERDO, J. C. D. M. Quantification of flooded areas of Pantanal by sub-pixel classification of MODIS time-series data. **Geografia**, [s. l.], v. 40, p. 39–53, 2015.

ANUSHA, N.; BHARATHI, B. Flood detection and flood mapping using multi-temporal synthetic aperture radar and optical data. **The Egyptian Journal of Remote Sensing and Space Science**, [s. l.], v. 23, n. 2, p. 207–219, 2020.

ASSINE, M. L. Brazilian Pantanal: A Large Pristine Tropical Wetland. In: VIEIRA, B. C.; S., RODRIGUES, A. A.; SANTOS, L. J. C. (org.). **Landscapes and Landforms of Brazil**. [S. l.]: Springer Dordrecht, 2015. p. 135–146.

BERGIER, I. River level sensitivity to SOI and NAO in Pantanal and Amazonia. Simpósio de Geotecnologias no Pantanal, 3, **Anais...** Cáceres, MT: Embrapa Informática Agropecuária/INPE, 2010. p. 25–34.

BIELSKI, Conrad *et al*. **Novel Approach for Ranking DEMs: Copernicus DEM Improves One Arc Second Open Global Topography**. IEEE Transactions on Geoscience and Remote Sensing, [s. l.], v. 62, p. 1–22, 2024.

BOIN, M. N. *et al*. Pantanal: The Brazilian Wetlands. In: SALGADO, A. A. R.; SANTOS, L. J. C.; PAISANI, J. C. (org.). **The Physical Geography of Brazil**. [S. l.]: Springer Cham, 2019. p. 75–91.

BRASIL. Projeto RADAMBRASIL. **Folha SE.21 Corumbá e parte da Folha SE.20: geologia, geomorfologia, pedologia, vegetação e uso potencial da terra**. Rio de Janeiro: [s. n.], 1982.

CAO, Y.; YAN, L.; ZHENG, Z. **Extraction of information on geology hazard from multi-polarization SAR images**. In: The International Archives of the Photogrammetry, Remote Sensing and Spatial Information Sciences. Beijing: International Society of Photogrammetry and Remote Sensing, 2008. p. 1529–1532.

CARDOZO, M. R. D.; MARCUZZO, F. F. N. Mapeamento de três decênios da precipitação pluviométrica total e sazonal do bioma Pantanal. Simpósio de Geotecnologias no Pantanal, 3, Cáceres, **Anais...** Cáceres-MT: Embrapa Informática Agropecuária/INPE, 2010. p. 84–94.

CARVALHO, N. de O. Hidrologia da Bacia do Alto Paraguai. In: Simpósio sobre Recursos Naturais e Sócio-econômicos do Pantanal, 1, **Anais...** Corumbá: EMBRAPA-DDT, 1984. p. 43–50.

CHIARAVALLOTI, Rafael Morais *et al*. Achieving conservation through cattle ranching: The case of the Brazilian Pantanal. **Conservation Science and Practice**, [s. l.], 2023.

CLEMENT, M.A.; KILSBY, C.G.; MOORE, P. Multi-temporal synthetic aperture radar flood mapping using change detection. **Journal of Flood Risk Management**, [s. l.], v. 11, n. 2, p. 152–168, 2018.

COFFELT, J.L.; LIVINGSTON, Russell K. **Second U.S. Geological Survey Wildland Fire Workshop: Los Alamos, New Mexico**, October 31-November 3, 2000. [S. l.: s. n.], 2002.

COSTA, Maycira P.F.; TELMER, Kevin H. Mapping and monitoring lakes in the Brazilian Pantanal wetland using synthetic aperture radar imagery. **Aquatic Conservation: Marine and Freshwater Ecosystems**, [s. l.], v. 17, n. 3, p. 277–288, 2007.

DAUGHTRY, C. Estimating Corn Leaf Chlorophyll Concentration from Leaf and Canopy Reflectance. **Remote Sensing of Environment**, [s. l.], v. 74, n. 2, p. 229–239, 2000.

ERWIN, Kevin L. Wetlands and global climate change: the role of wetland restoration in a changing world. **Wetlands Ecology and Management**, [s. l.], v. 17, n. 1, p. 71–84, 2009.

EVANS, Teresa L. *et al*. **Using ALOS/PALSAR and RADARSAT-2 to Map Land Cover and Seasonal Inundation in the Brazilian Pantanal**. IEEE Journal of Selected Topics in Applied Earth Observations and Remote Sensing, [s. l.], v. 3, n. 4, p. 560–575, 2010.

FERNANDES-FILHO, E. I. *et al*. Methods and Challenges in Digital Soil Mapping: Applied Modelling with R Examples. In: CARVALHO JUNIOR, W. de; *et al*. (eds.). **Pedometrics in Brazil**. Switzerland: Springer Cham, 2024. p. 263–283.

FERREIRA-JÚNIOR, W. G. *et al*. Flood regime and water table determines tree distribution in a forest-savanna gradient in the Brazilian Pantanal. **Anais da Academia Brasileira de Ciências**, [s. l.], v. 88, n. suppl 1, p. 719–731, 2016.

FRAMPTON, W. J. *et al*. Evaluating the capabilities of Sentinel-2 for quantitative estimation of biophysical variables in vegetation. **ISPRS Journal of Photogrammetry and Remote Sensing**, [s. l.], v. 82, p. 83–92, 2013.

FREITAS, J. G. *et al*. Interaction between lakes' surface water and groundwater in the Pantanal wetland, Brazil. **Environmental Earth Sciences**, [s. l.], v. 78, n. 5, p. 139, 2019.

FURQUIM, S. A. C. *et al*. Salt-affected soils evolution and fluvial dynamics in the Pantanal wetland, Brazil. **Geoderma**, [s. l.], v. 286, p. 139–152, 2017.

FURQUIM, S. A. C.; VIDOCA, T. T. Salt-Affected Soils of Pantanal Wetland. In: TALEISNIK, Edith; LAVADO, R. S. (org.). **Saline and Alkaline Soils in Latin America**. Cham: Springer International Publishing, 2021. p. 229–254.

GUERREIRO, Renato L. *et al*. The soda lakes of Nhecolândia: A conservation opportunity for the Pantanal wetlands. Perspectives in Ecology and Conservation, [s. l.], v. 17, n. 1, p. 9–18, 2019.

GUO, Zhishun *et al*. Water-Body Segmentation for SAR Images: Past, Current, and Future. **Remote Sensing**, [s. l.], v. 14, n. 7, p. 1752, 2022.

HAMILTON, S. K. Hydrological controls of ecological structure and function in the Pantanal wetland (Brazil). **The ecohydrology of South American rivers and wetlands**, [s. l.], v. 6, p. 133–158, 2002.

HAMILTON, S. K.; SIPPEL, Suzanne J.; MELACK, John M. Inundation patterns in the Pantanal wetland of South America determined from passive microwave remote sensing. **Archiv für Hydrobiologie**, [s. l.], v. 137, n. 1, p. 1–23, 1996.

HAWKER, Laurence *et al*. A 30 m global map of elevation with forests and buildings removed. **Environmental Research Letters**, [s. l.], v. 17, n. 2, p. 024016, 2022.

HUETE, A. A comparison of vegetation indices over a global set of TM images for EOS-MODIS. **Remote Sensing of Environment**, [s. l.], v. 59, n. 3, p. 440–451, 1997.

IVORY, Sarah J *et al*. Vegetation, rainfall, and pulsing hydrology in the Pantanal, the world's largest tropical wetland. **Environmental Research Letters**, [s. l.], v. 14, n. 12, p. 124017, 2019.

JIANG, Wei *et al*. An Effective Water Body Extraction Method with New Water Index for Sentinel-2 Imagery. **Water**, [s. l.], v. 13, n. 12, p. 1647, 2021.

KARIM, Fazlul *et al*. A Review of Hydrodynamic and Machine Learning Approaches for Flood Inundation Modeling. **Water**, [s. l.], v. 15, n. 3, p. 566, 2023.

KARPATNE, Anuj *et al*. Global Monitoring of Inland Water Dynamics: State-of-the-Art, Challenges, and Opportunities. In: LÄSSIG, J. *et al*. (eds.). **Computational Sustainability**, Switzerland: Springer, Cha, v. 645, p. 121–147, 2016.

KEDDY, Paul A. *et al*. Wet and Wonderful: The World's Largest Wetlands Are Conservation Priorities. **BioScience**, [s. l.], v. 59, n. 1, p. 39–51, 2009.

LANDSAT MISSIONS. Landsat Satellite Missions. [S. l.], 2024.

LANDSAT MISSIONS. Landsat Surface Reflectance and Normalized Burn Ratio 2. [S. l.], 2023.

LI, H. *et al*. Flood Monitoring Using Sentinel-1 SAR for Agricultural Disaster Assessment in Poyang Lake Region. **Remote Sensing**, [s. l.], v. 15, n. 21, p. 5247, 2023.

LI, Fei *et al*. Research on Methods of Complex Water Body Information Extraction Based on GF-1 Satellite Remote Sensing Data. **Journal of University of Jinan**, [s. l.], 2021.

MAPBIOMAS. MapBiomas - Coleção da série de Mapas de Superfície da Água do Brasil. [S. l.], 2024.

MARCUZZO, F. F. N. *et al*. Chuvas no Pantanal brasileiro: análise histórica e tendência futura. Simpósio de Geotecnologias no Pantanal, 3, Cáceres, **Anais...** Cáceres-MT: Embrapa Informática Agropecuária/INPE, p. 170–180, 2010.

MARENGO, J. A.; ALVES, LM; TORRES, RR. Regional climate change scenarios in the Brazilian Pantanal watershed. Climate Research, [s. l.], v. 68, n. 2–3, p. 201–213, 2016.

MARENGO, J. A.; OLIVEIRA, G. S.; ALVES, L. M. Climate Change Scenarios in the Pantanal. In: BERGIER, I; ASSINE, M. L. **Dynamics of the Pantanal Wetland in South America**. Switzerland: Springer, Cham, 2015. p. 227–238.

MARKOVIĆ, Miljana *et al*. Using Sentinel-1 data for soybean harvest detection in Vojvodina province, Serbia. In: NEALE, C. M. Neale; MALTESE, A. (org.). **Remote Sensing for Agriculture, Ecosystems, and Hydrology** [S. l.]: SPIE, 2023. p. 62.

MARTINIS, S.; RIEKE, C. Backscatter Analysis Using Multi-Temporal and Multi-Frequency SAR Data in the Context of Flood Mapping at River Saale, Germany. **Remote Sensing**, [s. l.], v. 7, n. 6, p. 7732–7752, 2015.

MCFEETERS, S. K. The use of the Normalized Difference Water Index (NDWI) in the delineation of open water features. **International Journal of Remote Sensing**, [s. l.], v. 17, n. 7, p. 1425–1432, 1996.

MERDY, Patricia *et al*. Processes and rates of formation defined by modelling in alkaline to acidic soil systems in Brazilian Pantanal wetland. **Catena**, [s. l.], v. 210, p. 105876, 2022.

MILCZAREK, M.; ROBAK, A.; GADAWSKA, A. **Sentinel Water Mask (SWM)-new index for water detection on Sentinel-2 images**. In: Advanced Training Course on Land Remote Sensing, 7, [S. l.: s. n.], 2017.

MONTERO, David *et al*. A standardized catalogue of spectral indices to advance the use of remote sensing in Earth system research. **Scientific Data**, [s. l.], v. 10, n. 1, p. 197, 2023.

MORAES, E. C.; PEREIRA, G.; CARDOZO, F. da S. Evaluation of reduction of Pantanal wetlands in 2012. **Geografia**, [s. l.], v. 38, p. 81–93, 2013.

NASA. **Terra & Aqua Moderate Resolution Imaging Spectroradiometer (MODIS)**. [S. l.], 2024.

NASIRZADEHDIZAJI, R. *et al*. Sensitivity Analysis of Multi-Temporal Sentinel-1 SAR Parameters to Crop Height and Canopy Coverage. **Applied Sciences**, [s. l.], v. 9, n. 4, p. 655, 2019.

NIU, L. *et al*. Triangle Water Index (TWI): An Advanced Approach for More Accurate Detection and Delineation of Water Surfaces in Sentinel-2 Data. **Remote Sensing**, [s. l.], v. 14, n. 21, p. 5289, 2022.

PADOVANI, C. R. **Dinâmica Espaço-Temporal das Inundações do Pantanal**. 2010. 1–175 f. Tese (Doutorado) - Escola Superior de Agricultura “Luiz de Queiroz”, Piracicaba, 2010.

POTT, A. *et al*. Plant diversity of the Pantanal wetland. **Brazilian Journal of Biology**, [s. l.], v. 71, n. 1, p. 265–273, 2011.

QI, J. *et al*. A modified soil adjusted vegetation index. **Remote Sensing of Environment**, [s. l.], v. 48, n. 2, p. 119–126, 1994.

R CORE TEAM. **R**: A language and environment for statistical computing. Viena: R Foundation for Statistical Computing, 2024.

ROUSE, J. W. Jr. *et al*. **Monitoring vegetation systems in the Great Plains with ERTS**. In: NASA. Goddard Space Flight Center 3d ERTS-1 Symp, **Annals…** [S. l.: s. n.], 1974. p. 309–317.

SCHULZ, C. *et al*. Physical, ecological and human dimensions of environmental change in Brazil’s Pantanal wetland: Synthesis and research agenda. **Science of The Total Environment**, [s. l.], v. 687, p. 1011–1027, 2019.

SHAERI KARIMI, S. *et al*. Application of Machine Learning to Model Wetland Inundation Patterns Across a Large Semiarid Floodplain. **Water Resources Research**, [s. l.], v. 55, n. 11, p. 8765–8778, 2019.

SHEN, L.; LI, C. **Water body extraction from Landsat ETM+ imagery using adaboost algorithm**. In: International Conference on Geoinformatics, 18, Beijing, China: IEEE, 2010. p. 1–4.

SILIO-CALZADA, A. *et al*. Long-term dynamics of a floodplain shallow lake in the Pantanal wetland: Is it all about climate? **Science of The Total Environment**, [s. l.], v. 605–606, p. 527–540, 2017.

TARIFA, J. R. O Sistema Climático do Pantanal: da compreensão do sistema à definição de prioridades de pesquisa climatológica. In: Simpósio sobre Recursos Naturais e Sócio-econômicos do Pantanal,1, 1984, Corumbá, **Anais...** Corumbá-MS: EMBRAPA-DDT, 1984. p. 9–28.

THEMISTOCLEOUS, K. *et al*. Investigating Detection of Floating Plastic Litter from Space Using Sentinel-2 Imagery. **Remote Sensing**, [s. l.], v. 12, n. 16, p. 2648, 2020.

TORRES, R. *et al*. GMES Sentinel-1 mission. **Remote Sensing of Environment**, [s. l.], v. 120, p. 9–24, 2012.

TULBURE, M. G. *et al*. Surface water extent dynamics from three decades of seasonally continuous Landsat time series at subcontinental scale in a semi-arid region. **Remote Sensing of Environment**, [s. l.], v. 178, p. 142–157, 2016.

TWELE, A. *et al*. Sentinel-1-based flood mapping: a fully automated processing chain. **International Journal of Remote Sensing**, [s. l.], v. 37, n. 13, p. 2990–3004, 2016.

USSAMI, N.; SHIRAIWA, S.; DOMINGUEZ, J. M. L. Basement reactivation in a sub-Andean foreland flexural bulge: The Pantanal wetland, SW Brazil. **Tectonics**, [s. l.], v. 18, n. 1, p. 25–39, 1999. Disponível em: Acesso em: 26 mar. 2024.

VELOSO, A. *et al*. Understanding the temporal behavior of crops using Sentinel-1 and Sentinel-2-like data for agricultural applications. **Remote Sensing of Environment**, [s. l.], v. 199, p. 415–426, 2017.

WWAP. **La Plata Basin Case Study: Final Report**. [S. l.: s. n.], 2007.

WWF-BRASIL; INSTITUTO SOS PANTANAL. **Monitoramento das alterações da cobertura vegetal e uso do Solo na Bacia do Alto Paraguai – Porção Brasileira – Período de Análise: 2012 a 2014**. Brasília: [s. n.], 2015.

XIAO, X. *et al*. Satellite-based modeling of gross primary production in an evergreen needleleaf forest. **Remote Sensing of Environment**, [s. l.], v. 89, n. 4, p. 519–534, 2004.

XU, H. Modification of normalised difference water index (NDWI) to enhance open water features in remotely sensed imagery. **International Journal of Remote Sensing**, [s. l.], v. 27, n. 14, p. 3025–3033, 2006.

ZUO, J. *et al*. Remote sensing dynamic monitoring of the flood season area of Poyang Lake over the past two decades. **Natural Hazards Research**, [s. l.], v. 4, n. 1, p. 8–19, 2024.

6 GENERAL CONCLUSION

The pedodiversity and biodiversity of the Nhecolândia Pantanal are primarily influenced by the hydrological regime, which directly affects soil formation and nutrient distribution across the landscape. On a predominantly sandy substrate, key soil-forming factors included relief, climate, and organisms, with processes such as bissialitization, gleyzation, podzolization, paludization, and pedoturbation playing central roles.

Salinas soils, rich in clay and nutrients, are dominated by 2:1 minerals, supporting Solonetz, Gleysols, and Spodosols. The presence of interstratified minerals suggests acidification linked to system opening and freshwater influence. The surrounding vegetation is less diverse due to high sodium content. The *Baías* soils, characterized by prolonged water saturation from freshwater interconnections, promote organic carbon accumulation. In the *Campos* and *Vazantes*, Arenosols dominate with acidic and dystrophic properties, respectively, while Podzols and ferrolysis occur in the lower *Vazantes* areas. Vegetation in *Baías*, *Campos*, and *Vazantes* is dominated by herbaceous species with low diversity, reflecting the impact of the seasonal flooding influence.

The *Cordilheiras* and *Murundus* Arenosols are marked by the influence of the organisms, with accumulation of soil organic matter and nutrients influenced by litter decomposition and termite activity. Our findings provide rare evidence of pedoturbation in Nhecolândia soils, highlighting the need for more detailed studies about the origins of these environments. These areas exhibit the richest and most diverse vegetation, dominated by arboreal species due to the absence of flooding.

The current Nhecolândia landscape is a complex evolving sandy wetland, formed under drier early-Mid Holocene conditions, driven by combined aeolian and fluvial processes, that became established at the beginning of the Late Holocene. During this period, the *Salinas* transitioned from a cerrado (savanna) to a grassy environment, while the higher *Vazantes* with mixed C3-C4 grass cover changed to a C4-dominated grassland. In contrast, lower areas, such as the *Baías* and lower *Vazantes*, remained dominated by hydrophilic and aquatic macrophytes due to a more persistent flooding regime. Non-floodable arboreal environments, such as *Cordilheiras* and *Murundus*, showed a δ13C signal enrichment with depth, suggesting a past mixed C3-C4 vegetation.

The frequency inundation monitoring, from 2018 and 2021, indicated a concentration of permanently inundated areas in the western portion of the Upper Paraguay River Basin, close to the Paraguay river, and in the south, close to the Nhecolândia's lakes. A decrease trend in the water extent was observed in the wet season, which was consistent with previous works in the Pantanal. A diminishing of the water availability in the Nhecolândia landscape would directly affect the soil nutrient distribution and, consequently, the vegetation communities, with an expanding of tree species in the non-floodable environments. The lakes would have their water level reduced, changing their soil physico-chemical characteristics, and, consequently, affecting the fauna surviving, and the sustainability of the Pantanal's cattle husbandry. This scenario reinforces the need to better understand the ecological dynamics of Pantanal aiming to support public politics in prone of a more sustainable development, and to mitigate the future climate change impacts.

APPENDIX A – Morphological description of the soils of Nhecolândia Pantanal, Brazil

PROFILE 1

GENERAL DESCRIPTION

Date – 08/20/2016
World Reference Base Classification – Reductigleyic Eutric Gleysol (Clayic, Alcalic, Sideralic, Humic, Protosodic, Uterquic)
Brazilian Soil Classification System (SiBCS) – GLEISSOLO HÁPLICO Sódico típico hipocarbonático êutrico
Location, municipality, state, and coordinates – 21 K 0541267 W 7883118 S
Landscape position, slope, and vegetation cover over the profile – Located at the margin of a saline lake
Altitude – 110 m
Lithology – Alluvial sediments
Geological formation – Pantanal Formation
Chronology – Quaternary period
Parent material – Weathering product of the aforementioned material
Stoniness – Non-stony
Rockiness – Non-rocky
Local relief – Flat
Regional relief – Flat
Erosion – Not apparent
Drainage – Poorly drained
Primary vegetation – Grasses
Current land use – Native pasture
Water table depth – 110 cm
Climate – AW (Köppen-Geiger classification)
Described and sampled by – Guilherme R. Corrêa and Roberta F. P. de Queiroz

MORPHOLOGICAL DESCRIPTION

An 0–11 cm; dark olive gray (5Y 3/2, moist); clayey; medium to large subangular blocky structure; hard, friable, plastic and sticky; clear and smooth transition.

ABgn 11–23 cm; dark gray (5Y 4/1, moist); clayey; moderate small to medium prismatic structure; very hard, friable, plastic and sticky; gradual and smooth transition.

Bgn1 23–57 cm; olive gray (5Y 4/2, moist); clayey; strong small to medium prismatic structure; very hard, friable, plastic and sticky; clear and smooth transition.

Bgn2 57–88 cm; black (5Y 2.5/2, moist); very clayey; strong small to medium prismatic structure; very hard, friable, plastic and sticky; abrupt and smooth transition.

Cn 88–110+ cm; reddish brown (2.5YR 5/4, moist); sandy; loose, loose consistency, non-plastic and non-sticky.

Roots – Many fine and very fine roots in the A and AB horizons; common very fine to fine roots in Bgn1 and Bgn2.

Observations – Seasonally flooded area. No grassland present, only lagoon and slightly elevated levee. Presence of Carandá palms along the edges. Horizon C is sandy, flooded, and structureless. Flat relief with slight depression. Mottles are few, small, and diffuse in Bgn1 and Bgn2.

PROFILE 2

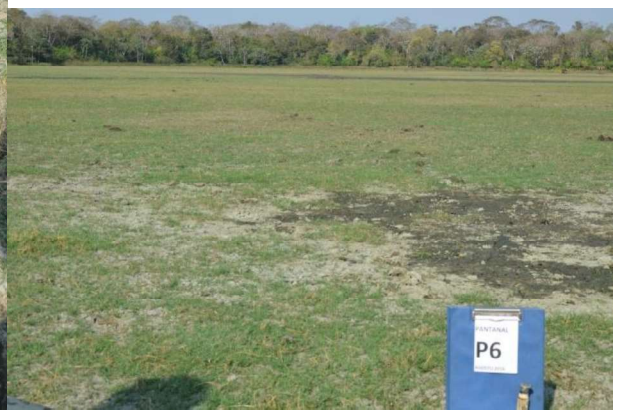

GENERAL DESCRIPTION

Date – 08/20/2016
World Reference Base Classification – Reductigleyic Eutric Gleysol (Arenic, Alcalic, Ochric, Sodic, Uterquic)
Brazilian Soil Classification System (SiBCS) – GLEISSOLO HÁPLICO Sódico típico hipocarbonático
Location, municipality, state, and coordinates – UTM 21 K 0541321 W 7883080 S
Landscape position, slope, and vegetation cover – Located inside a saline lagoon
Altitude – 106 m
Lithology – Alluvial sediments
Geological formation – Pantanal Formation
Chronology – Quaternary period
Parent material – Weathering product of the aforementioned material
Stoniness – Non-stony
Rockiness – Non-rocky
Local relief – Flat
Regional relief – Flat
Erosion – Not apparent
Drainage – Poorly drained
Primary vegetation – Grasses
Current land use – Native pasture
Climate – Aw, Köppen classification
Described and sampled by – Guilherme Resende Corrêa

MORPHOLOGICAL DESCRIPITION

An1 0–9 cm; dark olive gray (5Y 3/2, moist); sandy clay; moderate small to medium subangular blocky structure; slightly hard, friable, slightly plastic and slightly sticky; gradual and smooth transition.

An2 9–16 cm; olive (2.5Y 5/4, moist); sandy clay loam; weak small to medium subangular blocky structure; hard, friable, slightly plastic and slightly sticky; wavy and clear transition.

Bsgn 16–29 cm; olive gray (2.5Y 5/2, moist); sand; single grains; very hard, very firm, non-plastic and non-sticky; gradual and smooth transition.

Cg 29–70+ cm; weak red (2.5YR 4/2, moist); sand; single grains; very hard, very firm, non-plastic and non-sticky.

Roots – Many fine to very fine roots in An1 and An2; common very fine to fine roots in Bsgn and Cg.

Observations – Bichromic features in An1, An2, and Bsgn. Possible nodules in An2 and Bsgn.

PROFILE 3

GENERAL DESCRIPTION

Date – 08/20/2016
World Reference Base Classification – Dystric Sideralic Brunic Arenosol (Ochric, Claric)
Brazilian Soil Classification System (SiBCS) – NEOSSOLO QUARTZARÊNICO Órtico típico – RQo
Location, municipality, state, and coordinates – UTM 21 K 0541104 W 7883235 S
Landscape position, slope, and vegetation cover – Located on a levee near a saline lagoon
Altitude – 119 m
Lithology – Alluvial sediments
Geological formation – Pantanal Formation
Chronology – Quaternary period
Parent material – Weathering product of the aforementioned material
Stoniness – Non-stony
Rockiness – Non-rocky
Local relief – Flat
Regional relief – Flat
Erosion – Not apparent
Drainage – Excessively drained
Primary vegetation – Arboreal savannah with *Tingui*, *Acuri*, *Gravatá*, *Pau-Terra*, *Pequi*, *Bacuri*, and *Aroeira*
Current land use – Natural
Climate – Aw, Köppen classification
Described and sampled by – Guilherme Resende Corrêa

MORPHOLOGICAL DESCRIPTION

A1 0–19 cm; dark brown (10YR 3/3 moist); sand; single grain; loose, friable, non-plastic and non-sticky; clear, smooth transition.

A2 19–30 cm; brown (10YR 4/3 moist); sand; single grain; loose, friable, non-plastic and non-sticky; clear, smooth transition.

C1 30–73 cm; yellowish brown (10YR 5/6 moist); sand; single grain; loose, very friable, non-plastic and non-sticky; clear, smooth transition.

C2 73–94+ cm; brown (10YR 5/3 moist); sand; single grain; loose, very friable, non-plastic and non-sticky.

Roots – Many fine to very fine roots in A1; many very fine to very coarse roots in A2 and C1; and few fine roots in C2.

PROFILE 4

GENERAL DESCRIPTION

Date – 08/21/2016
World Reference Base Classification – Eutric Albic Gleyic Histic Planosol (Arenic, Alcalic, Sideralic, Humic, Sodic)
Brazilian Soil Classification System (SiBCS) – PLANOSSOLO HÁPLICO Eutrófico gleissólico solódico
Location, municipality, state, and coordinates – UTM 21 K 0522731 W 7875813 S
Landscape position, slope, and vegetation cover – Located in a bay
Altitude – 91 m
Lithology – Alluvial sediments
Geological formation – Pantanal Formation
Chronology – Quaternary period
Parent material – Weathering product of the aforementioned material
Stoniness – Non-stony
Rockiness – Non-rocky
Local relief – Flat
Regional relief – Flat
Erosion – Not apparent
Drainage – Very poorly drained
Primary vegetation – Grassland
Current land use – Natural
Climate – Aw, Köppen classification
Described and sampled by – Guilherme Resende Corrêa

MORPHOLOGICAL DESCRIPTION

An 0–10 cm; very dark gray (5Y 3/1 moist); sandy loam; single grain; soft, very friable, non-plastic and non-sticky; clear, smooth transition.

AEn 10–17 cm; dark gray (5Y 4/1 moist); loamy sand; single grain; soft, very friable, non-plastic and non-sticky; clear, smooth transition.

E 17–44 cm; olive (5Y 5/3 moist); sand; single grain; loose, very friable, non-plastic and non-sticky; clear, smooth transition.

Egn1 44–75 cm; very dark gray (5Y 3/1 moist); sand; single grain; soft, very friable, non-plastic and non-sticky; clear, smooth transition between horizons.

Egn2 75–108 cm; olive (5Y 5/3 moist); sand; single grain; soft, very friable, non-plastic and non-sticky; abrupt, smooth transition between horizons.

Bt 108–130+ cm; olive gray (5Y 4/2 moist); clay-loam-sandy; medium to large subangular blocks; hard, very friable, non-plastic and non-sticky.

Roots – Many fine to very fine roots in A and AE; common very fine to fine roots in E; few very fine to fine roots in Eg1 and Eg2.

Observations – Mottling near the roots due to oxidation.

PROFILE 5

GENERAL DESCRIPTION

Date – 08/21/2016
World Reference Base Classification – Eutric Sideralic Brunic Arenosol (Ochric, Claric)
Brazilian Soil Classification System (SiBCS) – NEOSSOLO QUARTZARÊNICO Órtico gleissólico - RQo
Location, municipality, state, and coordinates – UTM 21 K 0522853 W 7875719 S
Landscape position, slope, and vegetation cover – Located on a ridge near a bay
Altitude – 104 m
Lithology – Alluvial sediments
Geological formation – Pantanal Formation
Chronology – Quaternary period
Parent material – Weathering product of the aforementioned material
Stoniness – Non-stony
Rockiness – Non-rocky
Local relief – Flat
Regional relief – Flat
Erosion – Not apparent
Drainage – Excessively drained
Primary vegetation – Arboreal savannah with *Bacuri*, *Lixeira*, *Ipê*, *Cactus*, and *Bocaiúva*
Current land use – Natural
Climate – Aw, Köppen classification
Described and sampled by – Guilherme Resende Corrêa

MORPHOLOGICAL DESCRIPTION

A 0-23 cm dark yellowish brown (10YR 4/4 moist); sandy; simple grains; loose, very friable, non-plastic and non-sticky; diffuse and flat transition.

C 23-64 cm brown (10YR 5/3 moist); sandy; simple grains; loose, very friable, non-plastic and non-sticky; diffuse and flat transition.

Cg 64-120+ cm very pale brown (10YR 7/4 moist); sandy; simple grains; soft, friable, non-plastic and non-sticky; clear and flat transition.

Roots – Many very fine to very coarse in A and C; and many very fine to coarse in Cs.

Observations – Dominance of Bacuri. Common, distinct, medium to large mottles in Cs.

PROFILE 6

GENERAL DESCRIPTION

Date: 08/21/2016
World Reference Base Classification – Dystric Brunic Arenosol (Ochric, Protoargic)
Brazilian Soil Classification System (SiBCS) – NEOSSOLO QUARTZARÊNICO Hidromórfico típico
Location, municipality, state, and coordinates: UTM 21K 0627919 O 7902296 S
Situation, slope, and vegetation cover: Located in a bay, flat, with grassland vegetation.
Altitude: 129 m
Lithology – Alluvial sediments
Geological Formation – Pantanal Formation
Chronology – Quaternary period
Originating material – Alteration product of the aforementioned material
Stoniness – Not stony
Rockiness – Not rocky
Local relief – Flat
Regional relief – Flat
Erosion – Not apparent
Drainage – Poorly drained
Primary vegetation – Grassland
Current land use – Natural
Climate: Aw, Köppen classification.
Described and collected by: Guilherme Resende Corrêa

MORPHOLOGICAL DESCRIPTION

A 0-20 cm very dark grayish brown (10YR 3/2 moist); loamy sand; simple grains; soft, very friable, non-plastic, and non-sticky; gradual and flat transition.

A2 20-31 cm dark grayish brown (10YR 4/2 moist); sand; simple grains; soft, very friable, non-plastic, and non-sticky; gradual and flat transition.

AC 31-38 cm dark yellowish brown (10YR 4/4 moist); sand; simple grains; loose, very friable, non-plastic, and non-sticky; clear and flat transition.

Cg1 38-63 cm brown (10YR 5/3 moist); loamy sand; simple grains; loose, very friable, non-plastic, and non-sticky; clear and flat transition.

Cg2 63-110 cm brown (10YR 5/3 moist); sand; simple grains; loose, friable, non-plastic, and non-sticky.

Roots – Many fine to very fine in the A1 and A2 horizons; rare very fine to fine in AC, C1, and C2.

Observations – Common, medium, and distinct mottling in Cg1 and Cg2.

PROFILE 7

GENERAL DESCRIPTION

Data: 15/12/2016
World Reference Base Classification – Eutric Sideralic Brunic Arenosol (Ochric, Rubic)
Brazilian Soil Classification System (SiBCS) – NEOSSOLO QUARTZARÊNICO Órtico típico - RQo
Location, municipality, state, and coordinates: UTM 21K 0627965 O 7902277 S
Situation, slope, and vegetation cover: Located in a mountain range.
Altitude: 137 m
Lithology – Alluvial sediments
Geological Formation – Pantanal Formation
Chronology – Quaternary Period
Originating material – Altered material from the above-mentioned formation
Stoniness – Not stony
Rockiness – Not rocky
Local relief – Flat
Regional relief – Flat
Erosion – Not apparent
Drainage – Poorly drained
Primary vegetation – Arboreal savannah (*Cerradão*)
Current use – Natural
Climate: Aw, according to Köppen's classification
Described and collected by: Guilherme Resende Corrêa

MORPHOLOGICAL DESCRIPTION

A 0-27 cm brown (10YR 4/3 moist); sand; simple grains; loose, very friable, non-plastic, and non-sticky; diffuse and flat transition.

CA 27-44 cm brown (10YR 4/3 moist); sand; loose, very friable, non-plastic, and non-sticky; diffuse and flat transition.

C1 44-67 cm dark yellowish brown (10YR 4/4 moist); sand; simple grains; loose, very friable, non-plastic, and non-sticky; diffuse and flat transition.

C2 67-91 cm yellowish brown (10YR 5/8 moist); sand; simple grains; loose, very friable, non-plastic, and non-sticky; diffuse and flat transition.

C3 91-115+ cm light yellowish brown (10YR 6/4 moist); sand; simple grains; loose, very friable, non-plastic, and non-sticky.

Roots – Many very fine to very coarse in A, CA, C1, C2; and few very fine to medium in C3.

Observations – Presence of charcoal in the A and CA horizons. Predominance of Jatobás in the surrounding area. Small and medium distinct mottling in C1.

PROFILE 8

GENERAL DESCRIPTION

Date – 06/12/2016
World Reference Base Classification – Dystric Sideralic Brunic Arenosol (Ochric, Isopteric Claric)
Brazilian Soil Classification System (SiBCS) – NEOSSOLO QUARTZARÊNICO Órtico típico
Location, Municipality, State, and Coordinates – UTM 21K 0628006 O 7901826 S
Situation, Slope, and Vegetation – Located in Murundus
Altitude – 134 m
Lithology – Alluvial sediments
Geological Formation – Pantanal Formation
Chronology – Quaternary Period
Originating Material – Product of alteration of the aforementioned material
Stoniness – Non-stony
Rockiness – Non-rocky
Local Relief – Flat
Regional Relief – Flat
Erosion – Not apparent
Drainage – Excessively drained
Primary Vegetation – Arboreal savannah (*Cerradão*)
Current Land Use – Natural
Climate – Aw, in the Köppen classification
Described and collected by – Guilherme Resende Corrêa

DESCRIÇÃO MORFOLÓGICA

A 0–5 cm very dark grayish brown (10YR 3/2 moist); sand; single grains; soft, very friable, non-plastic, and non-sticky; clear and smooth transition.

CA 5–16 cm dark grayish brown (10YR 4/2 moist); sand; loose, very friable, non-plastic, and non-sticky; diffuse and smooth transition.

C1 16–67 cm dark grayish brown (10YR 4/2 moist); loamy sand; loose and very friable; diffuse and smooth transition.

C2 67–110+ cm grayish brown (10YR 5/2 moist); loamy sand; loose and loose; diffuse and smooth transition.

Roots – Many very fine to very coarse roots in A, CA, C1, and C2.

Observations – Presence of fauna such as termites, earthworms, spiders, and scorpions, and flora including *Jatobá, Faveiro, Sucupira Preta,* and *Lixeira.*

PROFILE 9

GENERAL DESCRIPTION

Date: 06/12/2016
World Reference Base Classification: Eutric Sideralic Brunic Arenosol (Ochric)
Brazilian Soil Classification System (SiBCS) – NEOSSOLO QUARTZARÊNICO Órtico típico
Location, municipality, state, and coordinates: UTM 21K 0628028 E 7901800 S
Topography, slope, and vegetation cover: Located in a field between Murundus
Altitude: 139 m
Lithology: Alluvial sediments
Geological formation: Pantanal Formation
Chronology: Quaternary Period
Parent material: Product of the alteration of the above-mentioned material
Stoniness: Not stony
Rockiness: Not rocky
Local relief: Flat
Regional relief: Flat
Erosion: Not apparent
Drainage: Excessively drained
Primary vegetation: Grassland
Current land use: Natural
Climate: Aw, Köppen classification
Described and collected by: Guilherme Resende Corrêa

MORPHOLOGICAL DESCRIPTION

C 0–3 cm; sand; single grains; loose, loose, non-plastic and non-sticky; abrupt and smooth transition.
2A 3–7 cm very dark grayish brown (10YR 3/2); sand; single grains; soft, friable, non-plastic and non-sticky; clear and smooth transition.

2CA 7–16 cm dark grayish brown (10YR 4/2 moist); sand; single grains; loose, friable, non-plastic and non-sticky; diffuse and smooth transition.
2C1 16–63 cm brown (10YR 4/3 moist); sand; loose, very friable, non-plastic and non-sticky; diffuse and smooth transition.
2C2 63–97 cm yellowish brown (10YR 5/4 moist); sand; single grains; loose, very friable, non-plastic and non-sticky.

Roots – Many very fine and fine roots in horizons C, 2A, 2C1, and 2C2.

Observations – Presence of termites and ants. Presence of "lixeiras" (termite mounds or waste piles). Small to medium, distinct mottles in horizon 2CA.

PROFILE 10

GENERAL DESCRIPTION

Date: 16/12/2016
World Reference Base Classification – Dystric Brunic Arenosol (Humic, Isopteric, Claric)
Brazilian Soil Classification System (SiBCS) – NEOSSOLO QUARTZARÊNICO Órtico típico
Location (municipality, state, and coordinates) – UTM 21K 0632735 E 7899156 S
Topographic position, slope, and vegetation cover – Located on a murundu
Altitude – 123 m
Lithology – Alluvial sediments
Geological formation – Pantanal Formation
Chronology – Quaternary period
Parent material – Weathering product of the aforementioned material
Stoniness – Non-stony
Rockiness – Non-rocky
Local relief – Flat
Regional relief – Flat
Erosion – Not apparent
Drainage – Excessively drained
Primary vegetation – Arboreal savannah (*Cerradão*) on termite mounds (Murundus), with woody-arboreal vegetation
Current land use – Natural
Climate – Aw, according to Köppen classification
Described and collected by – Guilherme Resende Corrêa

MORPHOLOGICAL DESCRIPTION

A 0–5 cm very dark grayish brown (10YR 3/2, moist); loamy sand; loose, loose, non-plastic and non-sticky; clear and smooth transition.

C1 5–47 cm dark grayish brown (10YR 4/2, moist); loamy sand; loose, very friable, non-plastic and non-sticky; clear and smooth transition.

C2 47–95 cm dark yellowish brown (10YR 3/4, moist); loamy sand; loose, very friable, non-plastic and non-sticky.

Roots – Many very fine to coarse roots in A and C1; and common very fine to very coarse in C2.

Observations – Presence of termites and ants. Understory dominated by Gravatás (bromeliads).

PROFILE 11

GENERAL DESCRIPTION

Date – 16/12/2016
World Reference Base Classification – Dystric Sideralic Brunic Arenosol (Ochric, Claric)
Brazilian Soil Classification System (SiBCS) – NEOSSOLO QUARTZARÊNICO Órtico típico
Location, municipality, state, and coordinates – UTM 21K 0632753 E 7899169 S
Topographic position, slope, and vegetation cover – Located in grassland between termite mounds (Murundus)
Altitude – 136 m
Lithology – Alluvial sediments
Geological formation – Pantanal Formation
Chronology – Quaternary period
Parent material – Weathered product of the aforementioned material
Surface stoniness – Non-stony
Rock outcrops – Non-rocky
Local relief – Flat
Regional relief – Flat
Erosion – Slight
Drainage – Excessively drained
Primary vegetation – Grassland
Current land use – Natural
Climate – Aw, in the Köppen classification
Described and sampled by – Guilherme Resende Corrêa

MORPHOLOGICAL DESCRIPTION

A1 0–2 cm grayish brown (10YR 5/2 moist); sand; single grains; loose, very friable, non-plastic and non-sticky; clear and smooth transition.

A2 2–35 cm brown (10YR 5/3 moist); sand; single grains; loose, very friable, non-plastic and non-sticky; diffuse and smooth transition.

C1 35–72 cm pale brown (10YR 6/3 moist); sand; single grains; loose, friable, non-plastic and non-sticky; diffuse and smooth transition.

C2 72–90+ cm very pale brown (10YR 7/3 moist); sand; single grains; loose, friable, non-plastic and non-sticky.

Roots – Many very fine and fine roots in A1; common very fine and fine in A2; and few very fine and fine in C1 and C2.

Observation – Presence of ants. From 0 to 1 cm, there is a concentration of coarse sand due to splashing.

PROFILE 12

GENERAL DESCRIPTION

Date – 12/16/2016
World Reference Base Classification – Dystric Sideralic Brunic Arenosol (Ochric)
Brazilian Soil Classification System (SiBCS) – NEOSSOLO QUARTZARÊNICO Órtico típico
Location, municipality, state, and coordinates – UTM 21K 0632791 E 7899002 S
Site position, slope, and vegetation cover – Located on a cordilheira with cerradão/forest
Altitude – 146 m
Lithology – Alluvial sediments
Geological formation – Pantanal Formation
Chronology – Quaternary period
Parent material – Product of the weathering of the aforementioned material
Stoniness – Non-stony
Rockiness – Non-rocky
Local relief – Flat
Regional relief – Flat
Erosion – Slight
Drainage – Excessively drained
Primary vegetation – Arboreal savannah (*Cerradão*)
Current land use – Natural
Climate – Aw, according to Köppen classification
Described and collected by – Guilherme Resende Corrêa

MORPHOLOGICAL DESCRIPTION

A1 0–14 cm brown (10YR 4/3 moist); sand; single grains; loose and very friable; diffuse and smooth transition.
A2 14–38 cm dark grayish brown (10YR 4/2 moist); sand; single grains; loose and friable; diffuse and smooth transition.

C1 38–66 cm brown (10YR 5/3 moist); sand; single grains; loose and very friable; diffuse and smooth transition.
C2 66–93+ cm brown (10YR 5/3 moist); sand; single grains; loose and very friable.

Roots – Many, ranging from very fine to coarse, in A1, A2, C1, and C2 horizons.

Observation – Presence of *Bacurizal, Angico, Tingui, Jatobá,* and *Baru*. Trees reach up to 20 meters in height.

PROFILE 13

GENERAL DESCRIPTION

Data: 12/16/2016
World Reference Base Classification – Dystric Sideralic Gleyic Arenosol (Ochric)
SBCS Classification – NEOSSOLO QUARTZARÊNICO Hidromórfico plintossólico - RQg
Location, Municipality, State, and Coordinates: UTM 21K 0632860 O 7898894 S
Situation, Slope, and Vegetation Cover: Located in a floodplain area
Altitude: 138 m
Lithology – Alluvial sediments
Geological Formation – Pantanal Formation
Chronology – Quaternary Period
Originating Material – Product of alteration of the aforementioned material
Pebbliness – Not pebbly
Rockiness – Not rocky
Local Relief – Flat
Regional Relief – Flat
Erosion – Light
Drainage – Poorly drained
Primary Vegetation – Grassland
Current Use – Natural
Climate: Aw, according to Köppen classification
Described and collected by: Guilherme Resende Corrêa

MORPHOLOGICAL DESCRIPTION

A 0–15 cm very dark gray (10YR 3/1, moist); sandy loam; soft, friable, non-plastic and non-sticky; clear and smooth transition.
CA 15–26 cm very dark grayish brown (10YR 3/2, moist); sand; single grains; soft, friable, non-plastic and non-sticky; clear and smooth horizon transition.
Cg 26–37 cm light yellowish brown (10YR 6/4, moist); sand; single grains; soft, friable, non-plastic and non-sticky; clear and smooth transition.

Cgf 37–50+ cm light yellowish brown (10YR 6/4, moist); sand; single grains; soft, friable, non-plastic and non-sticky.

Roots – Many very fine to fine roots in A, CA, Cg, and Cgf.

Observations – Presence of biological channels mainly in the first two horizons. Common, medium-sized, and diffuse mottles in A, CA, Cg, and Cgf.

PROFILE 14

GENERAL DESCRIPTION

Date – 12/18/2016
World Reference Base Classification – Eutric Sideralic Brunic Arenosol (Ochric)
Brazilian Soil Classification System (SiBCS) – NEOSSOLO QUARTZARÊNICO Órtico típico - RQo
Location, municipality, state, and coordinates – UTM 21K 0568794 E 7856308 S
Position, slope, and vegetation cover – Located on a sandy hill (*Cordilheira*)
Altitude – 175 m
Lithology – Alluvial sediments
Geological formation – Pantanal Formation
Chronology – Quaternary period
Parent material – Product of weathering of the aforementioned material
Stoniness – Non-stony
Rockiness – Non-rocky
Local relief – Flat
Regional relief – Flat
Erosion – Slight
Drainage – Excessively drained
Primary vegetation – Transition between *Cerradão* and seasonal forest with abundant *Bacuri*
Current land use – Natural
Climate – Aw, according to the Köppen classification
Described and collected by – Guilherme Resende Corrêa

MORPHOLOGICAL DESCRIPTION

A1 0–9 cm very dark grayish brown (10YR 3/2, moist); single grains; loose, very friable, non-plastic and non-sticky; gradual and smooth transition.
A2 9–23 cm very dark brown (10YR 2/2, moist); single grains; loose, very friable, non-plastic and non-sticky; gradual and smooth transition.

CA 23–59 cm dark brown (10YR 3/3, moist); single grains; loose, very friable, non-plastic and non-sticky; gradual and smooth transition.
C1 59–99 cm brown (10YR 4/3, moist); single grains; loose, very friable, non-plastic and non-sticky; diffuse and smooth horizon transition.
C2 99–130+ cm dark yellowish brown (10YR 3/4, moist); single grains; loose, very friable, non-plastic and non-sticky.

Roots – Many in A1, A2, and CA; common in C1 and C2.

Observations – *Cordilheira* associated with saline lake (Lagoa do Coração). Rings were collected for bulk density in all horizons.

PROFILE 15

DESCRIÇÃO GERAL

Date – 11/19/2017
World Reference Base Classification – Dystric Sideralic Arenosol (Ochric)
Brazilian Soil Classification System (SiBCS) – NEOSSOLO QUARTZARÊNICO Órtico típico
Location, municipality, state, and coordinates – UTM 21K 578572 E 7862927 S
Position, slope, and vegetation cover – Located on a *Cordilheira*
Altitude – 117 m
Lithology – Alluvial sediments
Geological formation – Pantanal Formation
Chronology – Quaternary period
Parent material – Product of weathering of the aforementioned material
Stoniness – Non-stony
Rockiness – Non-rocky
Local relief – Flat
Regional relief – Flat
Erosion – Not apparent
Drainage – Excessively drained
Primary vegetation – Semideciduous forest
Current land use – Natural
Climate – Aw, according to the Köppen classification
Described and collected by – Guilherme Resende Corrêa

MORPHOLOGICAL DESCRIPTION

A1 0–24 cm very dark grayish brown (10YR 3/2, moist); single grains; soft, friable, non-plastic and non-sticky; gradual and smooth transition.
A2 24–33 cm dark grayish brown (10YR 4/2, moist); single grains; soft, very friable, non-plastic and non-sticky; gradual and smooth transition.

CA 33–59 cm dark grayish brown (10YR 4/2, moist); single grains; soft, very friable, non-plastic and non-sticky; gradual and smooth transition.
C1 59–106 cm dark yellowish brown (10YR 4/4, moist); single grains; soft, very friable, non-plastic and non-sticky; diffuse and smooth transition.
C2 106–120+ cm dark yellowish brown (10YR 3/4, moist); single grains; soft, friable, non-plastic and non-sticky.

Roots – Many fine, medium, and coarse roots in A1, A2, and CA; and common fine and medium roots in C2.

Observations – Area with a large number of *Bacuri* trees. Color variegated in horizon C2. Volumetric rings were collected in all horizons. Environment associated with a saline lake (Lagoa da Ilha).

PROFILE 16

Date – 11/19/2017
World Reference Base Classification – Dystric Sideralic Brunic Arenosol (Ochric)
Brazilian Soil Classification System (SiBCS) – NEOSSOLO QUARTZARÊNICO Órtico típico
Location, municipality, state, and coordinates – UTM 21K 570473 E 7854651 S
Position, slope, and vegetation cover – Located on a *Cordilheira*
Altitude – 139 m
Lithology – Alluvial sediments
Geological formation – Pantanal Formation
Chronology – Quaternary period
Parent material – Product of weathering of the aforementioned material
Stoniness – Non-stony
Rockiness – Non-rocky
Local relief – Flat
Regional relief – Flat
Erosion – Not apparent
Drainage – Excessively drained
Primary vegetation – Cerradão
Current land use – Natural
Climate – Aw, according to the Köppen classification
Described and collected by – Guilherme Resende Corrêa

MORPHOLOGICAL DESCRIPTION

A 0–6 cm very dark grayish brown (10YR 3/2); single grains; loose, friable, non-plastic and non-sticky; clear and smooth transition.
CA 6–35 cm dark grayish brown (10YR 4/2, moist); single grains; loose, friable, non-plastic and non-sticky; diffuse transition.
C1 35–51 cm brown (10YR 4/3, moist); single grains; loose, friable, non-plastic and non-sticky; diffuse transition.

C2 51–97 cm dark yellowish brown (10YR 3/4, moist); single grains; loose, friable, non-plastic and non-sticky; diffuse transition.
C3 97–120 cm dark yellowish brown (10YR 4/4, moist); single grains; loose, friable, non-plastic and non-sticky.

Roots – Many coarse to very coarse roots in A, CA, C1, and C2; and abundant in C3.

Observations – Sub-canopy dominance with a predominance of *Gravatás* and *Bacuri*. *Cordilheira* near a saline lake (Lagoa do Gregório). Volumetric ring samples were collected in all horizons.

PROFILE 17

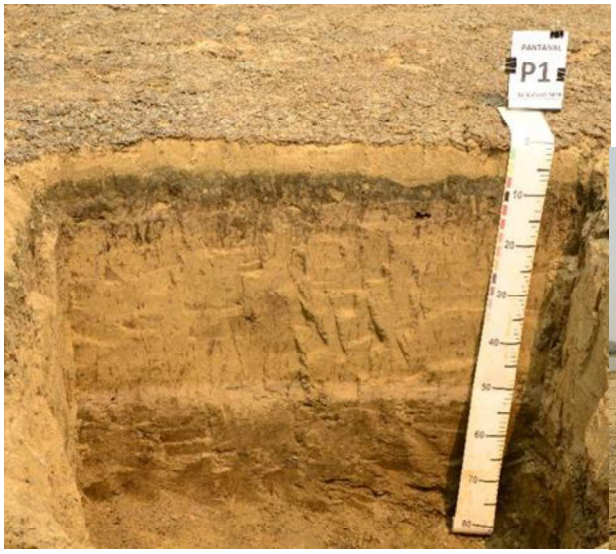

GENERAL DESCRIPTION

Date – 09/12/2019
World Reference Base Classification – Albic Solonetz (Arenic, Differentic, Endic, Hypernatric)
Brazilian Soil Classification System (SiBCS) – PLANOSSOLO NÁTRICO Órtico arênico
Location, municipality, state, and coordinates – UTM 21K 0570692 E 7855212 S
Position, slope, and vegetation cover – Located in a saline lake
Altitude – 110 m
Lithology – Alluvial sediments
Geological formation – Pantanal Formation
Chronology – Quaternary period
Parent material – Product of weathering of the aforementioned material
Stoniness – Non-stony
Rockiness – Non-rocky
Local relief – Flat
Regional relief – Flat
Erosion – Not apparent
Drainage – Imperfectly drained
Primary vegetation – Absent
Current land use – Natural
Climate – Aw, according to the Köppen classification
Described and collected by – Guilherme Resende Corrêa

MORPHOLOGICAL DESCRIPTION

An 0–6 cm light olive gray (5Y 6/2, moist); sand; weak, single grains, small and medium subangular blocks; loose, loose, non-plastic and non-sticky; clear and smooth transition.

2An 6–15 cm dark olive gray (5Y 3/2, moist); loamy sand; moderate, medium subangular blocks; slightly hard, firm, non-plastic and non-sticky; irregular and gradual transition.

E1 15–50 cm olive (5Y 5/4, moist); loamy sand; weak, medium to large angular blocks; very hard, firm, non-plastic and non-sticky; clear and smooth transition.

E2 54–90 cm pale yellow (5Y 7/3, moist); sandy loam; weak, small to medium angular blocks; hard, firm, non-plastic and non-sticky; clear and smooth transition.

Btn 90+ cm olive (5Y 5/3, moist); sandy clay loam; moderate, large and small angular blocks and prismatic structure; very hard, firm, slightly plastic and sticky.

Roots – Few, very fine roots in An and 2An.

Observations – Water table at 150 cm depth; presence of an Oo horizon (1–0 cm); weak cementation in E1 and E2.

PROFILE 18

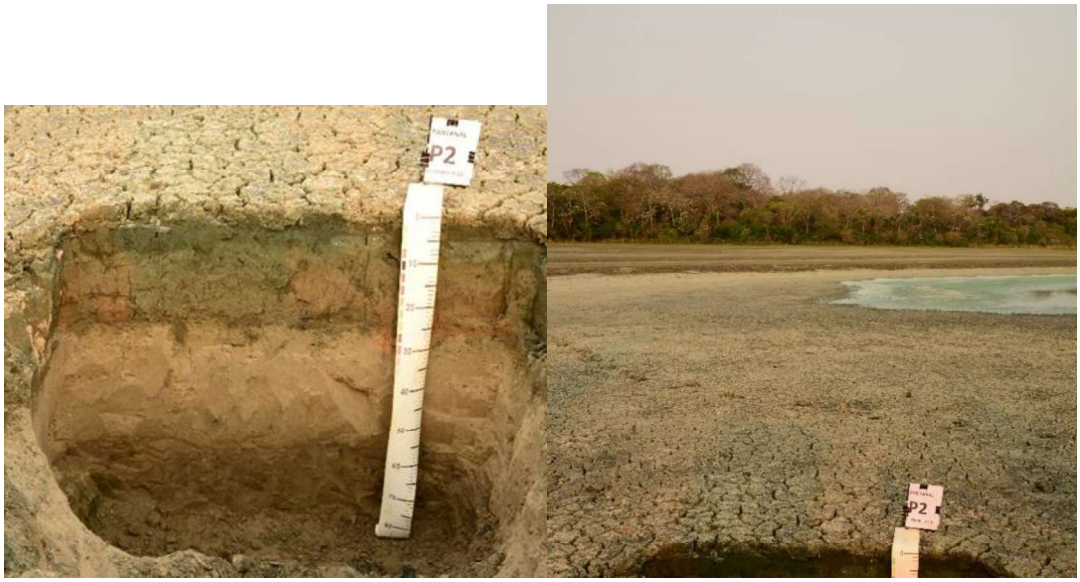

GENERAL DESCRIPTION

Date – 09/12/2019
World Reference Base Classification – Albic Nudinatric Protosalic Stagnic Gleyic Solonetz (Arenic, Differentic, Endic, Ochric, Hypernatric)
Brazilian Soil Classification System (SiBCS) – PLANOSSOLO NÁTRICO Sálico mésico hipocarbonático
Location, municipality, state, and coordinates – UTM 21K 0578491 E 7862531 S
Position, slope, and vegetation cover – Located in a saline lake
Altitude – 108 m
Lithology – Alluvial sediments
Geological formation – Pantanal Formation
Chronology – Quaternary period
Parent material – Product of weathering of the aforementioned material
Stoniness – Non-stony
Rockiness – Non-rocky
Local relief – Flat
Regional relief – Flat
Erosion – Not apparent
Drainage – Poorly drained
Water table depth – 100 cm
Primary vegetation – Absent
Current land use – Natural
Climate – Aw, according to the Köppen classification
Described and collected by – Guilherme Resende Corrêa

MORPHOLOGICAL DESCRIPTION

Agn1 0–16 cm very dark grayish green (5GY 3/2, moist); clay; strong to moderate and weak, very large to small and large angular blocks, prismatic and platy structure; very hard, firm, very plastic and very sticky; clear and smooth transition.

Agn2 16–27 cm dark grayish olive (10Y 4/2, moist); sandy clay loam; moderate, medium and large subangular blocks; hard; friable, slightly plastic and slightly sticky; abrupt and smooth transition.

E 27–60 cm light olive gray (5Y 6/2, moist); sand; single grains and massive when moist; medium and large subangular blocks; soft; very friable; non-plastic and non-sticky; clear and smooth transition.

Btn 60–90+ cm olive gray (5Y 5/2, moist); loamy sand; weak, medium and large subangular blocks; soft, very friable, non-plastic and non-sticky.

Btgn 90–106 cm very dark grayish olive (10Y 3/2, moist)

Btg 106–128 cm very dark greenish gray (5GY 3/1, moist)

Roots – Few and very fine in Agn1 and Agn2.

Observations – Bsc2 shows iron mottles; Bsc1 has degraded petroplinthite (ironstone); evidence of hydromorphism; mottles and nodules: Bsc1 – 50%, Bsc2 – 40%, Bsc2 – 30%.

PROFILE 19

GENERAL DESCRIPTION

Date – 09/13/2019
World Reference Base Classification – Stagnic Gleyic Entic Podzol (Arenic, Epic, Eutric, Sideralic)
Brazilian Soil Classification System (SiBCS) – ESPODOSSOLO FERRILÚVICO hidromórfico arênico
Location, municipality, state, and coordinates – UTM 21K 0569225 E 7855986 S
Position, slope, and vegetation cover – Located in a saline lake
Altitude – 89 m
Lithology – Alluvial sediments
Geological formation – Pantanal Formation
Chronology – Quaternary period
Parent material – Product of weathering of the aforementioned material
Stoniness – Non-stony
Rockiness – Non-rocky
Local relief – Flat
Regional relief – Flat
Erosion – Not apparent
Drainage – Poorly drained
Water table depth – 70 cm
Primary vegetation – Grassland
Current land use – Natural
Climate – Aw, according to the Köppen classification
Described and collected by – Guilherme Resende Corrêa

MORPHOLOGICAL DESCRIPTION

An1 0–5 cm dark olive gray (5Y 3/2, moist); sand; single grains when dry and massive when moist; soft, very friable, non-plastic, and non-sticky; clear and smooth transition.

An2 5–10 cm dark olive gray and olive (5Y 3/2 and 5Y 4/3, moist); sand; single grains when dry and massive when moist; soft, very friable, non-plastic, and non-sticky; abrupt and smooth transition.

Bsc1 10–28 cm dark reddish gray, pinkish gray, and very dark gray (5YR 4/2, 5Y 6/2, and 5Y 3/1, moist); sandy loam; single grains when dry and massive when moist; loose; very friable, non-plastic, and non-sticky; wavy and clear transition.

Bsc2 28–48 cm olive and reddish brown (5Y 5/3 and 5YR 4/3, moist); sand; single grains when dry and massive when moist; loose, very friable, non-plastic, and non-sticky; clear and smooth transition.

Bsc3 48–70+ cm olive gray and yellowish red (5Y 5/2 and 5YR 4/6, moist); sand; single grains when dry and massive when moist; loose, very friable, non-plastic, and non-sticky.

Roots – Abundant, very fine, and fine in An1 and An2; common, very fine, and fine in Bsc horizons.

Observations – 30% of the An2 horizon showed olive (5Y 4/3) mottles.

- 30% and 25% of the Bsc1 horizon showed mottles of light olive gray (5Y 6/2) and very dark gray (5Y 3/1), respectively.

- 40% of the Bsc2 horizon showed mottles of reddish brown (5YR 4/3) and degraded petroplinthite (ironstone).

- 30% of the Bsc3 horizon showed mottles of yellowish red (5YR 4/6).

PROFILE 20

GENERAL DESCRIPTION

Data: 09/13/2019
World Reference Base Classification – Eutric Sideralic Brunic Arenosol (Ochric, Protoargic, Claric, Protospodic)
Brazilian Soil Classification System (SiBCS) – PLANOSSOLO HÁPLICO Eutrófico solódico espessarênico
Location, municipality, state, and coordinates: UTM 21K 0572735 m O 7862261 m S
Situation, slope, and vegetation cover: Located at the top of a sand hill (*Cordilheira*)
Altitude: 114 m
Lithology – Alluvial sediments
Geological formation – Pantanal Formation
Chronology – Quaternary Period
Originating material – Product of alteration of the aforementioned material
Pebbliness – Non-pebbly
Rockiness – Non-rocky
Local relief – Flat
Regional relief – Flat
Erosion – Not apparent
Drainage – Well-drained
Primary vegetation – Semi-deciduous seasonal Forest with *Acuri* palm
Current use – Natural
Climate: Aw, in Köppen's classification
Described and collected by: Guilherme Resende Corrêa

MORPHOLOGICAL DESCRIPTION

A 0-36 cm; olive brown (2.5Y 4/3 moist); sand; simple grains when dry and massive when wet; soft, very friable, non-plastic, and non-sticky; clear and flat transition.

AE 36-53 cm; light yellowish brown (2.5 Y 6/3 moist); sand; simple grains when dry and massive when wet; soft, very friable, non-plastic, non-sticky; abrupt and flat transition.

E 53-96 cm; pale brown (2.5Y 7/3 moist); loamy sand; simple grains when dry and massive when wet; loose; very friable, non-plastic, and non-sticky; wavy and clear transition.

Bt 96-107 cm; dark grayish brown (2.5Y 4/2); loamy sand; simple grains when dry and massive when wet; hard, very friable, non-plastic, and non-sticky; clear and flat transition.

Btqnx (Bst2) 107-110 +; brown (7.5YR 4/2); sandy loam; simple grains when dry and massive when wet; extremely hard, very friable, non-plastic, and non-sticky.

Roots – Abundant with varied diameters in A, AE, and E horizons and rare, very fine roots in Bh and Bskm horizons

Observations – Bt and Btqnx horizons are poorly drained. In Bt, horizon densification occurs; Btqnx shows cementation by silica. Presence of the *Acuri* palm with medium density and height.

PROFILE 21

GENERAL DESCRIPTION

Data: 09/13/2019
World Reference Base Classification – Albic Podzol (Arenic, Epic, Eutric, Oxyaquic, Sideralic)
Brazilian Soil Classification System (SiBCS) – ESPODOSSOLO HUMILÚVICO Hidromórfico arênico
Location, municipality, state, and coordinates: UTM 21K 0572744 m O 7862293 m S
Situation, slope, and vegetation cover: Located at the edge of a bay
Altitude: 106 m
Lithology – Alluvial sediments
Geological formation – Pantanal Formation
Chronology – Quaternary Period
Originating material – Product of alteration of the aforementioned material
Pebbliness – Non-pebbly
Rockiness – Non-rocky
Local relief – Flat
Regional relief – Flat
Erosion – Not apparent
Drainage – Poorly drained
Primary vegetation – Grassland
Groundwater depth – 60 cm
Current use – Natural
Climate: Aw, in Köppen's classification
Described and collected by: Guilherme Resende Corrêa

MORPHOLOGICAL DESCRIPTION

A 0-5 cm; very dark grayish brown (2.5Y 3/2 moist); sand; simple grains when dry and massive when wet; soft, very friable, non-plastic, and non-sticky; clear and flat transition.

E 5-13 cm; dusky red (2.5YR 5/1 moist); sand; simple grains when dry and massive when wet; soft, very friable, non-plastic, non-sticky; clear and flat transition.

Bh 13-29 cm; reddish black (2.5YR 2.5/1 moist); sand; simple grains when dry and massive when wet; soft, very friable, non-plastic, and non-sticky; clear and flat transition.

C 29-60 cm; light yellowish brown (2.5Y 6/3 moist); loamy sand; simple grains when dry and massive when wet; loose, very friable, non-plastic, and non-sticky.

Roots – Few, very fine and fine in A and E horizons, rare, very fine and fine in Bh and C horizons.

Observations – Organic material cycling associated with macrofauna; abundant presence of decomposing aquatic macrophytes.

PROFILE 22

GENERAL DESCRIPTION

Data: 09/14/2019
World Reference Base Classification – Eutric Sideralic Arenosol (Ochric, Claric)
Brazilian Soil Classification System (SiBCS) – NEOSSOLO QUARTZARÊNICO Hidromórfico típico
Location, municipality, state, and coordinates: UTM 21K 0601692 m O 7857563 m S
Situation, slope, and vegetation cover: Located in a bay
Altitude: 113 m
Lithology – Alluvial sediments
Geological formation – Pantanal Formation
Chronology – Quaternary Period
Originating material – Product of alteration of the aforementioned material
Pebbliness – Non-pebbly
Rockiness – Non-rocky
Local relief – Flat
Regional relief – Flat
Erosion – Not apparent
Drainage – Poorly drained
Primary vegetation – Wetland hygrophilous vegetation
Current use – Natural
Climate: Aw, in Köppen's classification
Described and collected by: Guilherme Resende Corrêa

MORPHOLOGICAL DESCRIPTION

A 0-15 cm; black (2.5Y 2.5/1 moist); loamy sand; massive when dry and wet; soft, very friable, non-plastic, and non-sticky; flat and gradual transition.

AC 15-22 cm; dark gray (2.5YR 4/1 moist); sand; simple grains when dry and massive when wet; soft, very friable, non-plastic, non-sticky; flat and gradual transition.

Cg 22-50+ cm; weak red (2.5YR 5/2 moist); sand; simple grains when dry and massive when wet; loose, very friable, non-plastic, and non-sticky.

Roots – Common, very fine and fine in A and AC horizons, rare, very fine and fine in C horizon.

Observations – In the presence of moisture, all horizons exhibit a massive aspect; when dry, the A horizon maintains a massive appearance.

PROFILE 23

GENERAL DESCRIPTION

Data: 09/14/2019
World Reference Base Classification – Dystric Sideralic Brunic Arenosol (Ochric)
Brazilian Soil Classification System (SiBCS) – NEOSSOLO QUARTZARÊNICO Órtico típico
Location, municipality, state, and coordinates: UTM 21K 0601664 m O 7857459 m S
Situation, slope, and vegetation cover: Located at the top of a sand hill near a freshwater lake (*Baía*)
Altitude: 120 m
Lithology – Alluvial sediments
Geological formation – Pantanal Formation
Chronology – Quaternary Period
Originating material – Product of alteration of the aforementioned material
Pebbliness – Non-pebbly
Rockiness – Non-rocky
Local relief – Flat
Regional relief – Flat
Erosion – Not apparent
Drainage – Well-drained
Primary vegetation – Dense Cerrado without the presence of dry forest species
Current use – Natural
Climate: Aw, in Köppen's classification
Described and collected by: Guilherme Resende Corrêa

MORPHOLOGICAL DESCRIPTION

A 0-17 cm; light brownish gray (10YR 6/2 moist); sand; simple grains; loose, very friable, non-plastic, and non-sticky; flat and gradual transition.

CA 17-55 cm; light yellowish brown (10YR 6/4 moist); sand; simple grains when dry and massive when wet; loose, very friable, non-plastic, non-sticky; flat and gradual transition.

C1 55-103 cm; brownish yellow (10YR 6/6); sand; simple grains when dry and massive when wet; loose, very friable, non-plastic, and non-sticky; flat and gradual transition.

C2n 130+ cm; brownish yellow (10YR 6/6); sand; simple grains when dry and massive when wet; loose, very friable, non-plastic, and non-sticky.

Roots – Abundant, with varying diameters in A, CA, and C1 horizons, and rare, very fine and fine in C2.

Observations – When moist, all horizons show massive structure; No significant presence of the Acuri palm tree (Attalea phalerata); The area's vegetation appears to have undergone management practices involving fire use; Presence of species such as: *Cambará* (*Moquiniastrum polymorphum*), *Canjiqueira* (*Byrsonima cydoniifolia*), and *Pau-terra* (*Qualea parviflora*).

PROFILE 24

GENERAL DESCRIPTION

Data: 09/14/2019
World Reference Base Classification – Eutric Sideralic Gleyic Brunic Arenosol (Humic, Claric, Protospodic)
Brazilian Soil Classification System (SiBCS) – NEOSSOLO QUARTZARÊNICO Hidromórfico espodossólico
Location, municipality, state, and coordinates: UTM 21K 0571380 m O 7857418 m S
Situation, slope, and vegetation cover: Located at the edge of a lagoon/bay
Altitude: 110 m
Lithology – Alluvial sediments
Geological formation – Pantanal Formation
Chronology – Quaternary Period
Originating material – Product of alteration of the aforementioned material
Pebbliness – Non-pebbly
Rockiness – Non-rocky
Local relief – Flat
Regional relief – Flat
Erosion – Not apparent
Drainage – Imperfectly drained
Groundwater depth – 65 cm
Primary vegetation – Hygrophilous grasses
Current use – Natural
Climate: Aw, in Köppen's classification
Described and collected by: Guilherme Resende Corrêa

MORPHOLOGICAL DESCRIPTION

A 0-9 cm; very dark grayish brown (2.5Y 3/2 moist); loamy sand; simple grains; soft, very friable, non-plastic, and non-sticky; flat and gradual transition.

Bh 9-25 cm; very dark gray (2.5Y 3/1 moist); loamy sand; weak, small, subangular blocks; soft, very friable, non-plastic, and non-sticky; flat and undulating transition.

C 25-70+ cm; pale brown (2.5Y 7/3 moist); sand; simple grains; loose, very friable, non-plastic, and non-sticky.

Roots – Common and very fine and fine in A, few and very fine and fine in Bh, and rare and very fine and fine in C.

Observations – Evidence of podzolization (spodic horizon); The A horizon (0-9 cm) shows alterations due to macrofauna activity.

PROFILE 25

GENERAL DESCRIPTION

Data: 09/14/2019
World Reference Base Classification – Eutric Sideralic Gleyic Brunic Arenosol (Ochric)
Brazilian Soil Classification System (SiBCS) – NEOSSOLO QUARTZARÊNICO Órtico gleissólico
Location, municipality, state, and coordinates: UTM 21K 0571386 m O 7857479 m S
Situation, slope, and vegetation cover: Located at the top of a ridge
Altitude: 112 m
Lithology – Alluvial sediments
Geological formation – Pantanal Formation
Chronology – Quaternary Period
Originating material – Product of alteration of the aforementioned material
Pebbliness – Non-pebbly
Rockiness – Non-rocky
Local relief – Flat
Regional relief – Flat
Erosion – Not apparent
Drainage – Well-drained
Primary vegetation – Cerradão/Dry forest with abundant Acuri
Current use – Natural
Climate: Aw, in Köppen's classification
Described and collected by: Guilherme Resende Corrêa

MORPHOLOGICAL DESCRIPTION

A1 0-6 cm; dark grayish brown (2.5Y 4/2 moist); sand; simple grains; loose, very friable, non-plastic, and non-sticky; flat and clear transition.

A2 55-69 cm; very dark grayish brown (2.5Y 3/2 moist); sand; simple grains; loose, very friable, non-plastic, and non-sticky; flat and gradual transition.

CA 69-114 cm; light olive brown (2.5Y 5/3 moist); loamy sand; simple grains; loose, very friable, non-plastic, and non-sticky; flat and gradual transition.

Cg1 114-120 cm; light yellowish brown (2.5Y 6/4 moist); sand; simple grains; soft, very friable, non-plastic, and non-sticky; flat and gradual transition.

Cg2 120 cm +; pale brown (2.5Y 7/3 moist); sand; simple grains; soft, very friable, non-plastic, and non-sticky; large and hard mineral nodules and concretions, irregular and sparse.

Roots – Abundant and of varied diameter in A1, A2, CA, and C1; few and of varied diameter in Cg2.

Observations – Horizons C1 and Cg2 show mottling (10YR 6/6); A1 is under the influence of eluviation or recent deposition; abundant Acuri (Attalea phalerata) presence in height and density.

PROFILE 26

GENERAL DESCRIPTION

Data: 09/21/2021
World Reference Base Classification – Eutric Sideralic Brunic Gleyic Arenosol (Humic)
Brazilian Soil Classification System (SiBCS) – NEOSSOLO QUARTZARÊNICO Hidromórfico organossólico
Location, municipality, state, and coordinates – Pantanal of Nhecolândia, Aquidauana – MS, UTM 21K 572773 O 7862408 S
Situation, slope, and vegetation cover over the profile – Near a bay
Altitude – 105 m
Lithology – Alluvial sediments
Geological formation – Pantanal Formation
Chronology – Quaternary Period
Originating material – Product of alteration of the aforementioned material
Pebbliness – Non-pebbly
Rockiness – Non-rocky
Local relief – Flat
Regional relief – Flat
Erosion – Not apparent
Drainage – Very poorly drained
Primary vegetation – Macrophytes (Aguapé) and Poaceae
Current use – Natural
Depth of the water table – 100 cm
Climate – AW, according to Köppen-Geiger classification
Described and collected by – Guilherme R. Corrêa, Iorrana F. Sacramento, and Gabriel R. Palucci

MORPHOLOGICAL DESCRIPTION

H 0 – 21 cm; black (10YR 2/1 moist); clayey-sandy loam; massive; soft, very friable, non-plastic, and non-sticky; clear and undulating transition.

A 21 – 25 cm; very dark gray (10YR 3/1 moist); loamy sand; simple grains; loose, very friable, non-plastic, and non-sticky; clear and undulating transition.

C1 25-42 cm; brown (10YR 4/3 moist); sand; simple grains; loose, very friable, non-plastic, and non-sticky; clear and undulating transition.

C2 42-75 cm; brown (10YR 4/3 moist); sand; simple grains; loose, very friable, non-plastic, and non-sticky; clear and undulating transition.

Cg 75-105 cm; dark grayish brown (10YR 4/2 moist); sand; simple grains; loose, very friable, non-plastic, and non-sticky.

Roots – Common very fine to fine roots in horizon H, few very fine to fine roots in horizon A.

Observations – Mottling occurrence in horizon E or C1 (common, medium to large, and diffuse). Clay pellets (no clay migration). Polycyclic pedogenesis. No prominent spodic features like those of P21. Horizons E and B have more characteristics of C, although some features indicate the presence of pedogenetic processes (clay concentration and mottling). Samples of Btg (75 – 105+) horizon were collected for micromorphological analyses and a tube for ASL dating at 60 cm.

PROFILE 27

GENERAL DESCRIPTION

Data: 09/21/2021
World Reference Base Classification – Dystric Sideralic Brunic Arenosol (Ochric)
Brazilian Soil Classification System (SiBCS) – NEOSSOLO QUARTZARÊNICO Órtico gleissólico - RQo
Location, municipality, state, and coordinates – Pantanal of Nhecolândia, Aquidauana – MS, UTM 21K 570522 m O 7859182 m S
Situation, slope, and vegetation cover over the profile – Flat relief, field between Murundus
Altitude – 106 m
Lithology – Alluvial sediments
Geological formation – Pantanal Formation
Chronology – Quaternary Period
Originating material – Product of alteration of the aforementioned material
Pebbliness – Non-pebbly
Rockiness – Non-rocky
Local relief – Flat
Regional relief – Flat
Erosion – Not apparent
Drainage – Poorly drained
Primary vegetation – Grassland
Current use – Natural
Depth of the water table – Not identified
Climate – AW, according to Köppen-Geiger classification
Described and collected by – Guilherme R. Corrêa, Iorrana F. Sacramento, and Gabriel R. Palucci

MORPHOLOGICAL DESCRIPTION

A 0 – 9 cm; dark brown (7.5YR 3/2 moist); sand; simple grains; soft, very friable, non-plastic, and non-sticky; gradual and flat transition.

CA 9 – 21 cm; dark brown (7.5YR 3/2 moist); sand; simple grains; loose, very friable, non-plastic, and non-sticky; gradual and undulating transition.

C1g 21-66 cm; brown (7.5 YR 4/3 moist); sand; simple grains; loose, very friable, non-plastic, and non-sticky; diffuse and flat transition.

C2 66-105+ cm; brown (10YR 4/3 moist); sand; simple grains; loose, very friable, non-plastic, and non-sticky.

Roots – Abundant and fine in horizon A, common and fine in horizon CA, few and fine in horizon C1.

Observations – Mottling in CA (few, small, and diffuse), C1g (common, small, and diffuse), and C2 (few, small, and diffuse).

PROFILE 28

GENERAL DESCRIPTION

Data: 09/22/2021
World Reference Base Classification – Dystric Brunic Arenosol (Ochric, Isopteric)
Brazilian Soil Classification System (SiBCS) – NEOSSOLO QUARTZARÊNICO Órtico típico
Location, municipality, state, and coordinates – Pantanal of Nhecolândia, Aquidauana – MS, UTM 21K 570557 m O 7859177 m S
Situation, slope, and vegetation cover over the profile – Collected from Murundu, a small elevation with gentle undulating slope
Altitude – 106 m
Lithology – Alluvial sediments
Geological formation – Pantanal Formation
Chronology – Quaternary Period
Originating material – Product of alteration of the aforementioned material
Pebbliness – Non-pebbly
Rockiness – Non-rocky
Local relief – Gently undulating
Regional relief – Flat
Erosion – Not apparent
Drainage – Well-drained
Primary vegetation – Murundu
Current use – Natural
Depth of the water table – Not identified
Climate – AW, according to Köppen-Geiger classification
Described and collected by – Guilherme R. Corrêa, Iorrana F. Sacramento, and Gabriel R. Palucci

MORPHOLOGICAL DESCRIPTION

O 0 – 5 cm; sand; simple grains; loose, very friable, non-plastic, and non-sticky; gradual and flat transition.

A 5 – 18 cm; dark brown (7.5YR 3/2 moist); sand; simple grains; loose, very friable, non-plastic, and non-sticky; gradual and flat transition.

C1 18 – 62 cm; brown (7.5YR 4/3 moist); sand; simple grains; loose, very friable, non-plastic, and non-sticky; diffuse and flat transition.

C2 62 – 75+ cm; brown (7.5YR 4/2 moist); sand; simple grains; loose, very friable, non-plastic, and non-sticky.

Roots – Abundant and very fine to fine in O, and many fine to coarse roots in horizons A, C1, and C2.

Observations – High biological activity in the profile (ants and termites). Presence of termite mound fragments at 24 cm depth. Collection was made approximately 30 cm from the termite mound. Very little mottling in C2. Horizon O was not collected.

PROFILE 29

GENERAL DESCRIPTION

Data: 09/23/2021
World Reference Base Classification – Gleyic Histic Albic Ortsteinic Podzol (Arenic, Abruptic, Epic, Sideralic)
Brazilian Soil Classification System (SiBCS) – ESPODOSSOLO FERRILÚVICO Hidromórfico arênico dúrico
Location, municipality, state, and coordinates – Pantanal of Nhecolândia, Aquidauana – MS, UTM 21K 569717 m O 7857864 m S
Situation, slope, and vegetation cover over the profile – Collected in the lower portion of a floodplain
Altitude – 103 m
Lithology – Alluvial sediments
Geological formation – Pantanal Formation
Chronology – Quaternary Period
Originating material – Product of alteration of the aforementioned material
Pebbliness – Non-pebbly
Rockiness – Non-rocky
Local relief – Flat
Regional relief – Flat
Erosion – Not apparent
Drainage – Poorly drained
Primary vegetation – Grassland
Current use – Natural
Depth of the water table – 100 cm
Climate – AW, according to Köppen-Geiger classification
Described and collected by – Guilherme R. Corrêa, Iorrana F. Sacramento, and Gabriel R. Palucci

MORPHOLOGICAL DESCRIPTION

A 0 – 14 cm; black (5YR 2.5/1 moist); loamy; simple grains; loose, very friable, non-plastic, and non-sticky; abrupt and flat transition.

2A 14 – 23 cm; black (5YR 2.5/1 moist); loamy sand; simple grains; loose, very friable, non-plastic, and non-sticky; clear and flat transition.

2AE 23 – 29 cm; dark reddish brown (10YR 3/2 moist); sand; simple grains; loose, very friable, non-plastic, and non-sticky; gradual and flat transition.

2E 29 – 48 cm and 48 – 60 cm; reddish brown (7.5YR 5/4 moist); sand; simple grains; loose, very friable, non-plastic, and non-sticky; abrupt and irregular transition.

2Bsm1 45 – 53 cm and 53 – 63 cm; strong brown (7.5YR 4/4 moist); loamy sand; simple grains; massive, extremely hard, extremely firm, non-plastic, and non-sticky; abrupt and irregular transition.

2Bsm2 65 – 76 cm and 67 – 73 cm; strong brown (7.5YR 4/6 moist); loamy sand; simple grains; massive, very hard, very firm, non-plastic, and non-sticky; clear and undulating transition.

2Cg1 73/76 – 94 cm; strong brown (7.5YR 4/6 moist); sand; simple grains; loose, very friable, non-plastic, and non-sticky; clear and undulating transition.

2Cg2 94+ cm; dark grayish brown (10YR 4/2 moist); loamy sand; simple grains; loose, very friable, non-plastic, and non-sticky; clear and undulating transition.

Roots – Abundant in O, many in AO, common in AE, and few in E.

Observations – The A horizon appeared fibrillated. Mottles in the E horizon (common, medium, small, and prominent) and oxidation near the roots. This profile is affected by seasonal variations of the water table. The 2Bsm1 horizon is harder than 2Bsm2. Slightly obscured local relief. 2Bsm1 and 2Bsm2 are ancient Cg/Cf horizons. We collected micro samples at the E–Bsm1 transition and at the Cg1–Cg2 transition, and a tube for dating at 80–90 cm.

PROFILE 30

GENERAL DESCRIPTION

Date: 09/23/2021
World Reference Base Classification – Dystric Sideralic Arenosol (Ochric)
Brazilian Soil Classification System (SiBCS) – NEOSSOLO QUARTZARÊNICO Órtico típico
Location, municipality, state, and coordinates – Pantanal of Nhecolândia, Aquidauana – MS, UTM 21K 569548 m O 7857997 m S
Situation, slope, and vegetation cover over the profile – Collected in the higher portion of a floodplain
Altitude – 107 m
Lithology – Alluvial sediments
Geological formation – Pantanal Formation
Chronology – Quaternary Period
Originating material – Product of alteration of the aforementioned material
Pebbliness – Non-pebbly
Rockiness – Non-rocky
Local relief – Flat
Regional relief – Flat
Erosion – Not apparent
Drainage – Moderately drained
Primary vegetation – Grassland
Current use – Natural
Depth of the water table – Undetermined
Climate – AW, according to Köppen-Geiger classification
Described and collected by – Guilherme R. Corrêa, Iorrana F. Sacramento, and Gabriel R. Palucci

MORPHOLOGICAL DESCRIPTION

A 0 – 6 cm: very dark brown (7.5 YR 2.5/2 moist); sand; simple grains; loose, friable, non-plastic, and non-sticky; clear and flat transition.

AC 6 – 12 cm: dark brown (7.5 YR 3/2 moist); sand; simple grains; loose, friable, non-plastic, and non-sticky; gradual and flat transition.

C1 12 – 45 cm: dark brown (7.5 YR 3/2 moist); sand; simple grains; loose, friable, non-plastic, and non-sticky; gradual and flat transition.

C2 45 – 69 cm: brown (7.5 YR 4/3 moist); sand; simple grains; loose, very friable, non-plastic, and non-sticky; gradual and flat transition.

C3 69 – 90+ cm: brown (7.5 YR 5/4 moist); sand; simple grains; loose, very friable, non-plastic, and non-sticky; gradual and flat transition.

Roots – Many and very fine in A, few and fine to very fine in AC, few and fine to very fine in C1, and few and fine to very fine in C2.

Observations – A sample was collected for dating between 70–80 cm.

APPENDIX B – Physical attributes of the soils of Nhecolândia Pantanal, Brazil

Horizon	Depth	Munsell color		CS	FS	Silt	Clay	Texture	D_s
	cm	Moist		---------- % ----------					g/cm³
P1 - GLEISSOLO HÁPLICO Sódico hipocarbonático êutrico									
Reductigleyic Eutric Gleysol (Clayic, Alcalic, Sideralic, Humic, Protospodic, Uterquic)									
An	0-11	5Y 3/2	Dark olive gray	4.9	4.6	35.1	55.4	Clay	-
ABgn	11-23	5Y 4/1	Dark gray	7.1	11.4	32.6	48.9	Clay	-
Bgn1	23-57	5Y 4/2	Olive gray	7.6	7.7	31.1	53.6	Clay	-
Bgn2	57-88	5Y 2/2	Black	6.7	9.4	23.2	60.8	Clay	-
Cn	88-110	2,5 Y 5/4	Reddish brown	11.2	81.3	0.3	7.2	Sand	-
P2 - GLEISSOLO HÁPLICO Sódico Típico									
Reductigleyic Eutric Gleysol (Arenic, Alcalic, Ochric, Sodic, Uterquic)									
An1	0-9	5Y 3/2	Dark olive gray	13	29.8	17.2	40	Sand clay	-
An2	9-16	2,5 Y 5/4	Olive	24.7	45.5	2.8	27.1	Sandy clay loam	-
Bsgn	16-29	2,5Y 5/2	Olive gray	19.6	72.4	1.2	6.8	Sand	-
Cg	29-70	2,5 YR 4/2	Weak red	16.8	72.1	4.6	6.4	Sand	-
P3 - NEOSSOLO QUARTZARÊNICO Órtico típico									
Dystric Sideralic Brunic Arenosol (Ochric, Claric)									
A1	0-19	10YR 3/3	Dark brown	27.7	60.3	6.6	5.4	Sand	-
A2	19-30	10YR 4/3	Brown	26.6	66.6	1.6	5.2	Sand	-
C1	30-73	10YR 5/6	Yellowish brown	31.6	60.4	1.6	6.3	Sand	-
C2	73-94	10YR 5/3	Brown	27.7	65.9	0.5	5.9	Sand	-
P4 - PLANOSSOLO HÁPLICO Eutrófico gleissólico									
Eutric Albic Gleyic Histic Planosol (Arenic, Alcalic, Sideralic, Humic, Sodic)									
An	0-10	5Y 3/1	Very dark gray	8.4	49.9	24.8	16.9	Sandy loam	-
AEn	10-17	5Y 4/1	Dark gray	11.6	71.9	14.5	1.9	Loamy sand	-
E	17-44	5Y 5/3	Olive	16.5	76	6.8	0.7	Sand	-
Eg1	44-75	5Y 3/1	Very dark gray	10.2	75.9	5.6	8.3	Sand	-
Eg2	75-108	5Y 5/3	Olive	11.4	79.5	5.3	3.8	Sand	-
Bt	108-130	5Y 4/2	Olive gray	9.8	57.2	8.4	24.6	Sandy clay loam	-
P5 - NEOSSOLO QUARTZARÊNICO Órtico gleissólico									
Eutric Sideralic Brunic Arenosol (Ochric, Claric)									
A	0-23	10YR 4/4	Dark yellowish brown	13.1	78.2	4.6	4	Sand	-
C	23-64	10YR 5/3	Brown	11.9	78.8	6.4	3	Sand	-
Cg	64-120	10YR 7/4	Very pale brown	16.8	74.7	6.5	2	Sand	-

P6 - NEOSSOLO QUARTZARÊNICO Hidromórfico típico									
Dystric Brunic Arenosol (Ochric, Protoargic)									
A1	0-20	10YR 3/2	Very dark grayish brown	26.5	52.7	12.5	8.3	Loamy sandy	-
A2	20-31	10YR 3/2	Dark grayish brown	29.1	59.5	5	6.4	Sand	-
AC	31-38	10YR 4/4	Dark yellowish brown	29	62.1	2.2	6.6	Sand	-
Cg1	38-63	10YR 5/3	Brown	23.2	60.6	5.1	11.1	Loamy sandy	-
Cg2	63-110	10YR 5/3	Brown	32.2	57.7	4.3	5.8	Sand	-
P7 - NEOSSOLO QUARTZARÊNICO Órtico típico									
Eutric Sideralic Brunic Arenosol (Ochric, Rubic)									
A	0-27	10YR 4/3	Brown	28.5	61.6	4.7	5.2	Sand	-
CA	27-44	10YR 4/4	Brown	27.5	63.6	4.9	4	Sand	-
C1	44-67	10YR 4/4	Dark yellowish brown	24.3	64.5	6.8	4.3	Sand	-
C2	67-91	10YR 5/8	Yellowish brown	25.6	64.4	6.1	3.9	Sand	-
C3	91-115	10YR 6/4	Light yellowish brown	32.4	60.1	4.3	3.2	Sand	-
P8 - NEOSSOLO QUARTZARÊNICO Órtico típico									
Dystric Sideralic Brunic Arenosol (Ochric, Isopteric Claric)									
A	0-5	10YR 3/2	Very dark grayish brown	37.2	53.3	2.8	6.7	Sand	-
CA	5-1	10YR 4/2	Dark grayish brown	37.5	52.3	4.5	5.7	Sand	-
C1	16-67	10YR 4/2	Dark grayish brown	35.1	53.7	1.1	10.1	Loamy sandy	-
C2	67-110	10YR 5/2	Grayish brown	34.3	51.3	7.1	7.2	Loamy sandy	-
P9 - NEOSSOLO QUARTZARÊNICO Órtico típico									
Eutric Sideralic Brunic Arenosol (Ochric)									
C	0-3	-		50.3	44.5	1.4	3.9	Sand	-
2A	3-7	10YR 3/2	Very dark grayish brown	47	48.4	0.3	4.3	Sand	-
2CA	7-1	10YR 4/2	Dark grayish brown	39.8	54.2	1.8	4.2	Sand	-
2C1	16-63	10YR 4/3	Brown	39.3	55	0.9	4.8	Sand	-
2C2	63-97	10YR 5/4	Yellowish brown	47.4	46.9	2.1	3.5	Sand	-
P10 - NEOSSOLO QUARTZARÊNICO Órtico típico									
Dystric Brunic Arenosol (Humic, Isopteric, Claric)									
A	0-5	10YR 3/2	Very dark grayish brown	35	49.8	5.1	10.1	Loamy sandy	-
C1	5-47	10YR 4/2	Dark grayish brown	36.3	46.9	5.2	11.7	Loamy sandy	-
C2	47-95	10YR 3/4	Dark yellowish brown	36.8	45.6	6.5	11.1	Loamy sandy	-
P11 - NEOSSOLO QUARTZARÊNICO Órtico típico									
Dystric Sideralic Brunic Arenosol (Ochric, Claric)									
A1	0-2	10YR 5/2	Grayish brown	45.2	48.9	1.6	4.3	Sand	-
A2	2-35	10YR 5/3	Brown	45.6	48.3	1.6	4.5	Sand	-
C1	35-72	10YR 6/3	Pale brown	40.4	51.1	3.8	4.7	Sand	-
C2	72-90	10YR 7/3	Very pale brown	42.7	47.3	2.4	7.7	Sand	-
P12 - NEOSSOLO QUARTZARÊNICO Órtico típico									

			Dystric Sideralic Brunic Arenosol (Ochric)						
A1	0-14	10YR 4/3	Brown	50.2	45.3	0.8	3.6	Sand	-
A2	14-38	10YR 4/2	Dark grayish brown	49.7	45.7	1.3	3.2	Sand	-
C1	38-66	10YR 5/3	Brown	51.4	40.7	4.7	3.2	Sand	-
C2	66-93	10YR 5/3	Brown	48.5	45.1	2.4	4	Sand	-
			P13 - NEOSSOLO QUARTZARÊNICO Hidromórfico plintossólico						
			Dystric Sideralic Gleyic Arenosol (Ochric)						
A	0-15	10YR 3/1	Very dark gray	22.1	55.9	7	15	Sandy loam	-
CA	15-26	10YR 3/2	Very dark grayish brown	25	63.9	8	3.2	Sand	-
Cg	26-37	10YR 6/4	Light yellowish brown	26.9	66.6	5.8	0.7	Sand	-
Cgf	37-50	10YR 6/4	Light yellowish brown	22.3	68.3	5.8	2.6	Sand	-
			P14 - NEOSSOLO QUARTZARÊNICO Órtico típico						
			Eutric Sideralic Brunic Arenosol (Ochric)						
A1	0-9	10YR 3/2	Very dark grayish brown	23.6	65.9	5.3	5.2	Sand	-
A2	9-23	10YR 2/2	Very dark brown	24.2	67.9	4.1	3.8	Sand	-
CA	23-52	10YR 3/3	Dark brown	23.9	68.5	3.8	3.7	Sand	-
C1	52-99	10YR4/3	Brown	23.7	68.6	3.4	4.4	Sand	-
C2	99-130	10YR3/4	Dark yellowish brown	24.7	68.5	3.2	3.5	Sand	-
			P15 - NEOSSOLO QUARTZARÊNICO Órtico típico						
			Eutric Sideralic Arenosol (Ochric)						
A1	0-24	10YR 3/2	Very dark grayish brown	19.8	71.4	3.8	5	Sand	-
A2	24-33	10YR 4/2	Dark grayish brown	21.1	70.2	4.8	4	Sand	-
CA	33-59	10YR 4/2	Dark grayish brown	20.5	71.5	3.8	4.2	Sand	-
C1	59-106	10YR 4/4	Dark yellowish brown	19.8	72.4	3.1	4.7	Sand	-
C2	106-120	10YR 3/4	Dark yellowish brown	20.8	70.2	4.6	4.5	Sand	-
			P16 - NEOSSOLO QUARTZARÊNICO Órtico típico						
			Dystric Sideralic Brunic Arenosol (Ochric)						
A	0-6	10YR 3/2	Very dark grayish brown	37	55.6	1.7	5.7	Sand	-
CA	6-35	10YR 4/2	Dark grayish brown	37.1	57.2	1.6	4.1	Sand	-
C1	35-51	10YR 4/3	Brown	37.1	56.5	1.4	5	Sand	-
C2	51-97	10YR 3/4	Dark yellowish brown	42.2	51	1	5.8	Sand	-
C3	97-120	10YR 4/4	Dark yellowish brown	34.6	58.4	1.6	5.4	Sand	-
			P17 - PLANOSSOLO NÁTRICO Carbonático típico						
			Albic Solonetz (Arenic, Differentic, Endic, Hypernatric)						
An	0-6	5Y 6/2	Light olive gray	19.3	76.5	0.4	3.8	Sand	1.72
2An	6-15	5Y 3/2	Dark olive gray	18.8	67.6	0.6	13	Loamy sandy	1.8
E1	15-54	5Y 5/4	Olive	17.7	67.7	3	11.6	Loamy sandy	1.86
E2	54-90	5Y 7/3	Pale yellow	17.4	61.6	5.8	15.2	Sandy loam	1.95
Btn	90+	5Y 5/3	Olive	19.3	76.5	0.4	3.8	Sand	1.72

P18 - PLANOSSOLO NÁTRICO Sálico êndico									
Albic Nudinatric Protosalic Stagnic Gleyic Solonetz (Arenic, Differentic, Endic. Ochric, Hypernatric)									
Agn1	0-16	5GY 3/2	Dark olive gray	22.1	55.9	7	15	Clay	0.97
Agn2	16-27	10Y 4/2	Dark gray	25	63.9	8	3.2	Sandy clay loam	1.06
E	27-60	5Y 6/2	Olive gray	26.9	66.6	5.8	0.7	Sand	1.78
Btn	60-90	5Y 5/2	Black	22.3	68.3	5.8	2.6	Loamy sand	1.8
Btgn	90-106	10Y-SGY 3/2	Reddish brown	21.6	49.6	7.3	21.5	Sandy clay loam	-
Btg	106-128	Grey1 3/5GY	Dark grayish green	28.1	43.5	6.8	21.6	Sandy clay loam	-
P19 - ESPODOSSOLO FERRILÚVICO Hidromórfico arênico									
Stagnic Gleyic Entic Podzol (Arenic, Epic, Eutric, Sideralic)									
An1	0-5	5Y 3/2	Dark grayish green	22.9	69.7	0.7	6.6	Sand	1.52
An2	5-10	5Y 3/2 e 5Y 4/3	Light olive gray	25.4	66.2	0.2	8.2	Sand	1.66
Bsc1	10-28	5YR 4/2 e 5Y 6/2	Olive gray	31	55.4	1.4	12.2	Loamy sand	1.6
Bsc2	28-48	5Y 5/3	Very dark grayish olive	35	59.2	0.5	5.3	Sand	1.72
Bsc3	48-70+	5Y 5/2	Very dark greenish gray	37.4	58.1	1.2	3.3	Loamy sand	1.82
P20 - PLANOSSOLO HÁPLICO Eutrófico solódico espessarênico									
Eutric Sideralic Brunic Arenosol (Ochric, Protoargic, Claric, Protospodic)									
A	0-36	2,5 Y 4/3	Olive brown	20	69.7	4.7	4.6	Sand	1.53
AE	36-53	2,5 Y 6/3	Light yellowish brown	21.4	71	3.9	3.8	Sand	1.46
E	53-96	2,5 Y 7/3	Pale brown	19.4	74.4	2.1	4	Sand	1.64
Bt	96-107	2,5 Y 4/2	Dark grayish brown	15.5	71.1	5	8.6	Loamy sandy	1.5
Btnqx	107-110	7,5 YR 4/2	Brown	21.2	60	5	13.9	Sandy laom	-
P21 - ESPODOSSOLO HUMILÚVICO Hidromórfico arênico									
Albic Podzol (Arenic, Epic, Eutric, Oxyaquic, Sideralic)									
A	0-5	2,5Y 3/2	Very dark grayish brown	16	69.6	6.8	7.6	Sand	0.87
E	5-13	2,5 YR 5/1	Dusky red	15.9	72.7	4.3	7	Sand	1.66
Bh	13-29	2,5 YR 2,5/1	Reddish black	13.5	75.2	6.5	4.8	Sand	1.69
C	29-60	2,5 Y 6/3	Light yellowish brown	20.6	74.3	3.6	1.5	Loamy sandy	1.64
P22 - NEOSSOLO QUARTZARÊNICO Hidromórfico típico									
Eutric Sideralic Arenosol (Ochric, Claric)									
A	0-15	5GY 3/2	Black	12.9	56.6	16.8	13.6	Sandy loam	1.52
AC	15-22	10Y 4/2	Dark gray	18.3	70.1	5.6	6	Sand	1.73
C	22-50	5Y 6/2	Weak red	19.5	74.8	0.9	4.8	Sand	1.74
P23 - NEOSSOLO QUARTZARÊNICO Órtico típico									

Dystric Sideralic Brunic Arenosol (Ochric)									
A	0-17	10 YR 6/2	Light brownish gray	20.8	70.3	1.8	7.1	Sand	1.36
CA	17-55	10 YR 6/4	Light yellowish brown	20.4	71.2	2.3	6.1	Sand	1.53
C1	55-103	10 YR 6/6	Brownish yellow	19.7	71.6	3.7	5	Sand	1.52
C2n	103-130	10 YR 6/6	Brownish yellow	18.8	74.5	1.8	4.9	Sand	1.68
P24 - NEOSSOLO QUARTZARÊNICO Hidromórfico espodossólico									
Eutric Sideralic Gleyic Brunic Arenosol (Humic, Claric)									
A1	0-9	2,5 Y 3/2	Very dark grayish brown	18.5	61.7	7.5	12.2	Sandy loam	1.03
A2	9-25	2,5 Y 3/1	Very dark gray	21.1	65.7	4	9.2	Loamy sandy	1.52
C	25-70	2,5 Y 7/3	Pale brown	24.3	70.4	1.1	4.1	Sand	1.75
P25 - NEOSSOLO QUARTZARÊNICO Órtico gleissólico									
Eutric Sideralic Gleyic Brunic Arenosol (Ochric)									
A1	0-6	2,5Y 4/2	Dark grayish brown	20.4	69.6	3.9	6.1	Sand	1.48
A2	6-55	2,5Y 3/2	Very dark grayish brown	19.8	68.8	5.3	6.1	Sand	1.5
CA	55-69	2,5 Y 5/3	Light olive brown	19.6	67.6	7.1	5.7	Sandy loam	1.49
Cg1	69-114	2,5Y 6/4	Light yellowish brown	22	69.7	4.4	3.9	Sand	1.55
Cg2	114-120	2,5Y 7/3	Pale brown	22.7	70	2.1	5.2	Sand	1.58
P26 - NEOSSOLO QUARTZARÊNICO Hidromórfico organossólico									
Eutric Sideralic Brunic Arenosol (Humic)									
H	0-21	10YR 2/1	Black	15.4	46.3	9.8	28.5	Sandy clay loam	0.64
A	21-25	10YR 3/1	Very dark gray	32.1	50.6	11.8	5.6	Loamy sand	1.41
C1	25-42	10YR 4/3	Brown	54.3	36.9	6.2	2.6	Sand	1.42
C2	42-75	10YR 4/3	Brown	43.5	47.6	5.9	3	Sand	1.50
Cg	75-105	10YR 4/2	Dark grayish brown	62.1	27.6	6.2	4.1	Sand	1.60
P27 - NEOSSOLO QUARTZARÊNICO Órtico gleissólico									
Dystric Sideralic Brunic Arenosol (Ochric)									
A	0-9	7,5YR 3/2	Dark brown	56.7	34.1	4.4	4.8	Sand	1.39
CA	9-21	7,5YR 3/2	Dark brown	49.3	43.9	2.7	4.1	Sand	1.35
C1	21-66	7,5 YR 4/3	Brown	59.4	31.9	3.6	5.2	Sand	1.30
C2	66-105	10YR 4/3	Brown	59.2	32.8	4.2	3.8	Sand	1.33
P28 - NEOSSOLO QUARTZARÊNICO Órtico típico									
Dystric Brunic Arenosol (Ochric, Isopteric)									
A	5-18	7,5 YR 3/2	Dark brown	50.9	39.4	4.6	5.1	Sand	1.28
C1	18-62	7,5YR 4/3	Brown	64.6	26.3	4.8	4.3	Sand	1.24
C2	62-75	7,5YR 4/2	Brown	48.4	42.3	4.2	5	Sand	1.23
P29 - ESPODOSSOLO FERRILÚVICO Hidromórfico arênico									
Gleyic Histic Albic Ortsteinic Podzol (Arenic, Abruptic, Epic, Sideralic)									
A	0-14	5YR 2,5/1	Black	0.8	38.4	42.6	18.2	Loamy sand	
2A	14-23	5YR 2,5/1	Black	14.9	71	9.6	4.5	Loamy sand	1.24

2AE	23-29/48	10YR 3/2	Dark reddish brown	16.6	73.4	6.7	3.4	Sand	1.40
2E	29/45-53	7,5YR 5/4	Reddish brown	15.7	78.5	3.7	2.1	Sand	1.39
2Bsm1	45/53-53/63	7,5YR 4/4	Brown	20.9	61.8	7.6	9.6	Loamy sand	1.53
2Bsm2	65/67-76	7,5YR 4/6	Strong brown	15.3	72.6	5.6	6.5	Loamy sand	1.57
2Cg1	76-94	7,5YR 4/6	Strong brown	17.1	72.3	4.8	5.8	Sand	1.50
2Cg2	94+	10YR 4/2	Dark grayish brown	9.8	76.9	6.3	7.1	Loamy sand	1.49
P30 - NEOSSOLO QUARTZARÊNICO Órtico típico **Dystric Sideralic Arenosol (Ochric)**									
A	0-6	7,5 YR ,5/2	Dark brown	38.5	52.9	4.1	4.5	Sand	1.23
AC	6-12	7,5YR 3/2	Dark brown	44.8	48.8	4.1	2.3	Sand	1.32
C1	12-45	7,5YR 3/2	Dark brown	19.3	73	4.3	3.4	Sand	1.32
C2	45-69	7,5YR 4/3	Brown	23.5	67.5	6.8	2.2	Sand	1.36
C3	69-90	7,5YR 5/4	Brown	41.2	49.9	6.3	2.5	Sand	1.39

APPENDIX C – Chemical attributes of the soils of Nhecolândia Pantanal, Brazil

Horizon	pH H2O	pH KCl	ΔpH	P	K	Na	Ca^{2+}	Mg^{2+}	Al^{3+}	H+Al	SB	t	T	V	m	ISNa	COT	P-Rem	Cu	Mn	Fe	Zn	CE
				$mg.kg^{-1}$		---------- $cmol_c.kg^{-1}$ ----------								---------% ---------			$dag.kg^{-1}$	$mg.L^{-1}$		$mg.kg^{-1}$			dS/m
P1 - GLEISSOLO HÁPLICO Sódico hipocarbonático êutrico																							
Reductigleyic Eutric Gleysol (Clayic, Alcalic, Sideralic, Humic, Protosodic, Uterquic)																							
A	9.1	4.5	-4.6	32.4	2297.08	1004	8.4	1.0	0	0	19.6	19.6	19.6	100	0	22	1.0	20.2	0.4	755	17	0	0.89
ABgn	9.1	7.5	-1.7	42.8	3028.35	1105	8.0	0.7	0	0.7	21.3	21.3	22.0	97	0	22	1.2	29	0.5	507	30	0	1.19
Bgn1	9.4	7.6	-1.7	26.2	1823.91	986	7.5	1.2	0	0	17.7	17.7	17.7	100	0	24	1.0	17.8	0.3	949	9	0	0.70
Bgn2	9.4	7.8	-1.6	42.0	1388.93	853	6.4	1.4	0	0	15.1	15.1	15.1	100	0	25	1.1	18.4	0.3	1019	17	0	0.80
Cn	10.0	8.8	-1.1	9.5	132.16	101	0.6	0.1	0	0.2	1.5	1.5	1.7	88	0	26	0.5	50.4	0.2	53	12	0	0.95
P2 - GLEISSOLO HÁPLICO Sódico Típico																							
Reductigleyic Eutric Gleysol (Arenic, Alcalic, Ochric, Sodic, Uterquic)																							
An1	9.4	7.5	-1.8	19.5	2075.62	891	5.7	0.7	0	0.2	15.6	15.6	15.9	98	0	24	0.8	19	0.4	334	14	0	1.21
An2	9.5	7.7	-1.8	19.3	1476.53	555	3.4	0.4	0	0.0	10.0	10.0	10.0	100	0	24	0.8	21.6	0.5	543	13	0	0.71
Bsgn	9.7	8.6	-1.1	12.5	150.18	92	1.0	0.1	0	0.0	1.9	1.9	1.9	100	0	21	1.0	40.7	0.3	348	5	0	0.95
Cg	9.6	8.6	-1.1	35.8	173.44	85	1.2	0.1	0	0.1	2.1	2.1	2.2	94	0	17	0.7	30.3	0.4	412	29	0	0.76
P3 - NEOSSOLO QUARTZARÊNICO Órtico típico																							
Dystric Sideralic Brunic Arenosol (Ochric, Claric)																							
A1	6.2	4.9	-1.3	15.8	28.28	0	1.0	0.2	0.0	1.8	1.3	1.3	3047.0	42	0	0	0.3	42.5	0.2	65041	41	0	-
A2	5.2	4.0	-1.2	3.6	10.42	0	0.1	0	0.2	1.6	0.2	0.4	1786.0	11	53	0	0.1	41.5	0.1	14174	35	0	-
C1	5.2	4.1	-1.1	3.3	4.06	0	0.1	0	0.3	1.6	0.2	0.4	1711.0	9	64	0	0.0	43.9	0.1	10213	37	0	-
C2	5.2	4.1	-1.1	3.7	3.27	0	0.1	0	0.3	1.6	0.1	0.4	1765.0	7	67	0	0.4	44.5	0.2	84989	37	0	-
P4 - PLANOSSOLO HÁPLICO Eutrófico gleissólico																							
Eutric Albic Gleyic Histic Planosol (Arenic, Alcalic, Sideralic, Humic, Sodic)																							
An	6.5	4.9	-1.7	1.5	284.62	221	4.1	1117.0	0	6.8	6877.0	6877.0	13.7	50	0	7	6.0	28.6	0.9	135	1405	1	0.81
AEn	7.5	6.0	-1.5	0.7	113.44	36	0.8	0.3	0	0.7	1537.0	1537.0	2195.0	70	0	7	0.2	51.6	0.2	19317	268	0	0.39
E	8.6	6.8	-1.8	0.3	71.25	24	0.5	0.2	0	0.5	0.9	0.9	1404.0	66	0	7	0.3	55.2	0.1	13427	125	0	0.38
Eg1	9.0	8.0	-1.0	1.5	147.72	46	2.0	0.4	0	0.2	2969.0	2969.0	3118.0	95	0	6	0.2	43.2	0.4	271	448	0	0.65
Eg2	9.4	8.6	-0.8	5.7	75.85	31	1.0	0.2	0	0.0	1538.0	1538.0	1538.0	100	0	9	0.1	52.7	0.2	494	51	0	0.51
Bt	8.8	7.5	-1.3	7.2	408.32	89	4.3	1669.0	0	0.2	7381.0	7381.0	7544.0	98	0	5	0.5	43.3	0.9	929	305	0	0.43
P5 - NEOSSOLO QUARTZARÊNICO Órtico gleissólico																							
Eutric Sideralic Brunic Arenosol (Ochric, Claric)																							
A	6.8	5.9	-0.9	2.4	67.24	4581	1589.0	0.5	0	0.5	2291.0	2291.0	2808.0	82	0	1	0.8	55.8	0.3	61622	86	1	-
C	6.6	4.7	-1.9	0.6	30.37	0	0.3	0.0	0	0.5	0.4	0.4	1.0	44	0	0	0.2	49.7	0.0	32394	43	0	-
Cg	6.7	4.8	-1.9	0.3	17.62	0	0.2	0.0	0	0.2	0.3	0.3	0.4	58	0	0	0.2	57.4	0.1	27696	26	0	-
P6 - NEOSSOLO QUARTZARÊNICO Hidromórfico típico																							

Dystric Brunic Arenosol (Ochric, Protoargic)

A1	5.2	3.8	-1.4	0.8	9.58	8	0.1	0	0.8	2.4	0.2	1.0	2.7	8	78	1	0.5	37.7	0.1	175	7	0	0.21
A2	4.8	3.6	-1.1	0.4	9.01	5	0.1	0	0.5	1.3	0.2	0.7	1.5	11	76	1	0.2	40.8	0.1	188	6	0	0.16
AC	4.9	3.5	-1.4	0.6	7.69	4	0.1	0	0.5	1.2	0.2	0.7	1.4	14	71	1	0.2	41.1	0.1	167	7	1	0.13
Cg1	5.2	3.4	-1.8	0.2	11.46	25	0.2	0.1	1.0	1.9	0.4	1.4	2.3	16	74	5	0.2	32.6	0.1	204	8	1	0.04
Cg2	5.4	3.7	-1.7	0.1	8.82	5	0.1	0.1	0.3	0.3	0.2	0.5	0.5	32	67	4	0.2	47.2	0.1	70	5	0	0.07
P7 - NEOSSOLO QUARTZARÊNICO Órtico típico **Eutric Sideralic Brunic Arenosol (Ochric, Rubic)**																							
A	4.8	4.0	-0.8	8.0	38.02	0	0.7	0.2	0.2	1.9	1.0	1.2	2.9	34	17	0	0.8	46.4	1.1	39	34	0	-
CA	5.3	4.1	-1.3	0.8	29.60	0	0.2	0.2	0.2	0.0	0.4	0.6	0.4	100	34	0	0.3	44.5	0.1	112	6	0	-
C1	5.5	4.0	-1.5	0.6	54.30	0	0	0.2	0.1	1.0	0.3	0.5	1.3	26	30	0	0.2	48.7	0.1	88	6	0	-
C2	5.4	4.2	-1.2	0.3	57.38	1	0.1	0.1	0	0.2	0.3	0.3	0.5	59	0	1	0.2	50.5	0.1	50	8	0	-
C3	6.2	4.7	-1.5	0.2	25.95	0	0	0.1	0	0.2	0.2	0.2	0.4	46	0	0	0.1	52.1	0.2	21	5	0	-
P8 - NEOSSOLO QUARTZARÊNICO Órtico típico **Dystric Sideralic Brunic Arenosol (Ochric, Isopteric Claric)**																							
A	4.1	3.4	-0.8	4.8	41.63	0	0.2	0.1	0.7	3.4	0.4	1.1	3.7	10	64	0	1.0	43.9	0.3	41	7	0	-
CA	4.1	3.6	-0.5	1.7	21.97	0	0	0	0.7	2.2	0.1	0.8	2.3	5	85	0	0.6	39.9	0.1	60	2	0	-
C1	4.2	3.6	-0.6	0.7	12.51	4	0	0	0.7	1.8	0.1	0.8	1.9	4	90	1	0.3	39.8	0.1	79	2	0	-
C2	4.9	3.5	-1.4	0.5	20.19	14	0	0	0.6	1.1	0.1	0.7	1.2	11	81	5	0.1	46.9	0.1	91	3	0	-
P9 - NEOSSOLO QUARTZARÊNICO Órtico típico **Eutric Sideralic Brunic Arenosol (Ochric)**																							
C	5.5	4.3	-1.2	3.2	15.91	0	0.3	0.2	0.5	0	0.5	0.5	1.0	52	100	0	0.3	52.6	0.4	30	10	0	-
2A	5.5	4.3	-1.3	2.8	19.52	0	0.3	0.1	0.4	0	0.9	0.4	1.3	68	100	0	0.3	49.8	0.1	23	1	0	-
2CA	5.4	4.2	-1.2	1.0	15.94	0	0.1	0.1	0.2	0.2	0.6	0.4	0.8	77	49	0	0.3	44.5	0.0	11	0	0	-
2C1	5.1	4.2	-0.9	0.7	10.44	0	0	0.0	0.1	0.3	0.9	0.4	1.0	92	20	0	0.2	42.4	0.1	5	0	0	-
2C2	4.9	4.2	-0.8	0.6	3.48	0	0	0.0	0.0	0.3	0.4	0.3	0.5	91	13	0	0.2	47.6	0.0	4	0	0	-
P10 - NEOSSOLO QUARTZARÊNICO Órtico típico **Dystric Brunic Arenosol (Humic, Isopteric, Claric)**																							
A	4.1	3.4	-0.7	10.4	78.86	0	0.4	0.2	0.7	4.0	0.9	1.6	4.9	18	46	0	2.5	42.7	0.8	43	32	0	0.91
C1	4.3	3.6	-0.8	3.0	40.36	15	0.1	0.1	0.9	2.4	0.3	1.2	2.6	11	76	2	2.2	37.6	0.4	54	19	1	0.62
C2	4.9	3.6	-1.4	1.3	84.19	22	0	0.1	0.7	1.9	0.4	1.1	2.3	18	63	4	2.3	38.9	0.2	72	17	1	0.48
P11 - NEOSSOLO QUARTZARÊNICO Órtico típico **Dystric Sideralic Brunic Arenosol (Ochric, Claric)**																							
A1	5.1	4.1	-1.0	4.8	60.80	0	0.3	0.2	0.2	1.2	0.7	0.9	1.9	37	24	0	0.8	49.2	1.0	20	39	0	-
A2	5.1	4.1	-1.0	1.2	20.23	0	0.1	0	0.3	0.6	0.2	0.5	0.8	20	66	0	0.2	44.1	1.9	21	4	0	-
C1	5.0	4.0	-1.0	0.8	13.49	0	0.0	0	0.4	0.8	0.1	0.5	0.9	8	83	0	0.2	42	0.0	11	1	0	-
C2	4.8	4.0	-0.9	0.6	9.55	0	0.0	0	0.6	1.0	0.1	0.7	1.1	6	90	0	0.2	36.7	0.0	6	1	0	-
P12 - NEOSSOLO QUARTZARÊNICO Órtico típico																							

Dystric Sideralic Brunic Arenosol (Ochric)

A1	4.8	3.9	-0.9	7.9	33.95	0	0.4	0.2	0.1	1.1	0.6	0.7	1.7	34	18	0	0.4	51	0.5	24	33	0	-
A2	4.9	3.9	-1.0	16.3	13.62	0	0.1	0	0.3	0.7	0.2	0.5	0.9	20	63	0	0.2	45.7	0.2	35	15	0	-
C1	5.0	4.0	-1.0	9.2	9.79	0	0.1	0.1	0.2	0.5	0.2	0.4	0.7	26	51	0	0.2	49.2	0.2	40	13	0	-
C2	4.9	3.9	-1.0	3.7	8.68	0	0.1	0	0.3	0.6	0.1	0.4	0.7	15	68	0	0.2	45.7	0.2	43	4	0	-

P13 - NEOSSOLO QUARTZARÊNICO Hidromórfico plintossólico
Dystric Sideralic Gleyic Arenosol (Ochric)

A	4.5	3.5	-1.0	3.8	62.77	5	0.2	0.1	1.2	3.8	0.4	1.6	4.2	9	75	0	1.3	30.1	0.3	319	28	2	-
CA	4.7	3.6	-1.1	1.3	21.64	0	0.1	0	0.4	1.0	0.1	0.5	1.1	11	80	0	0.2	46.4	0.1	144	5	1	-
Cg	5.3	4.0	-1.3	0.5	8.48	0	0.1	0	0.1	0.1	0.1	0.2	0.2	36	57	0	0.2	53.1	0.1	39	1	0	-
Cgf	5.4	4.1	-1.3	0.7	7.23	0	0.0	0	0.0	0.0	0.1	0.1	0.1	100	0	0	0.2	51.8	0.1	47	1	0	-

P14 - NEOSSOLO QUARTZARÊNICO Órtico típico
Eutric Sideralic Brunic Arenosol (Ochric)

A1	6.7	6.0	-0.7	13.7	53.27	8	3.6	0.9	0.0	1.8	4.6	4.6	6.4	73	0	1	1.3	32.4	0.6	5	108	1	-
A2	6.5	5.1	-1.5	7.6	17.62	6	1.0	0.2	0.0	1.3	1.3	1.3	2.5	51	0	1	0.4	53.9	0.2	20	47	1	-
CA	6.3	4.7	-1.6	11.4	14.44	7	0.7	0.2	0.0	1.2	1.0	1.0	2.1	45	0	1	0.4	52.1	0.2	16	36	1	-
C1	6.1	4.4	-1.8	13.9	16.91	10	0.3	0.1	0.1	0.9	0.5	0.6	1.4	34	21	3	0.2	50.8	0.1	16	22	1	-
C2	6.2	4.3	-2.0	16.7	12.67	8	0.4	0.0	0.1	0.9	0.5	0.6	1.4	34	21	3	0.1	50.5	0.1	25	21	1	-

P15 - NEOSSOLO QUARTZARÊNICO Órtico típico
Eutric Sideralic Arenosol (Ochric)

A1	5.8	4.9	-0.9	6.4	46.98	5	1.8	0.3	0.0	1.6	2.3	2.3	3.9	59	0	1	0.9	52.7	0.4	15	100	0	0.29
A2	6.0	4.7	-1.3	5.3	26.73	7	0.9	0.2	0.0	1.1	1.1	1.1	2.2	49	0	1	0.4	52.7	0.2	17	46	0	0.19
CA	6.0	4.8	-1.2	7.4	23.73	6	0.8	0.1	0.0	1.0	1.0	1.0	2.1	50	0	1	0.1	54.8	0.2	18	36	0	0.17
C1	6.1	4.4	-1.7	12.3	26.09	7	0.4	0.1	0.0	0.9	0.6	0.6	1.5	38	0	2	0.1	54	0.2	23	22	0	0.12
C2	5.8	4.2	-1.6	14.9	29.22	7	0.3	0.1	0.1	0.8	0.5	0.7	1.3	40	20	2	0.1	50.7	0.2	33	26	1	0.14

P16 - NEOSSOLO QUARTZARÊNICO Órtico típico
Dystric Sideralic Brunic Arenosol (Ochric)

A	5.5	4.7	-0.9	5.6	10.29	9	0.1	0	0.0	2.1	2.1	2.1	4.2	49	0	1	1.1	57.3	0.9	12	66	0	-
CA	5.6	4.0	-1.6	2.8	9.25	5	0.1	0	0.2	1.5	0.2	0.4	1.7	13	49	1	0.3	55.2	0.2	44	18	0	-
C1	5.4	4.0	-1.4	3.5	7.65	4	0.1	0	0.3	1.1	0.2	0.5	1.3	17	54	0	0.3	48.6	0.2	53	10	0	-
C2	5.4	4.1	-1.4	2.1	10.34	23	0.1	0.1	0.2	1.1	0.2	0.4	1.3	16	49	0	0.1	50.2	0.1	54	8	0	-
C3	5.8	4.1	-1.7	2.0	9.03	5	0.1	0.1	0.3	0.9	0.2	0.5	1.1	18	57	1	0.1	52.1	0.1	53	6	0	-

P17 - PLANOSSOLO NÁTRICO Carbonático típico
Albic Solonetz (Arenic, Differentic, Endic, Hypernatric)

An	10.3	9.5	-0.8	9.9	277.93	304	0.3	0	0	0	2.3	2.3	2.3	100	0	57	0.1	38.7	0.1	15	7	0	3.91
An2	10.0	8.6	-1.4	7.3	1094.69	673	0.8	0	0	0	6.6	6.6	6.6	100	0	45	0.1	29.1	0.2	41	9	0	2.18
E1	10.3	9.3	-1.0	10.0	706.77	667	0.3	0	0	0	5.0	5.0	5.0	100	0	58	0.1	28.8	0.1	12	5	0	3.58
E2	10.3	9.3	-1.0	10.8	622.08	526	0.3	0	0	0	4.2	4.2	4.2	100	0	54	0.1	38.7	0.1	14	8	0	3.16

Btn	10.2	8.7	-1.5	15.2	1368.29	1300	0.6	0	0	0	9.7	9.7	9.7	100	0	58	0.1	36.6	0.1	14	9	0	3.93
P18 - PLANOSSOLO NÁTRICO Sálico êndico Albic Nudinatric Protosalic Stagnic Gleyic Solonetz (Arenic, Differentic, Endic. Ochric, Hypernatric)																					
Agn1	10.3	9.0	-1.4	287.5	2993.56	4282	1.3	0	0	0	27.6	27.6	27.6	100	0	67	1.4	5.3	0.4	403	5	0	8.46
Agn2	9.9	8.1	-1.8	35.7	977.58	1037	2.3	0.1	0	0	9.3	9.3	9.3	100	0	48	0.2	11.9	0.3	664	1	0	2.01
E	10.0	9.2	-0.8	12.9	183.75	183	0.6	0	0	0	1.8	1.8	1.8	100	0	43	0.1	27.2	0.2	168	3	0	2.01
Btn	10.0	8.8	-1.2	44.4	432.90	328	0.9	0	0	0	3.4	3.4	3.4	100	0	42	0.1	38	0.7	431	7	0	0.96
Btgn	10.1	8.5	-1.5	101.2	1147.06	96	1.0	0	0	0	6.5	6.5	6.5	100	0	9	0.1	36.5	1.0	1056	30	0	1.16
Btg	10.1	8.6	-1.5	21.8	2182.67	88	1.0	0	0	0	9.7	9.7	9.7	100	0	5	0.2	45.7	1.8	503	114	0	1.76
P19 - ESPODOSSOLO FERRILÚVICO Hidromórfico arênico Stagnic Gleyic Entic Podzol (Arenic, Epic, Eutric, Sideralic)																					
An1	8.6	7.0	-1.5	9.9	510.13	359	1.9	0.2	0	0.0	5.0	5.0	5.0	100	0	31	0.7	44.5	0.3	151	467	0	4.37
An2	7.4	5.6	-1.9	4.7	235.10	52	1.8	0.5	0	0.8	3.1	3.1	4.0	79	0	6	0.2	39.6	0.2	102	572	0	0.51
Bsc1	7.0	5.0	-2.0	2.0	137.12	12	1.3	0.5	0	1.3	2.2	2.2	3.5	64	0	2	0.2	29.8	0.1	229	643	0	0.10
Bsc2	6.6	5.2	-1.4	0.1	17.78	1	0.2	0	0	0.3	0.3	0.3	0.6	43	0	1	0.1	43.6	0.1	38	167	0	0.11
Bsc3	6.0	4.0	-2.0	0.7	12.88	0	0.1	0	0	0.3	0.1	0.1	0.5	29	0	0	0.1	52.1	0.1	5	126	0	0.15
P20 - PLANOSSOLO HÁPLICO Eutrófico solódico espessarênico Eutric Sideralic Brunic Arenosol (Ochric, Protoargic, Claric, Protospodic)																					
A	7.3	6.0	-1.3	6.2	76.28	3	1.0	0.2	0	0.5	1.4	1.4	2.0	72	0	1	0.3	55.2	0.3	45	8	0	0.31
AE	7.3	6.3	-1.0	6.4	18.92	0	0.8	0.1	0	0.1	1.0	1.0	1.1	88	0	0	0.1	56.7	0.3	32	4	0	0.21
E	8.5	8.0	-0.4	18.3	20.18	0	1.1	0.0	0	0	1.2	1.2	1.2	100	0	0	0.1	59.6	0.2	6	4	0	0.21
Bt	8.6	7.4	-1.2	37.2	178.30	21	1.9	0.4	0	0	2.8	2.8	2.8	100	0	3	0.1	52.1	0.4	15	9	0	0.48
Btnqx	8.9	7.4	-1.6	352.2	708.02	119	3.3	1.6	0	0	7.3	7.3	7.3	100	0	7	0.1	34.1	0.5	16	5	0	0.59
P21 - ESPODOSSOLO HUMILÚVICO Hidromórfico arênico Albic Podzol (Arenic, Epic, Eutric, Oxyaquic, Sideralic)																					
A	5.3	4.0	-1.3	1.8	75.13	18	1.1	0.2	0.2	4.2	1.6	1.8	5.8	27	9	1	1.7	45.8	0.3	53	179	1	-
E	5.6	4.1	-1.6	1.3	23.24	1	0.5	0.1	0.2	1.7	0.7	0.8	2.4	28	19	0	0.4	48.4	0.2	16	136	0	-
Bh	5.8	4.1	-1.7	1.3	18.71	1	0.4	0.1	0.1	1.4	0.6	0.7	1.9	29	19	0	0.4	42.9	0.2	15	117	0	-
C	5.3	4.0	-1.3	0.5	2.61	0	0.1	0	0.1	0.3	0.2	0.3	0.5	32	45	0	0.1	52.1	0.1	3	37	0	-
P22 - NEOSSOLO QUARTZARÊNICO Hidromórfico típico Eutric Sideralic Arenosol (Ochric, Claric)																					
A	5.6	4.4	-1.2	0.6	50.20	4	1.5	0.2	0	2.8	1.9	1.9	4.7	40	0	0	1.7	35.2	0.3	71	391	1	-
AC	5.3	4.2	-1.1	0.4	18.14	1	0.5	0.1	0	1.1	0.6	0.6	1.7	37	0	0	0.2	48.3	0.2	12	210	0	-
C	5.8	4.4	-1.4	0.1	5.23	0	0.1	0.0	0	0.1	0.2	0.2	0.3	57	0	0	0.2	58.5	0.1	3	70	0	-
P23 - NEOSSOLO QUARTZARÊNICO Órtico típico Dystric Sideralic Brunic Arenosol (Ochric)																					
A	5.2	4.1	-1.2	2.3	20.06	0	0	0	0.3	2.3	0.2	0.5	2.5	8	65	0	0.5	45	0.2	25	17	0	-
CA	5.6	4.2	-1.3	0.4	17.59	0	0	0	0.1	0.9	0.1	0.2	1.0	11	54	0	0.2	44.9	0.4	26	13	0	-
C1	5.4	4.3	-1.1	0.3	11.30	0	0	0	0.1	0.6	0.1	0.2	0.6	12	58	0	0.1	46.7	0.3	24	8	0	-

C2n	6.8	5.3	-1.4	0.7	1.47	65	0	0	0.0	0.2	0.3	0.3	0.6	60	0	51	0.1	51.2	0.3	13	41	0	-
P24 - NEOSSOLO QUARTZARÊNICO Hidromórfico espodossólico Eutric Sideralic Gleyic Brunic Arenosol (Humic, Claric)																							
A1	5.2	4.0	-1.2	1.7	33.42	11	1.4	0.3	0.2	3.7	1.8	2.0	5.5	33	9	1	1.5	38	0.4	38	430	0	-
A2	5.6	3.9	-1.6	0.6	30.91	0	1.1	0.1	0.2	2.4	1.3	1.4	3.6	35	11	0	0.5	35.4	0.2	39	567	0	-
C	5.6	3.9	-1.7	0.4	3.96	0	0	0.0	0.0	0.1	0.1	0.1	0.2	38	0	0	0.0	55	0.1	2	85	0	-
P25 - NEOSSOLO QUARTZARÊNICO Órtico gleissólico Eutric Sideralic Gleyic Brunic Arenosol (Ochric)																							
A1	5.7	4.7	-1.0	7.1	47.04	0	2.1	0.4	0.0	1.5	2.6	2.6	4.1	63	0	0	0.8	53.7	0.2	40	28	0	-
A2	5.4	4.1	-1.4	13.5	25.49	0	0.7	0.2	0.1	1.9	0.9	1.1	2.9	33	13	0	0.2	54.7	0.1	12	123	0	-
CA	5.5	4.0	-1.5	28.3	44.66	0	0.3	0.1	0.2	1.5	0.6	0.8	2.1	27	26	0	0.2	45.1	0.1	7	246	0	-
Cg1	6.4	4.4	-2.0	6.9	72.03	0	0.2	0.1	0.0	0.3	0.5	0.5	0.8	58	0	0	0.0	50.5	0.1	4	131	0	-
Cg2	6.4	4.6	-1.8	4.5	34.52	0	0.1	0.0	0.0	0.0	0.3	0.3	0.3	100	0	0	0.0	51.8	0.0	2	77	0	-
P26 - NEOSSOLO QUARTZARÊNICO Hidromórfico organossólico Eutric Sideralic Brunic Arenosol (Humic)																							
H	5.4	3.9	-1.5	1.0	200.04	34	2.6	0.6	0.2	12.8	3.9	4.1	16.7	23	5	1	11.3	29.4	0.8	179	823	2	0.60
A	6.5	3.8	-2.7	0.0	63.07	4	0.2	0.1	0.2	2.0	0.8	1.1	2.8	30	21	1	0.4	47.7	0.6	34	186	0	0.33
C1	6.2	4.2	-2.0	0.1	22.35	0	0	0	0	0.2	0.2	0.2	0.4	50	0	1	0.1	55.2	0.6	10	113	0	0.15
C2	5.9	4.0	-1.9	0.2	19.63	0	0	0	0	0.2	0.2	0.2	0.4	44	0	1	0.1	58.1	0.6	14	123	0	0.16
Cg	5.8	3.8	-2.0	0.5	24.24	0	0.1	0	0	0.7	0.4	0.4	1.1	39	0	0	0.1	54.9	0.9	106	189	0	0.20
P27 - NEOSSOLO QUARTZARÊNICO Órtico gleissólico Dystric Sideralic Brunic Arenosol (Ochric)																							
A	4.9	3.8	-1.1	2.6	21.77	0	0	0	0.7	2.5	0.2	0.8	2.7	6	81	0	0.5	48.8	0.7	4	69	0	0.39
CA	4.9	4.0	-0.9	1.2	8.52	0	0	0	0.4	1.5	0	0.5	1.6	3	91	0	0.4	52.5	0.6	2	43	0	0.17
C1	5.0	4.1	-0.9	0.5	2.80	0	0	0	0.4	1.2	0	0.4	1.2	1	98	0	0.2	49.7	0.6	1	48	0	0.10
C2	5.1	4.2	-0.9	0.2	0.53	0	0	0	0.4	0.9	0	0.4	0.9	0	100	0	0.1	51.2	0.5	0	10	0	0.09
P28 - NEOSSOLO QUARTZARÊNICO Órtico típico Dystric Brunic Arenosol (Ochric, Isopteric)																							
A	4.2	3.3	-1.0	3.3	28.90	0	0	0	1.1	5.2	0.2	1.3	5.4	3	86	0	0.9	50.5	0.6	10	72	0	-
C1	4.5	3.7	-0.9	1.2	28.09	0	0	0	0.8	2.1	0.1	0.9	2.2	6	84	0	0.2	51.4	0.5	4	88	0	-
C2	5.0	3.6	-1.4	1.2	41.17	14	0	0	0.7	2.1	0.3	1.0	2.4	14	66	5	0.2	49	0.6	3	137	0	-
P29 - ESPODOSSOLO FERRILÚVICO Hidromórfico arênico Gleyic Histic Albic Ortsteinic Podzol (Arenic, Abruptic, Epic, Sideralic)																							
Oo	4.5	3.8	-0.7	6.2	137.21	11	0.7	0.5	0.9	7.8	1.7	2.5	9.5	18	34	1	4.9	35	1.4	47	155	1	0.63
AO	5.2	3.7	-1.5	0.4	32.63	2	0	0	0.8	3.0	0.3	1.0	3.2	8	75	0	0.6	42.5	0.9	24	414	0	0.43
AE	5.2	3.7	-1.5	0.3	27.35	0	0	0	0.4	2.0	0.1	0.6	2.1	7	75	0	0.2	48.2	0.8	18	177	0	0.22
E	6.0	4.3	-1.7	0.1	11.96	0	0	0	0	0.2	0.1	0.1	0.3	23	0	1	0.1	56.5	0.5	12	119	0	0.31
Bsm1	5.9	4.9	-1.0	0.5	13.02	0	0	0	0	1.4	0.1	0.1	1.6	8	0	0	0.1	31.6	0.6	141	663	0	0.23
Bsm2	5.5	3.9	-1.7	1.4	10.03	2	0	0.1	0	1.5	0.3	0.3	1.8	14	0	1	0.1	39.9	0.7	101	162	0	0.36

Cg1	4.2	3.1	-1.1	2.9	15.24	2	0	0	0.7	1.4	0.2	0.8	1.6	10	81	1	0.1	45.3	1.1	38	175	0	0.33
Cg2	3.1	2.8	-0.3	2.0	4.09	0	0	0	2.2	3.4	0.0	2.2	3.4	1	99	0	0.1	45	1.8	15	131	1	0.23
P30 - NEOSSOLO QUARTZARÊNICO Órtico típico Dystric Sideralic Arenosol (Ochric)																							
A	5.0	3.7	-1.3	4.0	31.10	0	0.1	0	0.4	3.5	0.3	0.7	3.8	7	61	0	0.8	50.7	0.6	14	84	0	0.24
AC	5.0	4.0	-1.0	1.7	6.29	0	0	0	0.3	1.5	0.0	0.4	1.6	2	91	0	0.2	52.2	0.6	1	91	0	0.19
C1	5.1	4.4	-0.8	0.8	0.56	0	0	0	0.2	1.4	0.0	0.2	1.5	2	91	0	0.4	46.9	0.1	2	32	0	0.13
C2	5.8	4.4	-1.3	0.2	0.53	0	0	0	0.2	0.9	0.0	0.2	0.9	2	91	0	0.1	53.8	0.1	1	7	0	0.06
C3	5.8	4.4	-1.5	0.1	0.53	0	0	0	0.2	0.6	0.0	0.3	0.6	7	83	0	0.1	56.1	0.2	3	11	0	0.16

APPENDIX D – Phytosociological parameters of species sampled in two landscape units (*Cordilheiras* and *Murundus*), representing the arboreous environments, of the Nhecolândia Pantanal, Brazil. Data is presented in decreasing order of importance value index (IVI). Relative Density (RD), Relative Dominance (RDo), and Relative Frequency (RF).

Species	Family	RD	RDo	RF	IVI
		---------- % ----------			
	Cordilheiras				
Attalea phalerata Mart. ex Spreng.	Arecaceae	7.53	23.90	6.01	12.48
Protium heptaphyllum (Aubl.) Marchand	Burseraceae	8.33	2.17	7.65	6.05
Emmotum nitens (Benth.) Miers	Metteniusaceae	8.06	5.03	3.28	5.46
Sterculia apetala (Jacq.) H. Karst.	Malvaceae	3.23	7.33	3.83	4.79
Dipteryx alata Vogel	Fabaceae	3.76	5.35	4.37	4.50
Casearia silvestris Sw.	Salicaceae	6.45	0.67	5.46	4.20
Qualea parviflora Mart.	Vochysiaceae	6.18	2.04	3.83	4.02
Curatella americana L.	Dilleniaceae	4.84	3.62	3.28	3.91
Pouteria torta (Mart.) Radlk.	Sapotaceae	3.76	3.00	4.37	3.71
Alibertia edulis (Rich.) A. Rich. ex DC.	Rubiaceae	5.65	0.43	3.83	3.30
Caryocar brasiliense Cambess.	Caryocaraceae	0.81	7.08	1.64	3.18
Ficus sp.	Moraceae	0.27	7.89	0.55	2.90
Albizia polyantha (A. Spreng.) G.P. Lewis	Fabaceae	1.34	5.15	2.19	2.89
Hancornia speciosa Gomes	Apocynaceae	3.23	1.32	3.83	2.79
Trichilia elegans A. Juss.	Meliaceae	2.42	1.70	3.28	2.47
Astronium fraxinifolium Schott	Anacardiaceae	1.08	3.56	2.19	2.28
Unonopsis lindmanii R.E. Fr.	Annonaceae	4.03	0.37	2.19	2.20
Dalbergia frutescens (Vell.) Britton	Fabaceae	2.42	1.43	2.73	2.19
Hymenaea courbaril L.	Fabaceae	1.88	0.90	3.28	2.02
Myracrodruon urundeuva Allemão	Anacardiaceae	1.08	2.74	2.19	2.00
Licania minutiflora (Sagot) Fritsch	Chrysobalanaceae	1.88	1.25	2.19	1.77
Tabebuia heptaphylla (Vell.) Toledo	Bignoniaceae	1.08	2.01	1.64	1.58
Tabebuia aurea (Silva Manso) Benth. & Hook. f. ex S. Moore	Bignoniaceae	1.08	1.17	1.64	1.29
Mouriri elliptica Mart.	Melastomataceae	1.61	0.53	1.64	1.26
Brosimum gaudichaudii Trécul	Moraceae	1.34	0.40	1.64	1.13
Qualea grandiflora Mart.	Vochysiaceae	1.88	0.41	1.09	1.13
Acrocomia aculeata (Jacq.) Lodd. ex Mart.	Arecaceae	1.08	0.53	1.64	1.08
Xylopia aromatica (Lam.) Mart.	Annonaceae	1.61	0.42	1.09	1.04
Acrocomia totai Mart.	Arecaceae	0.81	0.64	1.64	1.03
Cecropia cf. pachystachya Trécul	Urticaceae	1.08	0.73	1.09	0.97
Cordia glabrata (Mart.) A. DC.	Cordiaceae	0.81	1.50	0.55	0.95

Eriotheca gracilipes (K. Schum.) A. Robyns	Malvaceae	0.81	0.39	1.64	0.95
Randia armata (Sw.) DC.	Rubiaceae	1.08	0.97	0.55	0.87
Andira humilis Mart. ex Benth.	Fabaceae	1.08	0.07	1.09	0.75
Simarouba versicolor A. St.-Hil.	Simaroubaceae	0.54	0.60	1.09	0.74
Rourea induta Planch.	Connaraceae	0.81	0.22	1.09	0.71
Zanthoxylum rhoifolium Lam.	Rutaceae	0.54	0.33	1.09	0.65
Luehea paniculata Mart.	Malvaceae	0.54	0.22	1.09	0.62
Myrtaceae	Myrtaceae	0.54	0.14	1.09	0.59
Sapium sp.	Euphorbiaceae	0.54	0.08	1.09	0.57
Pouteria ramiflora (Mart.) Radlk.	Sapotaceae	0.81	0.27	0.55	0.54
Vitex cymosa Bertero ex Spreng.	Lamiaceae	0.27	0.58	0.55	0.46
Buchenavia tomentosa Eichler	Combretaceae	0.54	0.30	0.55	0.46
Tabebuia roseoalba (Ridl.) Sandwith	Bignoniaceae	0.27	0.42	0.55	0.41
Celtis pubescens Spreng.	Cannabaceae	0.27	0.05	0.55	0.29
Kielmeyera coriacea Mart. & Zucc.	Calophyllaceae	0.27	0.04	0.55	0.28
Licania octandra (Hoffmanns. ex Roem. & Schult.) Kuntze	Chrysobalanaceae	0.27	0.02	0.55	0.28
Linociera hassleriana (Chodat) Hassl.	Oleaceae	0.27	0.01	0.55	0.28
Total	31	100	100	100	100
	Murundus				
Mouriri elliptica Mart.	Melastomataceae	20.66	18.94	10.38	16.66
Curatella americana L.	Dilleniaceae	11.05	11.04	9.69	10.59
Eugenia aurata O. Berg	Myrtaceae	8.29	4.68	6.92	6.63
Simarouba versicolor A. St.-Hil.	Simaroubaceae	6.41	7.59	5.88	6.63
Pouteria torta (Mart.) Radlk.	Sapotaceae	5.08	7.46	4.15	5.57
Diospyros burchellii Hiern	Ebenaceae	7.96	3.12	3.46	4.85
Hancornia speciosa Gomes	Apocynaceae	3.43	2.41	5.54	3.79
Erythroxylum suberosum A. St.-Hil.	Erythroxylaceae	4.75	1.67	4.15	3.53
Tabebuia aurea (Silva Manso) Benth. & Hook. f. ex S. Moore	Bignoniaceae	1.99	4.57	3.81	3.45
Byrsonima verbascifolia (L.) DC.	Malpighiaceae	3.98	1.84	3.81	3.21
Andira cujabensis Benth.	Fabaceae	1.88	3.38	2.77	2.68
Dipteryx alata Vogel	Fabaceae	1.99	1.85	2.77	2.20
Protium heptaphyllum (Aubl.) Marchand	Burseraceae	1.99	0.92	2.77	1.89
Hymenaea courbaril L.	Fabaceae	1.22	1.69	2.77	1.89
Cereus peruvianus (L.) Mill.	Cactaceae	0.99	2.12	2.08	1.73
Zanthoxylum rhoifolium Lam.	Rutaceae	1.66	1.02	2.42	1.70
Licania octandra (Hoffmanns. ex Roem. & Schult.) Kuntze	Chrysobalanaceae	0.88	2.28	1.73	1.63

Eriotheca pubescens (Mart. & Zucc.) Schott & Endl.	Malvaceae	0.55	3.21	1.04	1.60
Bowdichia virgilioides Kunth	Fabaceae	1.10	1.76	1.73	1.53
Ocotea diospyrifolia (Meisn.) Mez	Lauraceae	1.77	1.08	1.73	1.53
Aegiphila lhotzkiana Cham.	Lamiaceae	1.44	0.87	2.08	1.46
Handroanthus impetiginosus (Mart. ex DC.) Mattos	Bignoniaceae	0.44	2.39	1.04	1.29
Vitex cymosa Bertero ex Spreng.	Lamiaceae	0.22	2.88	0.69	1.26
Caryocar brasiliense Cambess.	Caryocaraceae	0.66	1.67	1.38	1.24
Alibertia sessilis (Vell.) K. Schum.	Rubiaceae	1.44	0.53	1.73	1.23
Stryphnodendron adstringens (Mart.) Coville	Fabaceae	0.55	1.13	1.38	1.02
Licania minutiflora (Sagot) Fritsch	Chrysobalanaceae	0.55	2.04	0.35	0.98
Callisthene major Mart.	Vochysiaceae	0.88	0.91	1.04	0.95
Qualea parviflora Mart.	Vochysiaceae	0.55	0.95	0.69	0.73
Andira paniculata Benth.	Fabaceae	0.44	1.00	0.69	0.71
Acrocomia aculeata (Jacq.) Lodd. ex Mart.	Arecaceae	0.33	0.69	1.04	0.69
Sapium haematospermum Müll. Arg.	Euphorbiaceae	0.44	0.55	0.69	0.56
Miconia albicans (Sw.) Steud.	Melastomataceae	0.77	0.07	0.69	0.51
Dalbergia miscolobium Benth.	Fabaceae	0.33	0.43	0.69	0.48
Alchornea discolor Poepp.	Euphorbiaceae	0.55	0.19	0.69	0.48
Couepia grandiflora (Mart. & Zucc.) Benth. ex Hook. f.	Chrysobalanaceae	0.55	0.09	0.69	0.44
Styrax ferrugineus Nees & Mart.	Styracaceae	0.44	0.19	0.69	0.44
Licania parviflora Benth.	Chrysobalanaceae	0.33	0.28	0.69	0.44
Rheedia brasiliensis (Mart.) Planch. & Triana	Clusiaceae	0.44	0.06	0.69	0.40
Sclerolobium paniculatum Vogel	Fabaceae	0.22	0.11	0.69	0.34
Aspidosperma macrocarpon Mart.	Apocynaceae	0.22	0.06	0.35	0.21
Rourea induta Planch.	Connaraceae	0.11	0.11	0.35	0.19
Buchenavia tomentosa Eichler	Combretaceae	0.11	0.06	0.35	0.17
Agonandra brasiliensis Benth. & Hook. f.	Opiliaceae	0.11	0.05	0.35	0.17
Qualea grandiflora Mart.	Vochysiaceae	0.11	0.03	0.35	0.16
Cecropia cf. pachystachya Trécul	Urticaceae	0.11	0.02	0.35	0.16
Total	29	100	100	100	100

APPENDIX E – Phytosociological parameters of species sampled in four landscape units (*Salinas*, *Baías*, *Vazantes*, and *Campos*), that represent the herbaceous environments, of the Nhecolândia Pantanal, Brazil. Data is presented in decreasing order of importance value (IV). Relative Cover (RC), Relative Frequency (RF), and Importance Value Index (IVI).

Species	Family	RC	RF	IVI
		---------- % ----------		
	Salinas			
Paspalum vaginatum Sw.	Poaceae	57.80	41.10	49.45
Cynodon dactylon (L.) Pers.	Poaceae	20.60	13.70	17.15
Paspalum sp.	Poaceae	6.36	10.96	8.66
Bulbostylis sp.	Cyperaceae	6.12	8.22	7.17
Eleocharis sp.	Cyperaceae	3.35	9.59	6.47
Poaceae 2	Poaceae	3.00	6.85	4.93
Ludwigia sp.	Onagraceae	1.24	4.11	2.67
Pluchea sagittalis (Lam.) Cabrera	Asteraceae	0.53	2.74	1.63
Portulaca sp.	Portulacaceae	0.88	1.37	1.13
Poaceae 1	Poaceae	0.12	1.37	0.74
Total	5	100	100	100
	Baías			
Typha domingensis Pers.	Typhaceae	15.26	10.78	13.02
Eichhornia azurea (Sw.) Kunth	Pontederiaceae	9.04	8.98	9.01
Eleocharis sp.	Cyperaceae	9.70	6.59	8.14
Coelorachis aurita (Steud.) A. Camus	Poaceae	10.09	5.99	8.04
Andropogon bicornis L.	Poaceae	7.78	5.39	6.59
Cyperus cf. polystachyus	Cyperaceae	5.26	6.59	5.92
Andropogon hypogynus Hack.	Poaceae	6.87	4.79	5.83
Rhynchospora sp.	Cyperaceae	6.70	4.79	5.74
Oryza sp.	Poaceae	7.17	4.19	5.68
Paspalidium paludivagum (Hitchc. & Chase) Parodi	Poaceae	4.13	6.59	5.36
Pontederia cordata L.	Pontederiaceae	2.70	6.59	4.64
Caperonia castaneifolia (L.) A. St.-Hil.	Euphorbiaceae	1.91	4.79	3.35
Aeschynomene paniculata Willd. ex Vogel	Fabaceae	1.91	4.19	3.05
Xyris sp. 1	Xyridaceae	0.91	4.79	2.85
Bulbostylis sp.	Cyperaceae	3.13	2.40	2.76
Asteraceae	Asteraceae	1.17	3.59	2.38
Melochia sp.	Malvaceae	2.48	1.80	2.14
Erechtites hieraciifolius (L.) Raf. ex DC.	Asteraceae	1.22	2.40	1.81

Scleria sp.	Cyperaceae	0.61	1.20	0.90
Xyris sp. 2	Xyridaceae	0.61	1.20	0.90
Waltheria albicans Turcz.	Asteraceae	0.39	1.20	0.79
Poaceae	Poaceae	0.65	0.60	0.63
Diodia sp.	Rubiaceae	0.30	0.60	0.45
Total	10	100	100	100
	Vazantes			
Bulbostylis sp.	Cyperaceae	23.36	29	12.08
Schizachyrium tenerum Nees	Poaceae	18.15	9.58	13.87
Andropogon hypogynus Hack.	Poaceae	15.88	8.75	12.31
Paspalum acuminatum Raddi	Poaceae	7.99	15.42	11.70
Eragrostis sp.	Poaceae	9.57	4.58	7.08
Phyllanthus stipulatus (Raf.) G.L. Webster	Phyllanthaceae	1.86	7.92	4.89
Paratheria sp.	Poaceae	6.00	3.75	4.87
Scleria sp.	Cyperaceae	2.27	5.42	3.84
Poaceae 1	Poaceae	4.14	2.92	3.53
Eichhornia azurea (Sw.) Kunth	Pontederiaceae	1.63	3.75	2.69
Cyperus cf. polystachyus R. Br.	Cyperaceae	1.76	3.33	2.55
Ludwigia sedoides (Bonpl.) H. Hara	Onagraceae	0.87	2.92	1.89
Panicum sp.	Poaceae	1.10	2.08	1.59
Reimarochloa sp.	Poaceae	0.64	2.08	1.36
Melochia sp.	Malvaceae	0.38	2.08	1.23
Eleocharis sp.	Cyperaceae	1.12	1.25	1.19
Sipanea biflora (Rottb.) Cham. & Schltdl.	Rubiaceae	0.59	1.67	1.13
Acisanthera sp.	Melastomataceae	0.33	1.67	1.00
Pontederia cordata L.	Pontederiaceae	0.54	1.25	0.89
Caperonia palustris (L.) A. St.-Hil.	Euphorbiaceae	0.28	1.25	0.77
Rhynchanthera novemnervia DC.	Melastomataceae	0.28	1.25	0.77
Waltheria albicans Turcz.	Asteraceae	0.15	1.25	0.70
Luziola sp.	Poaceae	0.36	0.83	0.60
Rhynchospora sp.	Cyperaceae	0.36	0.83	0.60
Hyptis lorentziana O. Hoffm.	Lamiaceae	0.10	0.83	0.47
Gamochaeta sp.	Asteraceae	0.18	0.42	0.30
Indeterminada	-	0.05	0.42	0.23
Xyris sp.	Xyridaceae	0.05	0.42	0.23
Total	12	100	100	82.28
	Campos			
Elyonurus cf. muticus (Spreng.) Kuntze	Poaceae	46.80	23.68	35.24

Poaceae 1	Poaceae	16.26	19.08	17.67
Eupatorium sp.	Asteraceae	11.90	17.76	14.83
Andropogon bicornis L.	Poaceae	9.97	7.24	8.60
Bulbostylis sp.	Cyperaceae	4.26	6.58	5.42
Axonopus leptostachyus (Flüggé) Hitchc.	Poaceae	2.78	5.26	4.02
Phyllanthus sp.	Phyllanthaceae	2.18	4.61	3.39
Waltheria albicans Turcz.	Malvaceae	0.59	3.95	2.27
Curatella americana L.	Dilleniaceae	1.39	2.63	2.01
Stilpnopappus pantanalensis H. Rob.	Asteraceae	1.39	2.63	2.01
Diospyros burchellii Hiern	Ebenaceae	0.79	1.97	1.38
Malpighiaceae	Malpighiaceae	0.79	1.97	1.38
Lippia sp.	Verbenaceae	0.45	1.32	0.88
Byrsonima verbascifolia (L.) DC.	Malpighiaceae	0.35	0.66	0.50
Chromolaena laevigata (Lam.) R.M. King & H. Rob.	Asteraceae	0.10	0.66	0.38
Total	9	100	100	100

APPENDIX F – Equivalent doses of the aliquots used for calibration curve in the Optically Stimulated Luminescence analysis

Aliquot	Equivalent dose	Recycle test	Variation (%)	Recovery test (%)
5596 sample – P18 A1 (5-15 cm depth)				
1	4.2 ± 0.2	1.02 ± 0.04	2%	0.50% ± 0.10%
2	4.3 ± 0.2	1.01 ± 0.04	1%	0.70% ± 0.10%
3	4.2 ± 0.2	0.99 ± 0.04	-1%	0.30% ± 0.10%
4	4.2 ± 0.1	1 ± 0.03	0%	0.40% ± 0.10%
5	4.4 ± 0.2	0.98 ± 0.04	-2%	0.70% ± 0.10%
6	4.1 ± 0.2	0.98 ± 0.04	-2%	0.50% ± 0.10%
7	3.8 ± 0.2	1.01 ± 0.04	1%	0.40% ± 0.10%
8	4.2 ± 0.2	0.98 ± 0.03	-2%	0.50% ± 0.10%
9	4.3 ± 0.2	1.01 ± 0.03	1%	0.30% ± 0.10%
10	4.1 ± 0.1	1 ± 0.03	0%	0.60% ± 0.10%
11	4.2 ± 0.2	0.99 ± 0.03	-1%	0.40% ± 0.10%
12	3.9 ± 0.2	1.01 ± 0.03	1%	0.40% ± 0.10%
13	4.1 ± 0.2	0.98 ± 0.04	-2%	0.40% ± 0.10%
14	4.1 ± 0.2	1.01 ± 0.04	1%	0.40% ± 0.10%
15	4.4 ± 0.1	1.02 ± 0.04	2%	0.40% ± 0.10%
5597 sample – P26 E2 (60 cm depth)				
1	7.3 ± 0.5	1.02 ± 0.03	2%	0.50% ± 0.10%
2	7.8 ± 0.5	0.99 ± 0.03	-1%	0.90% ± 0.10%
3	6.2 ± 0.4	0.99 ± 0.04	-1%	0.50% ± 0.10%
4	6.6 ± 0.5	0.98 ± 0.03	-2%	0.60% ± 0.10%
5	8.6 ± 0.5	0.99 ± 0.03	-1%	0.40% ± 0.10%
6	14.4 ± 0.6	0.98 ± 0.04	-2%	0.60% ± 0.10%
7	9.5 ± 0.5	0.97 ± 0.03	-3%	0.70% ± 0.10%
8	12.9 ± 0.5	0.96 ± 0.03	-4%	0.30% ± 0.00%
9	8.9 ± 0.6	1.05 ± 0.04	5%	0.60% ± 0.10%
10	9 ± 0.5	1 ± 0.04	0%	0.50% ± 0.10%
11	8 ± 0.4	1.02 ± 0.03	2%	0.30% ± 0.10%
12	8.8 ± 0.5	0.96 ± 0.03	-4%	0.70% ± 0.10%
13	16 ± 0.6	0.99 ± 0.03	-1%	0.30% ± 0.00%
14	12.5 ± 0.6	0.99 ± 0.03	-1%	0.20% ± 0.00%
15	8.2 ± 0.6	1 ± 0.03	0%	0.40% ± 0.10%
5598 sample – P29 2Cg1 (80-90 cm depth)				
1	15.2 ± 0.5	1.03 ± 0.04	3%	0.20% ± 0.00%
2	9.4 ± 0.6	1.03 ± 0.04	3%	0.30% ± 0.10%
3	11.2 ± 0.5	1.03 ± 0.03	3%	0.20% ± 0.00%
4	11.2 ± 0.6	1.05 ± 0.04	5%	0.20% ± 0.00%
5	8 ± 0.5	1.06 ± 0.04	6%	0.20% ± 0.10%
6	10.6 ± 0.5	1.04 ± 0.03	4%	0.40% ± 0.00%
7	10.2 ± 0.5	1.04 ± 0.04	4%	0.30% ± 0.10%
8	12 ± 0.5	1.02 ± 0.03	2%	0.20% ± 0.00%
9	8.3 ± 0.5	1.04 ± 0.04	4%	0.40% ± 0.10%
10	10.9 ± 0.5	1.01 ± 0.03	1%	0.40% ± 0.00%
11	14.5 ± 0.6	1 ± 0.03	0%	0.40% ± 0.00%
12	12.8 ± 0.6	0.99 ± 0.03	-1%	0.50% ± 0.00%
13	16.4 ± 0.6	1.01 ± 0.03	1%	0.20% ± 0.00%
14	12.1 ± 0.5	0.99 ± 0.03	-1%	0.20% ± 0.00%
15	13.9 ± 0.6	0.97 ± 0.03	-3%	0.30% ± 0.00%
5599 sample – P30 C3 (70-80 cm depth)				
1	7.9 ± 0.5	0.99 ± 0.03	-1%	0.30% ± 0.00%

2	7.9 ± 0.5	0.99 ± 0.03	-1%	0.40% ± 0.00%
3	8.1 ± 0.5	1.05 ± 0.04	5%	0.90% ± 0.10%
4	7.3 ± 0.5	0.99 ± 0.03	-1%	0.40% ± 0.10%
5	8.4 ± 0.5	0.96 ± 0.03	-4%	0.50% ± 0.10%
6	6.5 ± 0.4	1.03 ± 0.03	3%	0.40% ± 0.10%
7	6.6 ± 0.4	0.99 ± 0.03	-1%	0.40% ± 0.10%
8	6.5 ± 0.5	1 ± 0.03	0%	0.40% ± 0.10%
9	7.3 ± 0.5	1.04 ± 0.04	4%	0.40% ± 0.00%
10	6.4 ± 0.4	1.03 ± 0.03	3%	0.60% ± 0.00%
11	8.9 ± 0.6	0.99 ± 0.03	-1%	0.40% ± 0.10%
12	7.9 ± 0.5	1 ± 0.03	0%	0.30% ± 0.10%
13	7.9 ± 0.5	1.03 ± 0.04	3%	0.60% ± 0.10%
14	7.1 ± 0.5	1 ± 0.03	0%	0.40% ± 0.10%
15	9 ± 0.5	1 ± 0.03	0%	0.30% ± 0.00%

APPENDIX G – Micromorphometric parameters of the sand fraction: sorting (percentage of soil fractions), equivalent diameter (ED), and circularity index (K).

Sample	Size fraction class*	n	Percentage of fractions	Statistics	ED (mm)*	K*
			Salinas			
P18 Agn2-E	CS	196	34.33	Min.	0.04	0.53
	FS	362	63.4	Max.	0.98	1.72
	Silt	13	2.28	Mean	0.19	0.83
P18 Btgn	CS	390	36.65	Min.	0.03	0.44
	FS	671	63.06	Max.	1.20	0.97
	Silt	3	0.28	Mean	0.19	0.82
P19 Duripan	CS	388	23.79	Min.	0.03	0.46
	FS	1235	75.72	Max.	0.83	0.99
	Silt	8	0.49	Mean	0.16	0.82
P19 A	CS	476	38.42	Min.	0.04	0.40
	FS	760	61.34	Max.	0.60	0.97
	Silt	3	0.24	Mean	0.20	0.81
			Baías			
P26 Cg	CS	392	33.25	Min.	0.02	0.41
	FS	759	65.38	Max.	1.14	0.99
	Silt	28	2.37	Mean	0.18	0.81
			Vazantes			
P29 2E-2Bsm1	CS	477	32.9	Min.	0.02	0.36
	FS	947	65.31	Max.	1.35	0.98
	Silt	26	1.79	Mean	0.18	0.79
P29 Cg1-Cg2	CS	569	38.76	Min.	0.04	0.35
	FS	894	60.9	Max	1.13	0.97
	Silt	5	0.34	Mean	0.19	0.81
			Cordilheiras			
P20 Btnqx	CS	78	12.68	Min.	0.03	0.41
	FS	511	83.09	Max.	0.68	0.98
	Silt	26	4.23	Mean	0.13	0.81
			Murundus			
P8 A	CS	335	46.79	Min.	0.03	0.46
	FS	370	51.68	Max.	0.79	0.97
	Silt	11	1.54	Mean	0.21	0.81

Notes: ***Fraction percentage classification**: Perfectly sorted (occurrence of one size fraction), well sorted (5-10% of sizes other than the dominant one), moderately sorted (10-30% of sizes other than the dominant one), poorly sorted (>30% of sizes other than the dominant one), and unsorted (occurrence of a variety of sizes); **Sand size classes**: CS-Coarse sand (0.2< ED < 2), FS-fine sand (0.05 < ED < 0.2), and silt (0.002 < ED < 0.05); **Roundness classes**: angular (0 < K < 0.2), subangular (0.2 < K < 0.4), subrounded (0.4 < K < 0.7), rounded to well rounded (0.7 < K < 1).